TNO innovation for life

National scale modelling of nitrogen deposition in the Netherlands

Benchmark of policy support models - Nationaal Kennisprogramma Stikstof (NKS)

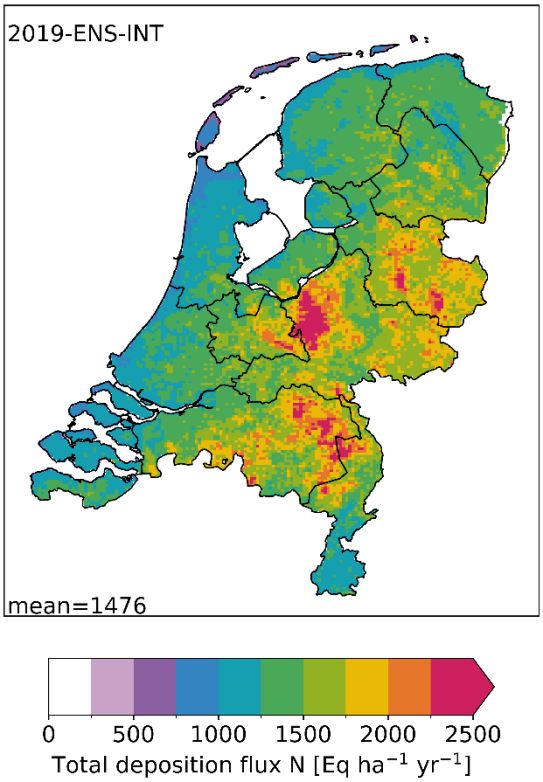

TNO Public ⟩ TNO 2025 R11248
December 2025

Energy & Materials Transition
www.tno.nl
+31 88 866 42 56
info@tno.nl

TNO 2025 R11248 – December 2025

National scale modelling of nitrogen deposition in the Netherlands

Benchmark of policy support models - Nationaal Kennisprogramma Stikstof (NKS)

Author(s)	TNO: M. Schaap, R. Kranenburg, C. H. Michaud van der Wal, L. Geers FMI: Rostislav Kouznetsov SMHI: Robert Bergström

Classification report	TNO Public
Title	TNO Public
Report text	TNO Public
Appendices	TNO Public
Number of pages	161 (excl. front and back cover)
Number of appendices	6
Sponsor	Nationaal Kennisprogramma Stikstof (NKS)
Project name	LNV Kennisprogramma Stikstof 2021 - 2024
Project number	060.46261
DOI	10.82135/tno-2025-r11248

Publiekssamenvatting

Dit is de eerste benchmarkstudie naar stikstofdepositie in Nederland op nationale schaal. Het doel van deze modelvergelijking was 1) inzicht te verschaffen in de robuustheid van regionale modellering van stikstofdepositie, die relevant is voor beleidsvorming, en 2) modelverbetering te stimuleren die relevant is voor beleidsvorming, door het OPS-model te benchmarken met een ensemble van modelleringssystemen. Uit de onderlinge vergelijking bleek dat de op nationale schaal ontwikkelde (OPS, LOTOS) en toegepaste (EMEP4NL) modellen in Nederland consistent zijn met de huidige modelpraktijk in Europa. Het ensemble blijkt een verfijnde manier om inzicht te geven in de onzekerheid in gemodelleerde stikstofdepositie en concentraties van verontreinigende stoffen. Op basis van de analyse van de resultaten konden we aanbevelingen doen voor modelontwikkeling voor de afzonderlijke ensemble-leden en voor het ensemble als geheel. We bevelen aan om de benchmark aan te vullen met een recent jaar (2025) en de volledige vergelijkingsstudie over twee jaar te herhalen als onderdeel van een structurele kwaliteitsborging van het modelinstrumentarium ter beleidsondersteuning. Door het herhalen van de benchmark profiteren we maximaal van huidige uitbreidingen van meetactiviteiten: die binnen het LML-netwerk, en de regionale netwerken in landbouwgebieden. Bovendien maakt de herhaling het mogelijk om de aanbevolen modelverbeteringen door te voeren, om de prestaties van het ensemble (gemiddelde) verder te vergelijken met een grotere set droge en natte depositie-metingen. Naast onze verdere samenvatting, bieden wij in Appendix F ook samenvattingsprompts voor Large Language Models (zoals CoPilot en ChatGPT).

Synopsis

This is the first national scale benchmark study of nitrogen deposition in the Netherlands. The aim of this model intercomparison was 1) to give insight in robustness of regional scale modelling of nitrogen deposition relevant to policy making, and 2) to foster model improvement relevant to policy making by benchmarking the OPS model with an ensemble of modelling systems. The intercomparison showed that the national scale models developed (OPS, LOTOS) and applied (EMEP4NL) in the Netherlands are consistent with the current state of modelling practice in Europe. The ensemble proves an elegant way to give insight in the uncertainty in modelled nitrogen deposition and pollutant concentrations. Based on the analysis of the results, we were able to give recommendations for model development for the individual ensemble members as well as for the ensemble as a whole. We recommend to complement the benchmark with a recent year (2025) and to repeat the full intercomparison exercise 2 years from now as part of a structural quality assurance of the modelling framework for policy support. Repeating the benchmark would also benefit from the current activities in expanding the LML network, and from activities in regional monitoring networks in agricultural areas. Moreover, the repetition allows for the incorporation of the advised model improvements and to further address the performance of the ensemble (mean) in comparison to a larger set of dry and wet deposition measurements. Next to our provided summary, we provide summary prompts for Large Language Models (such as Copilot or ChatGPT) in Appendix F.

Summary

Motivation

The government of the Netherlands strives for a transparent and scientifically robust basis of the national nitrogen policy. Dutch policy support is based on a combination of measurements and modelling (Marra et al., 2024). The OPS model is used for providing assessments on nitrogen deposition both on a national scale and on individual Natura 2000-areas. These assessments include the provision of deposition maps, the quantification of the contributions from source sectors responsible for the deposition, and impact analyses of proposed mitigation strategies. As such, the regional modelling results play a key role in informing all stakeholders in the societal debate concerning nitrogen deposition.

Modelling the fate of ammonia and nitrogen oxides in the atmosphere is a complicated task. Chemistry transport models used for this task aim to include all relevant physical process descriptions in a balanced way to explain observed concentration and deposition levels and the sensitivity to changing emissions and weather conditions as good as possible. The available models differ in the level of detail in which the processes are described, the targeted scale and resolution, and the degree in which they are operationally applied. The model performance and the uncertainty of model results are traditionally addressed through validation against observations and sensitivity analyses. During the last two decades, the intercomparison of groups of models in benchmark studies has been shown to be a powerful way to assess the robustness of modelling outcomes and to identify directions for improvement and thereby speed up model improvement. Participation in model intercomparison studies has become an integral part of evaluating a model system.

The spread between modelling outcomes is a measure of their robustness. A model may contain errors causing a part of the spread. Usually this would also be detected by validation against observations. Even for sufficiently validated models, there will be more fundamental uncertainties linked to gaps in scientific knowledge, requiring assumptions that can be made differently. Quantifying the ensemble spread provides an elegant way to assess uncertainty in modelling results. Moreover, the model ensemble mean (or median) often has most skill in comparison to observations. Experience shows that all model systems have their own strengths and weaknesses. It is this variability that often leads to a better performance of the ensemble model in air quality forecasting and analysis. Hence, the combined expertise and insights from multiple teams integrated into the ensemble model can provide added value. Until now, a national scale model benchmark and ensemble study aimed at nitrogen deposition was not available for the Netherlands.

Objectives

The central objectives of the present study are

1. To give insight in robustness of the regional scale modelling of nitrogen deposition relevant to policy making
2. To foster model improvement relevant to policy making by benchmarking the OPS model with an ensemble of modelling systems.

The objectives are met by obtaining these intermediate results:

1. A benchmark test using five national scale models with a focus on:
   a.Deposition of reduced and oxidized nitrogen compounds

   b. Concentration of reduced and oxidized nitrogen compounds
   c. Source attribution for domestic and international sectors to nitrogen deposition
2. An evaluation of the information provided by the ensemble model and its spread
3. An assessment of the differences between OPS and the other ensemble members
4. Recommendations for input data improvement and for model (input) development for the individual ensemble members and the ensemble as a whole.

Study design

The benchmark study presented here includes five modelling systems. Besides the OPS model, we used the LOTOS-EUROS (short: LOTOS) and EMEP4NL model systems as they are developed and/or applied at Dutch institutes. These three models were complemented by two international models: MATCH and SILAM. Except OPS, all models are Eulerian grid models. All models simulated concentrations and deposition of reduced and oxidized nitrogen compounds for the year 2019, using consistent annual emission distributions. The model results were compared between each other and, where possible, evaluated against observations from the Dutch Air Quality (LML) and ammonia in nature areas (MAN) monitoring networks. The comparison focuses on annual means or totals as current policy support activities using OPS are performed on an annual basis. For all quantities the ensemble mean and spread were computed. A consistency check was performed by running the three Dutch models also for the period 2016-2018. These three models also delivered source apportionment information for the year 2018 to compare the domestic and transboundary contributions for three main sectors.

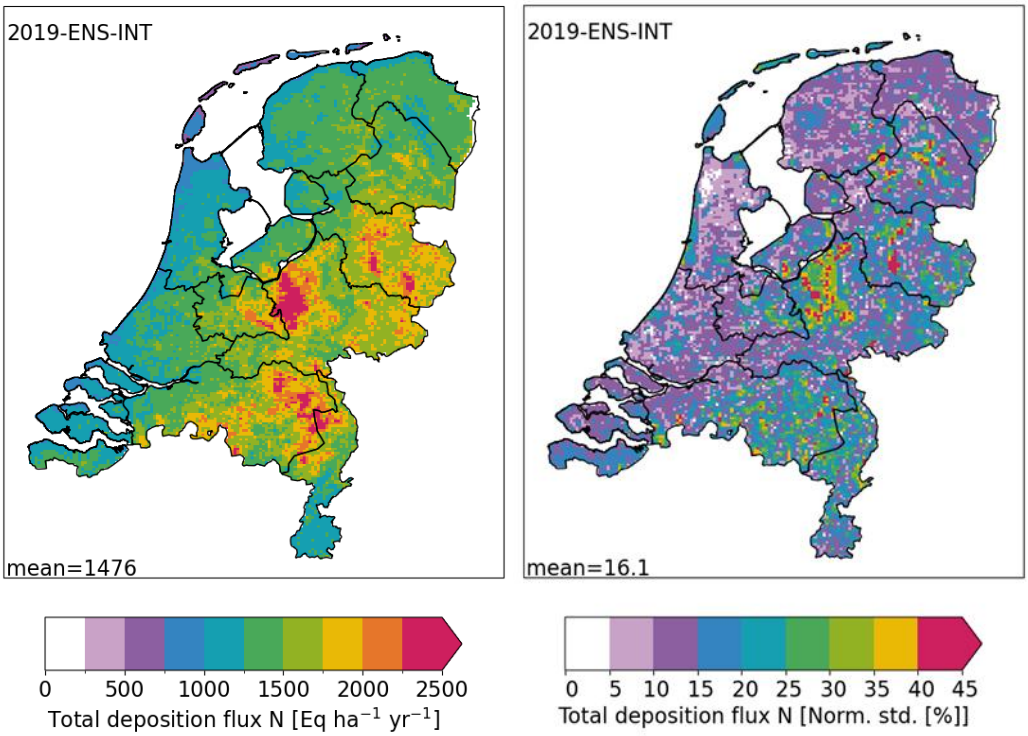

Figure 1: Left: Modelled ensemble mean total nitrogen deposition (left, eq ha^{-1} yr^{-1}) in the Netherlands, and right: Normalized standard deviation (%) as a measure of spread around the ensemble mean for total nitrogen deposition.

Modelled total deposition and spread between models

The mean total nitrogen deposition in the Netherlands as calculated by the five models is equal to 1476 eq ha^{-1} yr^{-1} (Figure 1, left). The individual model estimates are 1296 (EMEP4NL), 1334 (LOTOS), 1508 (SILAM), 1569 (OPS) and 1669 (MATCH) eq ha^{-1} yr^{-1} (Table 1). The standard deviation (1 σ) is 141 eq ha^{-1} yr^{-1} or 10 % of the mean.

The modelled total nitrogen deposition shows a large variability across the country. Highest deposition fluxes are calculated for the regions with intensive animal husbandry and for forested areas. In the maxima the modelled ensemble mean deposition exceeds 2000 eq ha^{-1} yr^{-1}. In the western coastal provinces of Zeeland, South and North Holland and outhern Limburg large areas show central estimates slightly below 1250 eq ha^{-1} yr^{-1}. The country-average standard deviation (1 σ) for the modelled deposition at a kilometer scale is about 15 % of the mean. Only for forested areas, most notably the Veluwe, the spread in the model results is considerably larger. These results suggest that in large parts of the Netherlands the modelled deposition of nitrogen is smaller than the observation-anchored uncertainty reported by Hoogerbrugge et al. (2024). Hoogerbrugge et al. (2024) estimated the uncertainty of the total deposition at a random location in the Netherlands to be around 30-35 % (1 σ). It should be noted that the spread or uncertainty provided in the present study does not include the uncertainty introduced due to uncertainty in emissions, but are solely due to differences in modelling practice, using the same emissions and not fully accounting for the uncertainty in model parameters. In this study of Hoogerbrugge et al. (2024), the uncertainty was estimated based (as much as possible) on a comparison of the model results with measurements.

Table 1: Overview of the modelled dry and wet deposition for reduced (NH_x), oxidized (NO_y) and total N deposition in 2019 for the country as a whole (eq N ha^{-1} yr^{-1}). For the ensembles the standard deviation of the mean is also provided.

	Dry-NH_x	Wet-NH_x	Dry-NO_y	Wet-NO_y	Total	% NH_x	% NO_y
OPS	733	374	260	201	1569	71	29
LOTOS	655	330	209	139	1334	74	26
EMEP4NL	573	308	268	147	1296	68	32
Ensemble mean NLD	654	337	246	162	1400	71	29
Std. ensemble mean NLD	131	38	32	30	173		
MATCH	968	356	184	162	1669	79	21
SILAM	952	220	246	90	1508	78	22
Ensemble mean INT	777	317	234	148	1476	74	26
Std. ensemble mean INT	246	59	44	38	250		

Reduced nitrogen (particularly the dry deposition of ammonia) explains a large part of the total deposition. The dry ammonia deposition contributes on average almost half of the total nitrogen deposition in the Netherlands. The wet reduced nitrogen deposition contributes about 20 – 25 %. The modelled contribution of oxidized nitrogen to total nitrogen deposition varies between 21 and 32 %. The models vary a lot regarding the relative importance of dry and wet deposition for oxidized nitrogen. Thus, the spread or uncertainty between the models increases when the different contributing fluxes to the

total are considered. The lower uncertainty in the totals is due to compensating effects. For example, when a model less efficiently removes nitrogen dioxide by dry deposition, dry or wet deposition of nitric acid will subsequently be enhanced. Similar compensation mechanisms apply to the spatial dimension. The uncertainty for the mean over the whole of the Netherlands is much smaller than for individual squares of one by one kilometre.

Reduced nitrogen deposition

The largest variability between the models was determined for the dry deposition of ammonia. On average across the Netherlands, the standard deviation was about 30 % of the mean. This number means that on average there is a 95 percent probability that a model outcome falls within the range of the mean plus or minus 60 %. For comparison, the mean normalized standard deviation was 23 % for the concentration of ammonia and 19 % for the reduced nitrogen wet deposition. The largest variability in the modelled reduced nitrogen dry deposition with a standard deviation of about 50 % is found for the Veluwe area. The latter is due to the contrasting results of MATCH and SILAM as compared to the other three models in the ensemble. This is illustrative for the fact that these two models were often the envelope within which the other models performed. The effective dry deposition velocity, computed from the mean concentration and deposition from the models, varies by a factor of two. This illustrates that the atmospheric lifetime and transport distances vary between models. An interesting case was provided by the different treatment of arable land and grassland in EMEP4NL as compared to OPS and LOTOS. This difference appears to affect the national-scale ammonia concentration and deposition patterns, highlighting the impact of differing approaches to describe ammonia exchange for agricultural land.

Oxidized nitrogen

Nitrogen dioxide is directly emitted or formed immediately after emission of nitrogen monoxide . The dry and wet deposition of nitrogen dioxide is a minor loss term (~20 %) for this component, which is largely due to the low water solubility of this compound. Most nitrogen dioxide is oxidized to nitric acid and may subsequently form particulate matter. The large similarity in the annual mean concentration distribution for nitrogen dioxide indicates that the mean dispersion is very similar among the models. Differences observed between the models near industrial areas and inland shipping lanes could be caused by differences in the assumptions on the effective emission height. The nationwide good agreement between modelled and observed annual mean concentrations provides evidence that the totals and spatial distribution of nitrogen oxides (NO_x) emissions are generally well understood. The variability between the model results increases for the reaction products of NO_x and their dry and wet deposition fluxes. This is understandable, as the number of processes involved, and the dependencies on the model skill for other reactants such as ammonia, become larger. For some key species, such as nitric acid, or key processes, such as particle deposition fluxes, no information was available for evaluation of the models. Moreover, in the regions where the models show some of the largest variability in wet deposition of oxidized nitrogen, likely related to differences in particulate nitrate, no wet deposition observations were available in the air quality monitoring networks. In these regions additional observations would be useful for model validation.

Skill of the ensemble

Evaluation against measurements indicates that the ensemble mean generally performs as well as, or better than, the best individual model for the quantities evaluated. The best performing model system varies per quantity. Hence, it is the consistency of the skill for all evaluated parameters that makes the ensemble model perform better than the ensemble

members. This also shows that models that individually perform not as well for a certain component, still contribute to the performance of the whole ensemble. The ensemble mean model shows the largest added value for parameters that are most uncertain. In other words, for components with little uncertainty such as the nitrogen dioxide the ensemble brings less added value than for parameters where the models are further apart, such as oxidized nitrogen deposition. These features could also be observed for the small ensemble of Dutch models. At the national scale the OPS model performs comparable to the other models for ammonia and nitrogen dioxide concentrations, where the more complex models performed better for secondary components. This is in line with earlier studies in which the OPS model has been compared with LOTOS and EMEP4NL (van der Swaluw et al., 2017, 2021).

Domestic contribution to reduced and oxidized nitrogen deposition

The domestic contribution may be the first indicator to assess the effectiveness of national mitigation measures. The contribution of Dutch sources to the total nitrogen deposition, the so-called domestic contribution, modelled by OPS is on average 66 % in the Netherlands. In an absolute sense, this is about 1000 eq ha^{-1} yr^{-1} (Figure 2). The source apportionment simulations using LOTOS and EMEP4NL yield domestic contributions of 53 %. In an absolute sense the nitrogen deposition attributed to domestic sources are 300 eq ha^{-1} yr^{-1} lower. Within the domestic contribution the shares of the source sectors are similar according to all models. The systematic differences in the contribution of domestic and international contributions highlight the different ‘source receptor relationships’ in the models. The transport distance in OPS is shorter than in EMEP4NL and LOTOS, for both nitrogen oxides and ammonia. The reason for the shorter transport distance in OPS might be partly attributed to the larger concentrations of precursor gas near source areas. Such higher concentrations are expected to yield higher deposition values on the average. Hence, more nitrogen is deposited in source areas in the OPS model than in the Eulerian models.

The source attribution results indicate that the fraction of the Dutch emissions exported is larger when calculated by LOTOS-EUROS and EMEP4NL than calculated by OPS, indicating a potentially 30 % lower effectiveness of national mitigation measures as compared to OPS. Correspondingly, the LOTOS and EMEP4NL model calculations would indicate that the Netherlands can benefit more strongly from international mitigation efforts. Because the differences between the models may lead to different policy conclusions, we recommend to conduct dedicated model simulations to compare the effectiveness of potential mitigation strategies.

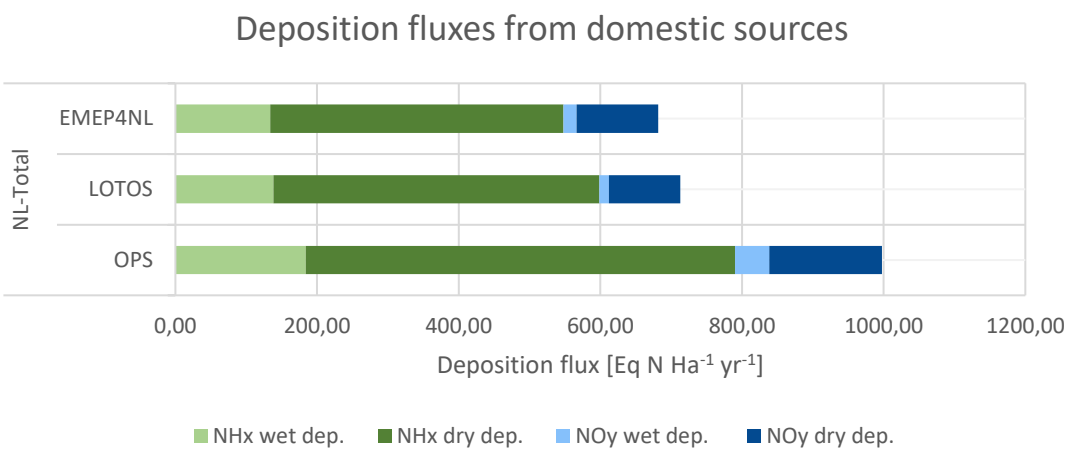

Figure 2: Total nitrogen deposition flux for 2018 from Dutch sources for each of the Dutch models (OPS, LOTOS, EMEP4NL).

An assessment of the differences between OPS and the ensemble members

The mean values for the different fluxes (i.e., dry and wet deposition of reduced and oxidized nitrogen), as modelled by the OPS model, are all within the range of the other models in this study. The only exception is the wet deposition of oxidized nitrogen, in which the OPS model yields the highest value of the five models (Table 2). This might be linked to the different spatial distributions of the modelled particulate nitrate ($pNO3^-$ concentrations in the OPS model as compared to the other models: the annual average particulate nitrate distribution from OPS shows gradients that resemble the ammonia emission distribution, whereas the other models show much smaller gradients across the country.

The OPS model uses chemical conversion rates derived from calculations by the EMEP4NL model (Hoogerbrugge et al., 2020). Rates for conversion from, for example, gaseous NO_x precursors to particulate $pNO3^-$ are derived which are consistent with the annual mass conversion computed by EMEP4NL. As such, annual mean conversion rates are produced for use in OPS on kilometre scale resolution over the Netherlands. In reality, conversion rates vary, depending on meteorological conditions and chemical regime, from day to day and from season to season. An improvement of the application of the chemical conversion rates from EMEP4NL in OPS could be established by differentiating them according to the meteorological classes in the OPS model, instead of using a constant value over the whole year. The same reasoning applies to the formation of particulate ammonium from ammonia.

Recommendations for model development for the individual ensemble members

The analysis of the results and discussions yielded model specific recommendations:

- For OPS we recommend to address the particulate matter formation conversion rates and subsequent wet removal efficiency (as explained above);
- For LOTOS we observed a lower dry and wet removal efficiency for (coarse) particles and we recommend to look into these aspects;
- For EMEP4NL we recommend to test the use of ECMWF meteorology and to incorporate an exchange module for arable land in line to that of OPS. Both aspects aim to improve consistency required for deriving the conversion rates to be used in OPS;
- For MATCH we recommend to look into the deposition efficiency above forests and the particulate ammonium formation;

- For SILAM we recommend to move away from the current approach for deposition and introduce a land use dependent scheme closer to those used in the other systems;

Recommendations for input data improvement and for model development for the ensemble as a whole

The differences between modelled and observed ammonia concentrations as well as the variability between the models is much larger for ammonia than it is for nitrogen dioxide (Figure 3).

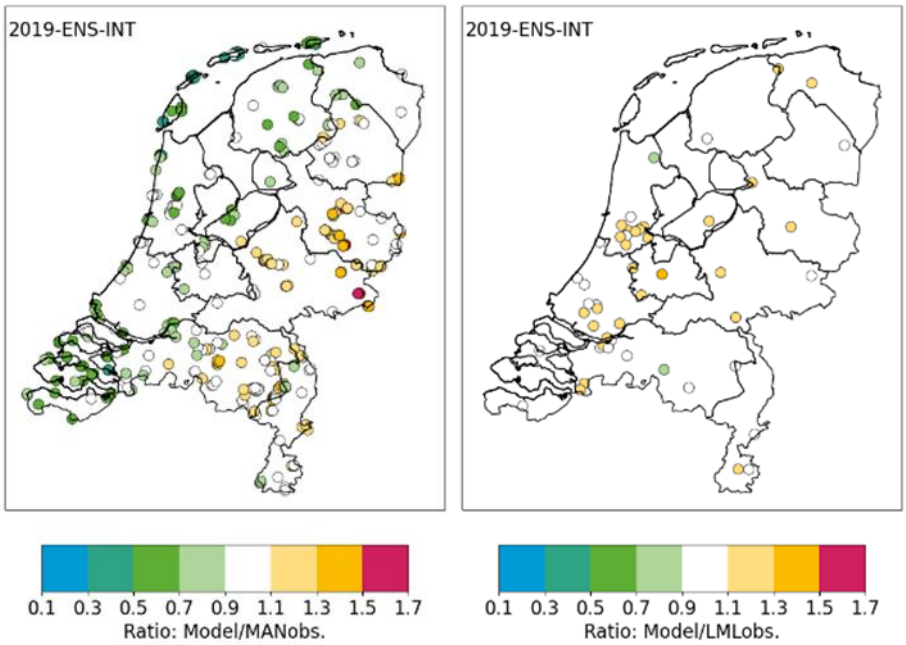

Figure 3: Left: ratio between modelled and observed ammonia concentration at locations of the MAN network. Right: Ratio between modelled and observed nitrogen dioxide concentrations at location of the LML-network.

We have identified that four models show a pattern in which annual mean ammonia concentrations in the western coastal provinces are underestimated and those in the eastern provinces overestimated. SILAM shows a systematic underestimation nationwide. The underestimation in the coastal provinces has been subject to discussions about the source contributions of ammonia from the sea and the underestimation is popularly called “Duinengat” (“Dune gap”) in the Netherlands, suggesting that the underestimation is limited to the Dune areas. The current study shows that the underestimation is also seen further inland, gradually turning into an overestimation by the models in the (south)eastern part of the country. Currently, an explanation for this underestimation in the west and overestimation in the east is lacking. However, we can conclude that this is not an OPS specific issue but a general feature.

Based on the current study (and previous experiences) we postulate that the underlying causes need to be sought in a number of directions. The common aspect in these directions of research is that they move away from using national scale assumptions that neglect regional variability towards detailing the spatiotemporal variability in the ammonia budget. Three directions of research are highlighted:

1. Detailing the regional variability in ammonia emissions for manure and fertilizer application. Instead of using a constant emission fraction for the whole country regional variability due to varying application practices, soil types, and soil characteristics should be introduced.
2. Detailing the temporal variability in ammonia emissions. The current practice assumes a single seasonal cycle in ammonia emissions across the country, whereas different crops and housing systems would induce variability within the country. Moreover, ammonia evaporation and its emissions are larger than average under fair weather conditions that are more often associated with south, southeasterly and easterly wind directions. First steps towards the detailing of the variability in ammonia emissions, largely based on German information, have shown a significant increase in model performance for ammonia (Ge et al., 2020; Ge, Schaap, Dammers, et al., 2023). We recommend to consolidate these efforts for the Dutch practice, and expand the methodology to incorporate managed grassland.
3. Detailing the role of agricultural land as a source and sink of ammonia. Arable land and pastures cover a large part of the Netherlands and are important for the nitrogen budget. Hence, the parameterization of exchange of ammonia for these areas impacts the travel distance of ammonia and the local to national reduced nitrogen budget. The coastal areas were shown to be sensitive to differences in transport distances. We recommend to expand the current efforts to measure ammonia dry deposition to natural ecosystems towards agricultural ecosystems and further develop modelling of ammonia exchange accordingly.

The preparation and execution on the benchmark study opens the possibility to track the impact of future developments in the national scale models. Moreover, it is possible to extend the effort by attracting more international modelling teams that bring international knowledge and experience to the Netherlands.

Closing remarks

This is the first national scale benchmark study of nitrogen deposition in the Netherlands. The model intercomparison showed that the national scale models developed (OPS, LOTOS) and applied (EMEP4NL) in the Netherlands are consistent with the current state of modelling practice in Europe. The ensemble proves to be an elegant way to quantify the uncertainty in modelled nitrogen deposition and pollutant concentrations. Based on the analysis presented here, we were able to give recommendations for model development of both the individual ensemble members as well as for the ensemble as a whole. We recommend to complement the benchmark with a recent year (2025) and to repeat the full intercomparison exercise 2 years from now as part of a structural quality assurance for policy modelling. Repeating the benchmark would also benefit from the current activities in expanding the LML network, and from activities in regional monitoring networks in agricultural areas. Moreover, the repetition allows for the incorporation of the advised model improvements and to further address the performance of the ensemble (mean) in comparison to a larger set of dry and wet deposition measurements.

Acknowledgement

Acknowledgement of the contribution of the partners

TNO is the main author of this report. TNO led the activity on the national scale benchmark for the duration of the project (2023-2025). TNO computed the LOTOS-EUROS simulations. TNO prepared and conducted the analysis of the benchmark results.

RIVM participated in the project throughout its entire duration. RIVM contributed to the definition of the benchmark protocol and provided the OPS-LT and EMEP4NL simulations. Additionally, RIVM contributed to the analysis and reviewed the report.

FMI and SMHI joined the project as external partners in 2024 and 2025. They computed SILAM and MATCH simulations, respectively. They contributed to the analysis and reviewed parts of the report.

Contents

Abbreviations

ABL	Atmospheric Boundary Layer
ACTM	Atmospheric Chemical Transport Model
AERIUS	Dutch calculation tool for nitrogen deposition (not an English acronym)
AQMEII	Air Quality Model Evaluation International Initiative
CAMx	Comprehensive Air Quality Model with Extensions
CAMS	Copernicus Atmosphere Monitoring Service
CBM-IV	Carbon Bond Mechanism IV (chemical mechanism)
CMAQ	Community Multiscale Air Quality model
COTAG	Continuous Ammonia Gradient (measurement network)
DEPAC	Deposition of Acidifying Compounds (dry deposition module)
ECMWF	European Centre for Medium-Range Weather Forecasts
EDGAR	Emissions Database for Global Atmospheric Research
EEA	European Environment Agency
EC	Elementary Carbon
EMEP	European Monitoring and Evaluation Programme
EMEP4NL	EMEP for the Netherlands (model configuration)
ENS-INT	International Ensemble (average of all five models)
ENS-NLD	Dutch Ensemble (average of the three Dutch models)
EQSAM	Equivalent Size Aerosol Model
ER	Dutch Pollutant Release and Transfer Register (Emissieregistratie)
EURODELTA	European Model Intercomparison Project
FMI	Finnish Meteorological Institute
FP7	Seventh Framework Programme (EU)
GFAS	Global Fire Assimilation System
GNFR	Gridded Nomenclature For Reporting (emission sectors)
HNO_2	Nitrous Acid
HNO_3	Nitric Acid
HTAP	Hemispheric Transport of Air Pollution
IFS	Integrated Forecasting System (ECMWF)
ISORROPIA	Aerosol thermodynamic equilibrium model
KNMI	Royal Netherlands Meteorological Institute
LAI	Leaf Area Index
LML	National Air Quality Monitoring Network (Netherlands)
LOTOS-EUROS	Long Term Ozone Simulation-European Operational Smog (model)
LRTAP	Long-range Transboundary Air Pollution (Convention)
MAN	Ammonia Monitoring Network in Nature Areas (Netherlands)
MATCH	Multi-scale Atmospheric Transport and Chemistry model
MEIC	Multi-resolution Emission Inventory for China

METPRO	Meterological Processor
MSC-W	Meteorological Synthesizing Centre-West
N_2	Nitrogen gas (molecular nitrogen)
N_2O_5	Dinitrogen pentoxide
NCP	North Sea Continental Platform
NCAR	National Center for Atmospheric Research
NCEP	National Centers for Environmental Prediction
NEC	National Emission Ceilings (Directive)
NH_3	Ammonia
NH_4^+	Ammonium
NH_x	Reduced nitrogen compounds (NH_3 + NH_4^+)
NMVOC	Non-Methane volatile organic compounds
NO	Nitric oxide
NO_2	Nitrogen dioxide
NO_x	Nitrogen oxides (NO + NO_2)
NO_y	Oxidized nitrogen compounds (NO + NO_2 + HNO_3 + pNO_3^- + HNO_2 + PAN + ...)
O_3	Ozone
OPS	Operational Priority Substances (model)
OSPARII	Oslo-Paris Convention Area II
PAN	Peroxyacetyl nitrate
PAR	Photosynthetically Active Radiation
PBL	Planetary Boundary Layer
PM	Particulate Matter
PM10	Particulate Matter <10 micrometers
PM2.5	Particulate Matter <2.5 micrometers
pNH_4^+	Particulate NH_4^+ (ammonium) i.e. in aerosol form
pNO_3^-	Particulate NO_3^- (nitrate) i.e. in aerosol form
PPM	Primary Particulate Matter
RIVM	National Institute for Public Health and the Environment (Netherlands)
RMSE	Root Mean Square Error
SIA	Secondary Inorganic Aerosol
SILAM	System for Integrated modeLling of Atmospheric coMposition
SMHI	Swedish Meteorological and Hydrological Institute
SO2	Sulfur dioxide
SOA	Secondary Organic Aerosol
TNO	Netherlands Organisation for Applied Scientific Research
UAT	Uncertainty Assessment Tool
UNECE	United Nations Economic Commission for Europe
US EPA	U.S. Environmental Protection Agency
VOC	Volatile Organic Compound
VMM	Flanders Environment Agency (Vlaamse Milieumaatschappij)
VLOPS	Flemish Air Research and Planning System (Vlaamse Lucht Onderzoeks- en PlanningSysteem)

VPD	Vapor Pressure Deficit
WRF	Weather Research and Forecasting (model)

1 Introduction

1.1 Motivation

The government of the Netherlands strives for a transparent and scientific sound basis of the national nitrogen policy. Dutch policy support activities build on a combination of measurements and modelling (Hoogerbrugge et al., 2020) The chemistry transport model (CTM) OPS is currently used for providing national scale assessments on nitrogen deposition. These assessments include the provision of deposition maps across the Netherlands, the quantification of the source sectors responsible for the deposition, and impact analyses of proposed mitigation strategies. As such these regional modelling efforts play a key role in informing all stakeholders in the societal debate concerning nitrogen deposition.

Modelling the fate of ammonia and nitrogen oxides in the atmosphere is a complicated task. The chemistry transport models (CTMs) used for this task aim to account for all relevant physical process descriptions in a balanced way to explain observed concentration and deposition levels and the sensitivity to changing emissions and weather conditions as good as possible. The available models differ in the level of detail in which the processes are described, the targeted scale and resolution, and the degree in which they are operationally applied. Given the policy context in which CTMs are often applied, an assessment of the quality of the modelling outcomes has been an important concern (e.g., Fox, D.G., 1984; Uusitalo et al., 2015).

Model evaluation has always been a major aspect of air quality modelling (Fox, D.G., 1984). Nowadays, model evaluation comprises a number of activities to answer questions like:

- Are we getting the right answers?
- Are we getting right answers for right (or wrong) reasons?
- Can we capture observed changes in concentration or deposition levels due to meteorological variability or emission changes?
- What is our confidence in the model predictions?
- Can we identify which improvements in process descriptions and input data are required?

The regional scale modelling community adopted a model evaluation framework to try to answer these questions as outlined by Dennis et al. (2010). In this framework the activities are grouped in operational, diagnostic, dynamic and probabilistic evaluation techniques.

Operational evaluation

In the operational evaluation the concentrations and deposition fluxes are compared to observations to obtain a quantitative insight in the (spatially and temporally varying) prediction errors or biases. For this process a number of standard statistical parameters is usually calculated for a large set of (standard) observations. As the operational evaluation is rather straightforward, it is often used to assess the performance of each new model version in the development and application of a CTM. Many modelling teams use a fixed protocol (period, domain, input data configuration, measurement data set, etc.) to track the model performance of individual development steps, a so-called benchmark. For example, the modelling team at TNO evaluates (new) LOTOS-EUROS versions against observations for two meteorological years (Manders et al., 2017). Every 4-5 years the older benchmark year is

exchanged for a recent year to be able to include new developments in observation and input data.

Previously performed studies, and the lessons learned from them, illustrate the usefulness of benchmarking exercises. Figure 4 (left) provides an example of a benchmark for modelled total nitrogen deposition in Germany, using the LOTOS-EUROS model. In this case the benchmark of a new model version was performed by excluding 9 updates in model descriptions one by one. The modelled mean total deposition over Germany was found to be very insensitive to the changes in model parametrizations. In Figure 4 (right), the change in the modelled NH_x-deposition distribution across the country is shown, by the exclusion of the compensation point.

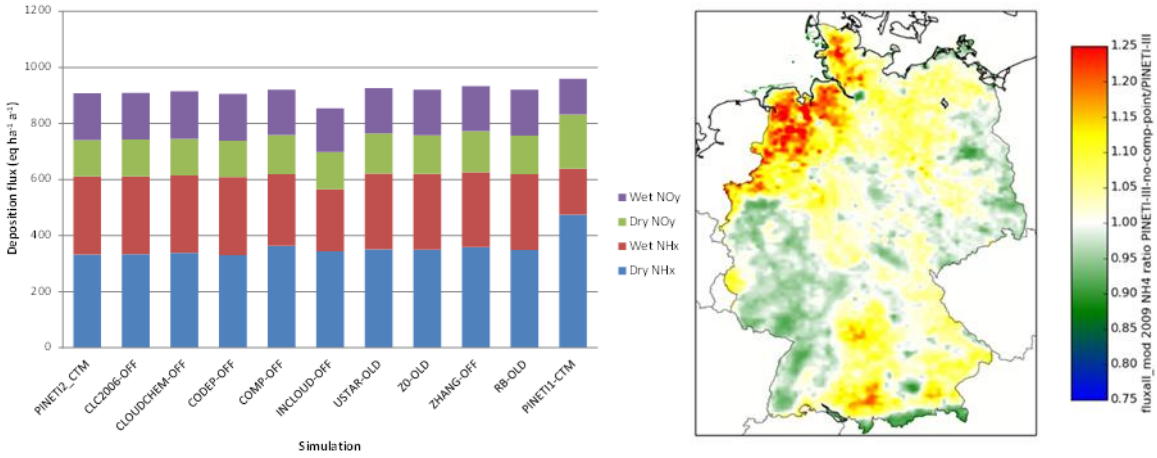

Figure 4: Left: Modelled total deposition averaged across Germany using the PINETI-2 version of LOTOS-EUROS as well as 9 development steps turned off. The PINETI-1 simulation excludes all development steps. Right: The fractional impact on total reduced nitrogen deposition by turning the compensation point in LOTOS-EUROS off (COMP-OFF) (Schaap et al., 2017).

The exclusion of the compensation point leads to an increased deposition in source regions. Thereby, it causes a decreased transport away from the source regions and a lower amount of ammonia deposition further downwind. This may be counterintuitive, as the exclusion of the compensation points causes the effective ammonia deposition velocity to be increased everywhere. Although the impact on the national mean (~4 %) is small, the regional patterns in N-deposition may change by -15 % to + 25 %. The latter are visible across regions with a similar size as the Netherlands. Furthermore, using this approach causes a shift between modelled wet and dry deposition. This example illustrates that modelling nitrogen deposition is a net zero game. As long as the emissions are considered constant, the mean total deposition across a large area hardly changes, although significant differences in the spatial distribution with the region and in the division between wet and dry deposition as well as between different land use types may occur. Hence, for the documentation of model developments and the comparison of different model systems, the choice of variables to investigate should encompass the spatial distributions across the Netherlands and the separate (land use specific) dry and wet deposition fluxes.

Currently, a benchmark protocol to track the impact of the model developments on the behaviour and performance of a model system within the national knowledge program on nitrogen (NKS) does not exist. ***The development of a benchmark protocol is needed to make evaluation results from different model systems and model versions comparable. Repeating the benchmark exercise makes it transparent and traceable which***

(combination of) development steps have caused specific changes in the model outcomes and performance.

Diagnostic and dynamic evaluation

More in-depth studies using diagnostic and dynamic evaluations demand much more effort to carry out and are only performed occasionally. Diagnostic evaluations are performed to diagnose the reasons behind good and bad model performances and often involve more detailed process-oriented measurement campaigns. Within NKS diagnostic model evaluation is applied by comparing calculated ammonia dry deposition using several parametrizations to novel dry deposition flux measurements (Jongenelen et al., 2025). Dynamic evaluations assess the ability of a model to reproduce the impact of emission reductions or meteorological variability. For example, Mues et al. (2012) addressed the ability of model systems to reproduce air pollution levels during the summer of 2003, which was exceptionally hot in large parts of Europe, whereas Stern et al. (2008) showed general difficulties of capturing pollutant distributions during very stagnant conditions. Recently, the ability to reproduce nonlinear behaviour observed in concentration and deposition trends across Europe were addressed (Banzhaf et al., 2015; Colette et al., 2017; R. J. Wichink Kruit et al., 2017). In addition to the traditional model evaluation strategies, a new perspective on assessing model performances is offered through comparison with satellite data. This topic is addressed in a parallel activity (NKS SAGEN-WP3) focused on the demonstration of satellite data applications, including important aspects of dynamic evaluation based on a long-term simulation and a focus of using dynamic ammonia emissions.

Probabilistic evaluation techniques

The quantification of the uncertainty range of model results and the identification of the most important factors contributing to this range is addressed in probabilistic model evaluation. The approaches include the well-known Monte-Carlo techniques in which a large number of simulations is performed to quantify the uncertainty induced by parameter settings or parameterizations. Within NKS the Monte-Carlo technique is applied to OPS in the uncertainty assessment tool (UAT). The application of the technique is feasible for OPS due to its highly parameterized nature and modest computational requirements. For most chemistry transport models the Monte Carlo approach is not feasible as the number of parameters and process descriptions to assess and the required computational demands are simply too large.

Nowadays probabilistic model evaluation is often performed through model comparison studies. The first European model intercomparison was launched within EUROTRAC-GLOREAM (Hass et al., 1997), which was extended into the review of the EMEP model in 2004 (Van Loon et al., 2004). The EMEP model is the central modelling system which is used within the UNECE-CLRTP convention and within the policy support activities for the European air quality policies such as the NEC-directive. The first operational evaluation studies were the basis of the CITYDELTA and EURODELTA-I and II studies, in which the consistency of responses to emission changes of the EMEP model in comparison to those of 6 other European systems was studied (Thunis et al., 2008; Van Loon et al., 2007). These exercises have increased the interaction between modelling teams through discussions and exchange of experiences and have contributed to the detection of model flaws and subsequent improvement.

Above mentioned model intercomparison studies as well as those organized within the Air Quality Modelling Evaluation International Initiative (AQMEII; Im et al., 2015a, 2015b) facilitated the development of ensemble approaches. *It was demonstrated that a model ensemble generally provides a better performance in comparison to observations (e.g.*

Vautard et al., 2009) *than the performance of each ensemble member.* Most studies have simply generated the ensemble model by taking the mean or median model at every location and time (based on hourly or daily time series). This recognition has led to the development of the regional ensemble within the Copernicus Atmosphere Monitoring Service (CAMS) (Marécal et al., 2015).

Few studies have compared N and S wet deposition estimated by regional and global CTMs with observed values in Europe, giving varying results (Dentener et al., 2006; Simpson et al., 2006, 2014; Vivanco et al., 2017, 2018). Compiling the results of these studies shows that model bias for wet deposition of oxidized nitrogen ranges from −86 % to +72 % of the average of the observed values with a median bias of −19 %. Model bias for wet deposition of reduced nitrogen ranges from −58 % to +21 % of the average of the observed values with a median bias of −20 %. The reason for the large deviation between the models is the complexity of the processes involved and the fact that quite a few models are not used for deposition assessment purposes. The only model intercomparison performed with OPS-like models for deposition is documented by Dore et al. (2015) for the UK. These authors compared the simpler UK FRAME and HARM models against Eulerian models (e.g. EMEP, EMEP4UK and CMAQ). They concluded that the simpler models performed well for NH_3, SO_2 and NO_x concentrations, and that the more complex models performed better for secondary components such as aerosol concentrations. Similar conclusions were drawn from the comparison between OPS-LT and LOTOS-EUROS (van der Swaluw et al., 2017), and OPS-LT and EMEP4NL (Van Der Swaluw et al., 2021). National nitrogen deposition estimates for the UK varied by 22–36 %. At a local scale estimates of both dry and wet deposition for individual 5 km × 5 km model grid squares were found to vary much more.

The past experience shows that model systems have their own strengths and weaknesses and that it is to be expected that different models show the best performance on different aspects. It is this variability that leads to a better performance of the ensemble model in air quality forecasting and analysis. Moreover, using an ensemble of models provides a way to assess the confidence or uncertainty in the model results and facilitates the identification of development steps for the participating models. Hence, by learning from each other the improvement of the model systems is sped up. A model intercomparison and evaluation of an ensemble of models does not exist for the Netherlands or the OPS-LT model. ***By performing a full benchmark, this study extends earlier work aimed at the comparison of two models to a broader scope, by taking into account a larger number of models, by using a common basis regarding emissions, by performing simulations at higher resolution and by evaluating more parameters.***

1.2 Objectives

The central objectives of this study were 1) to give insight in the robustness of the regional scale modelling of nitrogen deposition relevant to policy making and 2) to foster model improvement relevant to policy making by benchmarking the OPS model with an ensemble of modelling systems. The objectives are met by obtaining the following intermediate results:

1. A benchmark test using 5 national scale models with a focus on:
   a) Deposition of reduced and oxidized nitrogen compounds
   b) Concentration of reduced and oxidized nitrogen compounds
   c.) Source attribution for domestic and international sectors to nitrogen deposition
2. An evaluation of the information provided by the ensemble model and its spread
3. An assessment of the differences between OPS and the ensemble members;

4. Recommendations for input data improvement and for model development for the individual ensemble members and the ensemble as a whole.

1.3 Overall approach and reading guide

The benchmark study performed here includes five modelling systems. Besides the OPS model, we used the LOTOS-EUROS and EMEP4NL model systems as they are developed (LOTOS-EUROS) and applied (LOTOS-EUROS and EMEP4NL) at Dutch institutes. These three models were complemented by two international models. Invitations for participation were sent out based on a review of modelling systems and their application for nitrogen deposition. Two teams responded positively and the models MATCH and SILAM were added to the ensemble.

Chapter 2 provides a short overview on the atmospheric nitrogen budget. The main nitrogen components and relevant processes governing the transport, transformation and removal of nitrogen compounds are introduced. This chapter was added to guide non-experts into the topic of modelling nitrogen deposition.

Chapter 3 describes the participating models and the model simulations requested to all models in more detail. Furthermore, it outlines the methodologies used to analyse the results and generate the ensemble.

In chapter 4 the main results of the model intercomparison are provided. The presentation of the results starts with those for total nitrogen deposition, after which the variability in results is explained by the NH_x and NO_y dry and wet deposition fluxes and air concentrations. Where possible, comparison to in-situ observations from the different monitoring networks in the Netherlands (LML, MAN, COTAG) is provided. The main focus is on the comparisons on an annual basis (concentration means or deposition totals), although some attention is given to the evaluation of modelled time series. For quantities for which observations are sparse or lacking, such as the dry deposition fluxes or source attribution, the results are mainly based on model-to-model comparisons to identify the uncertainty envelope around the central Dutch values. The ensemble model was integrated in the analyses and the ensemble spread is given specific attention as a measure of uncertainty.

The final chapter synthesizes the lessons learned and provides recommendations for improvement for individual systems and the ensemble as a whole.

2 Overview of atmospheric reactive nitrogen budget

This chapter can guide non-experts into the topic of modelling nitrogen deposition. It provides a short overview on the atmospheric nitrogen budget. The main nitrogen components and relevant processes governing the transport, transformation and removal of nitrogen compounds are introduced.

2.1 Nitrogen compounds

Non-reactive nitrogen gas (N_2) makes up 78 % of our atmosphere. Additionally, nitrogen is present in the atmosphere in the form of reactive nitrogen (Nr) compounds, which are all nitrogen compounds directly and indirectly used for plant growth. Excessive anthropogenic emissions harm ecosystems through acidification and eutrophication. Anthropogenic reactive nitrogen emissions occur mainly in the form of nitric oxides (mainly NO and to a lesser extend NO_2) and in the form of ammonia (NH_3). These nitrogen compounds enter chemical reactions in the atmosphere, resulting in nitrogen-containing reaction products. These reaction products can be either in the form of gas or particulate matter. The reaction products are called secondary compounds, while substances emitted at the source are primary compounds. The primary nitrogen oxides are often grouped as NO_x ($NO_x = NO + NO_2$).

When speaking of the deposition of reduced (NH_x) or oxidized (NO_y) nitrogen, the sum of nitrogen deposition of all components in the respective group is referred to:

NH_x = main group of reduced nitrogen = $NH_3 + pNH_4^+$

NO_y = main group of nitrogen oxides = $NO + NO_2 + HNO_3 + pNO_3^- + HNO_2 + PAN + ...$

Since the weights of the different molecules differ, this summation should be done only in ‘moles’ or (kilo)grams of the element nitrogen (N). In chemistry, the mole is the unit for the quantity of molecules and is often referred to as equivalents in deposition research. Throughout the report we will report deposition in terms of these groups of species.

Below, we provide a short overview of the atmospheric nitrogen budget (Figure 5). For a more complete overview we refer to TNO (2024). The atmospheric nitrogen budget involves emission, dispersion, chemical transformation and deposition processes for all relevant reactive nitrogen compounds. Deposition processes are separated in dry and wet deposition. Dry deposition refers to the deposition of gaseous and aerosol species on the Earth’s surface. Wet deposition in turn refers to the removal of species caused by precipitation. All these processes takes place under variable meteorological conditions and depend in factors like land use. Hence, the atmospheric nitrogen budget is a complex system to understand and model. In this chapter we provide a short introduction to the topic.

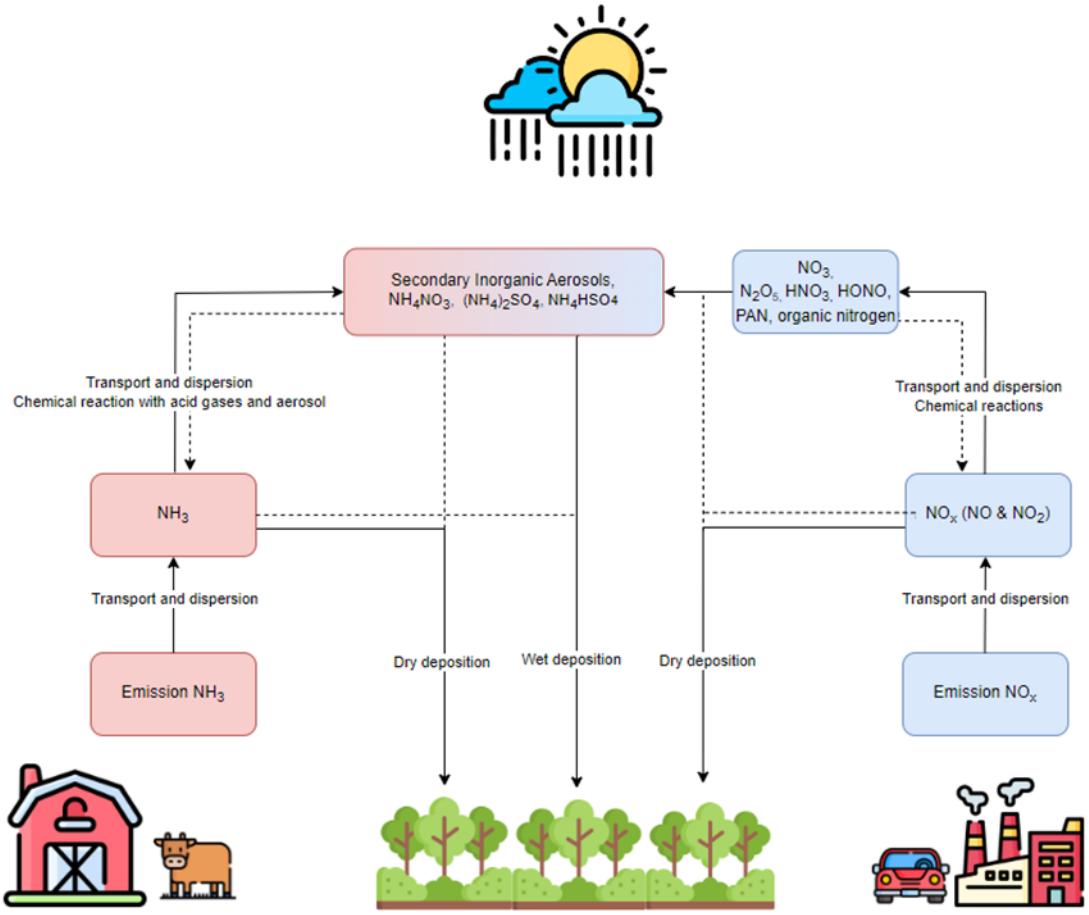

Figure 5: Schematic overview of the atmospheric budget of reactive nitrogen compounds as driven by emission of ammonia (NH_3) and nitrogen oxides (NO_x).

2.2 Sources

Ammonia is one of the most important sources of reactive nitrogen in the atmosphere. The emission of ammonia has risen on a global scale substantially during the twentieth century subsequently to population growth and the demand for food (Erisman et al., 2008). The most dominant source of ammonia emissions into the atmosphere is agriculture, accounting for more than 90 % of the emission total in the EU (Sintermann et al., 2012). Ammonia emissions from livestock housing, manure in storage systems, and manure and fertilizer application to fields, form the largest part of the total agricultural emissions at the European scale (De Vries et al., 2011; Leip et al., 2015). Other emissions are originating from traffic and road transport (less than 2 %) (EEA, 2017) and minor sources such as food processing and, biomass burning, (circa 4 %) (Erisman et al., 2008; Galloway et al., 2003; Krupa, 2003).

The dominant source of nitrogen oxides (NO_x) is fossil-fuel combustion, which takes place in many sectors such as traffic, shipping, agriculture, industry and energy production. Natural sources are rather limited, but can be substantial in the case of biomass burning (Seinfeld & Pandis, 2006). Moreover, NO is released from manured soils which means that agriculture is also a source of NO_x. The same processes also takes place in natural soils leading to a small natural biogenic emission over land. NO_x is mainly emitted as NO to the atmosphere, only a

small fraction is emitted as NO_2. In the atmosphere NO and NO_2 form an equilibrium with ozone under the influence of radiation.

In the chapter on the benchmark protocol the emission situation for the Netherlands and surrounding is elaborated. Detailed insights in emissions are provided in emission inventories, a key input for subsequent chemistry transport modelling to address the fate of the released pollutants.

2.3 Dispersion

The dispersion of reactive nitrogen compounds is described by turbulent (horizontal and vertical) mixing and advection (or transport) by wind. Dispersion thus relates the emission of a pollutant to its concentration distribution in the air. As nitrogen compounds are emitted in a dynamic atmosphere, and not in a static system, their dispersion changes with meteorological conditions.

Two thirds of the emissions of nitrogen oxides (NO_x) and almost all emissions of ammonia (NH_3) are emitted within a few meters of the ground and thus into the ‘planetary boundary layer’, also known as the ‘atmospheric boundary layer’. This is the lower atmospheric layer, in contact with an directly influenced by the earth’s surface. The height of the boundary layer is variable and determined by the amount of convective and turbulent forces. The behaviour of the boundary layer follows a diurnal cycle. At night, the height of the boundary layer is generally low. After sunrise, solar radiation warms the Earth's surface, which in turn warms the air above it. The warmer air starts rising and the air gradually starts mixing, causing the ‘mixed layer’ to gradually grow until the late afternoon. At the top of the mixed layer, a so-called ‘capping inversion’ develops. Here, the temperature gradient reverses and temperature rises with altitude, preventing air from rising higher. As the sun descends, the intensity of sunlight (per square meter) decreases. As a result, the surface heat fluxes drop and ultimately cools the lower air layer. As the result, the height of the mixed layer drops very rapidly, it ‘collapses’. During the day, the mixed layer is 500 to 1500 meters high, while at night it is much lower: usually 50 to 300 meters.

Pollutants are usually dispersed within the atmospheric boundary layer. As the top of the mixed layer acts as a ‘cap’ or ‘lid’, pollutant concentrations are contained within the boundary layer. Imagining an emission source within the mixing layer being constant over time, a pollutant’s concentration is higher during the night, as the mixing volume is significantly smaller due to the low mixing layer. Note that the term mixing layer can be misleading in this regard, since especially in nighttime conditions the air might not be mixed at all. During the day, when the mixing layer is high, the larger volume of air dilutes the pollutant’s concentration.

From their source, nitrogen compounds disperse in the form of plumes. Plumes, depending on the height of their source, are emitted into or above the atmospheric boundary layer. Only plumes within this mixed layer can lead to deposition at a short distance from the source, depending on meteorological conditions and the plume height. Plumes above the mixed layer will normally be transported far away. The latter occurs when emissions take place at large heights, such as emissions from air planes and stacks of industrial facilities and powerplant, or when the mixing layer is shallow. The latter tends to occur at night throughout the year and occasionally during the daytime in stagnant conditions in the winter. Still, the majority of emissions are within the atmospheric boundary layer. The direction in which the plume moves is determined by the prevailing wind direction. The amount and character of turbulence induced by momentum exchange with, and heating

from the earth's surface determine with what amplitude the plume will meander: in other words, how quickly the plume will widen and rise with distance from the source.

Different types of models are relevant to describe the dispersion process. A snapshot of a plume shows a complex pattern of varying concentrations due to the chaotic movements of air vortices. When one averages these snapshots over an hour, the result is a so-called Gaussian plume. The "Gaussian plume model" is a widely used mathematical and statistical approach to modelling a plume. It is the basis of many local scale atmospheric dispersion models. Plume models assume hourly-averaged meteorology. Therefore, the range of validity of plume models, from the source of emission to the modelled concentration location, is about 20 kilometers. Long range dispersion can be addressed with “Lagrangian trajectory models” or “Eulerian grid models”.

2.4 Chemistry

In the atmosphere the primary pollutants are transformed by a large number of reactions. These chemical conversions describe the process where primary species or ‘reactants’ are (partially) transformed into secondary species or ‘products’. In turn, these products can engage in further chemical conversions leading to further products. After the emission of ammonia (NH_3) and nitric oxide (NO) and during the dispersion of these compounds, chemical conversions take place in the atmosphere. Atmospheric chemical reactions are often referred to as multiphase reactions. They can occur in the gas, liquid or solid phase.

Ammonia mainly reacts in two manners. It dissolves in water droplets, and it converses to ammonium in particulate matter. To do the latter, ammonia, as the most abundant base in the atmosphere, reacts with an acid, forming for example ammonium nitrate (NH_4NO_3) or ammonium sulfate ($(NH_4)_2SO_4$).

For nitrogen oxides, the main chemical conversions after emission can be described in four steps:

1. Rapid conversion of NO to NO_2 immediately after emission, by reaction with ozone (O_3).
2. The settling of the photochemical balance between NO and NO_2.
3. The conversion of NO_2 to nitric acid (HNO_3) during day time and night time reaction pathways and small amounts of reservoir substances such as peroxy acetyl nitrate (PAN).
4. The conversion of HNO_3 into nitrate (pNO_3^-) in particulate matter.

These chemical conversions are schematically illustrated in Figure 6.

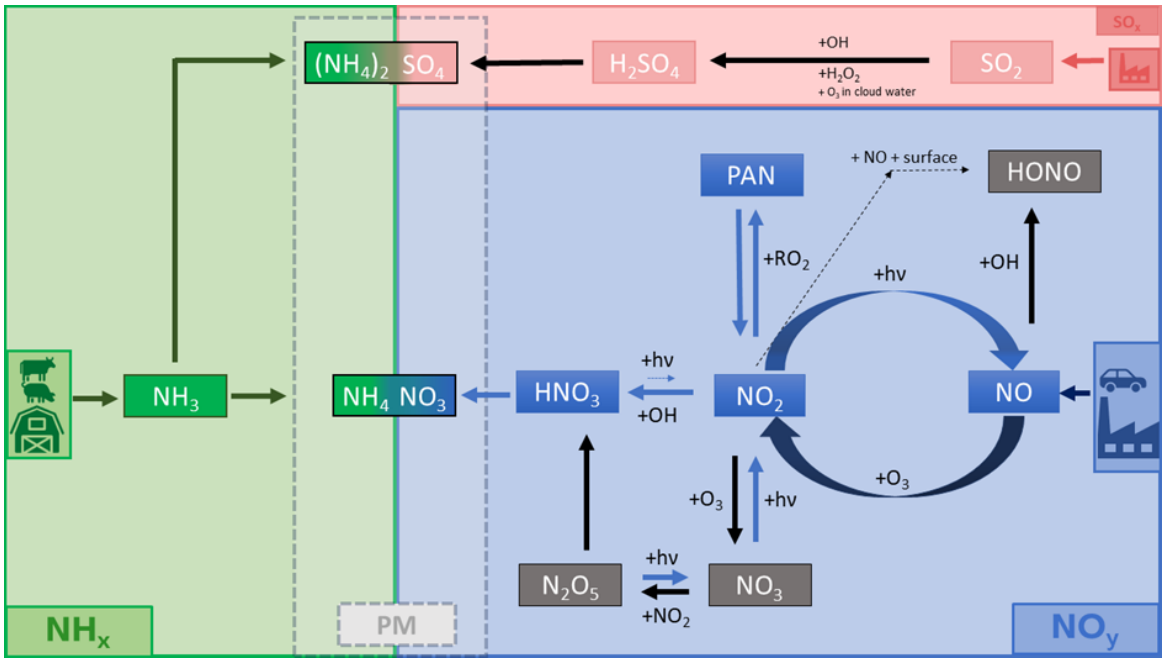

Figure 6: A simplified overview of the important chemical conversions related to atmospheric reactive nitrogen. Processes that take place during the day are highlighted with light blue arrows. 'hv' represents solar radiation.

Especially the chemistry involving steps 3 and 4 is complex and the oxidation of NO_x can lead to the formation of many other oxides of nitrogen. Though NO_2 can be directly removed from the atmosphere by dry deposition, it is mainly transformed into nitric acid (HNO_3) when it reacts with OH radicals during daytime. During nighttime, nitric acid is formed though a mechanism involving N_2O_5, which is formed out of NO_2 and ozone. HNO_3 usually has a short lifetime since it reacts fast with NH_3 to form new fine aerosol compounds (NH_4NO_3), it sticks to the surface (deposition), or forms a new coarse compound ($NaNO_3$) in reaction with sea salt aerosols (NaCl). Nitrate containing aerosols are mostly removed from the atmosphere by wet deposition (Hov et al., 1994; Wall et al., 1988).

Besides the main products described above a number of compounds play a minor role in the atmospheric nitrogen budget of polluted regions, such as western Europe. These involve the formation of nitrous acid (HNO_2), peroxy acetyl nitrates (PAN) and other organic nitrogen compounds. We refer to atmospheric chemistry textbooks for a complete overview of the chemistry involved.

2.5 Deposition

Nitrogen deposition is the removal of nitrogen compounds from the atmosphere to the Earth's surface. The earth's surface includes the soil, water surfaces and vegetation, and combinations of those. In general, there are three deposition pathways:

1. **Wet deposition** refers to the amount of nitrogen compounds removed from the atmosphere by rain, snow or hail.
2. **Dry deposition** refers to the amount of nitrogen compounds removed from the atmosphere at the Earth's surface by direct uptake or other surface removal processes.
3. **Occult deposition** refers to the amount of nitrogen compounds removed from the atmosphere at the Earth's surface, through direct interception of cloud or fog droplets at the surface, i.e. when clouds touch mountain ranges. This process is hardly relevant for the Netherlands.

Wet deposition depends on precipitation frequency and quantity. Over time, frequent light rains will remove more nitrogen than a heavy rain event for the same total volume of water. After all, substances cannot be removed by rain when there is no rain. In the Netherlands, statistically and on average, it rains about 10 % of the time at any specified location. However, significant rainfall only occurs on about a third of the days in a year. Therefore, hypothetically, well-soluble substances could be washed out once every three days. However, the duration of dry periods ranges from hours to weeks. This means that substances that are primarily wet deposited, such as PM, can be transported by the wind for many days. Gases that are not soluble in water such as nitrogen monoxide (NO) and nitrogen dioxide (NO2) are not scavenged by the rain and are also transported over larger distances.

Wet deposition is often split into in-cloud scavenging (or 'rainout'), and below-cloud scavenging (or 'washout') (Seinfeld & Pandis, 2006). Gaseous pollutants may dissolve into and evaporate from cloud water and precipitation, depending on the water solubility of the gas. Particulate pollutants collide with cloud and rain droplets, or serve as nuclei for condensation of water, thereby forming new droplets. The removal efficiency regarding the wet deposition of particles is mainly governed by the size of the particles. Coarse mode particulate matter is more effectively scavenged than fine mode particulate matter.

Dry deposition refers to the direct removal of a gas or particle at the surface from the atmosphere, without the intervention of precipitation. Dry deposition occurs continuously. It is governed by the concentration of a gas or particle in air and the vertical transport to the surface, mainly by turbulent motions, and subsequent removal at the surface.

Figure 7 describes three processes that control the dry deposition velocity. The first process that governs this velocity is the rate at which gases and particles are transported from a given height to the surface by vertical turbulent transport ('Process 1'). The second process is the rate of diffusion of the gas or particle through a thin layer of stagnant air directly at the surface ('Process 2'). The third process governing this velocity is the rate at which gases and particles are taken up by the vegetation or the surface ('Process 3').

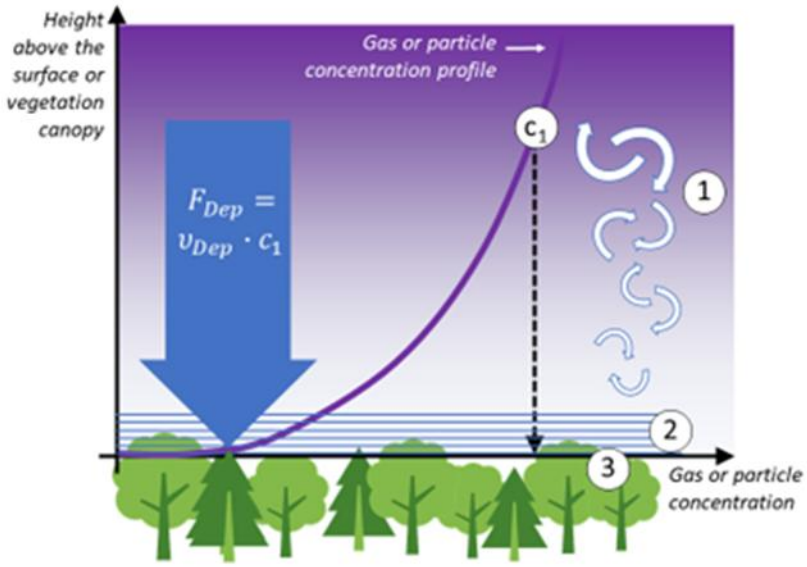

Figure 7: The dry deposition flux (FDep) of gases or particles, as driven by the deposition velocity (vDep) multiplied by the gas or particle concentration at a certain height (c1). Processes 1, 2 and 3 govern the deposition velocity.

In turn, this uptake at the surface is governed by several mechanisms. For example, plant leaves can take up water soluble gases in the same way they take up carbon dioxide (CO_2) for their photosynthesis through the stomata (small pores) in the leaves' skin. Other examples are water soluble gases such as ammonia (NH_3) or nitric acid (HNO_3) that stick to many surfaces, including leaves, branches, soils and artificial surfaces.

While the three described processes define the dry deposition velocity, the contributions of each of the three processes depends on many variables: on weather conditions, particle size, reactivity and water solubility of the gases, and the type of surface absorbing the gas or particle. Typical dry deposition velocities vary widely among nitrogen compounds and different land use types. For example, the dry deposition rates of HNO_3 and NH_3 are many times larger than those of low soluble nitrogen compounds (e.g. NO_2). For all compounds, dry deposition velocities (or fluxes) are lower on surfaces with low roughness, such as grass, than on surfaces with high roughness, such as forests. Due to leaf fall in winter, the dry deposition velocities (or fluxes) on a deciduous forest is lower than on a pine forest. Furthermore, some components (e.g. NH_3) can evaporate from the surface again, making the exchange with the surface bidirectional. Accounting for the bidirectional exchange is important for the calculation of the total nitrogen deposition. The air concentration at which no net exchange occurs is called the compensation point.

The dry deposition flux (*FDep*) is calculated as the product of a deposition velocity (*vDep*) and the concentration difference between the atmosphere and the surface (c1) (see Figure 8). The deposition velocity is mostly parametrized following an electrical analogy of a network of resistances. Each process determining the dry deposition route is represented by a resistance (i.e. resistance *against* deposition). These include the aerodynamic resistance (for process 1), the quasi laminar layer resistance (for process 2) and the surface resistance (for process 3). The reciprocal value of the total resistance of all these (often parallel) routes is used as the deposition velocity. More sophisticated schemes use compensation points, allowing the routes to be bidirectional (accounting for possible emissions from the surface).

One of such ‘surface-atmosphere exchange’ modules is the DEPAC module used in OPS and LOTOS-EUROS.

Figure 8 shows the modelled contributions to the total nitrogen deposition in the Netherlands. The relative importance of the dry and wet deposition contributions is about 2 to 1. Thus in a country with a high emission density such as the Netherlands, the dry deposition flux accounts for the majority of the total deposition. Unfortunately, few datasets with reliable dry deposition flux measurements of nitrogen components exist. Hence, the process description is highly parametrized and is performed for a small number of very broad vegetation classes, such as deciduous forest, grasslands and semi-natural vegetation.

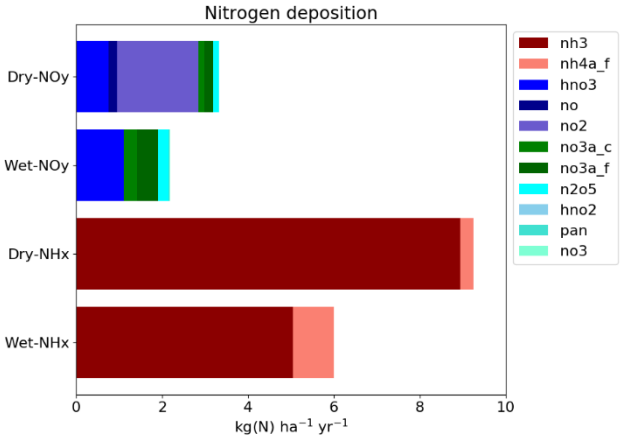

Figure 8: Contribution of the components to the modelled dry and wet deposition of oxidized and reduced nitrogen for the Netherlands.

2.6 Closing remarks

To arrive at a good understanding of the nitrogen budget and inform policy makers on the current situation and the effectiveness of potential policies, models have been developed to describe the atmospheric nitrogen budget and the relevant processes in variable degrees of complexity. These models are the focus of the current study.

3 Methodology

In this chapter, the participating models and the benchmark model simulations requested to all models are described. Furthermore, it outlines the methodologies used to analyse the results and generate the ensemble mean.

3.1 Participating models

Before introducing the models, it is important to understand a key difference between two modelling approaches, i.e. Lagrangian and Eulerian models. The fundamental difference between the Lagrangian and the Eulerian approach is the frame of reference. Lagrangian models follow individual parcels of air. Hence, they simulate the changes in the chemical composition of a given air parcel as it moves through space and time. Eulerian models perform model calculations on a fixed grid as time passes.

The OPS model is a combination of a Lagrangian system and a Gaussian plume model. In the Lagrangian approach, there is no mass exchange between the air parcels that are followed and their surroundings, other than emissions and deposition fluxes that are allowed to enter and leave, respectively. As the parcels constantly move, concentrations are simulated at different locations at different times. The advantage of the model is that it is relatively fast, enabling to perform many simulations in a short time, and that it explicitly calculates source-receptor relationships. A major advantage is that the resolution obtained with the calculations can be very high and that source receptor relations are simple to calculate. The disadvantage is that not all reactive nitrogen compounds are accounted for explicitly and that (chemistry) processes important for long range transport are simplified. This results for example in larger mismatches between modelled and measured concentrations of particulate nitrogen compounds compared to other systems (Dore et al., 2015b; van der Swaluw et al., 2017). In addition, the modelled annual mean concentration levels hamper the exploitation of hourly and daily observations to quantify model performance and diagnose deficiencies.

Internationally, Gaussian plume models (e.g., OPS, FRAME, AERMOD, IFDM, OML, etc.) are often used for local scale calculations, as these calculations generally need a high spatial resolution. For larger, regional scales, Eulerian models are more commonly used. The OPS model (similar to the FRAME model in the UK; https://www.pollutantdeposition.ceh.ac.uk/frame) is quite unique in the sense that it is also used in a Lagrangian approach (following the plumes in different wind directions) to calculate the air quality and nitrogen deposition on a (small) regional scale, typically at a country level. As the FRAME model is no longer maintained by CEH (UK), this benchmark study of OPS can only be performed using Eulerian modelling systems.

Eulerian models describe the concentration and deposition on a fixed grid. In the Eulerian approach, species enter and leave through the walls of these cells. The model simulates the species concentrations at all locations as a function of time. The equations of the model include all important atmospheric processes: advection, dispersion, emissions, reactions, and deposition. Eulerian grid models accommodate more detailed process descriptions than in

Lagrangian models and are internationally used for studying regional scale air quality. The advantage is that long range transport and chemical transformations are described in more detail and that the hour-by-hour calculations on the 3D regular grid allow direct comparison to observed time series from in-situ measurements and remote sensing instruments. The disadvantage is that the computation time is relatively large and the resolution is at least 1x1 km^2.

In the Netherlands, TNO develops the Eulerian LOTOS-EUROS model system. Furthermore, the Eulerian EMEP4NL system is applied at RIVM. Both models are included in the ensemble of the present study. To expand the ensemble to 5 models, an overview of international models was made (as presented in Appendix A). To attract interest an open invitation was sent to modelling groups in Europe. Three teams reacted positively: SILAM, MATCH and MINNI. The first two were able to deliver the results in time for this report.

In conclusion, the five modelling systems in this study are OPS-LT, LOTOS-EUROS, EMEP4NL, MATCH and SILAM. A short description of these models is provided next.

OPS-LT (Short: OPS) is the long-term version of the Operational Priority Substances (OPS-LT) model, which has been developed at RIVM to assess the present state and trends of the concentration and deposition within the Netherlands of pollutants like NH_3, NO_x, SO_2 and particulate matter. Official background maps of these quantities, based on computations with OPS-LT, are provided annually (e.g. Hoogerbrugge et al., 2022) and an outlook of the developments is given as well. The information is provided in support of policy making and licensing practice. The OPS-LT-model is an important component of AERIUS, the calculation tool for the living environment, ultimately targeting assessment of nitrogen deposition (www.aerius.nl). OPS-LT has also been applied to analyze the air quality in specific situations, e.g., where there may be an impact on public health in a particular region (e.g. Elberse et al., 2021) as well as for research applications (see Van Der Swaluw et al. (2021) for more references in this regard).

OPS-LT is a source-receptor model. The equations governing the transport, dispersion and deposition processes are solved analytically. Since OPS-LT is a source-receptor model it has implemented source apportionment in its calculations by construct. Thus, sectoral contributions from local, regional and foreign sources can be easily combined and distinguished (De Vries & Sauter, 2020). The area for which concentrations and depositions can be calculated is determined by the size of the area for which meteorological parameters are known. Since the standard climatological data set used for this model is based on observations from the Royal Netherlands Meteorological Institute (KNMI), the maximum size of the receptor area becomes, in effect, the Netherlands and adjoining regions (F. Sauter et al., 2022).

The long-term version of the model used in this study, OPS-LT, simulates the process sequence of emission into the atmosphere, transport and dispersion, chemical conversion and deposition of pollutants. It is based on the well-established principles of Gaussian dispersion in the atmosphere (Seinfeld & Pandis, 2006). Gaussian plumes from point or area sources are combined with a Lagrangian trajectory model for long-range transport. The model is considered statistical in the sense that concentration and deposition values are calculated for a number of typical situations, called classes. Long-term values are obtained by summation of the outcomes per class, weighted with their relative frequencies of occurrence. Classes are defined by meteorological conditions in combination with travel distance of air parcels between source and receptor.

LOTOS-EUROS (short: LOTOS) is an open source air quality model developed by TNO in cooperation with national and international partners for scientific applications and for policy support (Schaap et al., 2008). The model is aimed at the simulation of air pollution in the lower troposphere. The model is of intermediate complexity in the sense that the relevant processes are parameterized in such a way that the computational demands are modest enabling hour-by-hour calculations over extended periods of several years within acceptable computational time. The model is a so-called Eulerian grid model, which means that the calculations for advection, vertical mixing, chemical transformations and removal by wet and dry deposition are performed on a three dimensional grid. Applications in Europe typically cover the continent as a whole, with higher resolution domains on the region of interest. Meteorological data are standard taken from ECMWF. The LOTOS-EUROS model has a long history studying the atmospheric nitrogen budget, and is also applied for ozone, particulate matter, methane and other organic compounds. It is operationally applied to provide air quality analyses and forecasts within the CAMS service. The system contributes to the benchmarking of the UNECE EMEP model and is used for policy support for national authorities of the Netherlands, Germany and Croatia. LOTOS is an integral part of the nitrogen deposition mapping approach for Germany. The resulting deposition maps are used for international reporting obligations and are provided as a background deposition for use in permit applications in Germany.

TNO has developed a system to track the impact of emission categories within a LOTOS-EUROS simulation based on a labelling technique (Kranenburg et al., 2013). In addition to species concentrations and deposition fluxes, the contributions of predefined source categories are calculated and tracked for each process description in the model. The labelling routine is designed for chemically active tracers with a C, N (reduced and oxidized), S or O atoms. The source attribution module for LOTOS-EUROS provides source attribution valid for current atmospheric conditions, since all chemical transformations occur at the same concentrations of oxidants. For details and validation of this source attribution module, we refer to (Kranenburg et al., 2013). The source attribution technique has previously been used to study the origin of particulate matter (Timmermans et al., 2022), nitrogen dioxide (Thürkow et al., 2023) as well as nitrogen deposition (Schaap et al., 2018a).

EMEP4NL is configuration of the EMEP model specifically for the Netherlands. The European Monitoring and Evaluation Programme (EMEP) / Meteorological Synthesizing Centre-West (MSC-W) model is an Eulerian chemical transport model described in (Simpson et al., 2012a) and developed at the Norwegian Meteorological Institute. The EMEP model supports the development of air quality policies in the European Union (see https://emep.int) and is available under an open-source GPLv3 license. It includes a detailed atmospheric chemistry scheme and is used to monitor the yearly developments in particulate matter, photo-oxidants, acidifying and eutrophying components across Europe (see e.g. Eggerli et al., 2024). Specifically for the Netherlands, the EMEP4NL configuration was developed (Van Der Swaluw et al., 2021). The current version of EMEP4NL is based on the EMEP/MSC-W model version 4.45. EMEP4NL uses one-way nested horizontal grids, to scale up from a coarser resolution on a European level, to a higher resolution over the domain over the Netherlands. The EMEP4NL model is driven by meteorological data input obtained from the Weather Research Forecast (WRF) model version 3.8 (Skamarock et al., 2008). The grid configuration as used in the WRF model is identical to the grid configuration in the EMEP4NL model.

EMEP4NL uses a so-called brute-force method to calculate source contributions. A brute-force method (BF or emission reduction impact) is a sensitivity analysis technique which estimates the change in pollutant concentration or deposition (impact) that results from a change in one or more emission sources. Typically, the emissions of a source are reduced by

15 % in this process. The impact or difference to the base simulation in terms of concentration or deposition is attributed to the source of the emission change.

MATCH - the Multi-scale Atmospheric Transport and Chemistry model (MATCH; Bergström, R. & Olenius, T., 2025; *MATCH - Transport and Chemistry Model — SMHI*, n.d.; Robertson et al., 1999) is an off-line chemical transport model (CTM). It is developed at the Swedish Meteorological and Hydrological Institute (SMHI). It is used to study and monitor particulate matter, photo-oxidants, acidifying and eutrophying components across Europe and Scandinavia. The model has a flexible design, accommodating different weather data forcing on different resolutions and projections, and a range of alternative schemes for deposition and chemistry calculations. It is operationally applied to provide air quality analyses and forecasts within the CAMS service.

SILAM - The System for Integrated modeLling of Atmospheric coMposition SILAM (http://silam.fmi.fi) is a Eulerian chemical transport model that can be applied at global and regional scales. In this study version v.6.1 was applied. The main developer is the Finnish Meteorological Institute (FMI). It is developed for atmospheric composition, air quality, and emergency decision support applications, as well as for pollen. The model has a flexible design, accommodating different resolutions and projections, and a range of alternative schemes for deposition and chemistry calculations. It is operationally applied to provide air quality analyses and forecasts within the CAMS service.

3.2 Main model characteristics

The overview of the model versions used and their main characteristics is provided in Table 2. The main takeaways are:

- All models use scavenging rates based on water solubility for gases using Henry coefficients and particle size for particulate matter size to describe the removal efficiency for wet deposition. In principle, the formulations are very similar but implementation with respect to the precipitation information from the meteorological driver is known to be challenging.
- All models use a method based on resistances to calculate deposition velocities. For gases OPS and LOTOS use the DEPAC module, whereas in MATCH the EMEP scheme for dry deposition is applied, with the exception that MATCH implemented the compensation point approach from DEPAC (R. J. Wichink Kruit et al., 2012). Hence, three out of five models account for the compensation point using the same scientific basis.
- For the dry deposition of particulate nitrate and ammonium OPS applies a scheme based on experimental data from the Netherlands. LOTOS uses the scheme based on (Zhang et al., 2001). EMEP and MATCH use a similar scheme as LOTOS, but increase the dry deposition rates for particulate N compounds in comparison other particulate matter components, to account for the notion that few observations have shown larger deposition velocities for particulate nitrate than for the non-volatile particulate sulfate (Simpson et al., 2012a).
- All models use a land use dependent scheme, except SILAM. In SILAM a distinction is made between vegetated and non-vegetated areas is made.
- EMEP4NL assumes no dry deposition to occur on arable land during the growing season for crop land-covers. The surface resistance is set very large, ensuring zero deposition. This procedure was designed to account for the fact that many croplands are net emitters of NH_3, rather than sinks (Simpson et al., 2012a). All other models include emission and deposition to both take place (independently). Hence, in all other models crop land are a sink for ammonia during the growing season.

The variability in the applied schemes for dry deposition is not large, when one realizes that important parts of the EMEP and DEPAC modules are very similar. For example, the stomatal conductance is based on the same implementation in both schemes. Also the scientific basis for the wet deposition is basically the same, although implemented in different model structures and fed by different meteorological data. Hence, a large part of the variability between modelling results may derive from the other process descriptions in the models or from individual model assumptions (as for EMEP4NL). Therefore, we also added the information on chemical schemes and input data.

It is important to realize that OPS works with observed meteorological data for six regions in the Netherlands, whereas the Eulerian models use gridded data sets. EMEP4NL is ran with high resolution WRF meteorology, whereas the other models use ECMWF information. Further, the spatial distribution of the emissions is harmonized between the models (Appendix B), while model used their own temporal and height distribution. The OPS model is the only model that performs a meteorological dependent scaling of the inventoried ammonia emissions mainly based on temperature. Given the little variability between the mean temperatures between meteorological classes and years, this correction for annual simulations is expected to be rather small.

The OPS model uses the chemical conversion rate maps as calculated by the EMEP4NL model (Hoogerbrugge et al., 2020). These maps yield annual averaged conversion rates from e.g. gaseous NO_x precursors to particulate pNO_3^- in OPS on kilometer scale resolution over the Netherlands. In reality, these conversion rates vary throughout the year, depending on meteorological conditions and chemical regime from day to day and from season to season. This variability is modelled in the Eulerian models using a gaseous chemistry scheme to predict the transformation of NO_x to nitric acid. As a next step, a thermodynamic equilibrium module or aerosol chemistry module to applied to calculate the formation (or loss) of particulate ammonium nitrate. Although the schemes applied here are different, the aerosol chemistry modules provide very similar results when applied in a single model and are not expected to give rise to significant differences.

For a more detailed description of the models we refer to Appendix A and the references therein.

Table 2: Main model characteristics for the five participating models.

	OPS	LOTOS	EMEP4NL	SILAM	MATCH
Version	V5.1.1.0	V2.2.9	4.45	V6.1	vFFP_bd
Institute	RIVM	TNO	RIVM	FMI	SMHI
Model type	Langrangian	Eulerian	Eulerian	Eulerian	Eulerian
Resolution	0.015x0.09 lon/lat	1/40x1/80 lon/lat	1/54x1/54 lon/lat	1/30x1/60 lon/lat	2.5x2.5km
Vertical layers	-	12 up to 8 km	21 up to 15 km	10 up to 8 km	18 up to ~4km (for NL-domain)
Surface layer depth	Any height within mixing layer	20m	50m	25m	40m
Meteorology	KNMI weather stations for 6 regions	ECMWF-IFS	WRF (nudged by NCEP/NCAR GFS)	ECMWF-IFS	ECMWF-IFS
Land use	LGN2020	CORINE-2018	CORINE + SEIY (EMEP MSC-W, 1x1km)	IFS lai climatology	ECOCLIMAP-SG

	OPS	LOTOS	EMEP4NL	SILAM	MATCH
Emission inventory	OPS inventory	NKS-inventory	NKS-inventory	NKS-inventory	NKS-inventory
Emission time profiles	Apportioned to meteo classes proportionally + temperature correction for agricultural NH_3	Static + HDD for residential combustion + (Skjøth et al., 2011) for agricultural NH_3	CAMS-TEMPO + Adaption for agricultural NH_3	CAMS-TEMPO + static_HDD for residential combustion	CAMS-TEMPO v3.1
Natural emissions	-	Soil-NO_x, GFAS forest fires	Included: Soil NO_x, sea salt, isoprene, monoterpenes, wind-blown dust.	Lightning NO_x climatology SILAM soil-NO_x model: simplified Berkeley-Dalhousie emission with CAMS_GOB_SOIL base-map	GFAS forest fires, sea salt, isoprene, monoterpenes, wind-blown dust.
Boundary conditions	Climatology	CAMS-EAC4	Climatology/observations, (Simpson et al., 2012a)		MATCH-Europe
Wet deposition	In- and below-cloud scavenging rates described in Sauter et al. (2023)	Scavenging rates following Banzhaf et al. (2012)	In-cloud Scavenging (Simpson et al., 2012a), Sub-cloud (Berge & Jakobsen, 1998)	Scavenging rates with sub-grid exchange (Sofiev, 2000a)	In cloud Scavenging rates, Sub-cloud (Berge, 1993)
LLDry deposition					
Particles	Slinn (1982)	(Zhang, (2001)	Simpson et al. (2012a)	(Kouznetsov & Sofiev, 2012a)	(Simpson et al., 2012a)
Gases	DEPAC (van Zanten et al., 2010)	DEPAC v	(Simpson et al., 2012a)	(Wesely, 1989)	(Simpson et al., 2012a)
Stomatal conductance	(Emberson, Wieser, et al., 2000)	(Emberson, Wieser, et al., 2000)	(Emberson, Wieser, et al., 2000)	Wesely et al. (1989)	(Emberson, Wieser, et al., 2000)
Compensation point NH_3	Yes (R. J. Wichink Kruit et al., 2010, 2012, 2017)	Yes (R. J. Wichink Kruit et al., 2010, 2012, 2017)	No	No	Yes, (Frohn et al., 2025; R. J. Wichink Kruit et al., 2012)
Gas phase chemistry	Pseudo first-order reaction rates.	CBM-IV	EMEP EMCHEM09	Modified CBM-V+SOA (Hänninen et al., 2023a)	MATCH-VSOA; similar to EMEP EMCHEM09 + rates update CHEM19
Aerosol chemistry	Chemical conversion rates based on the MARS chemistry	ISORROPIA-2	MARS Eq. module	(Sofiev, 2000a)	(Mozurkewich, 1993)

	OPS	LOTOS	EMEP4NL	SILAM	MATCH
	scheme in EMEP4NL				
Coarse mode pNO_3^-	Yes, as above	Yes, on sea salt	Yes, on sea salt	Yes, on sea salt	Yes, on sea salt (Hov et al., 1994)

3.3 Simulation setup

To execute the benchmark exercise and enable the generation of an ensemble a benchmark protocol was defined, describing the simulations as calculated by the participating models.
Simulation years: The central meteorological year for the benchmark was 2019. In addition, to check for consistency of the results OPS, EMEP4NL and LOTOS also ran the years: 2016, 2017, and 2018.

Simulation domains:

- Europe
  - Use own domain, as long as Netherlands can be nested in
- Netherlands (shown in Figure 9)
  - Lon: 3.15 – 7.50
  - Lat: 50.65 – 53.70
  - Circa 1/40 x 1/80 lon-lat resolution
  - Model resolution preferably 2.5x2.5 km or higher.

Anthropogenic emissions: Prescribed inventory delivered by the consortium (See section 3.3.1).

Other inputs: Models use their own settings. This includes meteorological input, land use maps, natural emissions (soil-NO_x, wildfires, and lightning) and boundary conditions.

Figure 9: Preferred model domain for simulations on highest spatial resolution.

3.3.1 Emission inventory

The settings were chosen as such to mimic the situation in which a modelling team was required to perform a simulation based on the official emission data from the Pollutant Release and Transfer Register (Emissieregistratie) in the Netherlands. Therefore a central emission inventory was generated (NKS emission inventory), which includes all requirements. This set with harmonized input was used by all models. This dataset contains the following data:

- Europe
  - CAMS – v5.1 REF2 (submission 2020, year 2018)
  - 0.1x0.05 lon/lat resolution
  - GNFR sector classification
- NCP and OSPARII
  - ER-emissions based on MARIN data (spatial distribution 2016, year 2018)
  - 1x1 km resolution on NCP, spatial distribution + emission totals 2021
  - 5x5 km resolution on OSPARII except NCP, emission totals updated according to relative change in NCP emission totals
  - GNFR sector classification
- Netherlands
  - ER-emissions (submission 2022, year 2018)
  - 1x1km resolution
  - ER-sector-classification converted to GNFR sector classification
- Germany
  - Greta (submission 2022, year 2018)
  - 1/60 x 1/120 lon/lat resolution
  - GNFR sector classification
- Belgium
  - VMM-emissions (VLOPS) for 2018, from submission 2020.
  - Only for NO_x and NH_3
  - 1x1km resolution for Flanders, 5x5 km resolution for Wallonia
  - GNFR-classification

Unfortunately, it was not feasible to fully use the same identical set of emissions by all models. By design, the OPS model is able to use point sources in the standard settings using a Gaussian plume. In the OPS model, point sources are an integral part of the parametrization, allowing more precise modelling of localized sources such as industrial or agricultural exhausts. Utilizing this important model feature requires an emission set which includes explicit definitions of point sources, their emission heights and codes for diurnal variations, heat content etc. The NKS emission set provided for this study does not include this specific information. Therefore, a special set of emissions was generated for OPS (“OPS emission inventory”). To design this set, an existing set of emissions for OPS was taken as base and adjusted as much as possible to match the emission totals and the spatial distribution of the NKS set, especially for the Netherlands and neighboring countries.

The spatial differences in emissions between the NKS and OPS emissions inventories were determined for the smallest domain (highest resolution) because this is the most important part of the emission set, with the largest expected impact on concentrations in the Netherlands. A detailed analysis can be found in Appendix B. In conclusion, in spite of the effort to homogenize the emissions, differences remain, especially in spatial distribution. Because the differences are very small, these were not considered as an important

shortcoming for this study. Further note that by using grid models like LOTOS or EMEP4NL, emissions are directly spread over a complete grid cell, thus in these models this impact is even smaller.

For other emissions specifications such as temporal profiles, height distribution, and tracer composition, models used their own settings.

3.4 Model-to-model intercomparison

3.4.1 Output

To compare the model simulation results, the output was harmonized in the same netCDF format. Results were calculated on a regular grid as described. For the Langrangian model (OPS), this means automatic generation of multiple sub-receptors in each receptor grid cell, such that representative grid cell averages are obtained. For Eulerian grid models, the result was calculated for a domain with a resolution which matches the requested output. For all calculation points/grid cells, variables of interest were calculated. For the calculation of the variables, two tiers are defined. Tier 1 consists of all variables necessary for constructing the ensemble, while tier 2 contains all other variables of interest, which are used to gain more insight in the model processes. The requested output is split into four parts: concentrations, depositions, emissions, and meteorological parameters. An extended list of all variables is listed in 0.

3.4.2 Source apportionment

Dedicated simulations were performed using the Dutch models to compare source contributions to the nitrogen deposition in the Netherlands. It has to be noted here that not every model system can deliver a detailed overview of source sector contribution, as for models without a dedicated source apportionment technique (i.e. EMEP4NL) this would require about 20 full simulations. Therefore, a prioritized list was made of the source contribution sectors to be quantified. Priority was given to the sector “Agriculture” as the dominant source of ammonia, the “Transport” sector as an important near surface source of nitrogen oxides and “Energy and Industry” sector as an important source of nitrogen oxides from point sources. These sectors were addressed for the Netherlands, Belgium and Germany:

- Dutch - Agriculture
- Dutch - Transport
- Dutch - Energy and Industry
- Belgium - Agriculture
- Belgium - Transport
- Belgium - Energy and Industry
- Germany - Agriculture
- Germany - Transport
- Germany - Energy and Industry

The source apportionment system in LOTOS requires labelling of all sources. The output of this model was used to verify that the main contributions are covered with the shortlist provided above.

In the LOTOS labelling run labels were given to the 3 main sectors in each of the listed countries. All other sectors were combined in a sector called 'Other' and all emissions outside these countries were labelled as 'Other countries'. Boundary conditions were called "intercontinental", while the biogenic NO emissions and wildfire emissions were represented by the label "Natural". In Figure 10, results are shown for the simulation with LOTOS for 2019. NH_x explains 72 % of the total deposition in the Netherlands and NO_y the other 28 %. The LOTOS source apportionment results show that ~55 % of the total N deposition in the Netherlands have a Dutch origin, with the largest share for agriculture. Belgium (12 %), Germany (14 %), and France (9 %) also have significant contributions. All other countries together contribute slightly more than 5 % to the total N deposition in the Netherlands. Next to agriculture, also traffic and industry show significant contributions to nitrogen deposition, especially for NO_y. These findings indicate that the focus on the three main sectors and the neighbouring countries actually covers almost the whole N deposition in the Netherlands and thus should provide a representative picture.

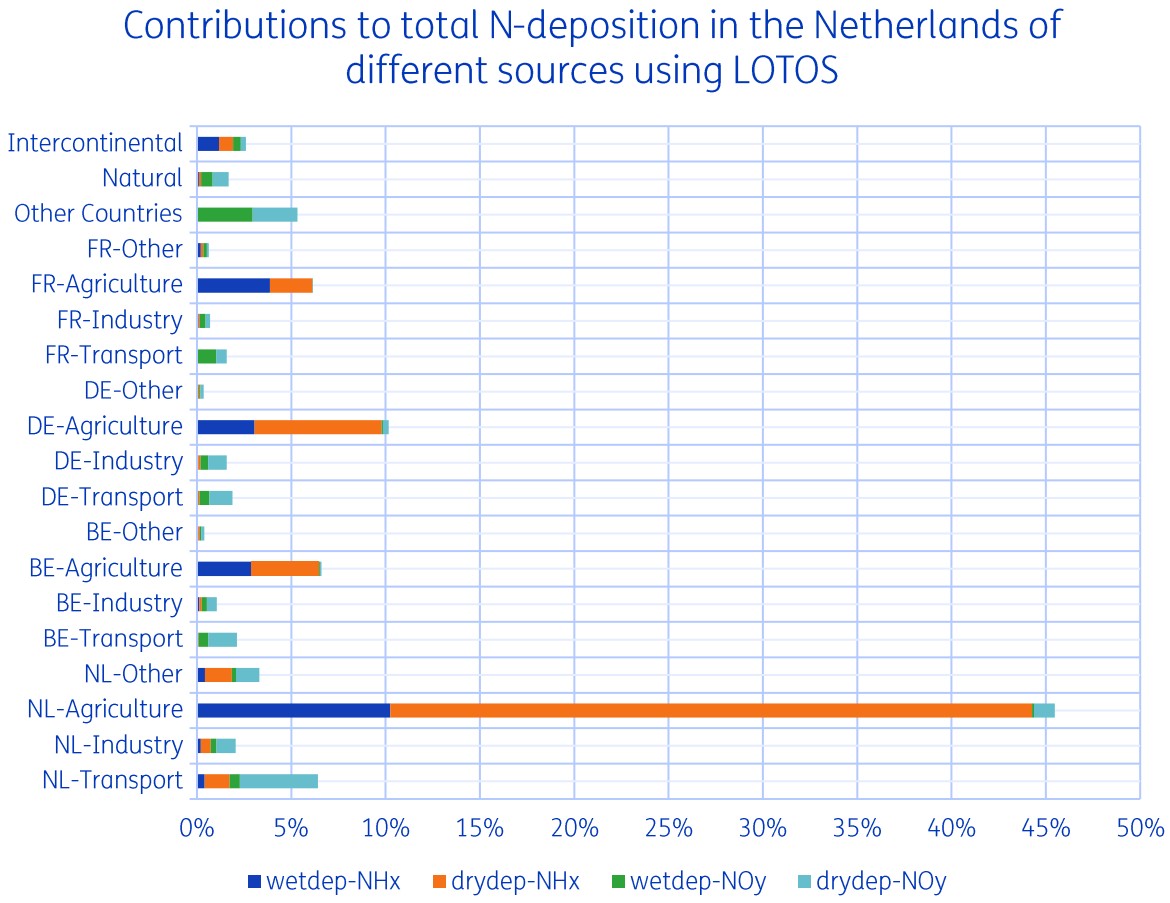

Figure 10: Contribution of different countries and sectors to total nitrogen deposition in the Netherlands. In green colours, wet and dry deposition of NH_x, and in blue depositions of NO_y.

3.5 Evaluation against observations

3.5.1 Observation data

The results of the benchmark were evaluated against the following observation data:

- LML – hourly temporal resolution
  - Concentrations of NO_2 (Dataset contain also data provided by GGD-Amsterdam and DCMR)
  - Concentrations of NH_3
- LML – daily temporal
  - Concentrations of pNO_3^-
  - Concentrations of pNH_4^+
- LML – irregular temporal resolution
  - Wet deposition of NO_y
  - Wet deposition of NH_x
- MAN – monthly temporal resolution
  - Concentrations of NH_3
- COTAG – monthly temporal resolution
  - Dry deposition of NH_3

All the locations of the monitoring systems are shown in Figure 11 (left panel shows all LML-stations, right shows all MAN and COTAG stations).

Note that the number of observation stations differs for each observation type. The COTAG NH_3 dry deposition measurements have the fewest number of stations (3). Five measurements time series were available for the particulate (pNH_4^+ and pNO_3^-) concentrations and eight locations of NH_x and NO_y. For nitrogen dioxide, 49 stations were available. For ammonia, 6 and 375 stations were available from LML and MAN, respectively.

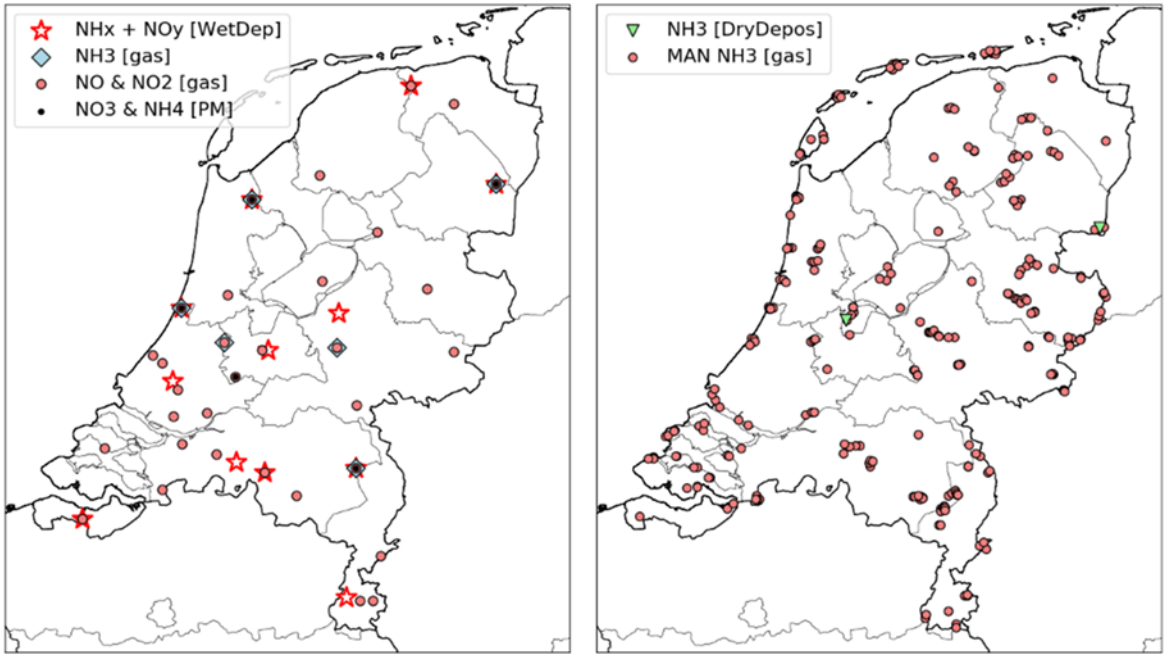

Figure 11: Map of all observation sites in the Netherlands. Left: LML-network for gaseous concentrations of NO_2 and NH_3, particulate concentrations of pNO_3^- and pNH_4^+, and wet deposition fluxes for NO_y and NH_x. Right: MAN network with tube samples for NH_3 and COTAG network for dry deposition of NH_3.

3.5.2 Operational evaluation

For all comparisons to observations a number of metrics were calculated to provide a quantitative analysis of model skill (Table 3). The bias and root-mean-square error (RMSE) provide insight into the deviation of the modelled data with the observations. These metrics allow us to assess how far off the model estimates are from the real-world measurements. The bias will provide systematic errors while the RMSE will give us the relative scatter of the modelled values which is sensitive to both systematic and random errors. The correlation coefficient (R) measures the linear relationship with the observations and is insensitive to an additive or a multiplicative factor. The metrics can be used on annual mean comparisons with data points for different stations or for time series analysis. Hence, the correlation coefficient can provide the explained variability for the spatial distribution (when mean are used) or for the temporal distribution (when time series are used). To provide an overview for different compounds in one graph we also used the normalized metrics.

Table 3: Statistical model quality indicators used in this study, which include the mean bias, Root Mean Square Error (RMSE), Ratio, and Correlation coefficient (R).

Parameter	Name	Formula
MB	Mean bias	$\text{Bias} = \overline{\text{Mi}} - \overline{\text{Oi}}$
NMB	Normalized mean bias	$\text{NMB} = \frac{\text{Bias}}{\overline{\text{Oi}}}$

Parameter	Name	Formula
Ratio	Ratio of means	$\text{Ratio} = \overline{\text{Mi}}/\overline{\text{Oi}}$
RMSE	Root mean squared error	$\text{RMSE} = \sqrt{\overline{(\text{Mi} - \text{Oi})^2}}$
NRMSE	Normalized RMSE	$\text{NRMSE} = \frac{\text{RMSE}}{\max(\text{Oi}) - \min(\text{Oi})}$
Corr	Correlation coëfficiënt	$\text{R} = \frac{\overline{\left(\text{Oi} - \overline{\text{Oi}}\right)\left(\text{Mi} - \overline{\text{Mi}}\right)}}{\sigma_{c_M}\sigma_{c_O}}$

3.6 Land use dependent effective deposition velocity comparison

To determine the deposition fluxes over a country or region it is important to notice that deposition velocities differ per chemical compound and per land use class. Land use classes with a higher roughness length (for example, forest) typically have a relatively large deposition velocity due to a lower atmospheric resistance.
To investigate the nitrogen deposition on different land use classes, an analysis of the deposition velocities was performed. Some of the models are able to calculate land use specific deposition velocities, but this is not possible for all model systems. Therefore a generic method was applied as follows. In each grid cell, the dry deposition flux from each model was divided by the corresponding concentration. This results in what is called “the effective dry deposition velocity”. Then for each land class, the cells in which this class is dominant (>80 %) were selected. The average of these cells was used as an estimate for the land use specific effective deposition velocity for a particular class. In the top panels of Figure 12, the maps of the land use fractions (derived from the Corine land use map) are shown for grass, arable land, coniferous forest and semi-natural vegetation. The lower panels indicates the cells which have a coverage over 80 % for these classes.

It needs to be noticed that this method provides a rough indication of the land-use specific effective deposition velocity as there remains an influence of land use types other than the dominant one in the result. Moreover, the effective deposition velocity does not equal the average deposition velocity. Usually, the effective deposition velocity is lower than the average deposition velocity due to covariances between concentration and deposition velocity. This can be understood by the fact that under (stable) conditions when the concentrations are high, the dry deposition velocity is small. In contrast, during instable daytime conditions the concentrations are low due to large vertical mixing, which also causes a high deposition velocity. Nonetheless, we consider the effective deposition velocity an useful metric for a first-order comparison of model results.

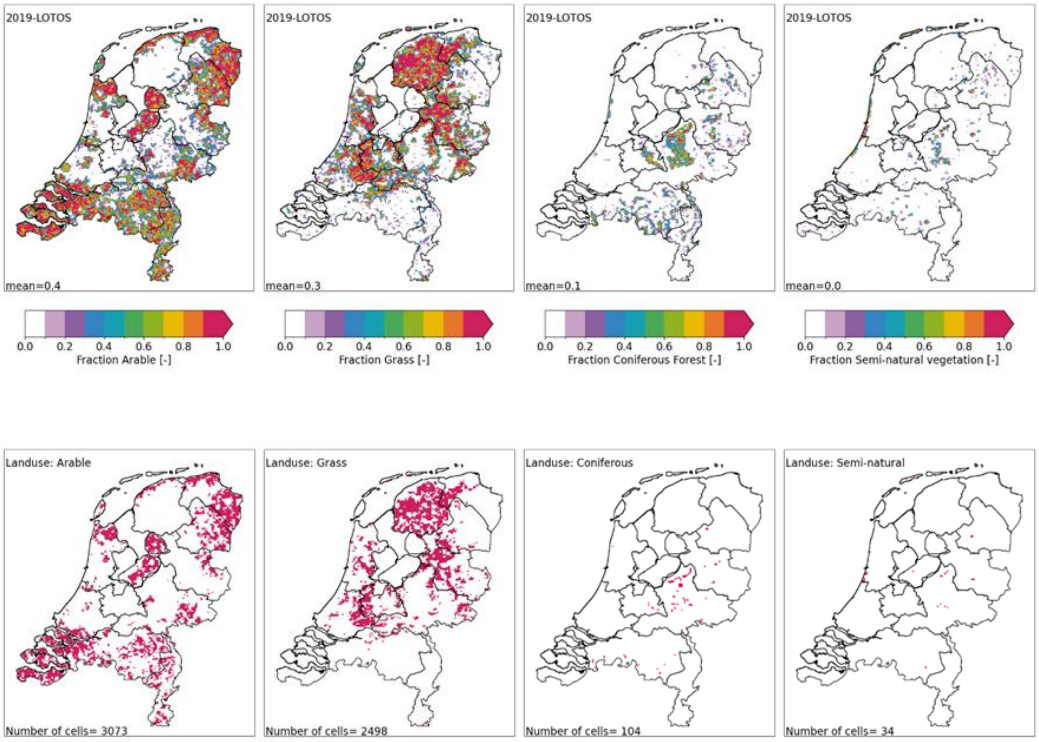

Figure 12: Top panels: Land use fractions per grid cells for the following land use classes from left to right: grass, arable land, coniferous forest and semi-natural vegetation. The lower panels indicates the grid cells with a coverage of more than 80 % for each of the classes.

Land use dependent total deposition over the country

For further reference we assessed the total contribution of nitrogen deposition per land use type in the Netherlands as calculated with LOTOS. In Figure 13, the relative land use cover (in percentage) over the Netherlands is shown in green, and its contribution to the total modelled N deposition is shown in blue. Note that most of the country is covered with grass (30 %) and arable land (38 %). Urban areas is the third most important land use (14 %). The protected nature area's coincide with the forest and semi-natural vegetation classes, which cover 12 % of the country. In the blue bars, the fraction of the total nitrogen deposition on all land use classes is shown. Because of the large area, most of the deposition takes place on grass (28 %) and arable land (37 %). For semi-natural and forest the combined contribution to the total deposition is about 14 %, which is slightly higher than their fractional area as explained by the roughness of the forest types and the evergreen nature of coniferous forest.

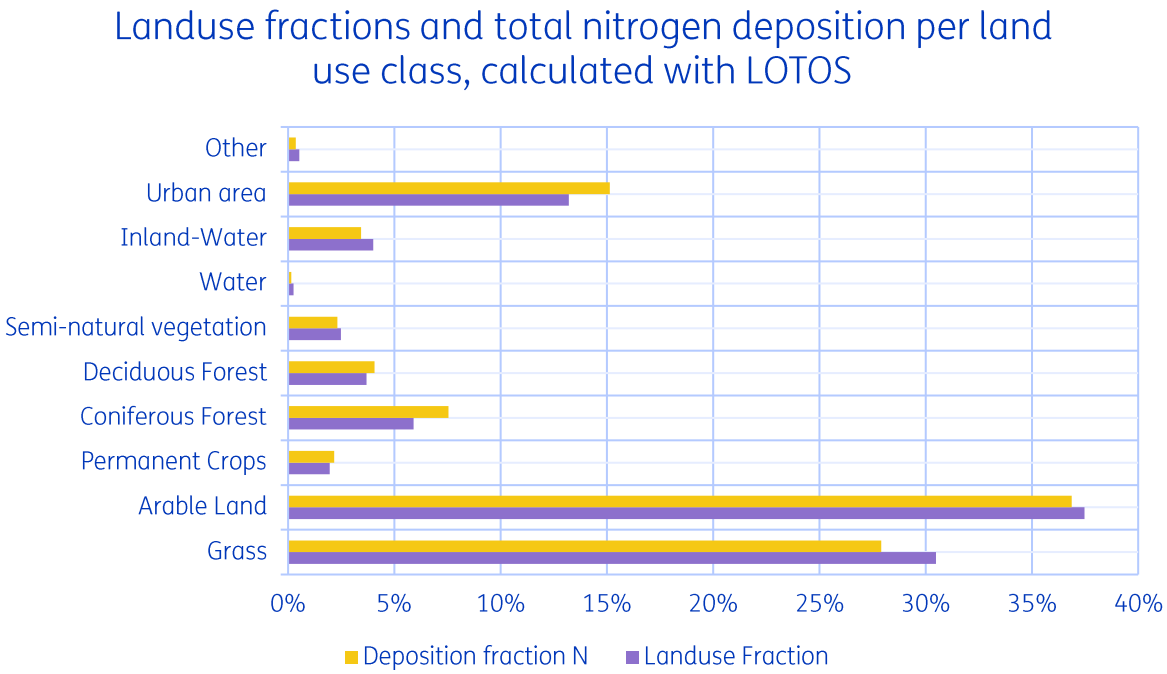

Figure 13: Land use fractions and fraction of total modelled nitrogen deposition over the Netherlands using LOTOS.

3.7 Ensemble model creation

A model ensemble can be constructed from the model results of the participating models. In this study, two ensembles were made. First, an ensemble was created including all five models: OPS, LOTOS, EMEP4NL, SILAM, and MATCH. This ensemble is called ENS-INT and is only available for 2019 because the two international models only participated for this year. The second ensemble was created using only the models used in the Netherlands: OPS, LOTOS, and EMEP4NL. This ensemble is called ENS-NLD in this document and is available for all years in this study (2016-2019).

To create these ensembles, two approaches are considered in this study: taking the average or the median value from the modelled concentrations and depositions. The largest advantage of taking median values is that in case a single model shows large systematic differences compared to the other models, it will not influence the ensemble result. On the other hand, this study focuses on the nitrogen budget including emissions, concentrations and deposition. Each of the models keeps its own internal mass balance and should be mass or nitrogen conserving through all processes. By creating an ensemble using the median of the models, the value of a specific model (the central one) is taken in the ensemble. So, this might lead to a concentration field dominated by one model and a deposition field from another model. Hence, the mass balance maintained by the individual models is violated by taking the median. Taking the mean value everywhere also maintains the mass balance in the ensemble. For this reason, it was chosen to base the ensembles used in this study on the average of the participating models, rather than the median.

4 Results and discussion

In this chapter, we present the results of the benchmark exercise. First, the total deposition estimates of the ensemble and the ensemble members are presented. Next, we walk through the results of the different contributing fluxes, starting with the largest contribution of dry NH_x deposition. After the deposition results the modelled concentration distributions are evaluated. Finally, the comparison of the source apportionment results are discussed.

4.1 Total nitrogen deposition

4.1.1 Ensemble mean and spread

The average total nitrogen deposition in the Netherlands as calculated by the five models amounts to 1476 eq ha^{-1} yr^{-1}. The individual model estimates are 1296 (EMEP4NL), 1334 (LOTOS), 1508 (SILAM), 1569 (OPS) and 1669 (MATCH) eq ha^{-1} yr^{-1}. The standard deviation (1 σ) of the total nitrogen deposition in the Netherlands is about 141 eq ha^{-1} yr^{-1}, or 10 % of the mean. In Table 4, all calculated results are displayed and split between reduced and oxidized nitrogen for both dry and wet deposition. In Appendix E, results for all years and for the individual components are displayed in tables.

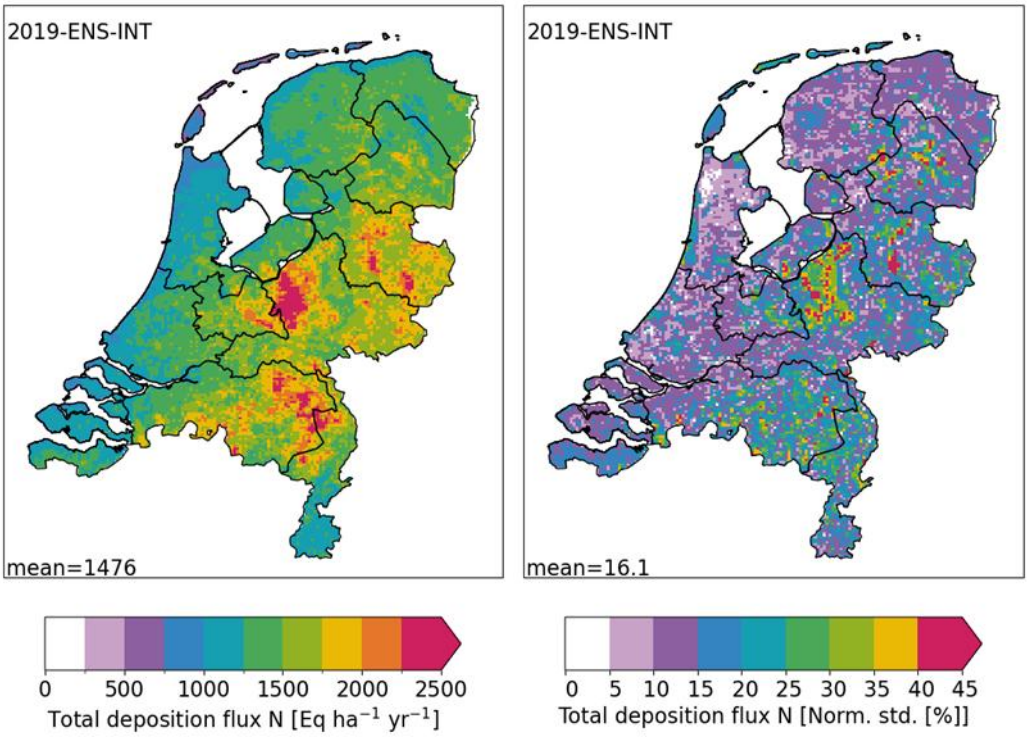

Figure 14: Left: Ensemble mean for all five models for total nitrogen deposition on the Netherlands. Right: Normalized standard deviation [%] of the models taken in the international ensemble.

Following the approach from section 3.7, an average based ensemble is created for the total deposition of nitrogen (Figure 14). The modelled total N deposition shows a large variability across the country. Highest deposition fluxes are calculated for the regions with intensive animal husbandry and for forested areas. In these areas the modelled ensemble mean deposition exceeds 2000 eq ha^{-1} yr^{-1}. In the western coastal provinces of Zeeland, South and North Holland and southern Limburg large areas show central estimates slightly below 1250 eq ha^{-1} yr^{-1}. The country average value for the standard deviation (1 σ) of the modelled deposition at a kilometer scale is about 16 %. For large parts of the country, the spread between the models for total nitrogen deposition is in fact between 10 and 20 % (1 standard deviation) around the average. Only for forested areas, most notably the Veluwe, the spread of the model results is considerably larger. These results may indicate that in large parts of the Netherlands the uncertainty in the modelled total N deposition is considerably smaller than reported by Hoogerbrugge et al. (2024). Hoogerbrugge et al. (2024) determined the uncertainty of the total deposition at a random location in the Netherlands to be at around 30-35 % (1σ). It should be noted that the spread provided here does not include the uncertainty introduced due to uncertainty in emissions, nor the uncertainties in model parameters. It is solely due to differences in modelling practice, using harmonized emissions and model specific parameter settings.

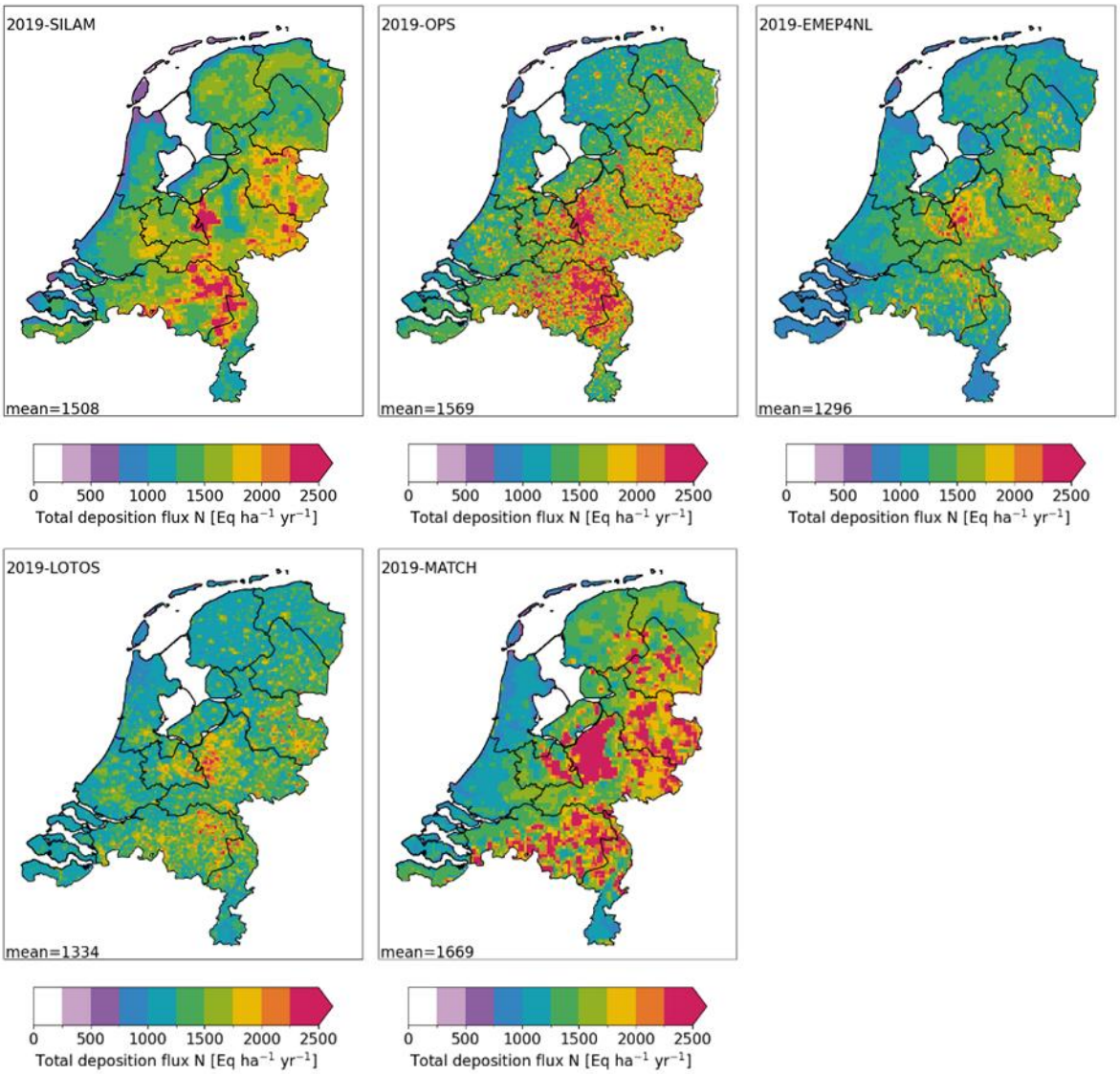

Figure 15: Total deposition flux of N in the Netherlands in 2019, for all models used in this benchmarking study, and the Dutch ensemble (ENS-NLD) and the ensemble of the five models used in the benchmarking study (ENS-INT).

Figure 15 shows the spatial pattern of total modelled N deposition for the year 2019 from all models used in this benchmarking study. The main patterns described for the ensemble mean are also obtained using the individual models, although some distinctive differences can be observed. The large variability in total modelled N deposition for the Veluwe area can be explained by the large contrast in the results of the international models MATCH and SILAM. Whereas MATCH shows a large deposition across the whole Veluwe, SILAM shows very low values. The Dutch models with values around 2000 eq ha^{-1} yr^{-1} are much more consistent. Focusing on other parts of the Netherlands, the EMEP4NL model shows lower total deposition in areas with a lot of arable farming (such as Zeeland, Brabant, Limburg and Flevoland). To determine the origin of the differences between models, similar analyses were performed for subcomponents of the total deposition (wet and dry deposition of both NH_x and NO_y) and the modelled concentrations for the most important nitrogen species.

Table 4: Overview of the modelled dry and wet deposition for NHx, NOy and total N deposition for the country as a whole (eq N ha^{-1} yr^{-1}). For the ensembles the standard deviation of the mean is also provided.

	Dry-NH_x	Wet-NH_x	Dry-NO_y	Wet-NO_y	Total	% NH_x	% NO_y
OPS	733	374	260	201	1569	71	29
LOTOS	655	330	209	139	1334	74	26
EMEP4NL	573	308	268	147	1296	68	32
Ensemble mean NLD	654	337	246	162	1400	71	29
Std. ensemble mean NLD	131	38	32	30	173		
MATCH	968	356	184	162	1669	79	21
SILAM	952	220	246	90	1508	78	22
Ensemble mean INT	777	317	234	148	1476	74	26
Std. ensemble mean INT	246	59	44	38	250		

The contribution to the total deposition is largest from the dry NH_x deposition, followed by wet NH_x deposition, dry NO_y and finally wet NO_y deposition (Table 4). The relative uncertainty derived from the spread of the model results for these four contributing fluxes is larger than the one of the total deposition, as is described in the next sections. The lower uncertainty in the total deposition is due to compensating effects. E.g., when NO_2 is less efficiently removed by dry deposition in a certain model, its removal by dry or wet deposition in the form of, e.g., nitric acid is expected to be enhanced. A similar reasoning applies to the spatial scale. The uncertainty for the country mean is much smaller than for individual square kilometres because of the interaction between concentrations and deposition.

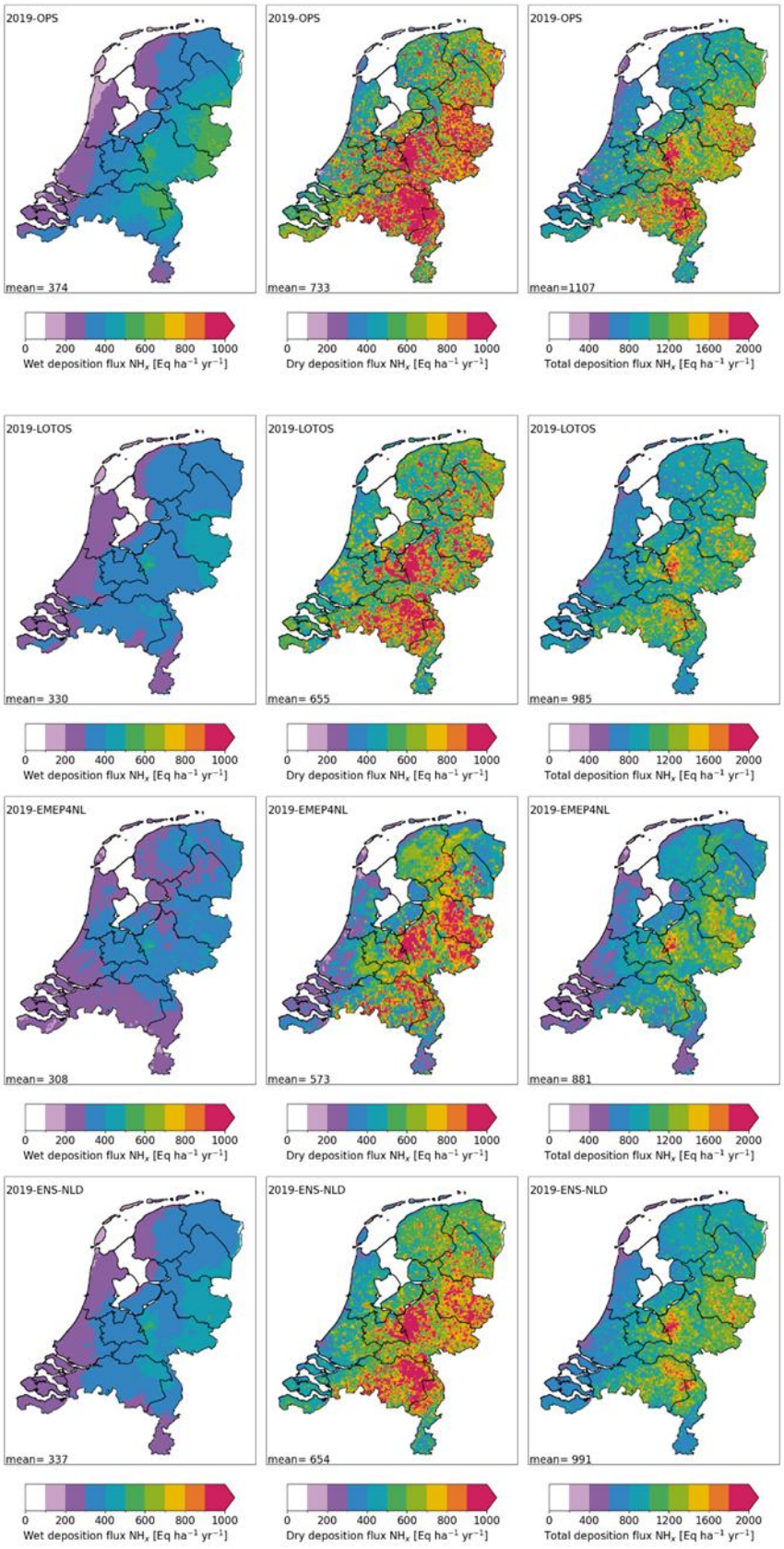
2019-OPS
mean= 374
2019-OPS
mean= 733
2019-OPS
mean=1107
0 200 400 600 800 1000
Wet deposition flux NHx [Eq ha-1 yr-1]
0 200 400 600 800 1000
Dry deposition flux NHx [Eq ha-1 yr-1]
0 400 800 1200 1600 2000
Total deposition flux NHx [Eq ha-1 yr-1]
2019-LOTOS
mean= 330
2019-LOTOS
mean= 655
2019-LOTOS
mean= 985
0 200 400 600 800 1000
Wet deposition flux NHx [Eq ha-1 yr-1]
0 200 400 600 800 1000
Dry deposition flux NHx [Eq ha-1 yr-1]
0 400 800 1200 1600 2000
Total deposition flux NHx [Eq ha-1 yr-1]
2019-EMEP4NL
mean= 308
2019-EMEP4NL
mean= 573
2019-EMEP4NL
mean= 881
0 200 400 600 800 1000
Wet deposition flux NHx [Eq ha-1 yr-1]
0 200 400 600 800 1000
Dry deposition flux NHx [Eq ha-1 yr-1]
0 400 800 1200 1600 2000
Total deposition flux NHx [Eq ha-1 yr-1]
2019-ENS-NLD
mean= 337
2019-ENS-NLD
mean= 654
2019-ENS-NLD
mean= 991
0 200 400 600 800 1000
Wet deposition flux NHx [Eq ha-1 yr-1]
0 200 400 600 800 1000
Dry deposition flux NHx [Eq ha-1 yr-1]
0 400 800 1200 1600 2000
Total deposition flux NHx [Eq ha-1 yr-1]

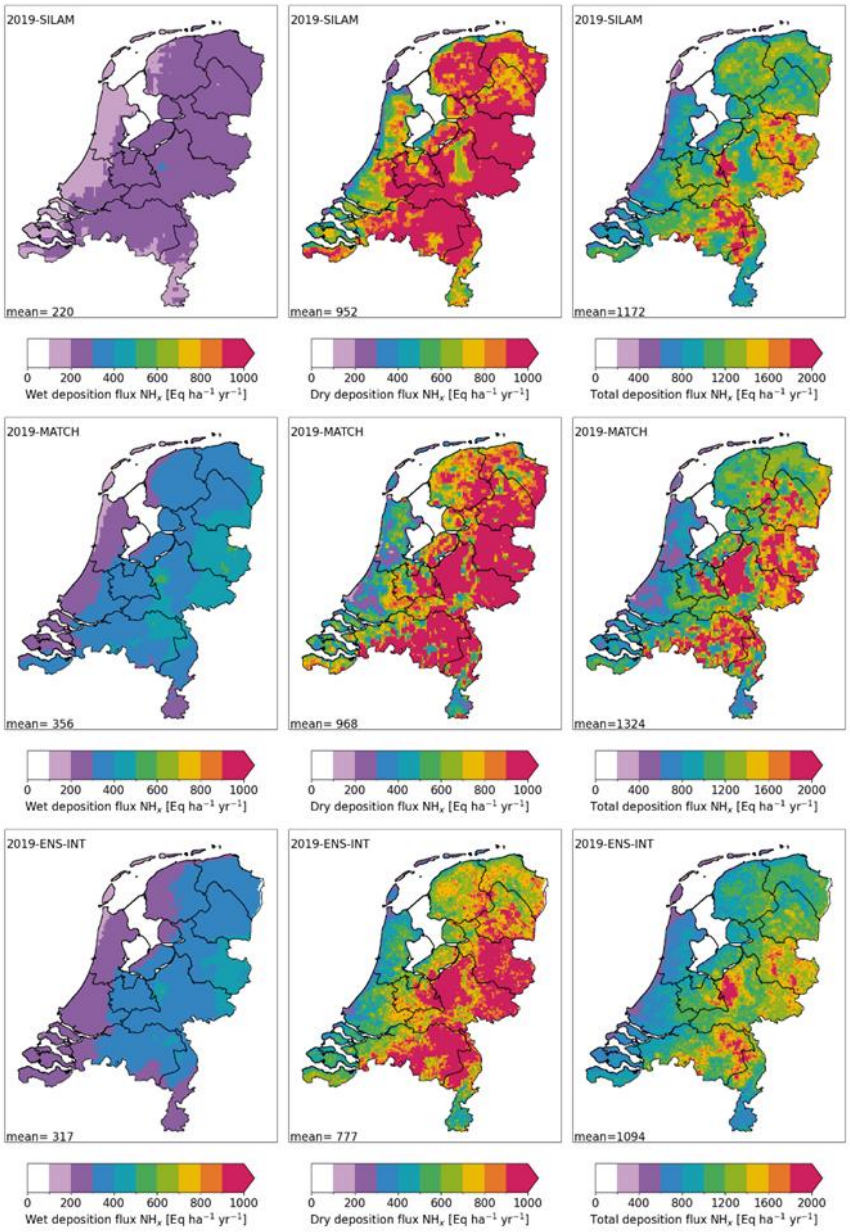

Figure 16: Simulated yearly averaged wet, dry and total deposition of NH_x for the year 2019. Dutch models represented are OPS, LOTOS-EUROS, an EMEP4NL, with their averaged values in their ensemble. International models represented are the Finish SILAM model and the Swedish MATCH model. The extended ensemble reflects the average values of all five models. Left: Simulated yearly averaged wet deposition over the year 2019. Middle: Simulated yearly dry deposition over the year 2019. Right: Simulated total deposition over the year 2019.

4.2 Reduced nitrogen (NH_x) deposition

4.2.1 Overview

Figure 16 provides an overview of the modelled annual total wet, dry and total NH_x deposition flux for all models in this benchmark study for the year 2019. The modelled average total NH_x deposition over the Netherlands varies between 881 (EMEP4NL) and 1324 (MATCH) eq ha^{-1} yr^{-1}. OPS (1107), LOTOS (985) and SILAM (1172) provide results in between

these ensemble bounds. OPS, LOTOS and EMEP4NL indicate about ratio of dry to wet deposition for NH_x to be 2:1 on average. MATCH has a more effective dry deposition and arrives at a ratio of 3:1. SILAM provides the largest ratio of over 4:1, as it predicts the second largest average dry NH_x deposition and the lowest wet NH_x deposition of all models.

4.2.2 Ensemble mean and spread

Reduced nitrogen (particularly the dry deposition of ammonia) explains a large part of the total deposition and the variability between the models (Figure 17). The dry reduced nitrogen deposition (777 eq ha^{-1} yr^{-1}) contributes 45-60 % of the total N deposition in the Netherlands. The wet NH_x deposition (317 eq ha^{-1} yr^{-1}) contributes about 20 – 25 %.
The largest variability between the models was found for the dry deposition of NH_3. On average across the Netherlands, the normalized standard deviation of the ensemble mean was 30 % for the dry deposition of NH_x. This number means that on average there is a 95 percent probability that a model outcome is within 60 % from the mean. For comparison, the average normalized standard deviation was 23 % for NH_3 and 18 % for the wet NH_x deposition. The largest variability in total modelled NH_x dry deposition with a relative standard deviation of about 50 % is seen for the Veluwe area. As for total N, the relative standard deviation is largest in the regions with the highest emission densities and in forested and urbanized areas. For wet deposition of NH_x, a country average standard deviation of 18 % is found with a clear spatial pattern. Maximum deviations are found in the southeast of the country up to ~25 %. The different pattern hints at a different origin of the spread between the models, when recognizing that the wet deposition of ammonia is an important part of the wet NH_x deposition flux.

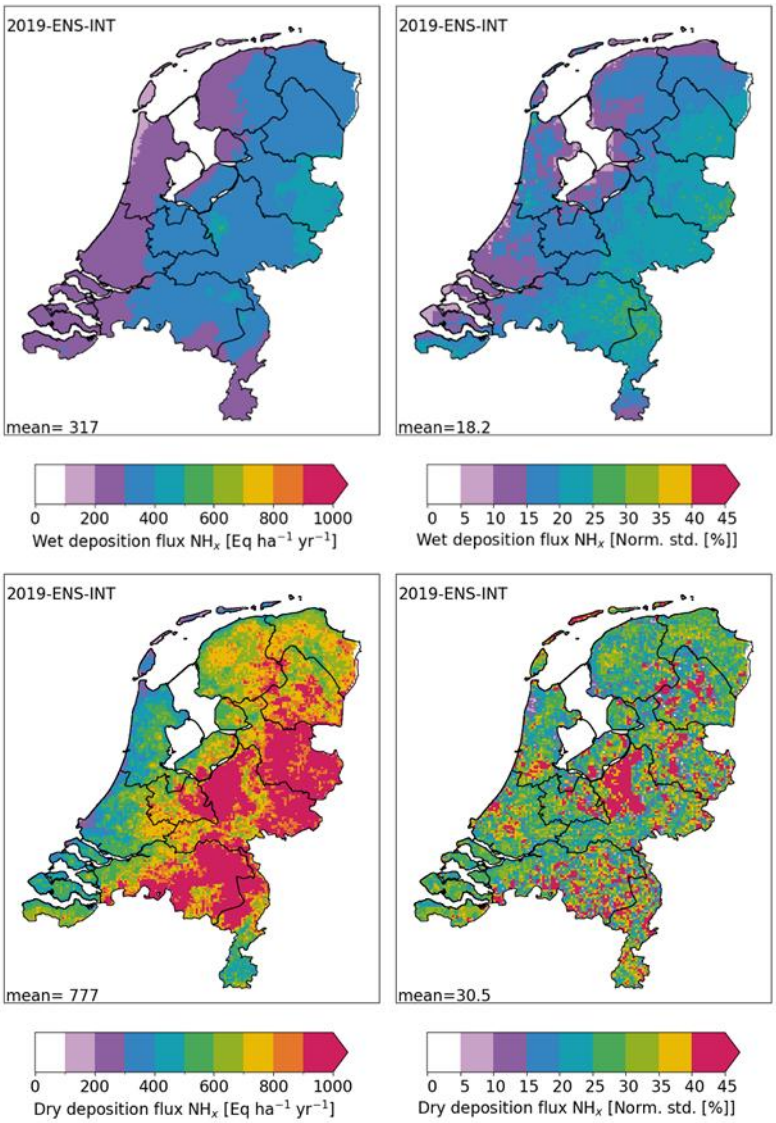

Figure 17: Left panels: Ensemble mean for all five models of wet (top) and dry (bottom) deposition of NH_x on the Netherlands. Right panels: Normalized standard deviation [%] of the models is shown for both components.

4.2.3 Dry deposition

The variability of the results between the models for the NH_x dry deposition, as previously shown in Figure 16, provides an interesting picture. These distributions can be interpreted as the dry deposition maps for ammonia, as the particulate NH_4^+ dry deposition flux is only a small fraction of NH_x. The average dry deposition ranges from 573 (EMEP4NL) to 968 (MATCH) eq ha^{-1} yr^{-1}, with LOTOS (655), OPS (733) and SILAM (952) between the bounds. Besides the range in the overall dry deposition numbers, the spatial variability modelled across the country differs substantially between the models. In terms of the spatial variability the largest similarity is observed between OPS and LOTOS, which may be expected as both models use the same DEPAC module. The modelled dry deposition is largest in the regions with intensive animal husbandry, in forested regions and urban areas in both models. In comparison, the EMEP4NL model yields much lower dry deposition in for example Zeeland, areas in North Holland, the east of Groningen and Flevoland. As a consequence, the

west-east gradient in the modelled dry deposition appears stronger in the EMEP4NL model compared to the other models. On the other hand, the dry deposition of NH_x in EMEP4NL is larger over large parts of Gelderland and Friesland. These differences could be related to the prevalent land use in these regions. In Figure 18 the NH_x dry deposition distributions for OPS and EMEP4NL are repeated and compared to the land use cover maps for the Netherlands that are used in LOTOS. In regions where EMEP4NL computes low dry deposition of NH_x (purple or blue colours) the arable land fraction tends to be comparatively large, whereas dry deposition from EMEP4NL tends to be larger in regions with high grassland cover. These results clearly illustrate the impacts of the different parameterizations for agricultural land uses plays in the EMEP model compared to the models that apply DEPAC (OPS and LOTOS).

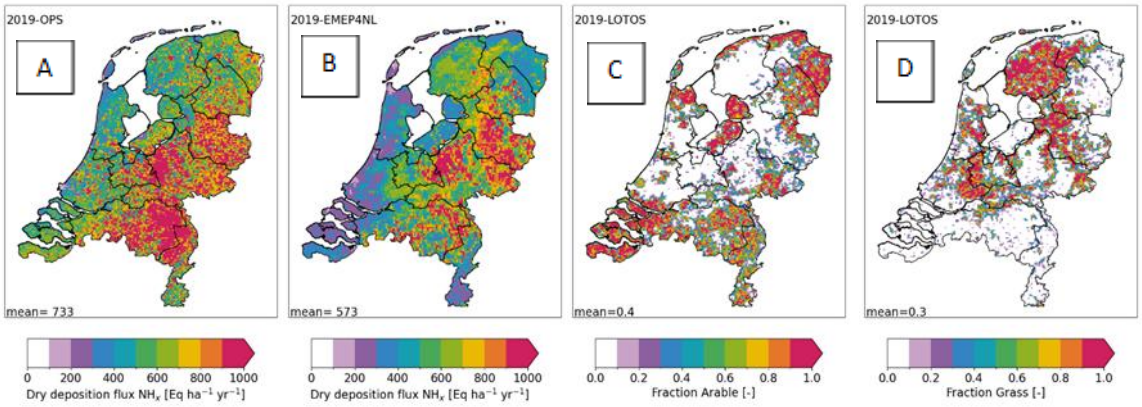

Figure 18: A) Dry deposition flux of NH_x as modelled in OPS, total yearly value for 2019. B) Simulated dry deposition flux of NH_x modelled with EMEP4NL. C) Fractional land use map depicting cells that in LOTOS-EUROS are assigned as land use type 'arable land' (no modelled values). D) Fractional land use map with cells assigned land use type 'Grassland' in LOTOS-EUROS (no modelled values).

MATCH and SILAM both provide country mean values of about 950 eq ha^{-1} yr^{-1} for the dry deposition of NH_x. These values are about 200 eq ha^{-1} yr^{-1} larger than modelled by OPS and 400 eq ha^{-1} yr^{-1} larger than EMEP4NL. Additionally, MATCH and SILAM show much larger areas in the Netherlands with values above 1000 eq ha^{-1} yr^{-1}. The MATCH model computes large dry deposition fluxes throughout the country, except for urbanized areas, which stand out as areas with relatively low deposition. A similar behaviour for urbanized areas is observed in the EMEP4NL results. In contrast, the dry deposition to urban areas are recognizable as maxima in the results from both LOTOS and OPS. The SILAM model does not show an impact of urban areas. The SILAM dry deposition pattern closely resembles the modelled ammonia concentration pattern. This can be explained by the fact that SILAM used vegetation cover rather than land use to model deposition. This choice tends to limit differences in land surface properties with a significant impact on dry deposition, like surface resistance.

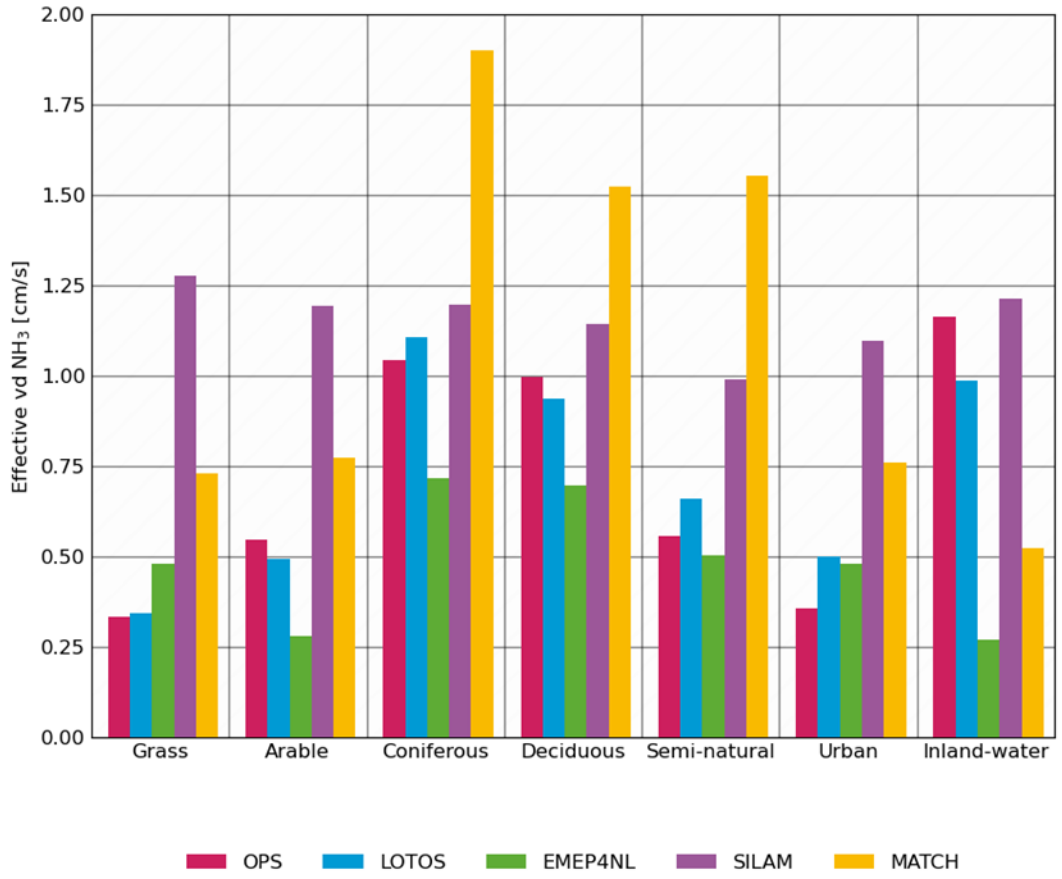

Figure 19: The effective dry deposition velocity of ammonia (NH_3) over various land use types in the Netherlands, as obtained from the different models, averaged over the year 2019. The land use classification includes grass, arable land, coniferous forest, deciduous forest, semi-natural vegetation, urban areas and inland water.

In Figure 19, we show the average annual effective deposition velocity for ammonia over various land use types in the Netherlands for 2019. The effective dry deposition velocities obtained from OPS and LOTOS are very similar. This is expected because they use the same dry deposition module. The analysis illustrates that at a given concentration, EMEP4NL computes a 40 % larger dry deposition to grassland than LOTOS and OPS. For arable land, the reverse is true. In this case, ammonia deposition is about twice as large in LOTOS and OPS than in EMEP4NL. Over forest areas (coniferous and deciduous), the effective deposition velocity in OPS and LOTOS is about 1 cm s^{-1}, whereas in EMEP4NL it is about 0.75 cm s^{-1}. MATCH shows systematically larger effective dry deposition velocities than OPS, LOTOS and EMEP4NL. The MATCH effective dry deposition velocity is over 1.5 cm s^{-1} for forests and semi-natural land uses. The effective deposition velocities for ammonia in SILAM are between 1 and 1.25 cm s^{-1} over the whole country, independent of land use. The country mean is considerably larger than the one of the other models.
The urban land use type presents a special case. The effective dry deposition velocity does not match the observed variability in the dry deposition fluxes for cities between the models. In other words, the deposition velocity is not much larger in LOTOS than in EMEP4NL, whereas the fluxes are different. This could partially be explained by differences in modelled ammonia concentrations, but we suspect that the translation of the urban land use classes in the original, detailed land use data datasets into the limited set of classes used in the dry deposition modelling may differ and impact the results as well. For example, modellers may make assumptions about discontinuous urban areas and assume these to be a combination

of urban fabric and vegetated surfaces. But how to translate those into urban fabric, grass, forest of semi-naturel classes that are used in the deposition routine is not trivial and can be done very differently.

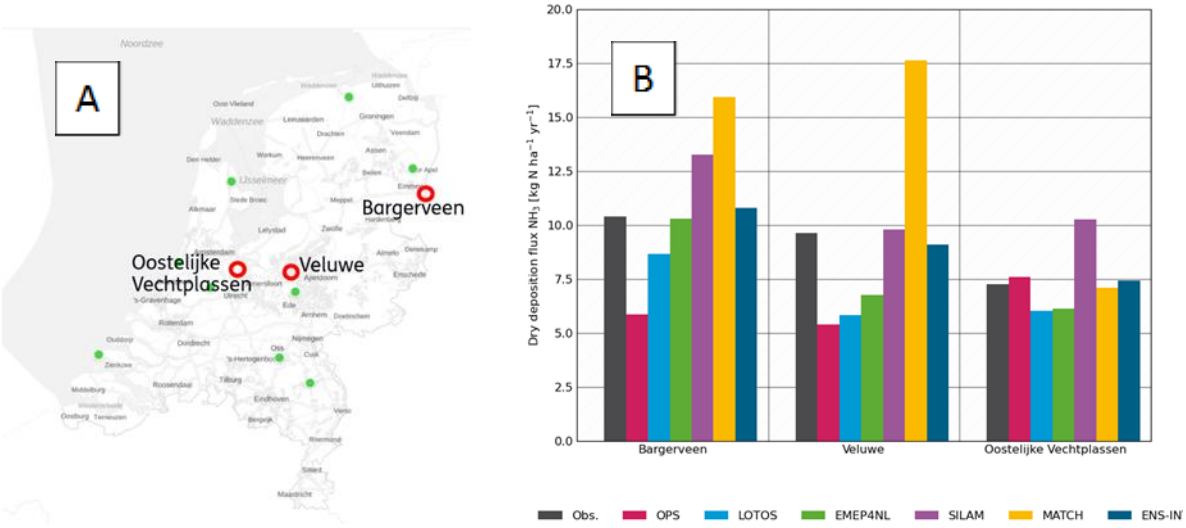

Figure 20: A) Locations of NH_3 dry deposition measurements with COTAG instruments in the Netherlands, as part of the LML (Landelijk Meetnet Luchtkwaliteit) as operated by RIVM. B) Simulated and observed dry deposition flux values of NH_3 at the three stations, annual total for the year 2019.

Simulated and observed dry deposition flux values of NH_3 at the three COTAG measurement stations are depicted in Figure 20. These results should be interpreted as very indicative as the land uses in the foot print of the measurements may not reflect those model grid cells. The modelled fluxes represent the flux calculated for the land use mosaic of the grid cell in which the station is located. The results show that the models can vary by about a factor 2 around the observation. Surprisingly, the mean of all models performs perfectly in line with the observations, which can of course be purely coincidental. Also notice that the measurements take place in areas where typically 500 eq ha^{-1} yr^{-1} is measured, whereas the country mean modelled values are typically 1000 eq ha^{-1} yr^{-1}.
The currently ongoing extension of the COTAG network to 10 locations may provide a better basis for future model evaluation studies. In this respect, it is important to mention that more detailed flux measurements are also ongoing and planned, which enable to evaluate dry deposition parameterizations in detail, in so-called “diagnostic evaluation”.

4.2.4 Wet deposition

Focusing on the NH_x wet deposition, we see the low bound at 220 (SILAM) and high bound at 374 (OPS) eq ha^{-1} yr^{-1}. EMEP4NL (308), LOTOS (330) and MATCH (356) are within those bounds. All models show an east-west gradient across the Netherlands, where values in the west are lower and values in the east are higher. The strength of the gradient varies between the models. It is strongest in OPS and MATCH and less pronounced in EMEP4NL and SILAM. All models indicate increased wet deposition across the ammonia source regions. Ammonia, which is highly water soluble, is thus effectively removed by washout in source regions. The spatial gradients in the wet deposition of NH_x is lower than that in ammonia concentrations or in dry deposition of NH_x. The reason is twofold. First, rain droplets fall though a column of air. Close to sources the average concentrations near the ground are larger due to the plumes of local sources. These plumes have not yet fully mixed into the full mixing layer. Hence, the concentration at the ground shows more variability than the

column mean concentrations. Second, particulate ammonium (NH_4^+) also contributes significantly to the NH_x wet deposition and this secondary component shows much less spatial variability than ammonia. The international model MATCH shows a similar pattern and total wet deposition to the that of the Dutch models. The wet deposition of NH_x of SILAM is lower than that of all other models, and the pattern shows little spatial differentiation.

Figure 21A shows the locations of the wet deposition fluxes as used in this study. In Figure 21B the simulated and observed annual total wet deposition fluxes at the 8 LML-stations for the year 2019 are depicted. The stations are ordered from (south)west to north(east). The most western stations in Phillippine, De Zilk, and Wieringerwerf, show the lowest observed and predicted NH_x wet deposition. In fact, the observations confirm the general west-east gradient depicted in the results of all models. Except that SILAM is clearly too low everywhere, it is hard to see a general picture in the comparison. MATCH yields the lowest biases to the observations. The modelled fluxes by OPS are quite comparable those measured at 5 of the 8 stations. The region close to the German border (Twente and Achterhoek) where the difference between the models is the largest is unfortunately not covered by Dutch stations. At the 2 stations close to the border to the south (Vredepeel) and north (Valthermond) OPS overestimates observed wet deposition fluxes.

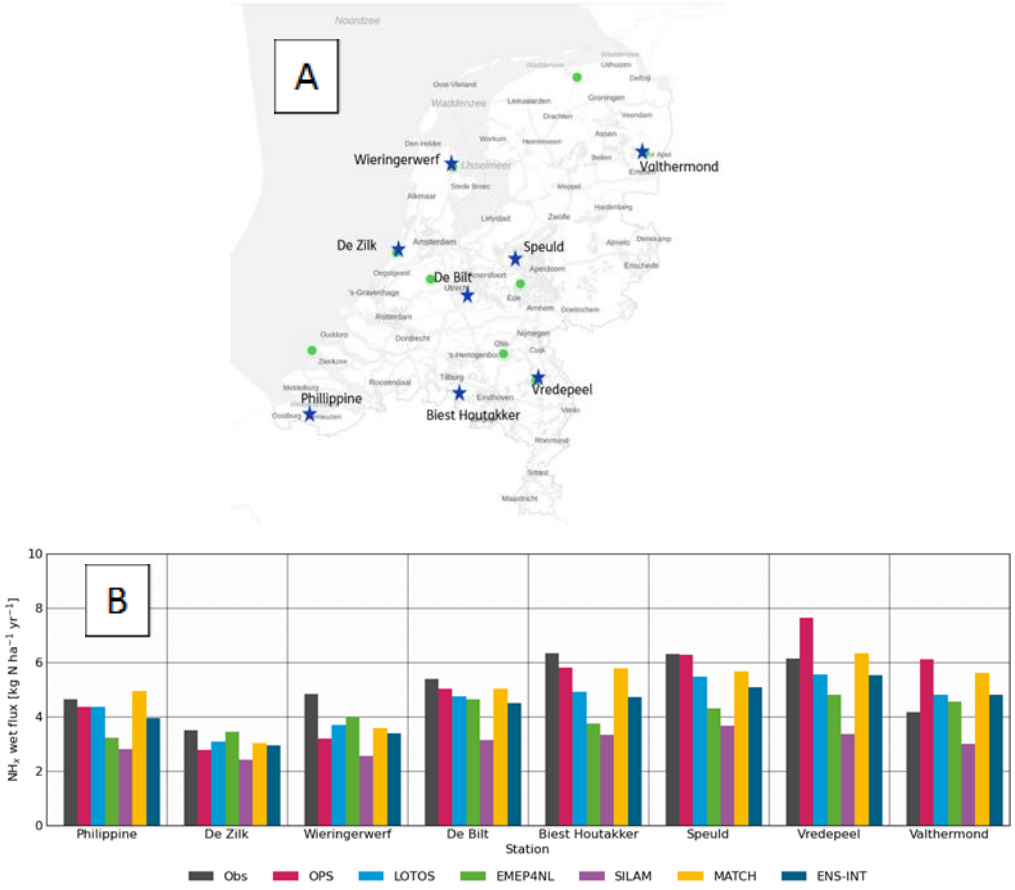

Figure 21: A) Locations of the observations of wet deposition fluxes of NH_x as used in this study, indicated with the blue stars. B) Simulated and observed NHx annual total wet deposition flux values at LML-stations for the year 2019. The locations are ranked from west to east. The five included models are: OPS, LOTOS-EUROS and EMEP4NL (all Dutch), SILAM (Finnish) and MATCH (Swedish).

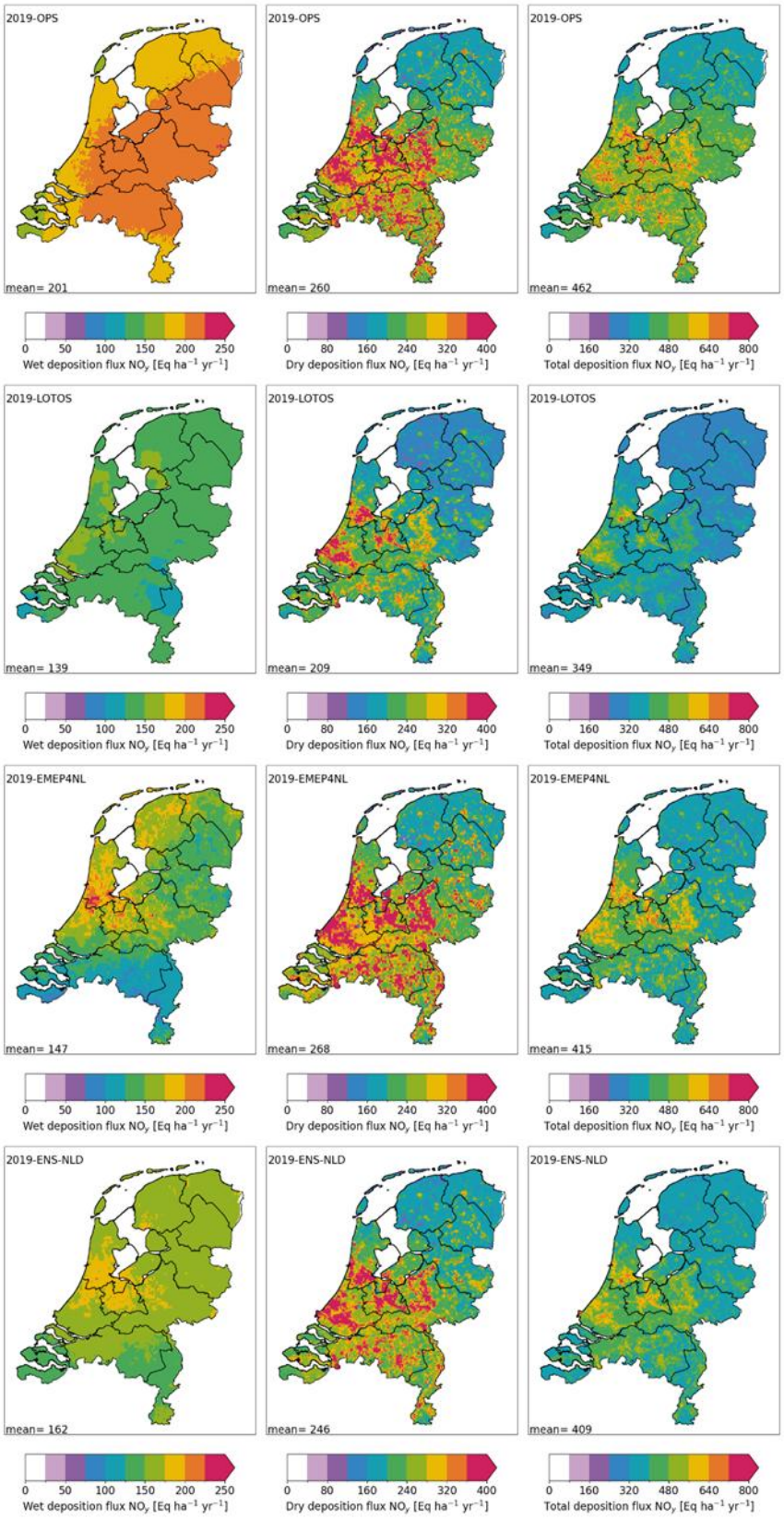
2019-OPS
mean= 201
2019-OPS
mean= 260
2019-OPS
mean= 462
0 50 100 150 200 250
Wet deposition flux NOy [Eq ha-1 yr-1]
0 80 160 240 320 400
Dry deposition flux NOy [Eq ha-1 yr-1]
0 160 320 480 640 800
Total deposition flux NOy [Eq ha-1 yr-1]
2019-LOTOS
mean= 139
2019-LOTOS
mean= 209
2019-LOTOS
mean= 349
0 50 100 150 200 250
Wet deposition flux NOy [Eq ha-1 yr-1]
0 80 160 240 320 400
Dry deposition flux NOy [Eq ha-1 yr-1]
0 160 320 480 640 800
Total deposition flux NOy [Eq ha-1 yr-1]
2019-EMEP4NL
mean= 147
2019-EMEP4NL
mean= 268
2019-EMEP4NL
mean= 415
0 50 100 150 200 250
Wet deposition flux NOy [Eq ha-1 yr-1]
0 80 160 240 320 400
Dry deposition flux NOy [Eq ha-1 yr-1]
0 160 320 480 640 800
Total deposition flux NOy [Eq ha-1 yr-1]
2019-ENS-NLD
mean= 162
2019-ENS-NLD
mean= 246
2019-ENS-NLD
mean= 409
0 50 100 150 200 250
Wet deposition flux NOy [Eq ha-1 yr-1]
0 80 160 240 320 400
Dry deposition flux NOy [Eq ha-1 yr-1]
0 160 320 480 640 800
Total deposition flux NOy [Eq ha-1 yr-1]

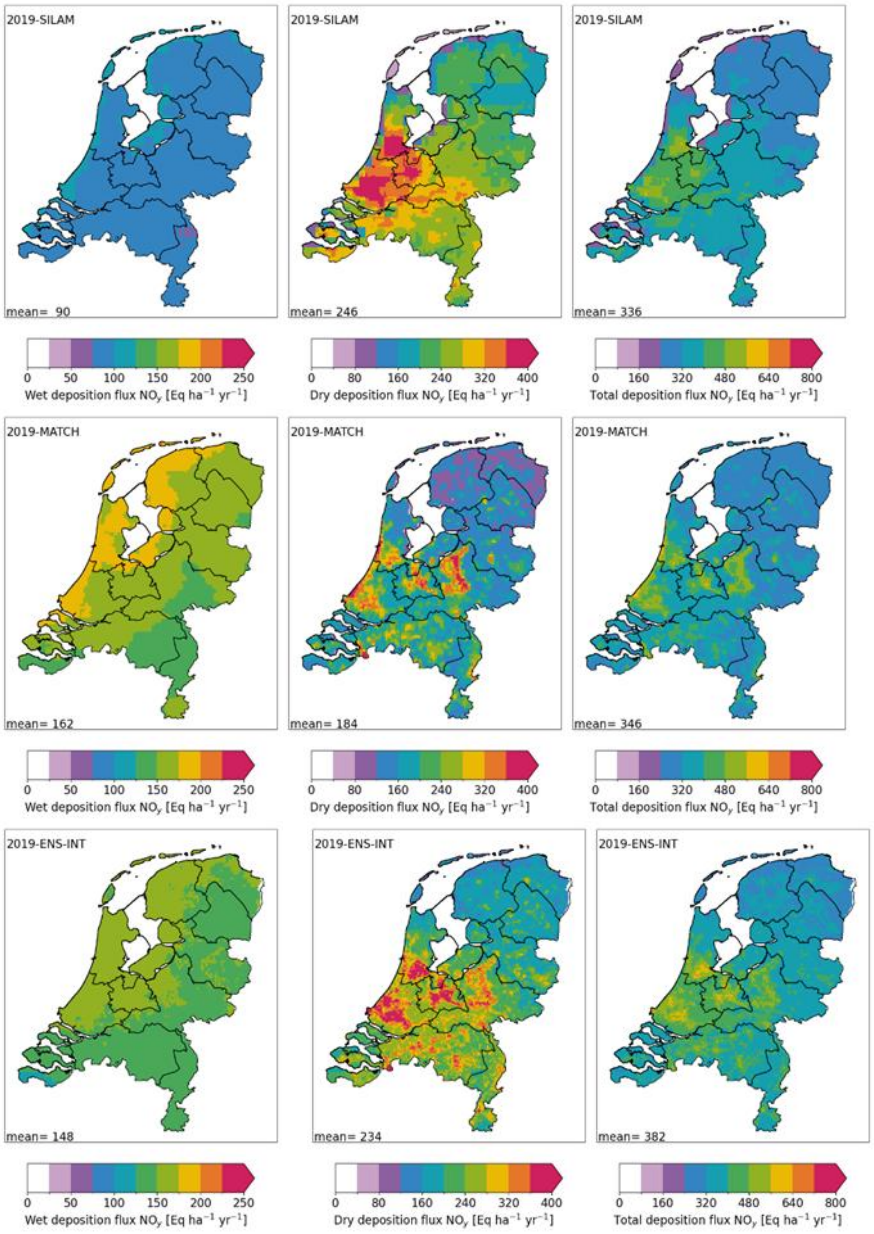

Figure 22: Deposition fluxes of NO_y in the three Dutch models (OPS, LOTOS-EUROS, EMEP4NL), their ensemble, the two international models (MATCH, SILAM) and the ensemble of all models. All data are averaged for the year 2019. Left column: Wet deposition fluxes, Middle column: Dry deposition fluxes, Right column: Total deposition fluxes, which equals the sum of the wet and dry deposition fluxes.

4.3 Oxidized nitrogen (NO_Y) deposition

4.3.1 Overview

Figure 22 provides an overview of the modelled annual total wet, dry and total NO_y deposition flux for all models in this benchmark study for the year 2019. The modelled average total NO_y deposition over the Netherlands varies between 336 (SILAM) and 462 eq ha^{-1} yr^{-1} (OPS). EMEP4NL (415), LOTOS (349) and MATCH (346) models provide results in between these ensemble bounds. The models do not agree on the relative importance of dry and wet deposition. OPS and MATCH show almost equal wet and dry fluxes on average, whereas LOTOS and EMEP4NL indicate ratios of dry to wet deposition to be closer to 2:1 on average. SILAM provides the largest ratio as it predicts the second largest average dry NO_y deposition and the lowest wet NO_y deposition of all models.

4.3.2 Ensemble mean and spread

Deposition of NO_y

The ensemble mean modelled contribution of oxidized nitrogen (382 eq ha^{-1} yr^{-1}) to total N deposition varies between 21 and 32 %. The model outcomes vary considerably regarding the contributions of dry and wet deposition to total oxidized nitrogen deposition. The dry NO_y deposition shows a spatial pattern with maxima around the cities and industrial regions. In addition, the ensemble mean shows the contours of the main transport corridors (highways and waterways). This is of course explained by the underlying emission pattern of nitrogen oxides. The secondary maxima can be found in the forested areas of the Veluwe. The relative standard deviation of the dry NO_y deposition is on average 19 %. Except for some small areas, mainly close to the coast, the relative standard deviation hardly exceeds 25 %. Also, no clear spatial pattern is recognizable. For wet deposition of NO_y, a larger country average standard deviation of 26 % is found. The ensemble spread (Figure 23) shows a clear spatial pattern that shows a resemblance to the distribution of the ensemble spread for wet NH_x deposition. Maximum relative standard deviations are found in the southeast of the country, up to ~35 %.

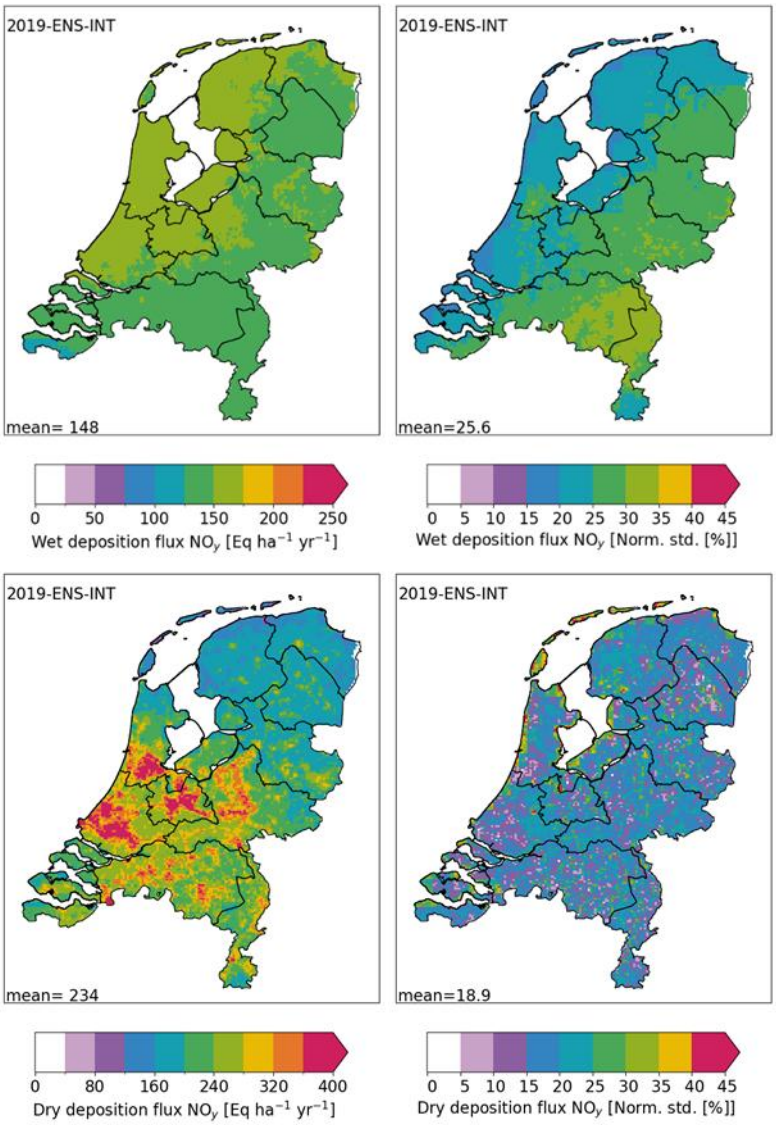

Figure 23: Left panels: Ensemble mean for all five models of wet (top) and dry (bottom) deposition of NO_y on the Netherlands. Right panels: Normalized standard deviation [%] of the models is shown for both components.

4.3.3 Dry deposition

In the middle panels of Figure 22, the modelled distributions of the annual total NO_y dry deposition across the Netherlands are presented. The modelled annual dry NO_y deposition averaged over the Netherlands varies between 184 (MATCH) and 268 eq ha^{-1} yr^{-1} (EMEP4NL). The OPS (260), SILAM (246) and LOTOS (209) models provide results in between these ensemble bounds, with the ensemble value of 233 eq ha^{-1} yr^{-1}. The NO_y dry deposition is a sum of several components. The differences in the modelled spatial distributions can be largely explained by the variable contributions of these components. In fact, the differences between the modelled NO_y national mean total deposition means are almost one to one explained by the differences in the dry deposition flux of NO_x ($NO+NO_2$), as the country means for nitric acid and particulate nitrate are rather consistent. The clear imprint of the road network in the OPS distribution results from the relatively large contribution of NO_x dry deposition.

Unfortunately, there are no observations of the dry deposition for oxidized nitrogen components available within the monitoring networks. Hence, it is not possible to say anything about the realism of the modelled NO_2 contributions.

With the method described in section 3.6, the effective dry deposition velocities for NO_x (NO + NO_2) were calculated for each model for the most important land use classes. The results are shown in Figure 24. Note that these values are not available for MATCH, because the deposition flux is not available for NO_x (only for NO_y). The figure shows that OPS has higher effective deposition velocity values for all land use classes than LOTOS, even though these model use the same dry deposition scheme to calculate the surface resistance used in the dry deposition calculation. Hence, it is likely that the covariance between the modelled concentrations and the deposition velocity in OPS differ from those of LOTOS.

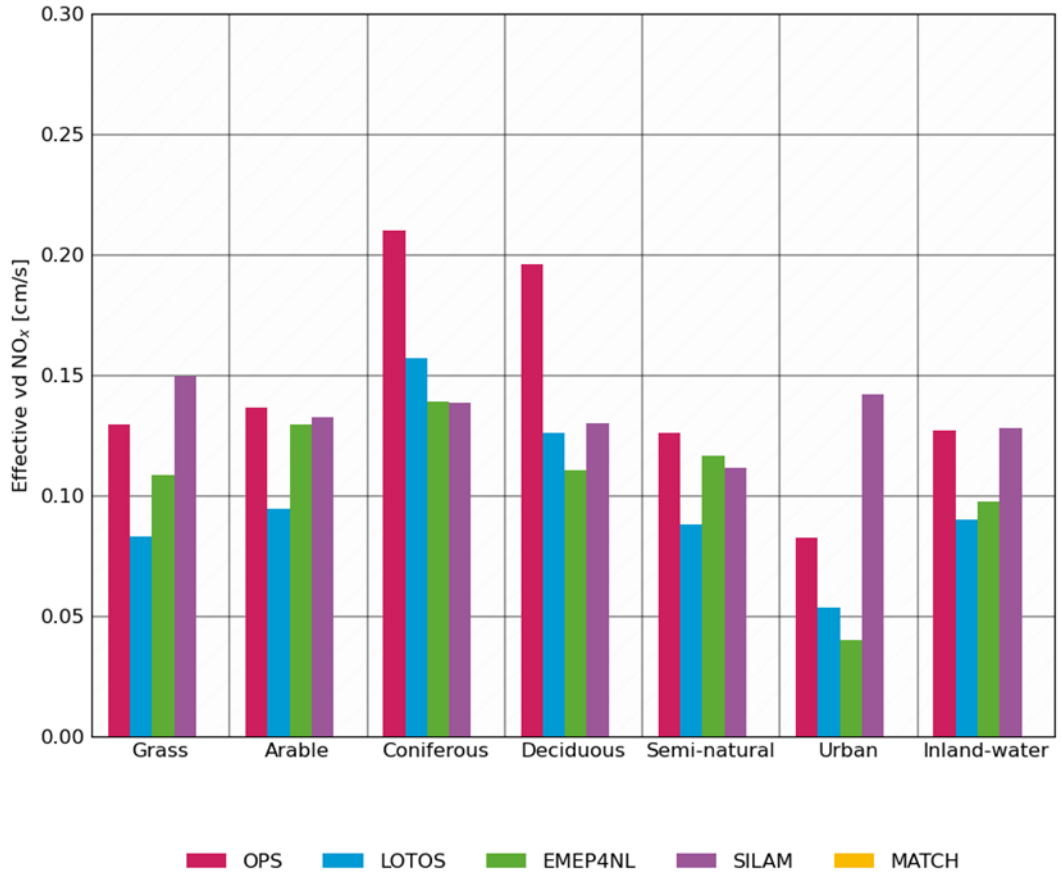

Figure 24: The effective dry deposition velocity of nitrogen dioxide (NO_x) over various land use types in the Netherlands, as obtained from the different models, averaged over the year 2019. The land use classification includes grass, arable land, coniferous forest, deciduous forest, semi-natural vegetation, urban areas and inland water.

4.3.4 Wet deposition

Most models show the largest NO_y wet deposition in the northwest of the Netherlands during 2019. The exception is the OPS model, which produces a maximum NO_y wet deposition across the east of the country. Inspection of the results for the other years (2016-2019 shown in Figure 25) shows that the OPS model produces a similar pattern each year with lower totals in dryer years than in wetter years, whereas the other models show a

spatial distribution pattern that varies from year to year. The variability in the NO_y wet deposition is much more dependent on the rain distribution than NH_x wet deposition. This is because the primary NO_x compounds are poorly soluble in water. In addition, the concentration of the secondary, readily solvable components, and of particulate nitrate, shows relatively little variability across the country. Hence, the variability must be largely due to the variability of the precipitation field.

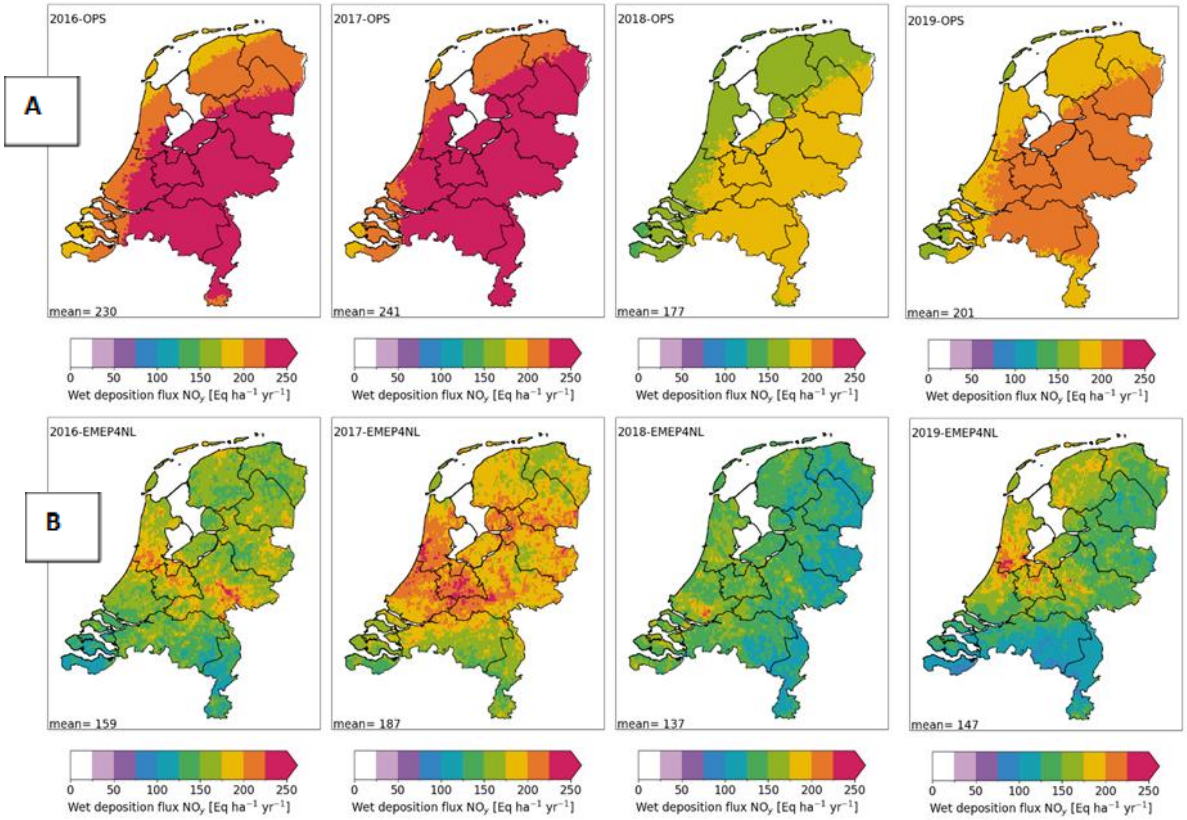

Figure 25: Simulated wet deposition flux of NO_y for the year 2016 to 2019 for the models A) OPS and B) EMEP4NL.

Figure 26 shows the measured and modelled wet deposition fluxes of NO_y at eight LML measurement stations in 2019. OPS has the largest wet deposition fluxes and tends to overestimate, especially at the stations located in the east of the country. MATCH and EMEP4NL show rather comparable picture to the observations, whereas the LOTOS and SILAM models are systematically underestimating. The precipitation fields are very similar in these models. We conclude that the removal efficiency for the latter models may need to be addressed. As the interannual variability in OPS does not respond to that in precipitation patterns, the treatment of the precipitation information needs to be addressed in OPS.

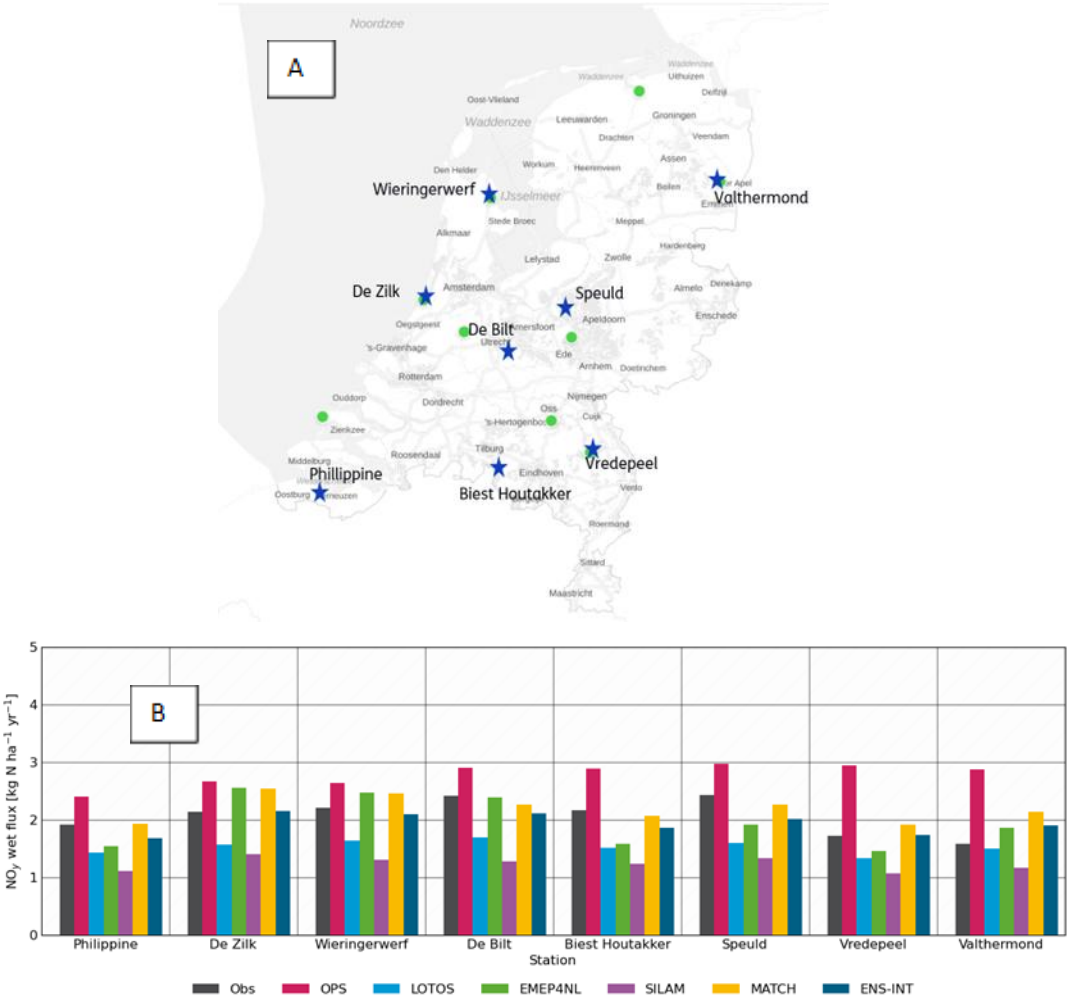

Figure 26: A) Measurement locations of NO_y wet deposition in the LML measurement network, indicated by blue stars. B) Annual total NO_y wet deposition fluxes measured and modelled at eight Landelijk Meetnet Luchtkwaliteit (LML) measurement stations for the year 2019. Models included are: three Dutch models (OPS, LOTOS-EUROS, EMEP4NL); two international models (MATCH, SILAM) and the ensemble of the five models.

4.4 Concentrations of reduced nitrogen (NH_X) compounds

4.4.1 Ensemble mean and spread

The modelled annual mean concentrations of ammonia (NH_3) vary about a factor of 10 within the Netherlands (Figure 27). At the coastline the ensemble mean concentrations for 2019 are close to 2 µg m^{-3}, whereas values around 20 µg m^{-3} are found in the areas with the largest animal husbandry densities in the centre (Gelderse Vallei) and the southeast (de Peel) of the country. Large areas of the eastern part of the country show concentrations between 6 and 14 µg m^{-3}.
A country mean relative standard deviations of 23 % is found. The modelled concentrations in the hotspot areas are shown to have the largest spread between the models, with

maximum relative standard deviations of 40 %. Over large parts of the country, the spread varies between 15 and 25 %. Some regions, such as the east of Drenthe and Groningen, and the area between the largest cities, called the “Groene Hart” (“Green Heart”) also show standard deviations above the average (~30 %). For particulate ammonium (NH4-aer) the mean concentration is about 1.5 µg m^{-3}, with largest concentrations modelled in parts of Gelderland and Noord Brabant. The average relative spread for ammonium is found to be 30 %, which is larger than for ammonia, and shows a clear south to north gradient.

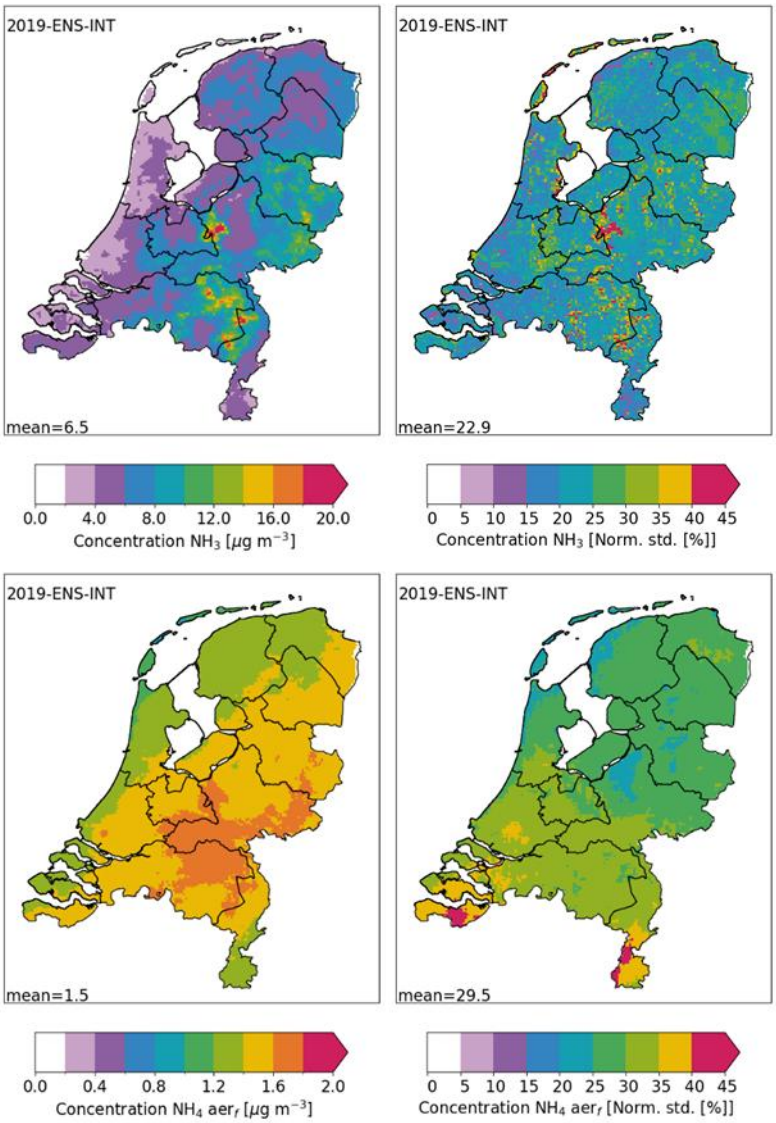

Figure 27: Left panels: Ensemble mean for all five models of concentrations of NH_3 (top) and pNH_4^+ (bottom) in the Netherlands. Right panels: Normalized standard deviation [%] of the models is shown for both components.

Ammonia

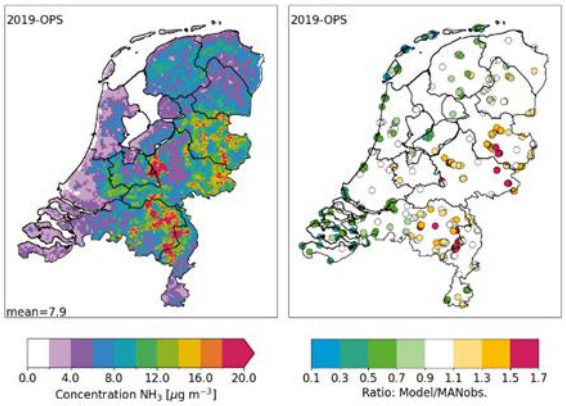

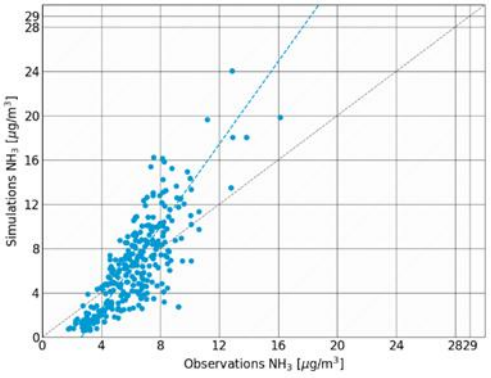

OPS; y=1.86x + -4.95; r^2=0.68; RMSE=2.66; NMB=0.06

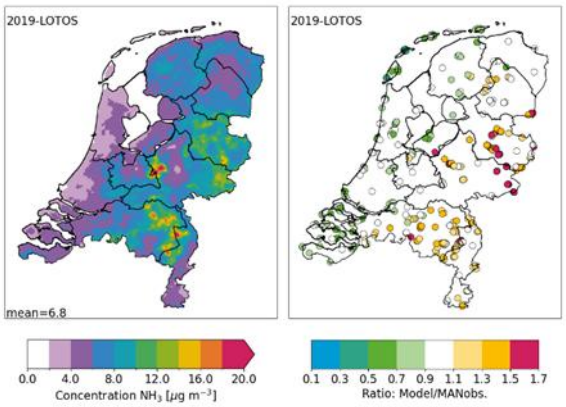

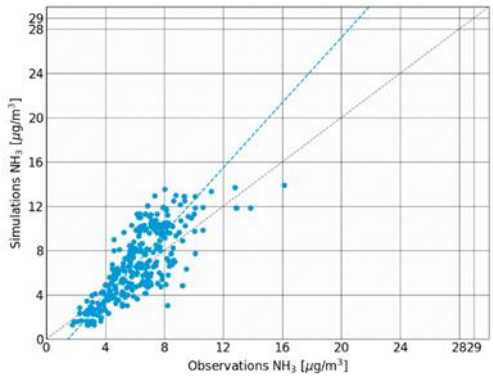

LOTOS; y=1.47x + -2.16; r^2=0.62; RMSE=2.16; NMB=0.12

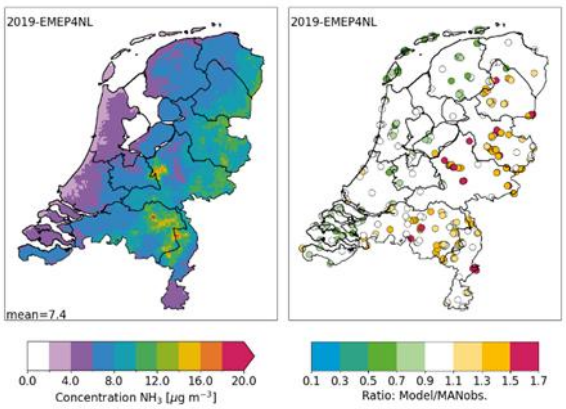

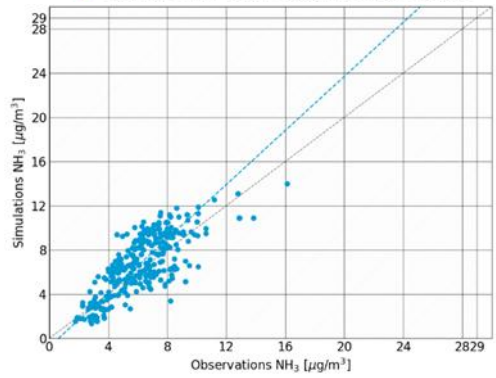

EMEP4NL; y=1.22x + -0.76; r^2=0.60; RMSE=1.82; NMB=0.10

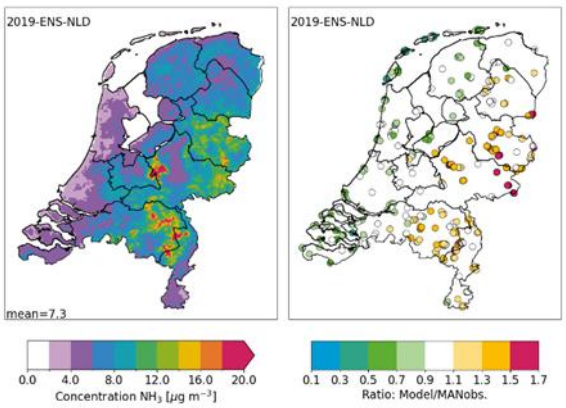

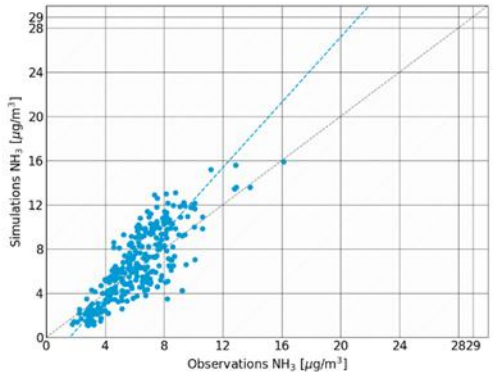

ENS-NLD; y=1.48x + -2.35; r^2=0.67; RMSE=2.01; NMB=0.09

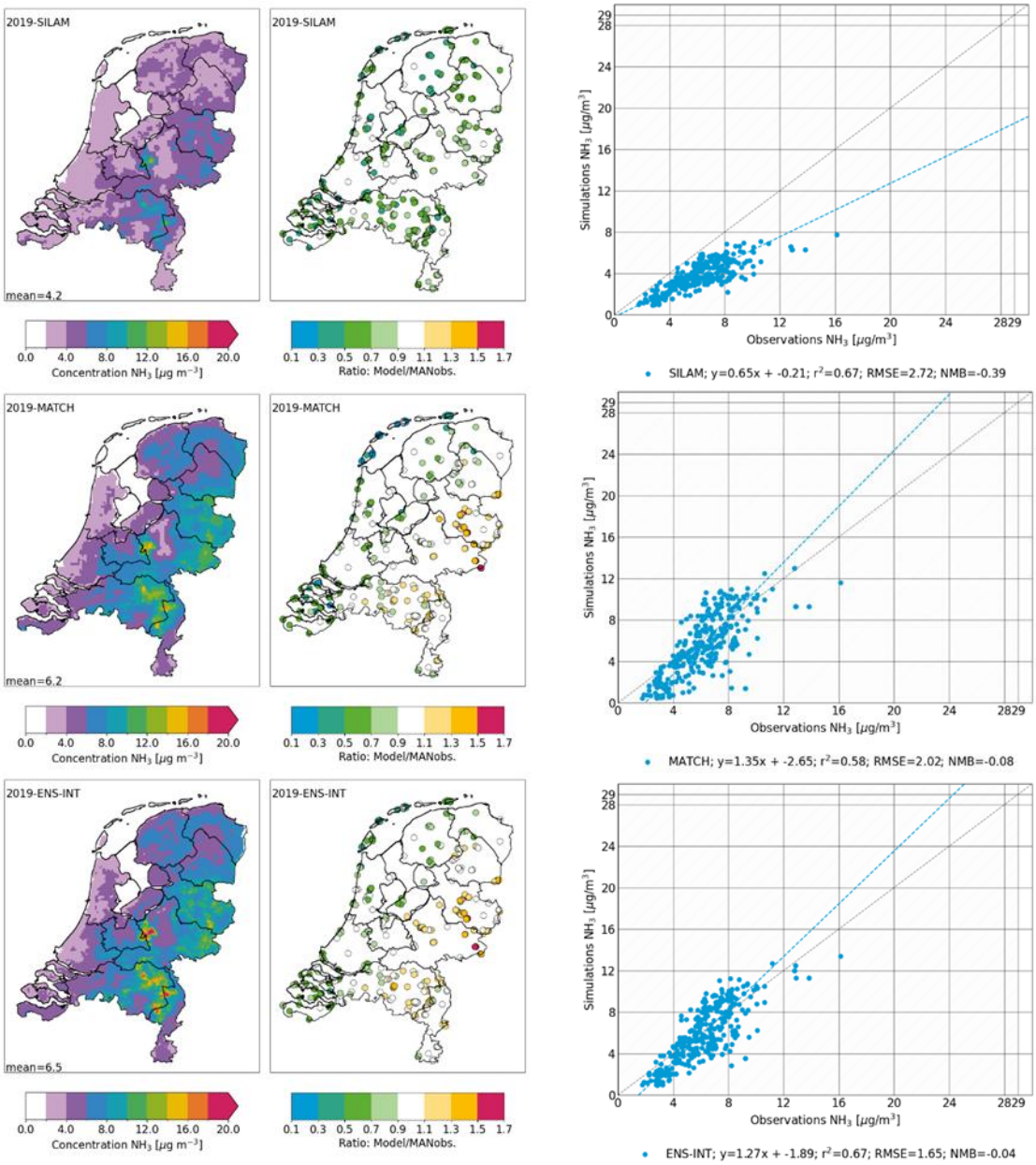

Figure 28: Comparison of the five models and ensembles, each showing yearly averaged ammonia (NH_3) concentrations in the Netherlands in 2019. Left plots: Modelled concentrations of NH_3 by the five models, first the Dutch models: OPS, LOTOS and EMEP4NL and their mean concentration in the ensemble, next the international models: SILAM and MATCH and the mean concentration of all five models in the extended ensemble. Middle plots: Ratios of modelled concentrations over the observed concentration values, first the Dutch models, next the international models. Right plots: Scatter plots of the modelled NH_3 concentrations and the observations of the MAN measurement network, following the same order of models as the left and middle columns.

4.4.2 Concentrations

In Figure 28, left panels, the modelled annual average ammonia (NH_3) concentration distributions over the Netherlands for 2019 are shown. All models show lower concentrations in the west of the Netherlands and higher concentrations in the east. The maxima reflect those in the emission inventory and correspond with the regions with intense animal husbandry (pigs and poultry). Additionally, all models show lower values in

the far southeast of the country (Zuid-Limburg). The Dutch models show country average values in the range of 6.8 to 7.9 µg m^{-3}. The OPS model shows a larger dynamic range in modelled concentrations than LOTOS and EMEP4NL. Strikingly, the average NH_3 concentrations modelled by the international models SILAM and MATCH are overall significantly lower. This causes lower overall values in the international ensemble, that includes all five models.

In the middle panel of Figure 28, we show the ratio of the modelled annual mean concentrations of NH_3 to those observed in the MAN measurement network. The three models used in the Netherlands (OPS, LOTOS, EMEP4NL) all show a higher model value in the east, compared to the measurements, while in the west, the model values are lower than those of the measurements. The Swedish MATCH model also shows this pattern, but to a lesser extent. Only the Finnish SILAM-model does not show this spatial pattern. In other words, all models except SILAM underestimate low concentrations and overestimate high concentrations. This is also shown in the scatterplots of the comparison, which are shown in the right panel of Figure 28. EMEP4NL shows less spatial gradients and generally overestimates more observation locations. In contrast to the Dutch models, the international models show an overall underestimation of the model compared to the MAN observations. Similar to the Dutch models, the MATCH model does show the same S-shape in the scatter plot. This illustrates greater underestimations for low observed values and smaller underestimations, even some overestimation, for high observed values.

Spatial correlations, in terms of r^2, vary from 0.60 (EMEP4NL) to 0.68 (OPS) for the individual models. While RMSE and NMB values are similar for the different models, EMEP4NL provides the lowest mean deviation from observations, with an RMSE of 1.82 µg m^{-3} and an NMB of 0.10. The indicator values of the ensemble resembles those of the values of the 'best' performing model for each indicator. All statistics for all models and other years (2016-2019) can be found in 0.

In Figure 29A, we see the locations of the six LML 'Landelijk Meetnet Luchtkwaliteit' measurement stations of NH_3 concentrations that are used in this study. Figure 29B shows the annual average modelled and measured concentrations of NH_3 for the six LML sites. The sites are located in regions with different intensity of animal husbandry in the Netherlands and therefore show a large range of observed mean ammonia concentrations. It is seen that for the two stations in the coastal west of the country, Wieringerwerf, and the De Zilk, all models underestimate the observed annual mean. The OPS model results approaches the observed values for the Vredepeel and Zegveld stations. At these two locations, all other models underestimate the observation. OPS overestimates the observations of the Wekerom station, while the other models (slightly) underestimate the observations at this station. Unfortunately, there is no LML location in the region of overestimations in Gelderland and Overijssel identified in the comparison to the MAN network. The spread between the lowest and highest concentration modelled by the individual models at a station is typically a factor of 2 to 3. The largest range is found for the stations in the agricultural source regions.

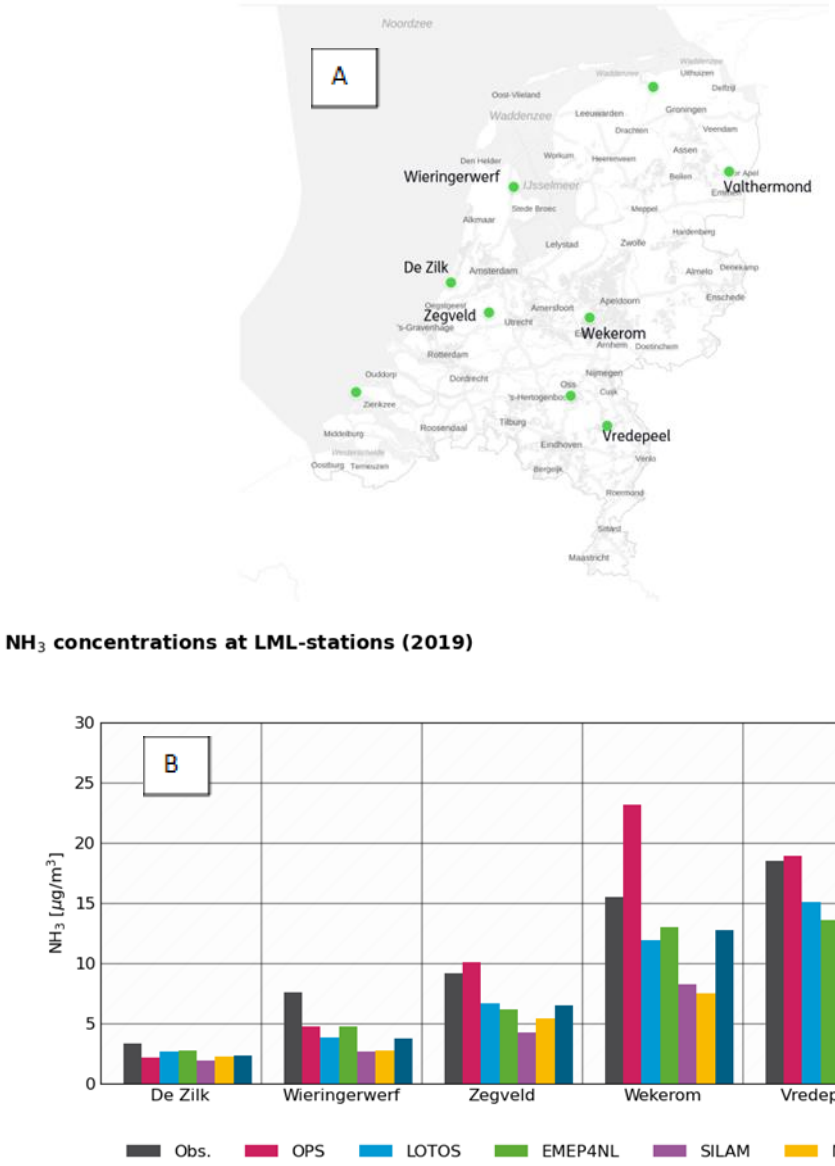

Figure 29: A) The LML-stations used in this study that measure ammonia (NH_3) concentrations in the Netherlands, indicated by their location name and corresponding green dots. B) Average modelled and measured concentrations of ammonia (NH_3) in the year 2019 at said 6 Dutch national measurement stations of the 'Landelijk Meetnet Luchtkwaliteit' (LML) measurement network. Modelled concentrations for the five models included in this study, the Dutch ensemble, and the total ensemble.

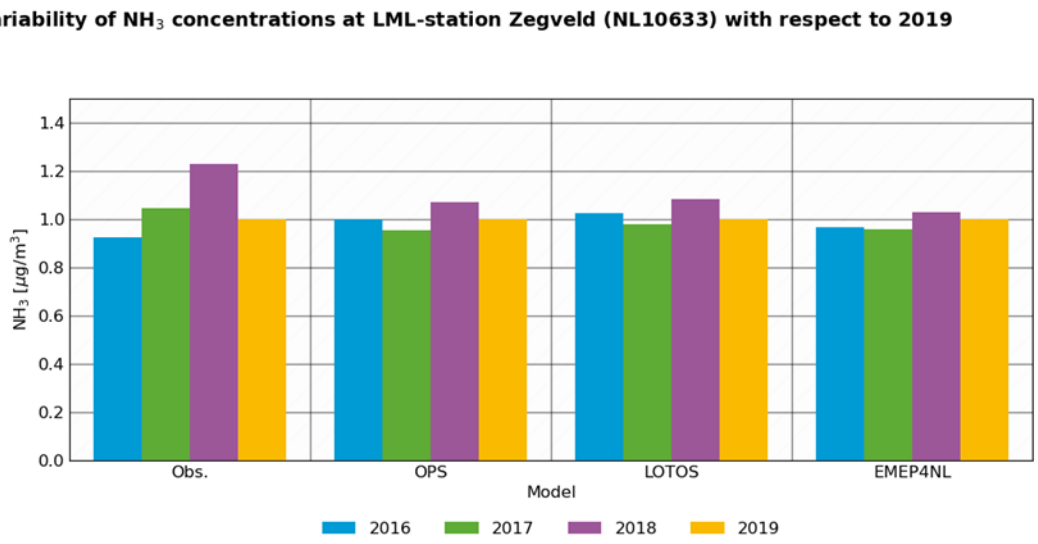

Figure 30: Observed and modelled NH_3 concentrations of the years 2016 to 2019 for the 'Zegveld' measurement station relative to the observed/modelled concentration of 2019.

Figure 30 illustrates the observed and modelled concentrations at the LML measurement stations in Zegveld for the years 2016-2019, normalized to the (observed and modelled) concentrations of 2019. In this figure, we see that the variability between the years is relatively large for the observations. Especially in 2018, which was a very dry and warm year, the observed NH_3 concentration is relatively high. However, this observed variability is hardly captured by the models. All models simulate rather constant annual NH_3 concentrations across the years, with only small increments for 2018. This indicates that models can improve their performances by using weather-dependent emissions for NH_3. For example, emissions of NH_3 are higher in warm periods, while this is currently not reflected by the models. Also OPS, which includes a simple approach to incorporate weather impacts on emission, does not show different results in comparison to LOTOS or EMEP4NL.

Particulate ammonium

Annual mean distributions of particulate ammonium (pNH_4^+) as modelled by all systems is shown in Figure 31. As for ammonia, the ensemble range is bound at the low and high bound by SILAM and MATCH, respectively. Except OPS all models show lower concentrations northwest and southeast of a band with similar levels across the country from Zeeland to Groningen. Whereas there is a slight indication of increased particulate ammonium concentrations in the source areas of NO_x and SO_2 (Rotterdam, Amsterdam) in models such as EMEP and LOTOS, the concentrations simulated by OPS are correlated with the ammonia emission distribution. The difference between the models is likely related to the way the particulate matter formation is treated. In the Eulerian models, the ammonium formed is limited by the formation of ammonium nitrate and ammonium sulphate. Hence, ammonium cannot be formed without its counterparts. The ammonium nitrate formation and concentrations are sensitive to meteorological conditions, with limited formation during hot summer conditions and effective formation during cold winter conditions (as discussed in the previous section). In OPS the particulate matter formation is represented by applying the annual average formation rate from the EMEP4NL model. This approach linearizes the many non-linear effects of weather and availability of reactants during the year and does not limit the ammonium formation to the available sulphate and nitrate. As such, the linearized formation rate applied will mirror the pattern of the ammonia emissions.

The comparison to the observations in Figure 32 shows that, except for SILAM, there is a tendency to overestimate the observed concentrations. The results of LOTOS and EMEP4NL are very close together. MATCH shows considerably larger concentrations than the other models. The time series in section 4.7 show that these patterns of overestimation are visible throughout the year, although LOTOS, SILAM and EMEP4NL follow a seasonal pattern, while the higher values of MATCH are explained by the summer time values.

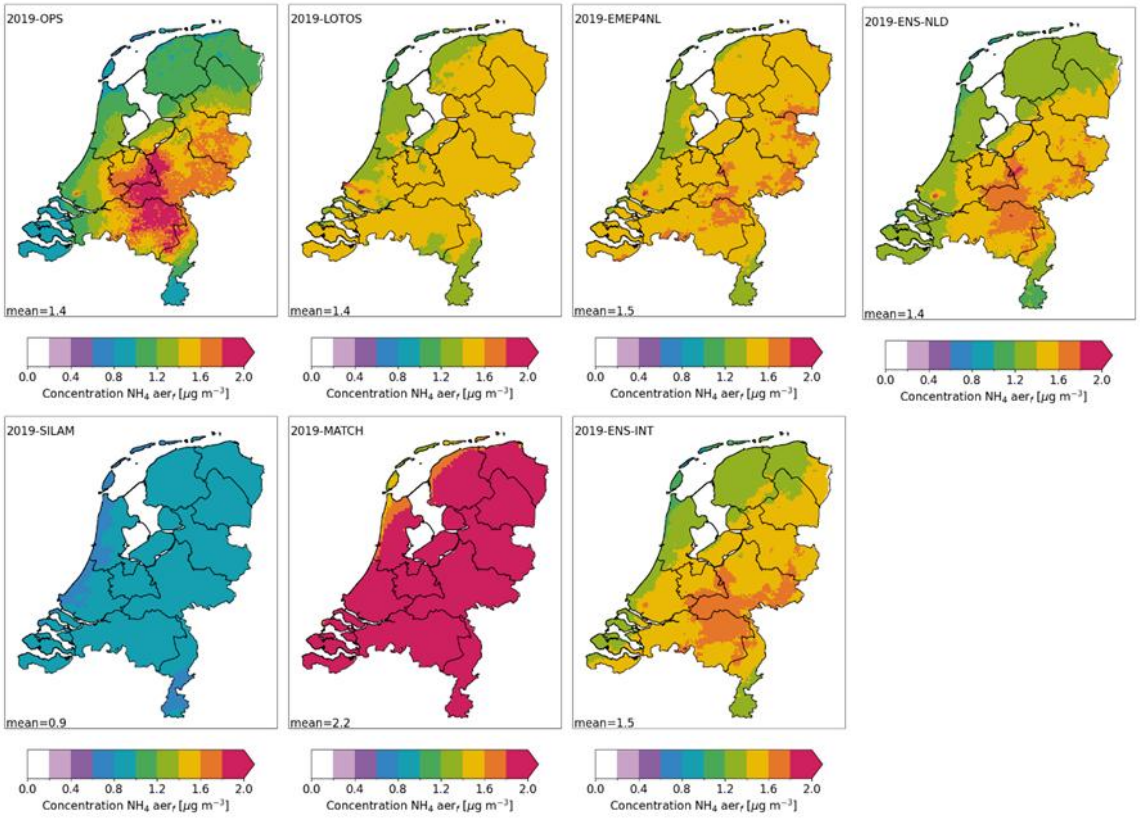

Figure 31: Concentrations of the fine portion of pNH_4^+ particles as modelled across the Netherlands by the models included in this study, the ensemble of the three Dutch models (ENS-NL), and the ensemble of the five models (ENS-INT).

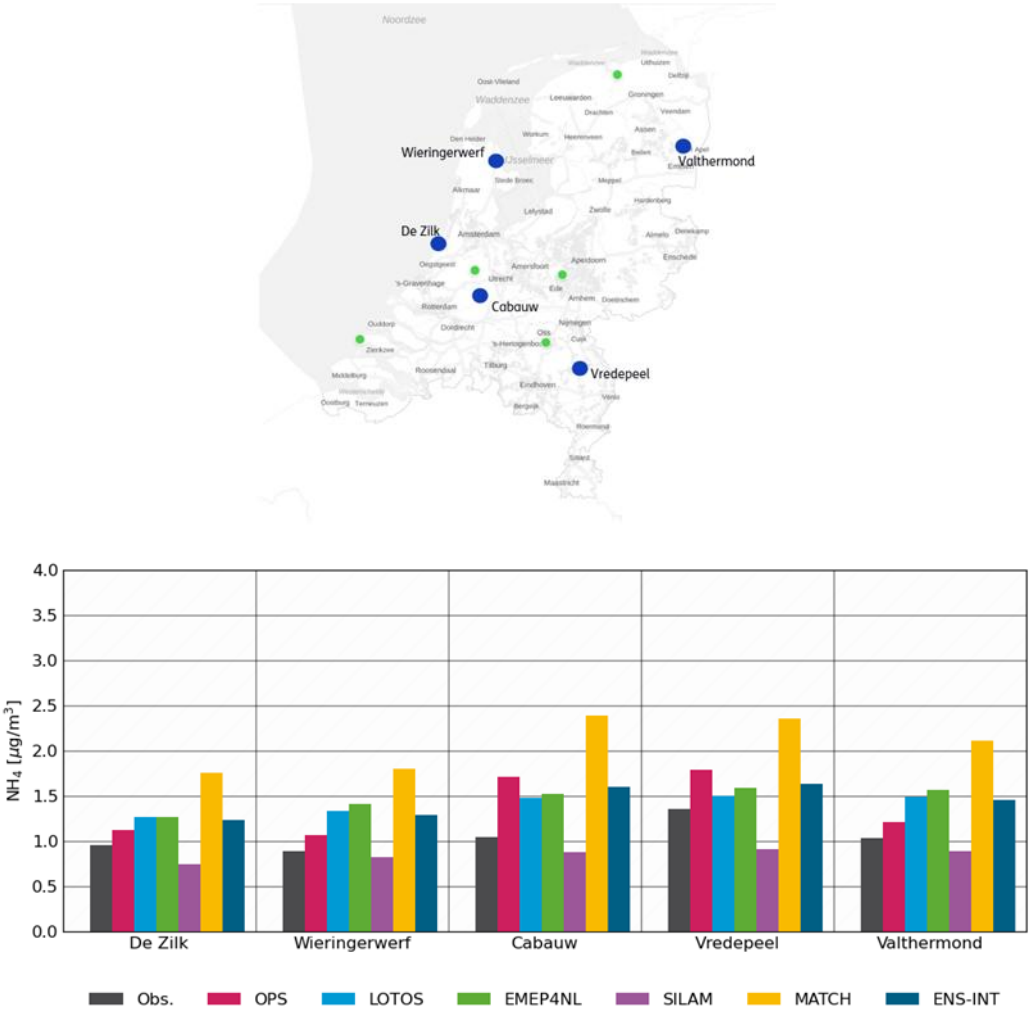

Figure 32: A) Measurement locations of concentrations of pNH_4^+ in particulate matter as measured at the LML measurement stations. Locations indicated with blue dots and location names. B) Observed and modelled values of pNH_4^+, at the measurement stations, by the models used in this study and their ensemble.

4.5 Concentrations of oxidized nitrogen (NO_y) compounds

4.5.1 Ensemble mean and spread

For oxidized nitrogen compounds nitrogen dioxide, nitric acid and particulate nitrate are most important (Figure 33). The modelled annual mean NO_2 concentration shows maxima in the urban areas, with declining concentrations away from the source areas. Nitric acid (HNO_3) shows a pattern opposite to that of ammonia. In other words, in areas with little ammonia, e.g. along the coastline, the nitric acid concentrations are relatively large and in the areas with the largest ammonia concentrations the lowest nitric acid levels are modelled. This is explained by the reaction of nitric acid with ammonia to form ammonium

nitrate. The particulate nitrate (pNO_3^-) levels (4.3 µg m^{-3} on average) hardly show any gradient, but small enhancements in the ammonia source regions. The standard deviation around the ensemble mean is small for NO_2. Averaged over the country the normalized standard deviation is only 5 %, with maxima of about 15 % further away from the main source areas in, e.g., Zeeland. For HNO_3, the spread is on average larger (12 %) with clearly higher values in the northern part of the country as well as in the coastal areas. The spread between the model outcomes for particulate nitrate is on average comparable to the one for HNO_3, but the spatial pattern shows a maximum in the southeast of the country.
The results for the oxidized N components illustrate that the uncertainty in the modelled concentrations are typically smaller than in the modelled dry and wet deposition fluxes. This means that the differences in the deposition routines applied in the models result in larger uncertainties.

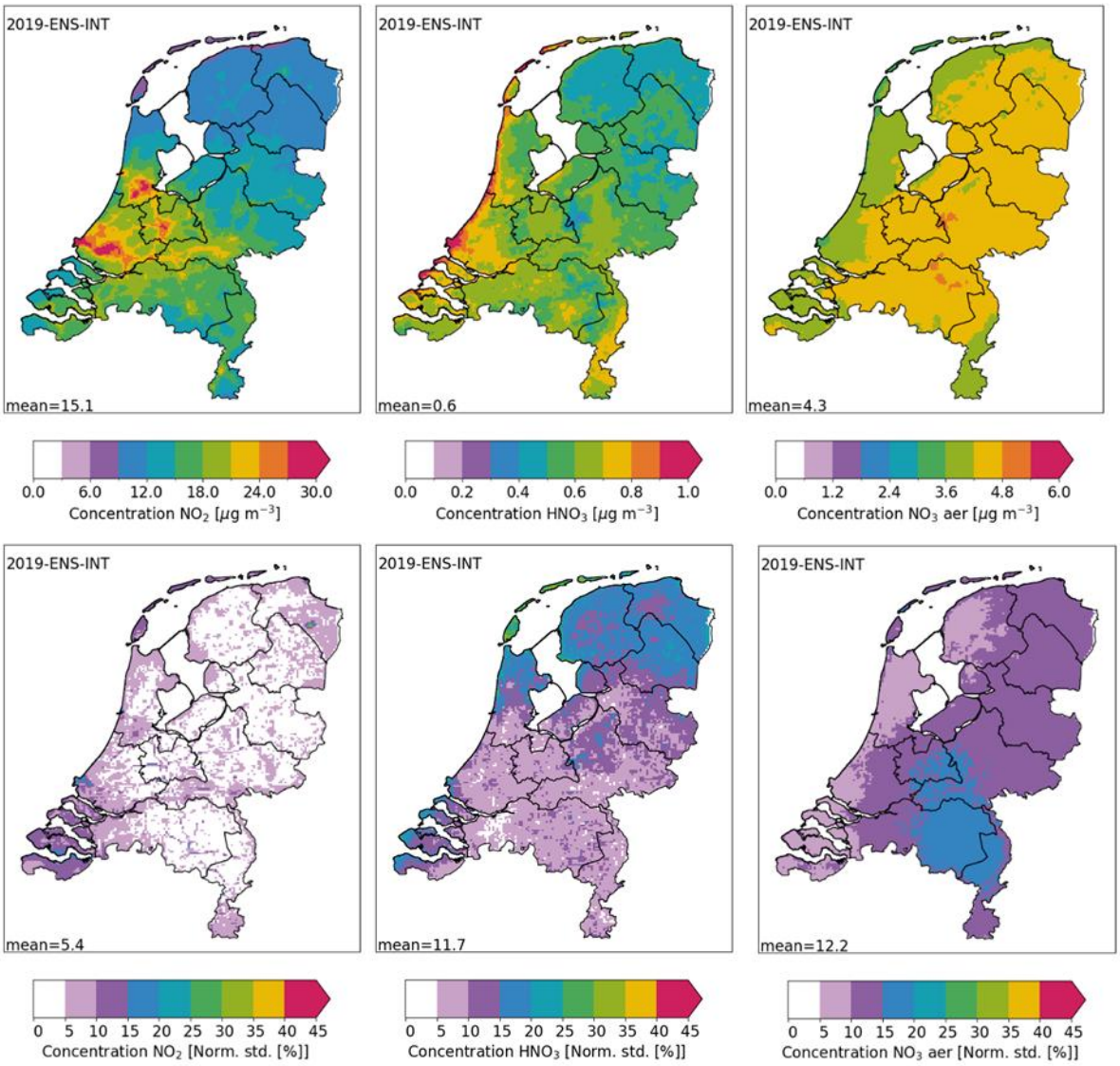

Figure 33: Ensemble mean for all five models of concentrations of NO_2 (left), HNO_3 (middle) and pNO_3^- (right) in the Netherlands. Bottom panels: Normalized standard deviation [%] of the models is shown for those components.

4.5.2 Concentrations

Nitrogen dioxide

Figure 34 shows an overview of the simulated NO_2 concentrations across the Netherlands and their evaluation against observed concentrations, for the year 2019. The mean simulated NO_2 concentration over the Netherlands as a whole shows very comparable values between 14.4 and 15.5 µg m^{-3}. All models show maxima in the Rotterdam-Rijnmond and the greater Amsterdam region. Furthermore, the location of many cities can be recognized. Although the similarity in the model results is large there are features where the models show some differences. For example, the impact of the highways is more pronounced in the OPS results, whereas the impact of the inland shipping on the Lek and Rhine are more pronounced in MATCH and EMEP4NL than in the other models. LOTOS shows higher concentrations in the vicinity of industrial areas. Sector-dependent assumptions on the effective emission height play a key role in some of these patterns. For example, in SILAM all shipping emissions, both inland and seagoing, occur at a height of 90m altitude. Hence, they are not introduced in the first model layer near the surface and this model does not show a pronounced inland shipping pattern. Unfortunately, there are no measurement stations in the affected areas.

In Figure 34 middle and right panels, the comparison of the model results to the observed values is shown. The scatter plots show that most modelled annual mean concentrations are close to the 1:1 line with the observed concentrations. The spatial distribution of the model to observed ratio is very similar among the models. Spatial correlations, in terms of r^2, vary from 0.79 (MATCH) to 0.84 (SILAM, LOTOS) for the individual models, which also indicates that the models performs well for NO_2. The international ensemble shows an even larger spatial correlation of 0.86. Also RMSE and NMB values are similar between the different models. According to those statistics, the ensemble does not show a better performance compared to the individual models. The individual models have an RMSE range of 3.92 µg m^{-3} (LOTOS) to 2.62 µg m^{-3} (EMEP4NL), where the ensemble RMSE is 2.76 µg m^{-3}. All statistics for each model and other years (2016-2019) can be found in 0.

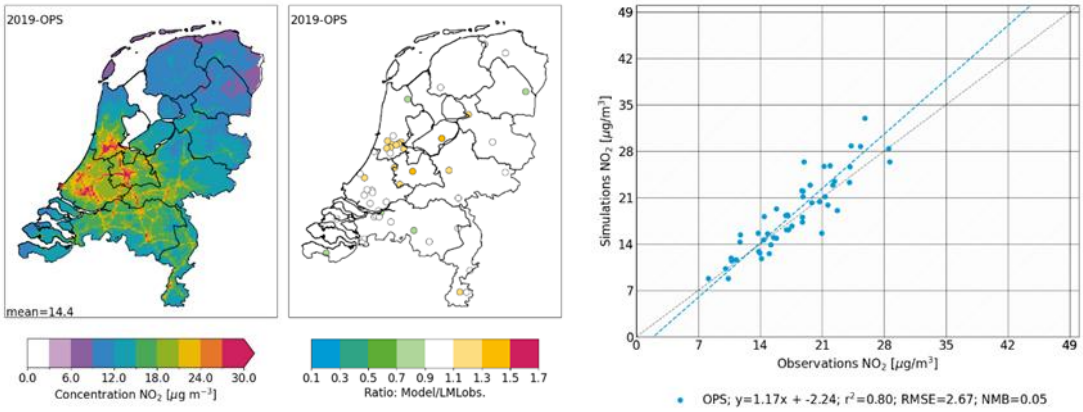

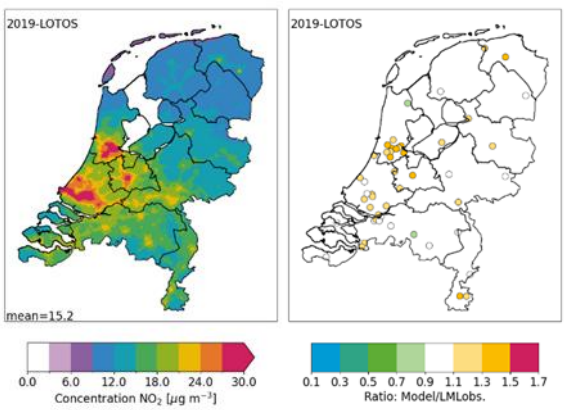

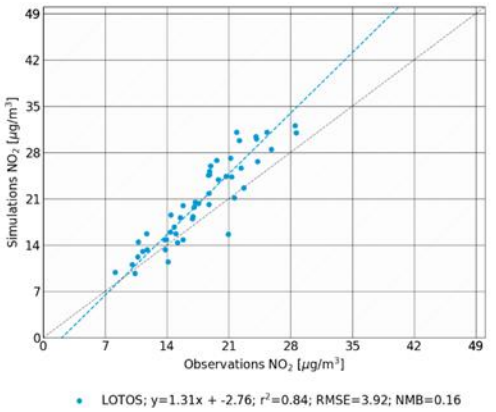

LOTOS; y=1.31x + -2.76; r^2=0.84; RMSE=3.92; NMB=0.16

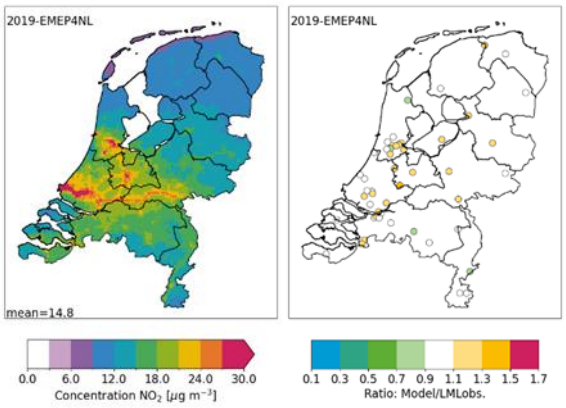

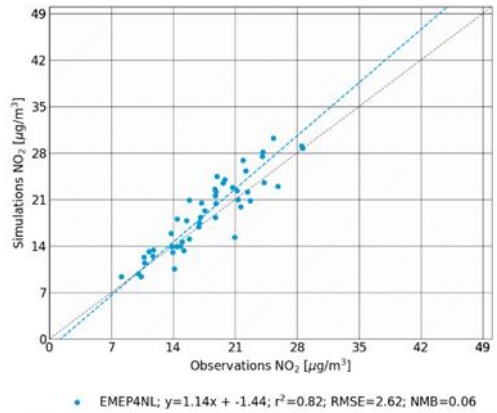

EMEP4NL; y=1.14x + -1.44; r^2=0.82; RMSE=2.62; NMB=0.06

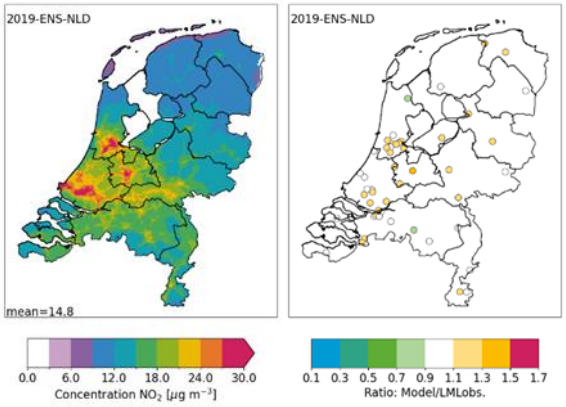

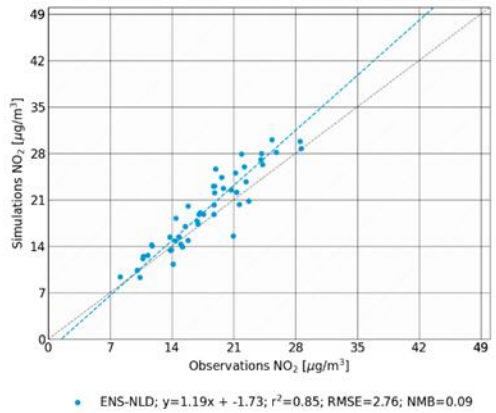

ENS-NLD; y=1.19x + -1.73; r^2=0.85; RMSE=2.76; NMB=0.09

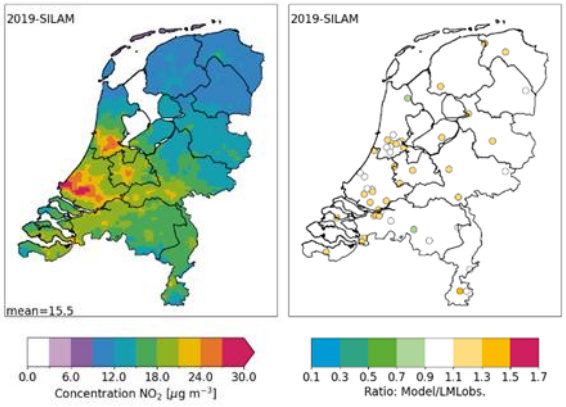

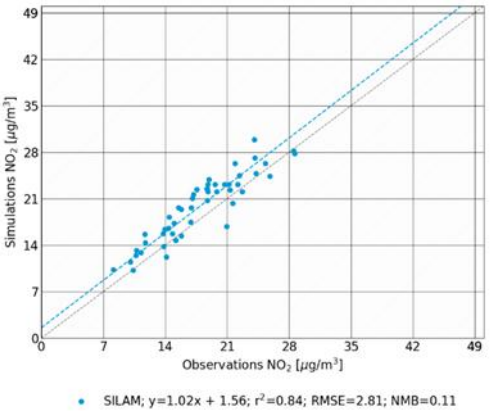

SILAM; y=1.02x + 1.56; r^2=0.84; RMSE=2.81; NMB=0.11

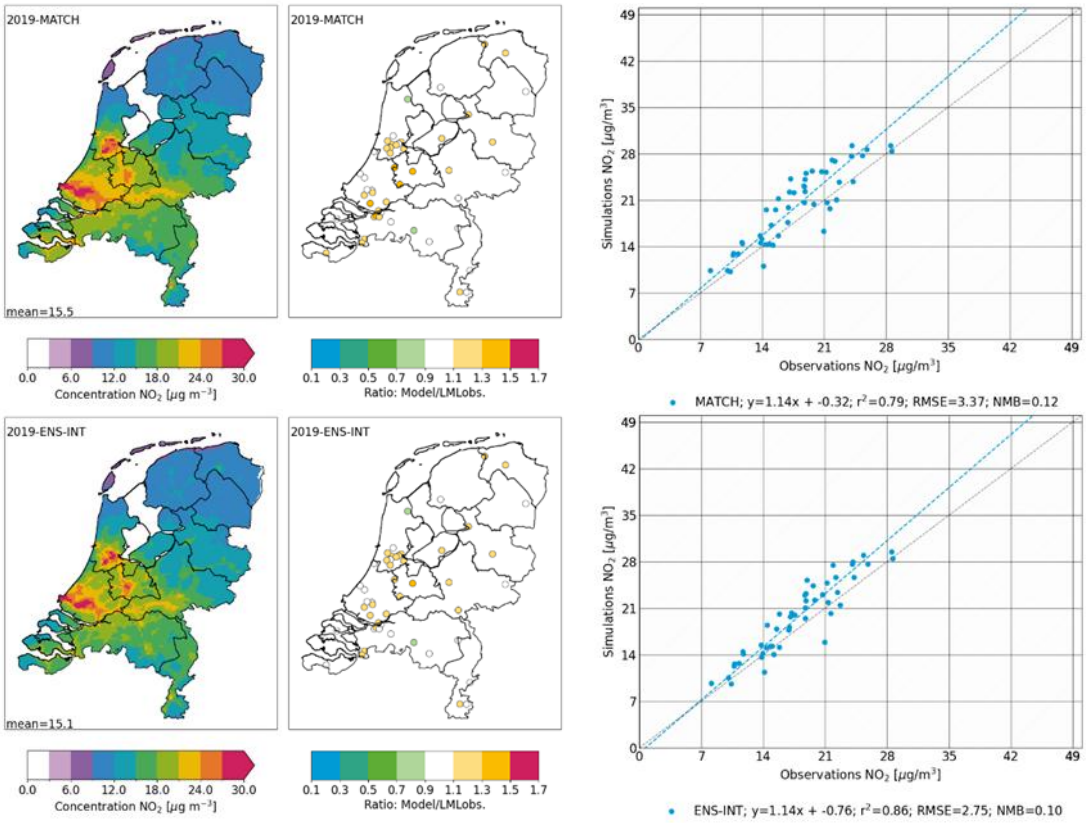

Figure 34: Modelled and observed concentrations of NO_2 in the Netherlands for the year 2019. Left plots: Modelled concentrations of NO_2. First, for the Dutch models OPS, LOTOS-EUROS and EMEP4NL and their mean taken as an ensemble. Second, the international models SILAM and MATCH, and the mean of all models in the extended ensemble. Middle plots: Ratios of simulated data over observed data in the Landelijk Meetnetwerk Luchtkwaliteit (LML), in the same order as for the left plots. Right plots: Scatter plots of the modelled values versus the observations of NO_2 in the LML-network.

The similarity between the models and observations is further illustrated in Figure 35, which shows the annual average simulated and observed concentrations of NO_2 at 6 LML stations. For all stations, the models provide a very consistent picture. The spread between the models is very small and they all behave the same. This feature is also recognized in the distribution of the under- and overestimation across the country shown in middle panels of Figure 34. The observed NO_2 concentrations in the locations of Zegveld and Wekerom are overestimated by all models, whereas the observed NO_2 concentrations in the locations of Vredepeel, Wieringerwerf and Valthermond are underestimated by all models. Only in the 'De Zilk' location, there is no clear pattern for the models relative to the observations.

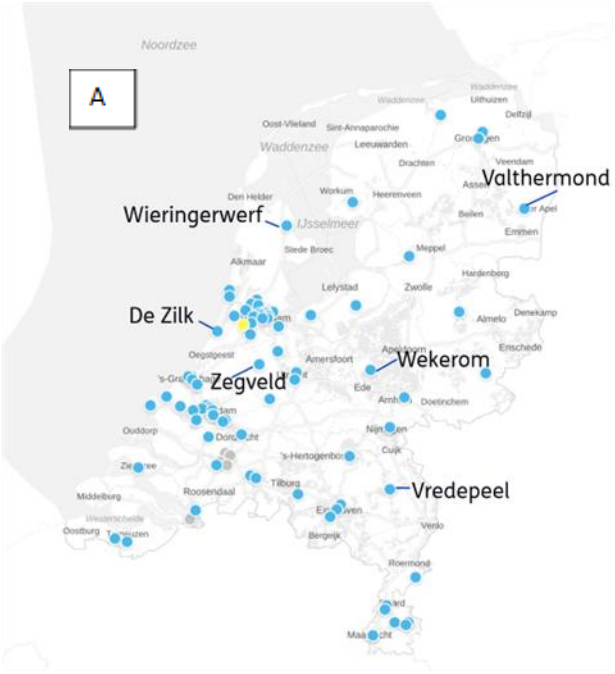

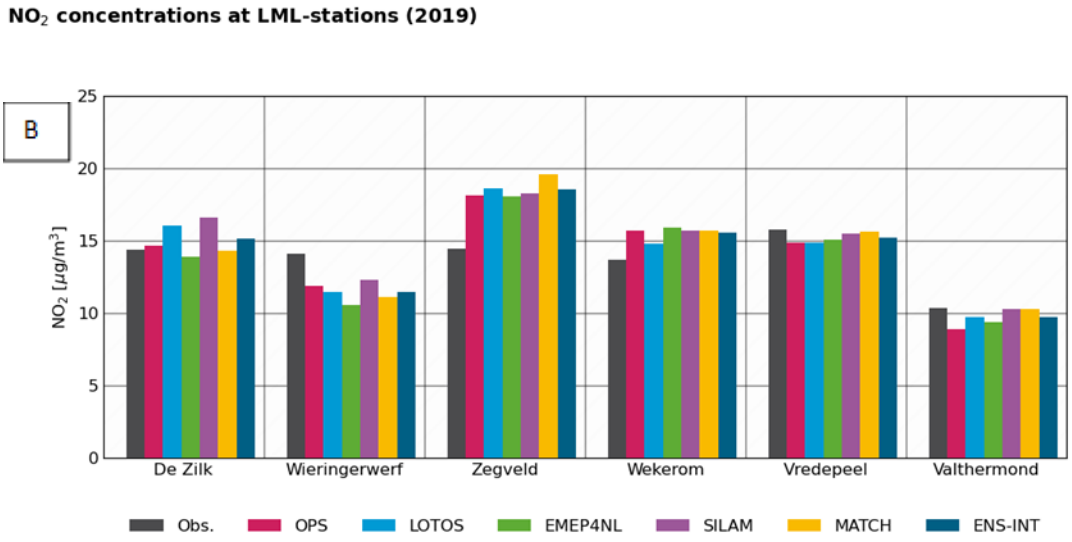

Figure 35: A) Indication of six measurement locations of LML (Landelijk Meetnetwerk Luchtkwaliteit) NO_2 measurement stations, operated by RIVM. In this study, 49 operational measurement stations for NO_2 are used. Locations indicated are used for modelling exercise of B) Histogram of observed and simulated averaged concentrations of NO_2 in 2019, at six selected LML measurement stations in the Netherlands that measure NO_2.

Nitric Acid

As discussed in section 2.5 (Figure 8), HNO_3 is the third largest contributor to total nitrogen deposition in the Netherlands after NH_3 and NO_2. As there were no observations of HNO_3 for 2019 at time of writing, we only compare the models with each other and with the ensemble mean. Annual mean concentrations of HNO_3 are shown in Figure 36 for all models and both ensembles.

In Figure 37, annual mean concentrations are shown at the same six locations as shown for NO_2 in the previous paragraph. The short life time of HNO_3 translates into a rather low mean

concentration of about 0.5 µg m^{-3}. Nitric acid concentration is negatively correlated with ammonia concentration. In areas with little ammonia, such as along the coastline, the nitric acid concentrations are relatively large and in the areas with the largest ammonia concentrations the lowest nitric acid levels are modelled. This is explained by the reaction of nitric acid with ammonia to form ammonium nitrate. The spatial patterns reveal that OPS provides larger modelled nitric acid levels in and near the NO_x source areas, e.g. the cities. Nitric acid concentration declines as function of distance to these source areas. In the other models this pattern is less pronounced. The other models also show maxima in regions downwind of the NO_x source areas with little ammonia, such as the Veluwe, albeit to a variable extent. LOTOS, SILAM and MATCH show increased nitric acid concentrations over the Veluwe (and correspondingly reduced particulate nitrate levels). The impact of the ammonia fields on the amount of nitric acid and particulate nitrate is strongest in MATCH. The modelled nitric acid distributions are differ in the gradients towards the north of the country. OPS shows the strongest decline and MATCH the weakest. The chemical regime involving nitric acid and particulate nitrate can be determined using a MARGA instrument, which is available in the Netherlands. Based on largest difference between the model results deploying a MARGA in the north of the Netherlands, e.g. in Valthermond, seems worthwhile.

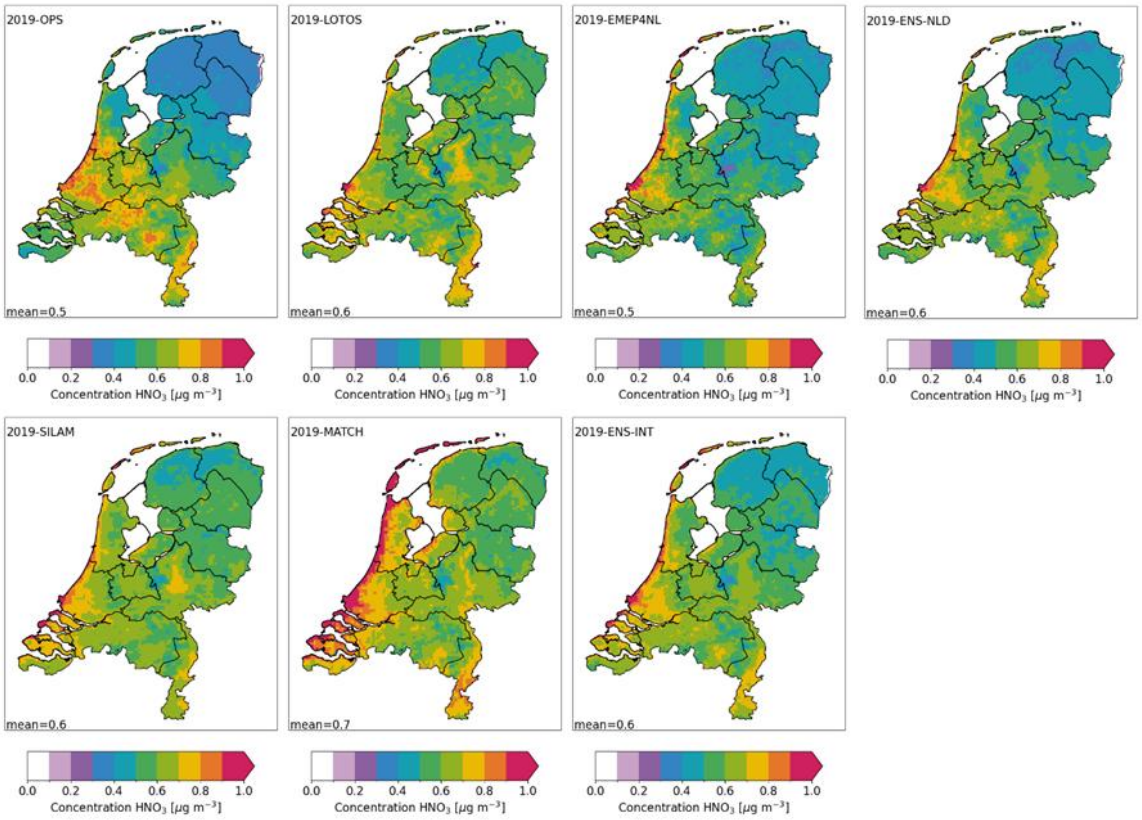

Figure 36: Simulated concentrations of nitric acid (HNO_3), averaged over the year 2019. Top row, left to right: Dutch models (OPS, LOTOS, EMEP4NL) and Dutch ensemble. Bottom row: international models (SILAM, MATCH) and the ensemble of all five models included in the study.

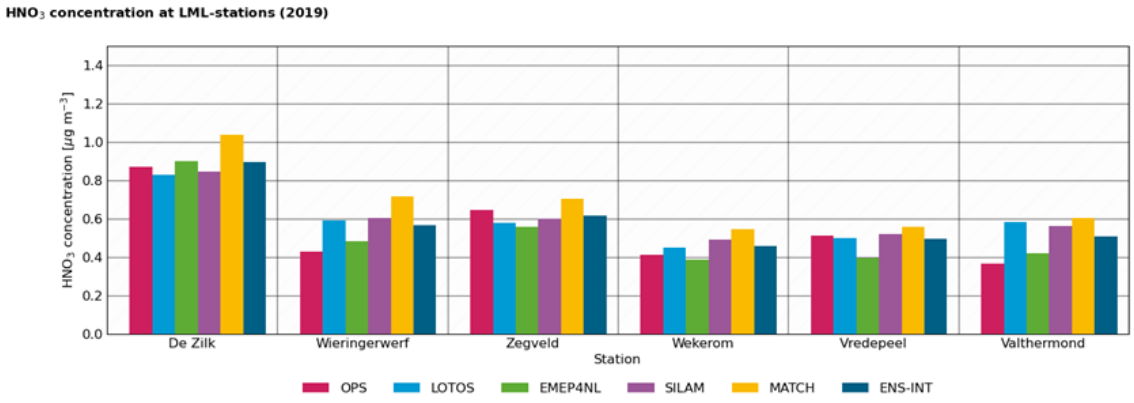

Figure 37: A) Indication of six measurement locations of LML (Landelijk Meetnetwerk Luchtkwaliteit) NO_2 measurement stations, operated by RIVM. B) Histogram of simulated averaged concentrations of HNO_3 in 2019, at six selected LML measurement stations in the Netherlands that measure NO_2.

Particulate nitrate

Annual mean distributions of particulate nitrate (pNO_3^-) as modelled by all systems are shown in Figure 38. LOTOS, EMEP4NL and MATCH show lower concentrations northwest and southeast and a band of similar levels across the country: from Zeeland to Groningen. OPS shows a distribution that is spatially correlated with the ammonia emission distribution. As for ammonium (Section 4.4.1), the reasoning is likely to be found in the way the particulate matter formation is treated. In OPS, the particulate nitrate formation is represented by applying the annual average conversion rate of NO_x to particulate nitrate from the EMEP4NL model. The semi-volatile nature of ammonium nitrate makes the formation strongly temperature dependent. During warm conditions less or no particulate (ammonium) nitrate forms because higher temperatures shift the equilibrium between particulate ammonium nitrate and gaseous ammonia and nitric acid towards the gas phase. In areas with larger

ammonia emissions the ammonium nitrate level can be sustained at higher level than in areas with little ammonia. During cooler summer time conditions ammonium nitrate may be effectively be formed everywhere. Due to contrasting conditions ammonium nitrate levels also show a strong diurnal cycle during summer time. In contrast, at cold winter temperatures the particulate ammonium nitrate is stable. Ammonia is typically abundant, making it non-limiting, which results in effective nitrate formation rather independent of the ammonia concentration. The varying meteorological conditions cause the formation rate to vary from seasonally, from day to day and between night and day. During summer, the formation rates increase with ammonia levels. Hence, by using an annual mean formation rate, the OPS model applies a constant but spatially variable formation rate for each meteorological class, independent of the associated conditions. The spatial variability includes the fingerprint of the ammonia distribution, which is then applied to all meteorological classes, independent of the fact if such a class would favour effective ammonium nitrate formation or not.

The comparison to the observations in Figure 39 indicates that the spatial variability of particulate nitrate in OPS is too strong. LOTOS, EMEP4NL and MATCH models are relatively consistent between each other for particulate nitrate, while SILAM shows and consistent small underestimation over the whole country.

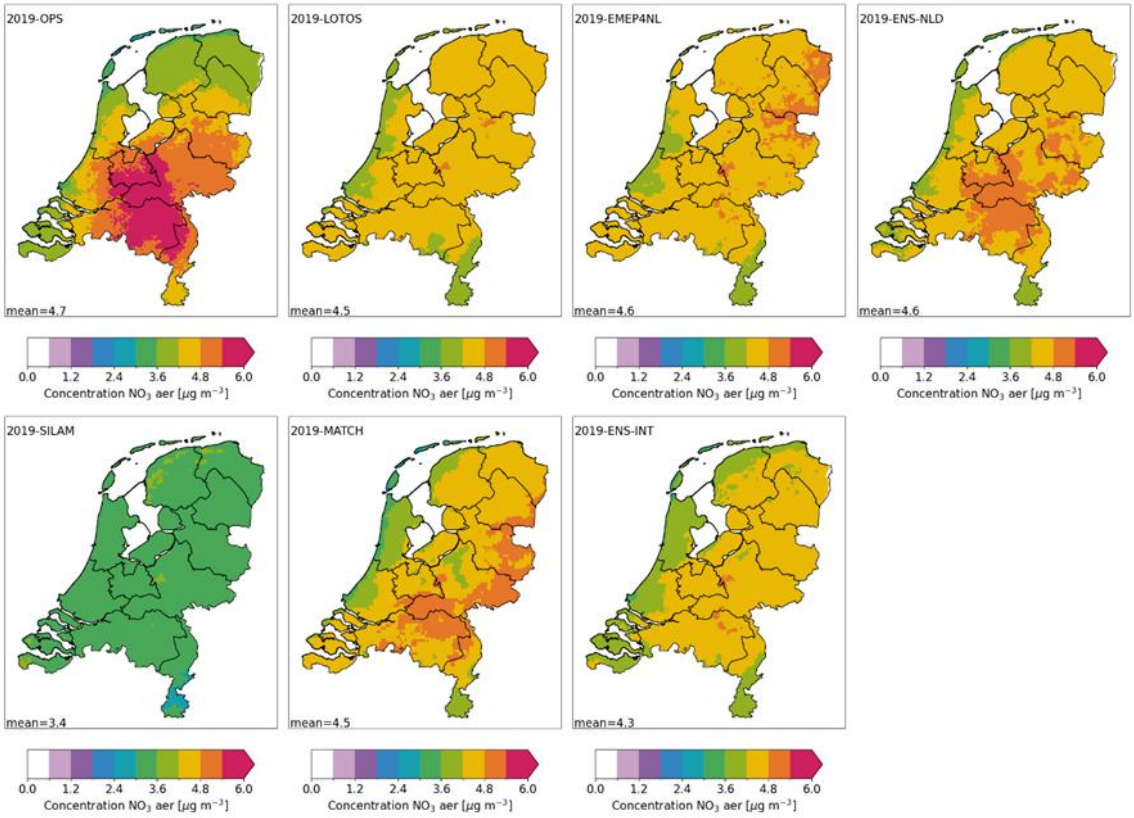

Figure 38: Simulated concentrations of particulate nitrate (pNO_3^-), averaged over the year 2019. Top row, left to right: Dutch models (OPS, LOTOS, EMEP4NL) and Dutch ensemble. Bottom row: international models (SILAM, MATCH) and the ensemble of all five models included in the study.

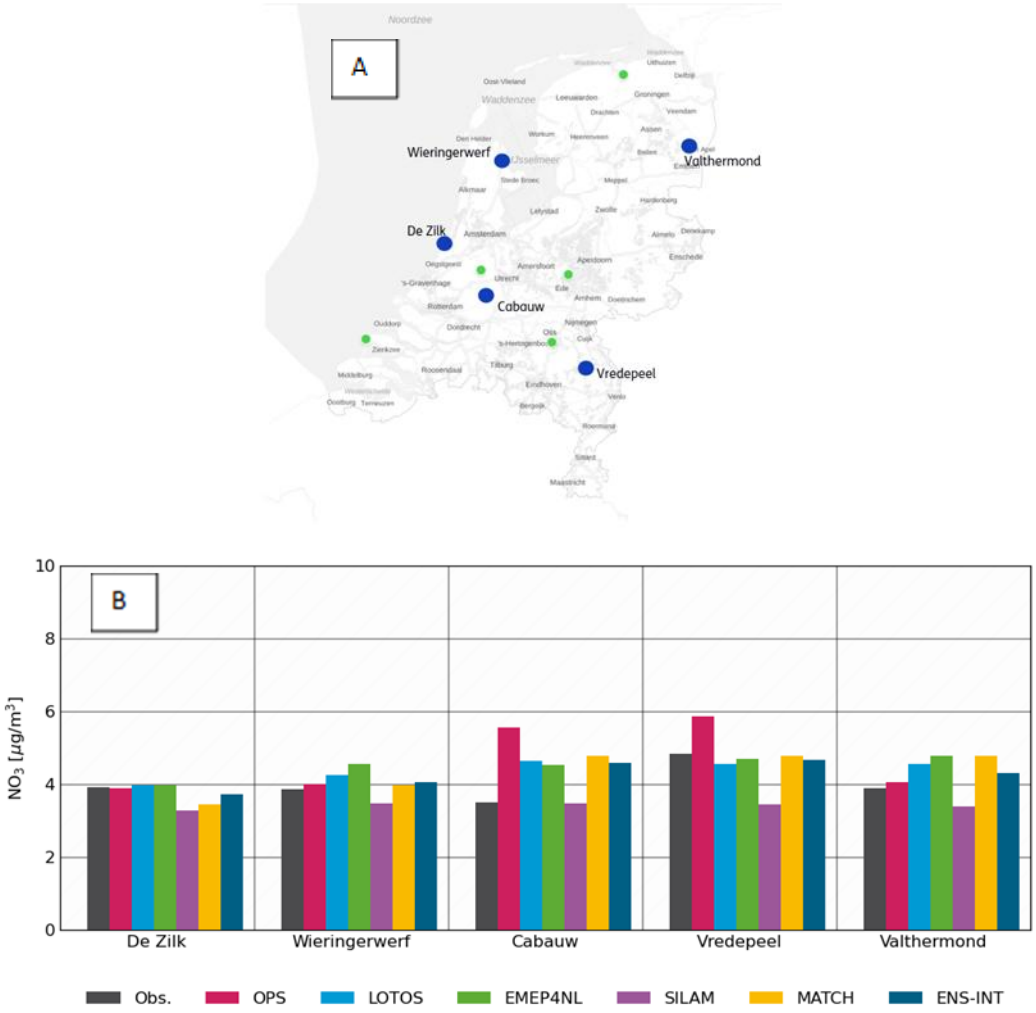

Figure 39: A) Locations used in this study within the LML measurement network that measure pNO_3^-. B) Observations and modelled values of pNO_3^- at the measurement locations in the Netherlands, and the ensemble value of the models.

4.6 Overview of annual performance statistics

In this chapter, we collected the statistical parameters on the modelled to observed ratios, the correlation coefficients, and NMRSE for all evaluated parameters and put them together. An overview in tabular form is provided by the statistical measures for the annual mean comparison for all observation types in 0. Note that the number of stations per component differs.

Ratios

In Figure 40, we averaged all modelled data paired to an observation to investigate the ratio between them. The goal here was to evaluate the modelled concentration and deposition values in comparison to all measurements.
We see reasonable agreement between the models and observations for NH_3-MAN, NO_2-LML, and particulate nitrate (pNO_3^-). Considering the ensemble ratios of the models to the observations of NH_3 concentrations in the MAN network are 1.06 for ENS-NLD and 0.93 for ENS-INT, showing agreement between model and observations. There, the ratios range from

0.62 (SILAM) to 1.10 (EMEP4NL). The average ratios close to 1 indicate that for ammonia the challenge lies in spatial distribution. For modelled and observed values at the NO_2 concentration observations in the LML network, the ensembles show ratio values of 1.09 (ENS-NLD) and 1.10 (ENS-INT), with ranges from 1.05 (OPS) to 1.15 (LOTOS), and a low spread of 5 % across the models. Regarding particulate nitrate (pNO_3) concentrations, the ensemble ratios between modelled and observed values show some agreement with an ENS-NLD value of 1.14 and an ENS-INT value of 1.09. The ratio values here range from 0.86 (SILAM) to 1.17 (OPS).

The largest systematic overestimation of the observations by the models is noticeable in the ratios of pNH_4^+ particle concentrations, .with values of 1.3 (OPS) to 1.99 (MATCH) with the exception of SILAM (0.81). For this compound, the spread of the ratios is the greatest with a 30 % spread across all models. On the other hand, the largest underestimations are seen for NH_3 concentrations in the LML network, NH_x wet deposition, and NO_y wet deposition. For NH_3 in LML, the ensemble values are 0.83 (ENS-NLD) and 0.74 (ENS-INT). The ratio values here range from 0.49 (SILAM) to 0.94 (OPS). Taking NO_y wet deposition, the ensemble values are 0.79 (ENS-NLD) and 0.92 (ENS-INT). The separate model ratios range from 0.60 (SILAM) to 1.37 (OPS). Looking at NH_4 wet deposition, the ensemble ratio values are the lowest of all compounds 0.71 (ENS-NLD) and 0.83 (ENS-INT), with ratios of models ranging from 0.60 (SILAM) to 0.99 (OPS).

Looking at the ratios of models to observations, the three Dutch models are often the three central models. We see that the international models SILAM and MATCH often provide the upper of lower bound of the ensemble, respectively. SILAM underestimates many indicators systematically, which seems to be related to the very efficient dry deposition assumed to occur throughout its model domain.

Correlations

The correlation reported in Figure 41 is the explained variability in the spatial distribution, since the parameters describe the spatial comparison. It becomes evident that the highest correlations coefficients are seen for NH_3 LML. There, the ENS-NLD and ENS-INT ensembles both show a value of 0.95. The individual models range from 0.80 (MATCH) to 0.97 (LOTOS). It is rather easy to arrive at large correlation coefficients when a considerable variability is observed between the concentrations at a limited number of measurement sites and these are also reflected in the model results, as is the case for ammonia. Other high correlations are found for NO_2 LML, where the ensemble values are 0.85 (ENS-NLD) and 0.86 (ENS-INT). The models range from 0.79 (MATCH) to 0.84 (LOTOS & SILAM).

Reasonable spatial correlations are found for particulate ammonium (pNH_4) concentrations, where the ENS-NLD value is 0.7 and ENS-INT is 0.66. The model values range from 0.48 (SILAM) to 0.69 (OPS). Somewhat similarly, NH_3 MAN correlations show ensemble values of 0.67 for both ENS-NLD and ENS-INT. Here, model values range from 0.58 (MATCH) to 0.68 (OPS).

Correlations slightly less strong are seen in wet deposition NH_4 correlations, which show ensemble values of 0.56 for ENS-NLD and ENS-INT. Here, model correlation values range from 0.49 (OPS) to 0.77 (SILAM). Similarly, both ENS-INT and ENS-NLD wet deposition NO_3 correlation values are 0.40. The models here range from 0.01 (OPS) to 0.62 (LOTOS). Wet deposition correlations are low for EMEP4NL, although the mean bias and RMSE is small. This may hint at a role of the precipitation fields rather than the removal efficiencies.
The lowest correlations are found for pNO_3^- concentrations range from 0.01 (LOTOS) to 0.17 (OPS), with ensemble values of 0.13 (ENS-NLD) and 0.10 (ENS-INT). This is explained by the

very low contrast in observed annual mean levels, yielding a low spatial correlation although biases are relatively low.
Looking at the spatial correlations between the modelled values and observations, it is very evident that the correlations of ENS-NLD and ENS-INT are almost identical to each other in all compounds.

NRMSE

The normalized root mean squared error (NRMSE) as shown in Figure 42 shows the lowest values for NH_3-MAN, NH_3-LML and NO_2-LML. Medium values are calculated for the wet deposition fluxes and largest values for the particulate components. The lowest NRMSE is found for the components with the largest spatial correlation coefficients. The relative error for the primary components is smaller than for the secondary components.

Overall

The evaluation against measurements showed that the skill of the ensemble mean model was better or as good as the best performing model system for all three presented quantities. The ensemble ensures that no excessively small or large values persist. The best performing model system varies per component. Hence, it is the consistency of the skill for all evaluated parameters that makes the ensemble model perform better than the ensemble members. The ensemble mean model shows the largest added value for parameters that are most uncertain (i.e. show the largest spread between models). In other words, for components with little uncertainty such as the NO_2 the ensemble brings less added value than for parameters where the models are further apart, such as NO_y deposition. At the national scale the OPS model performs comparable to the other models for NH_3 and NO_2 concentrations, where the more complex models performed better for secondary components.

The added value of the ensemble is also observed for the small ensemble of Dutch models. Hence, a pragmatic way to evaluate the impact of using an ensemble in more operational policy support applications is to test the methodology and impact using this small sized ensemble.

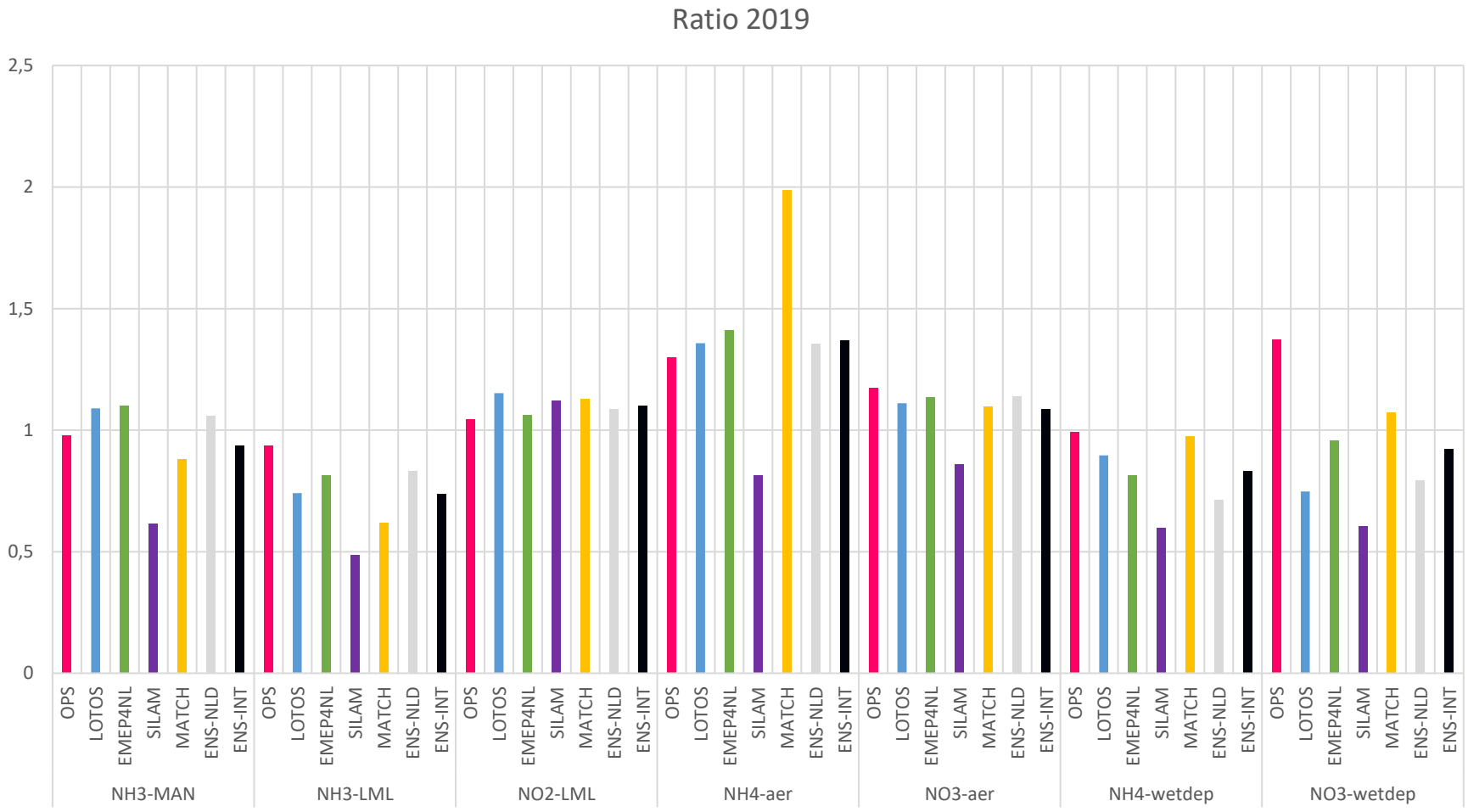

Figure 40: Ratio between model and observations for all models for each set of observations for 2019.

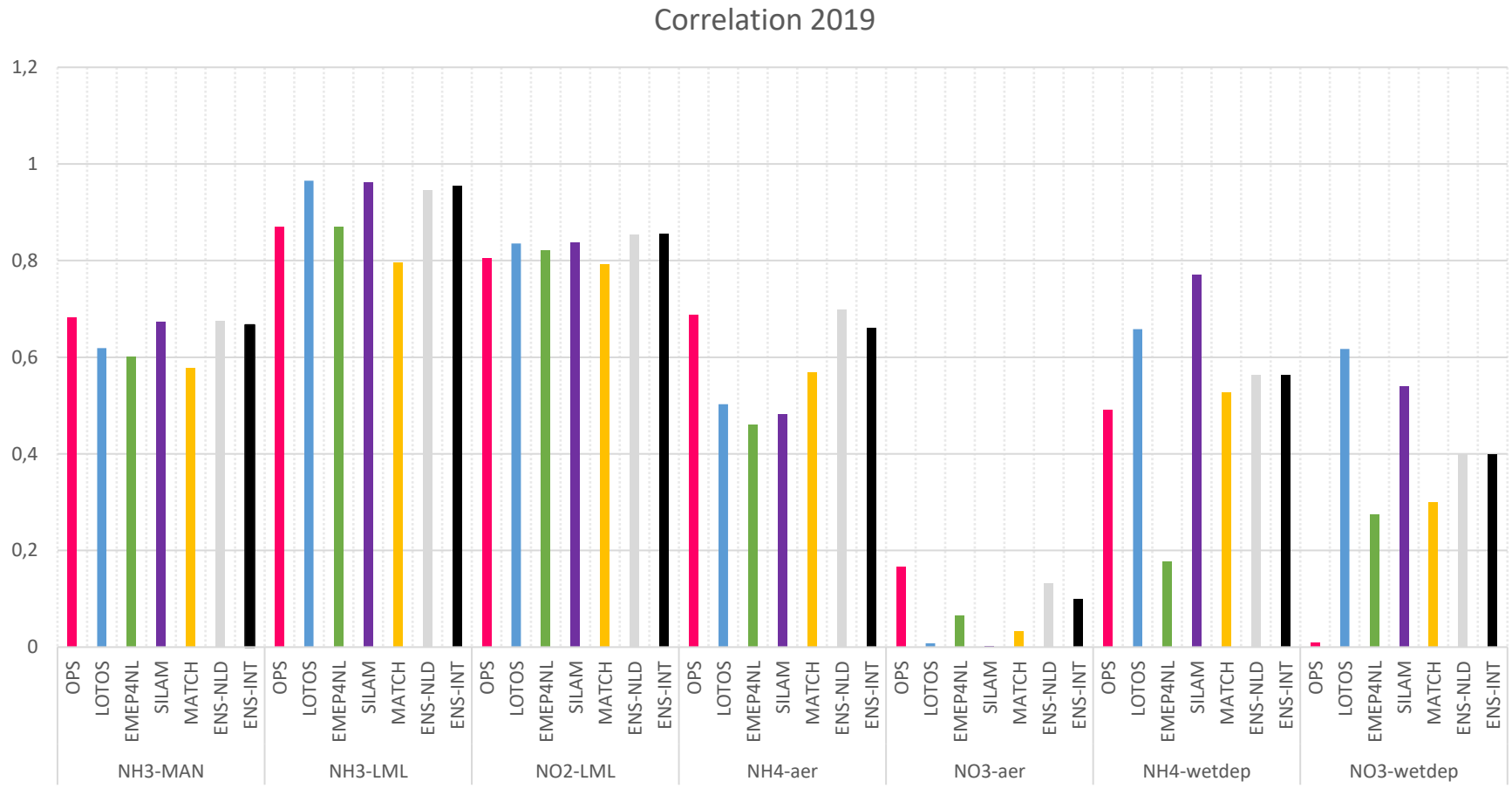

Figure 41: Correlation coefficient for all models for each set of observations for 2019.

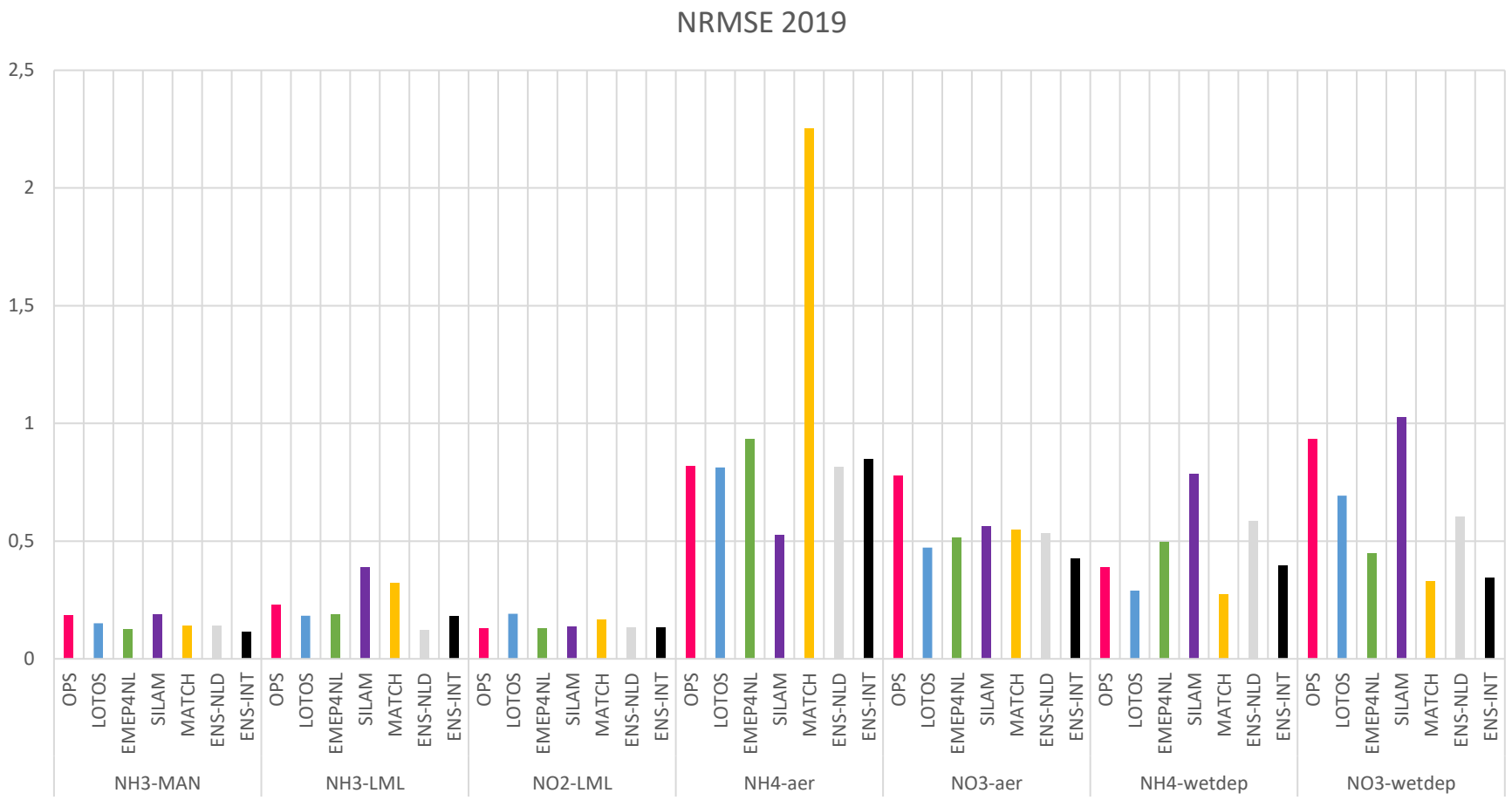

Figure 42: Normalized root mean squared error (NMRSE) for all models for each set of observations for 2019.

4.7 Evaluation of modelled time series

In this section, a short overview of the temporal behaviour of the different models is provided for the gaseous tracers NH_3 and NO_2, as well as for particulate ammonium (NH_4) and nitrate (pNO_3^-). The paired analysis on a daily basis is possible for the Eulerian grid models only, so OPS is not used for this comparison. Therefore, only four models are available for 2019. Hence, the ensemble presented here is also built with these four models. For this analysis, observations from the LML-network are used, excluding monitoring stations classified as traffic or industry. This results in analysis of 49 stations for NO_2, 6 stations for NH_3 and 5 stations for particulate nitrate and ammonium. The analyses were done on daily basis, to provide insight in the seasonal and synoptic variability. For this purpose, the hourly observations of NO_2 and NH_3 are recalculated to daily values, while observations for particulate matter are available on daily basis. For each of the compounds, timeseries are shown in comparison with the observations for all models (LOTOS, EMEP4NL, SILAM, MATCH) and the ensemble mean. In the statistics tables four indicators are displayed: Bias, Normalized mean bias (NMB), Root mean square error (RMSE) and temporal correlation (R^2). The latter represents the explained variability by the models.

For ammonia, the models show different temporal behaviour (Figure 43). LOTOS and EMEP4NL show two peak periods in spring, the first at the end of February and second at the end of March. This double peak is also represented by the observations. MATCH show one peak period in April, while SILAM models relatively constant concentrations during spring. All models except SILAM have also a small peak at the end of summer, which is also visible in the observations. Looking at the statistics (Table 5), LOTOS and EMEP4NL show the largest temporal correlations (explained variability almost 60 %) and lowest biases. Again, using the ensemble shows a better performance compared to the individual models.

In Figure 44, timeseries are shown for NO_2. All models show good agreements with respect to the observations. Biases are small and temporal correlations differ from 0.74 to 0.83, with the ensemble showing the largest correlation of 0.84 (shown in Table 6). This behaviour is as expected because the model performances on annual basis, shown in Section 4.5, were also very good for NO_2. In comparison to ammonia, the explained variability is considerably larger for NO_2.

All models show a good comparison with respect to the observations of particulate ammonium and nitrate (Figure 45 and Figure 46). As expected, both compound show similar behaviour with higher values in winter and lower values in summer. All models follow this pattern which gives low biases and high temporal correlations. Again the ensemble shows the best performance for these indicators (Table 7 and Table 8).

These results build confidence in the models to reproduce the variability of these compounds. Two findings stand out. 1) the assumed ammonia seasonal cycle differs between models and 2) the ensemble mean performs better than the individual models or provides a skill comparable to the best individual model. The latter was already observed for the spatial statistics of the annual evaluation presented above. This means that the ensemble contains generally more information than the individual models.

For OPS a paired comparison of modelled and observed timeseries is not possible as the model performs calculations for a limited number of meteorological classes. It would, however, be possible to classify both the observations and the results of all models in these meteorological classes to assess if such an activity yields additional information. In addition,

one could compare monthly simulations from OPS to the model results to investigate the performance during different seasons. Although out of scope for the present study, these directions may improve the use of observations and the Eulerian model outputs for the evaluation of the OPS model. The results of this study focused on the annual mean validation, which reduce the comparison to observations to a very limited number of numbers, depending on the component.

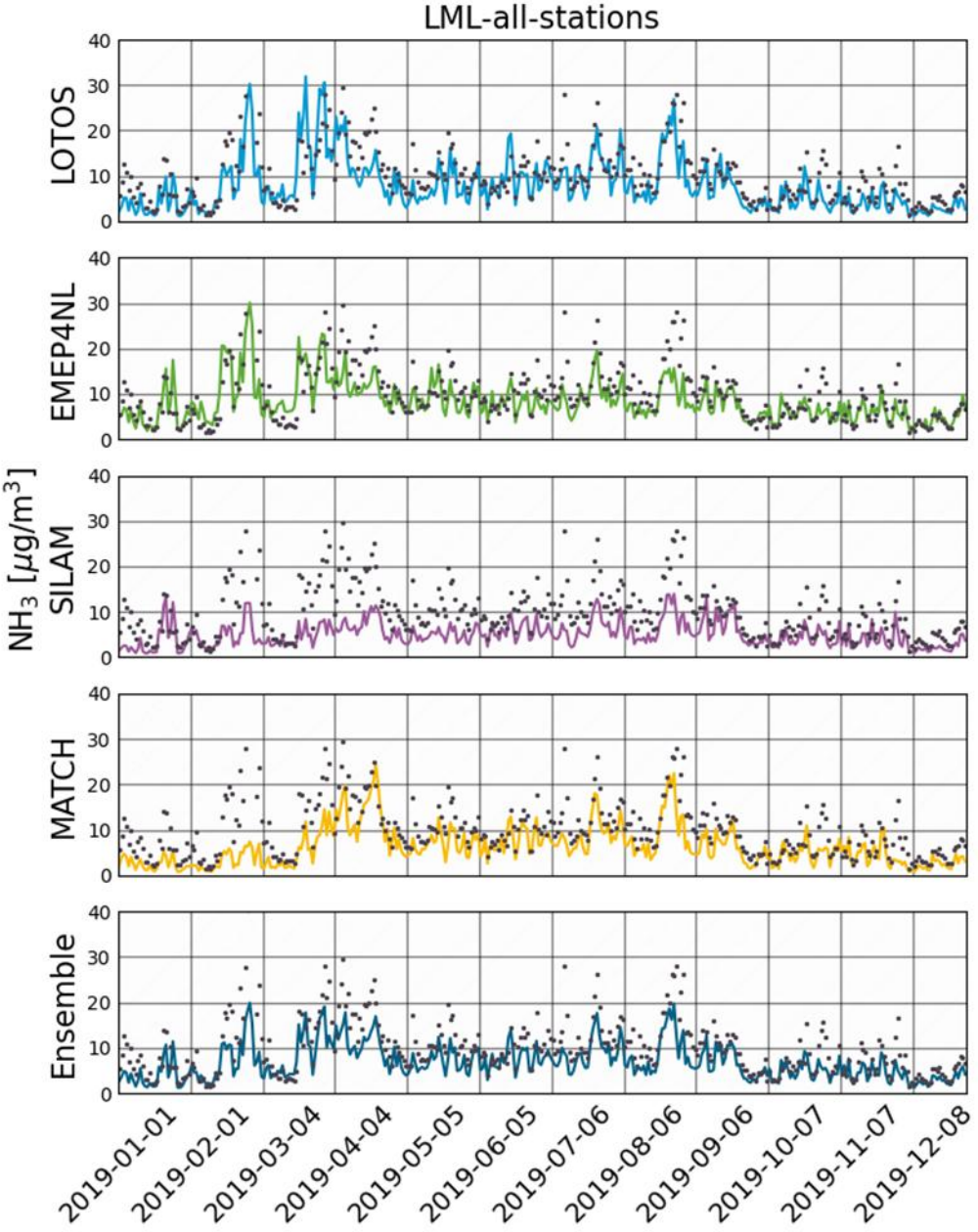

Figure 43: Ammonia concentrations for 2019 averaged over all LML-stations for each model and the ensemble. Top to bottom: LOTOS, EMEP4NL, SILAM, MATCH and Ensemble.

Table 5: Temporal statistics for ammonia concentrations on the average observations of the LML-stations.

Model	Bias	NMB	RMSE	Corr
LOTOS	-2.4	-0.23	5.2	0.59
EMEP4NL	-1.9	-0.19	5.1	0.58
SILAM	-5.2	-0.51	7.7	0.42
MATCH	-4.0	-0.39	6.8	0.39
Ensemble	-3.4	-0.33	5.8	0.62

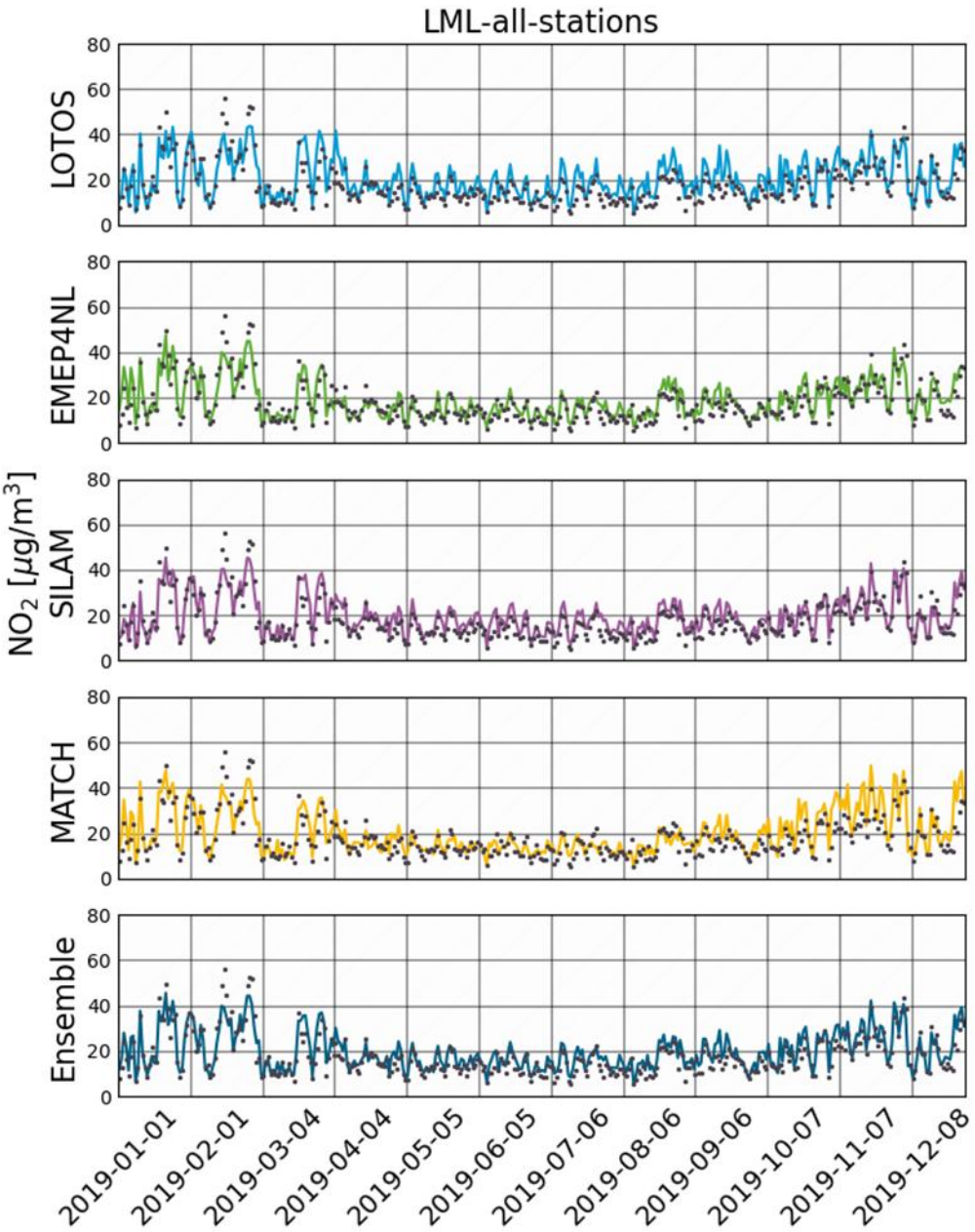

Figure 44: Nitrogen dioxide concentrations for 2019 averaged over all LML-stations for each model and the ensemble. Top to bottom: LOTOS, EMEP4NL, SILAM, MATCH and Ensemble.

Table 6: Temporal statistics for nitrogen dioxide concentrations on the average observations of the LML-stations.

Model	bias	NMB	RMSE	Corr
LOTOS	2.8	0.16	5.3	0.76
EMEP4NL	1.2	0.06	3.9	0.82
SILAM	2.0	0.11	4.2	0.83
MATCH	2.3	0.13	5.4	0.74
Ensemble	2.0	0.11	4.1	0.84

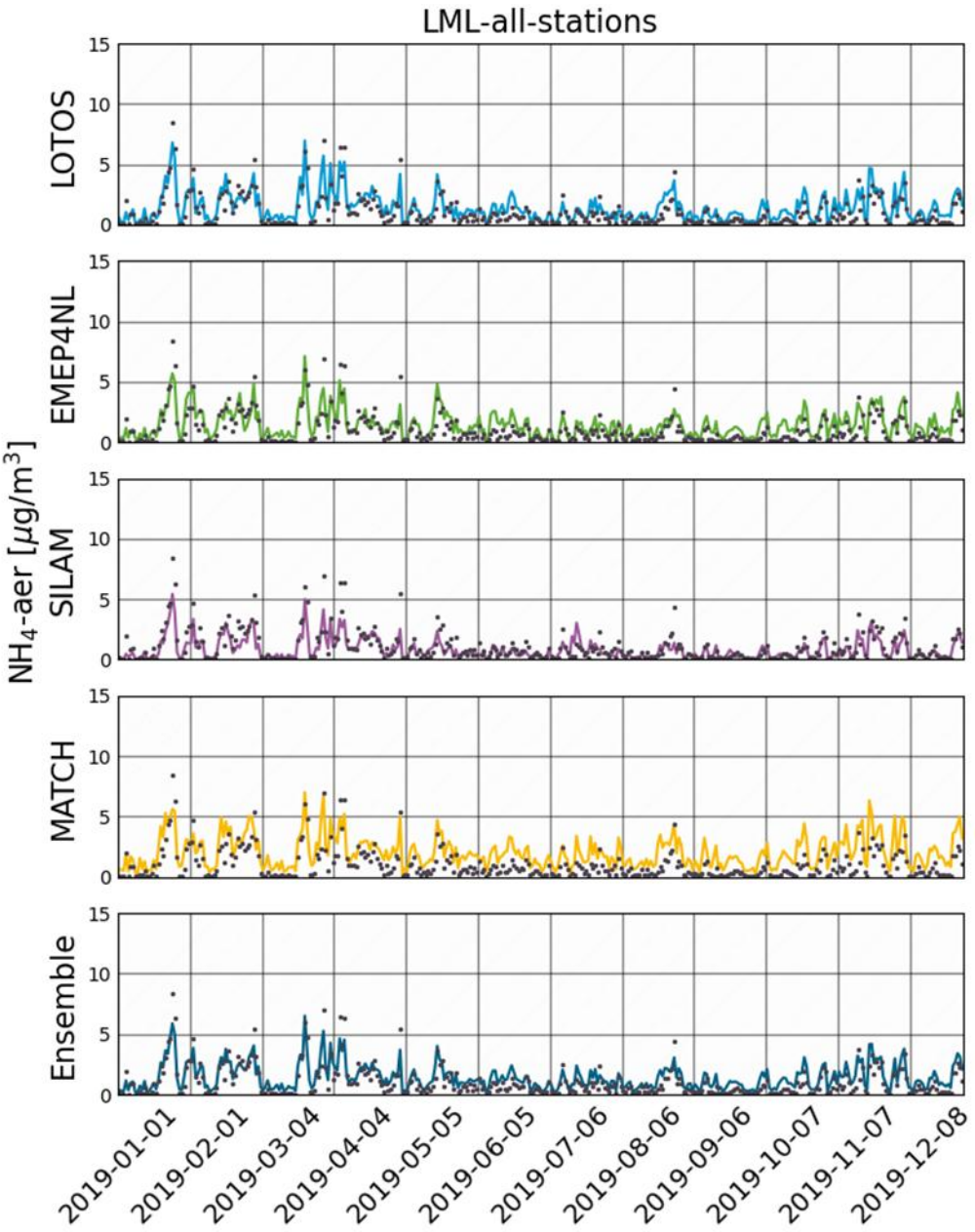

Figure 45: Ammonium aerosol concentrations for 2019 averaged over all LML-stations for each model and the ensemble. Top to bottom: LOTOS, EMEP4NL, SILAM, MATCH and Ensemble.

Table 7: Temporal statistics for ammonium aerosol concentrations on the average observations of the LML-stations.

Model	bias	NMB	RMSE	Corr
LOTOS	0.3	0.32	0.6	0.83
EMEP4NL	0.4	0.38	0.7	0.76
SILAM	-0.2	-0.2	0.7	0.80
MATCH	1.0	0.9	1.2	0.71
Ensemble	0.4	0.35	0.6	0.84

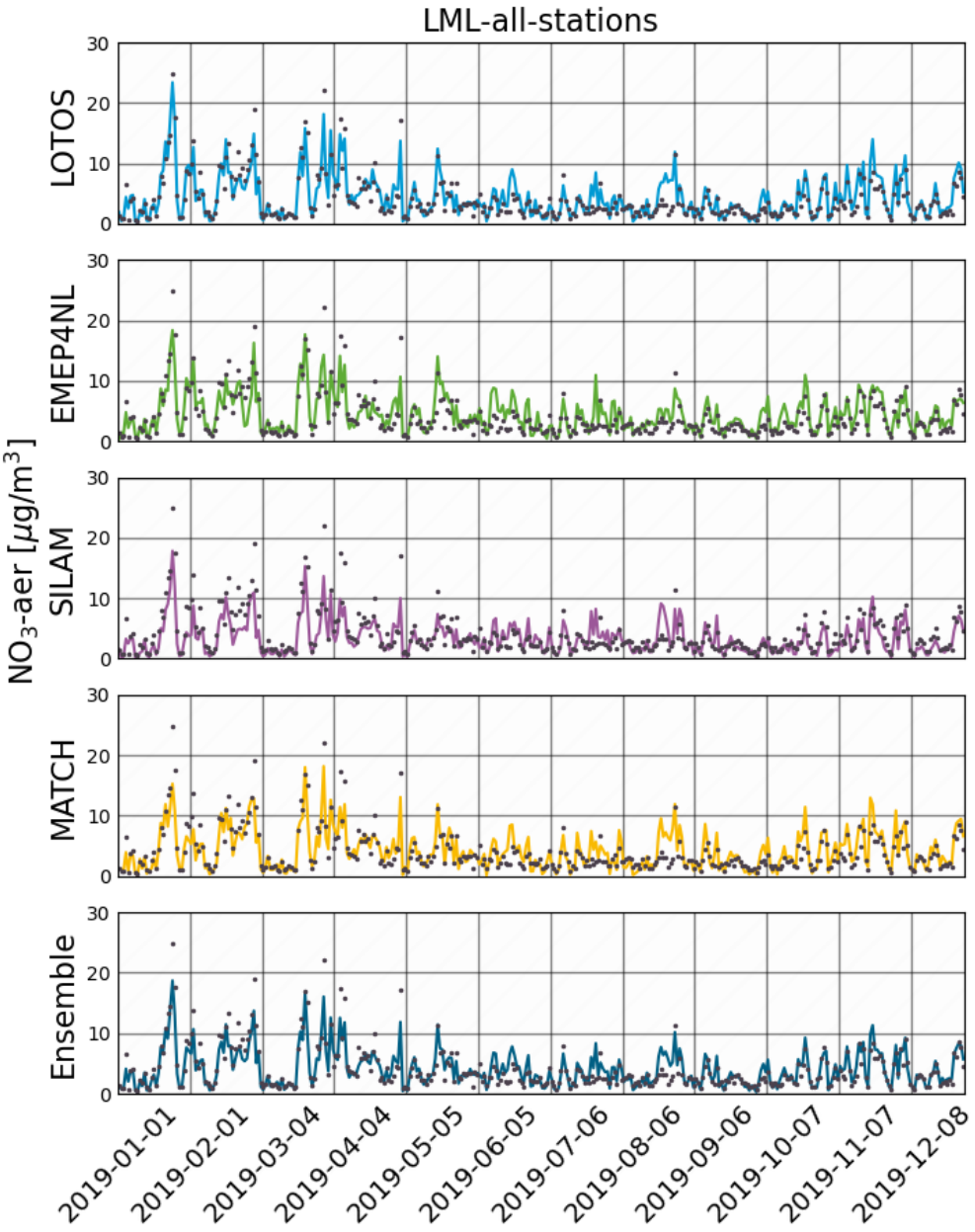

Figure 46: Nitrate aerosol concentrations for 2019 averaged over all LML-stations for each model and the ensemble. Top to bottom: LOTOS, EMEP4NL, SILAM, MATCH and Ensemble.

Table 8: Temporal statistics for nitrate aerosol concentrations on the average observations of the LML-stations.

Model	bias	NMB	RMSE	Corr
LOTOS	0.3	0.07	1.6	0.81
EMEP4NL	0.4	0.10	1.9	0.73
SILAM	-0.72	-0.17	2.1	0.73
MATCH	0.2	0.05	1.9	0.72
Ensemble	0.04	0.01	1.6	0.82

4.8 Modelled source apportionment

One of the key applications of the national scale models is source attribution. In this section we provide an overview of the results on the contributions from large source sectors in the Netherlands, Belgium, Germany and France. In this section, source apportionment results for 2018 for total N, NH_x, and NO_y are compared between the models used in the Netherlands (OPS, LOTOS, and EMEP4NL).

Total nitrogen

Averaged across the country, the OPS model explains a total nitrogen deposition of 997 eq ha^{-1} yr^{-1} by Dutch sources (Figure 47). This is 66 % of the total N deposition of 1513 eq ha^{-1} yr^{-1}. Based on a considerably lower deposition attributed to Dutch sources (about 300 eq ha^{-1} yr^{-1}) and a lower total N deposition, EMEP4NL and LOTOS both arrive at domestic contributions of 53 %. Similar findings have been reported before, but this is the first time the information is available from a direct comparison based on harmonized emission input. The ensemble results and the spread of the ensemble are shown in Figure 48.

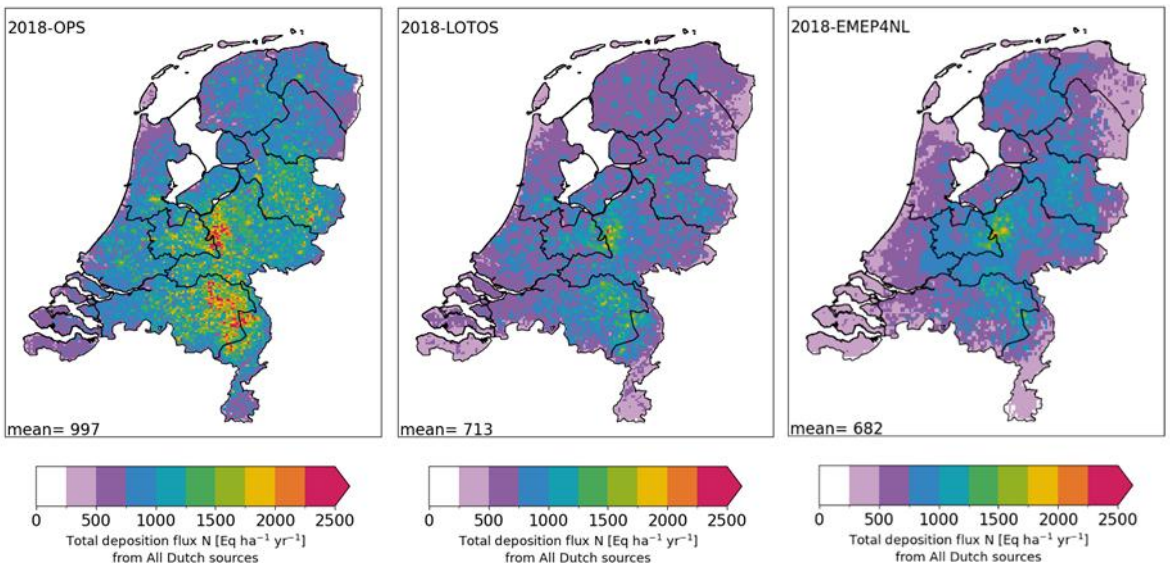

Figure 47: Total nitrogen deposition from Dutch sources in 2018 for OPS (left), LOTOS (middle), and EMEP4NL (right).

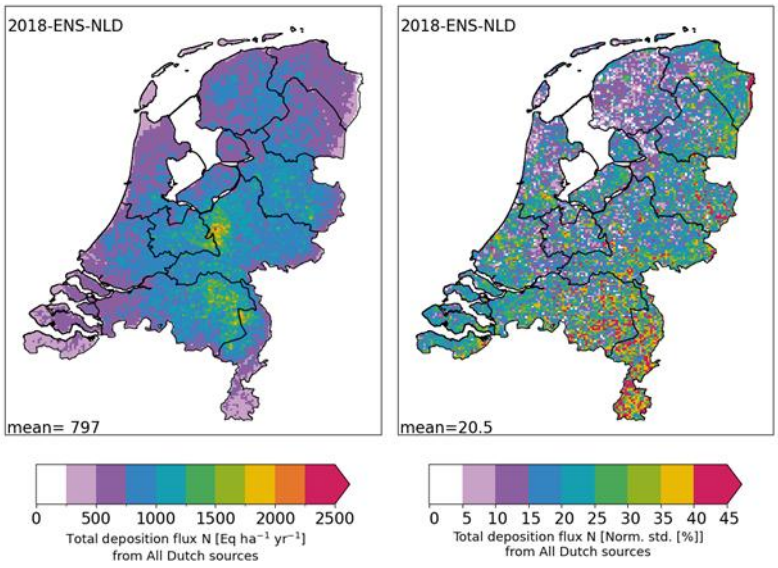

Figure 48 Total nitrogen deposition from Dutch sources for the ensemble of three Dutch models (OPS, LOTOS, and EMEP4NL). In the right plot, the normalized standard deviation is shown.

Table 9: Nitrogen depositions and country contributions of the different models and the ensemble of three Dutch models.

Tracer	Model	Total	Netherlands	Belgium	Germany	France
N	OPS	1513	997 (66%)	108 (7%)	222 (15%)	56 (4%)
NH_x	OPS	1057	790 (75%)	65 (6%)	145 (14%)	22 (2%)
NO_y	OPS	455	207 (46%)	42 (9%)	77 (17%)	34 (7%)
N	LOTOS	1349	713 (53%)	107 (8%)	260 (19%)	89 (7%)
NH_x	LOTOS	1002	599 (60%)	72 (7%)	197 (20%)	67 (7%)
NO_y	LOTOS	347	114 (33%)	35 (10%)	64 (18%)	22 (6%)
N	EMEP4NL	1291	682 (53%)	91 (7%)	262 (20%)	
NH_x	EMEP4NL	882	548 (62%)	65 (7%)	195 (22%)	
NO_y	EMEP4NL	409	134 (33%)	26 (6%)	67 (17%)	
N	ENS-NLD	1385	797 (58%)	102 (7%)	248 (18%)	
NH_x	ENS-NLD	981	646 (66%)	67 (7%)	179 (18%)	
NO_y	ENS-NLD	404	152 (38%)	35 (9%)	69 (17%)	

Reduced nitrogen (NH_x)

An overview of the source attribution for the Netherland as a whole is provide in Table 9. For NH_x, the total modelled deposition of NH_x in OPS (1057) is larger compared to LOTOS (1002) and EMEP4NL (882). The source apportionment results in this section shows that these differences are driven by different contributions from the Netherlands. In modelled depositions of NH_x from Dutch sources are shown in the top panel Figure 49 OPS, LOTOS and EMEP4NL. The lower panels show the most important Dutch source of NH_x deposition (agriculture) for the three models. The ensemble results and the spread of the ensemble are shown in Figure 50. The normalized standard deviation is on average 21 % for the contribution of all Dutch sources (20 % for only Dutch agriculture), this is comparable to the spread of the total nitrogen deposition as shown in the previous paragraph. The largest spread is found in the southeast of the country in Brabant and Limburg.

The modelled contribution from Dutch sources is 191 and 242 eq ha^{-1} yr^{-1} larger in OPS than in LOTOS and EMEP4NL respectively. For OPS, Dutch contribution to NH_x deposition is 75 % (790/1057), while LOTOS and EMEP4NL have contributions of 60 % and 62 % respectively.

For the Belgian and German contribution the results of OPS are in between the results from the other two models. Using EMEP4NL, the largest contribution from Germany is assessed, whereas LOTOS provides the largest Belgian contribution. For France, there is an obvious difference between OPS and LOTOS, with LOTOS providing a three times larger contribution than OPS. The results for Germany are difficult to interpret as the country is rather large and incorporates both nearby and distant sources. In a follow-up it is advised to differentiate the neighbouring federal states from those further away to investigate if there is a similar pattern as for Belgium and France.

When comparing the foreign contributions (Figure 51), one can observe that contribution of wet deposition becomes relatively more important for regions further away from the Netherlands. This can be explained by the important role of particulate matter components in the long range transport of reactive nitrogen. The particulate compounds are most effectively deposited by wet deposition.

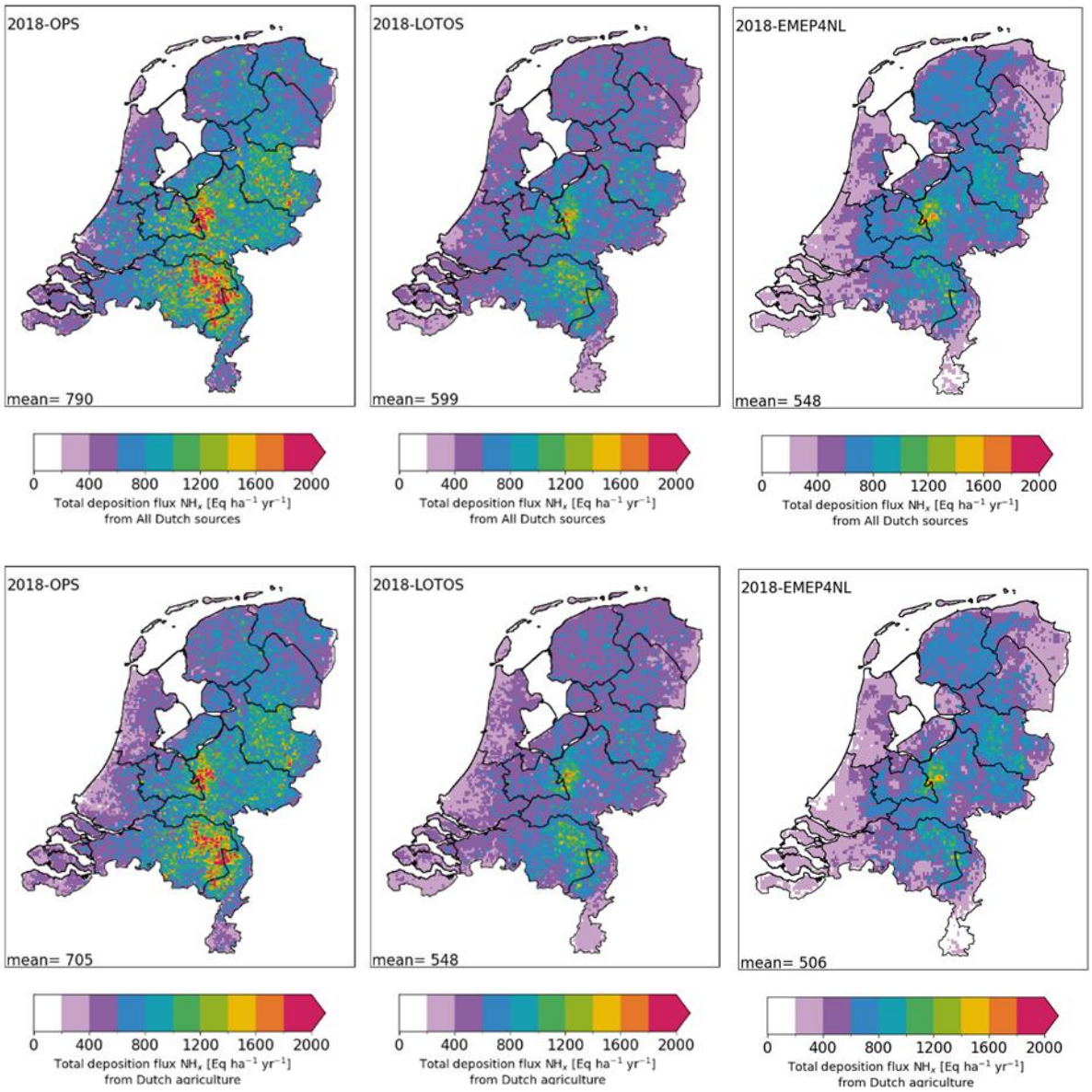

Figure 49: Total deposition of NH_x in 2018 from all Dutch sources (top panels) and from Dutch agriculture (bottom panels) for OPS (left), LOTOS (middle) and EMEP4NL (right).

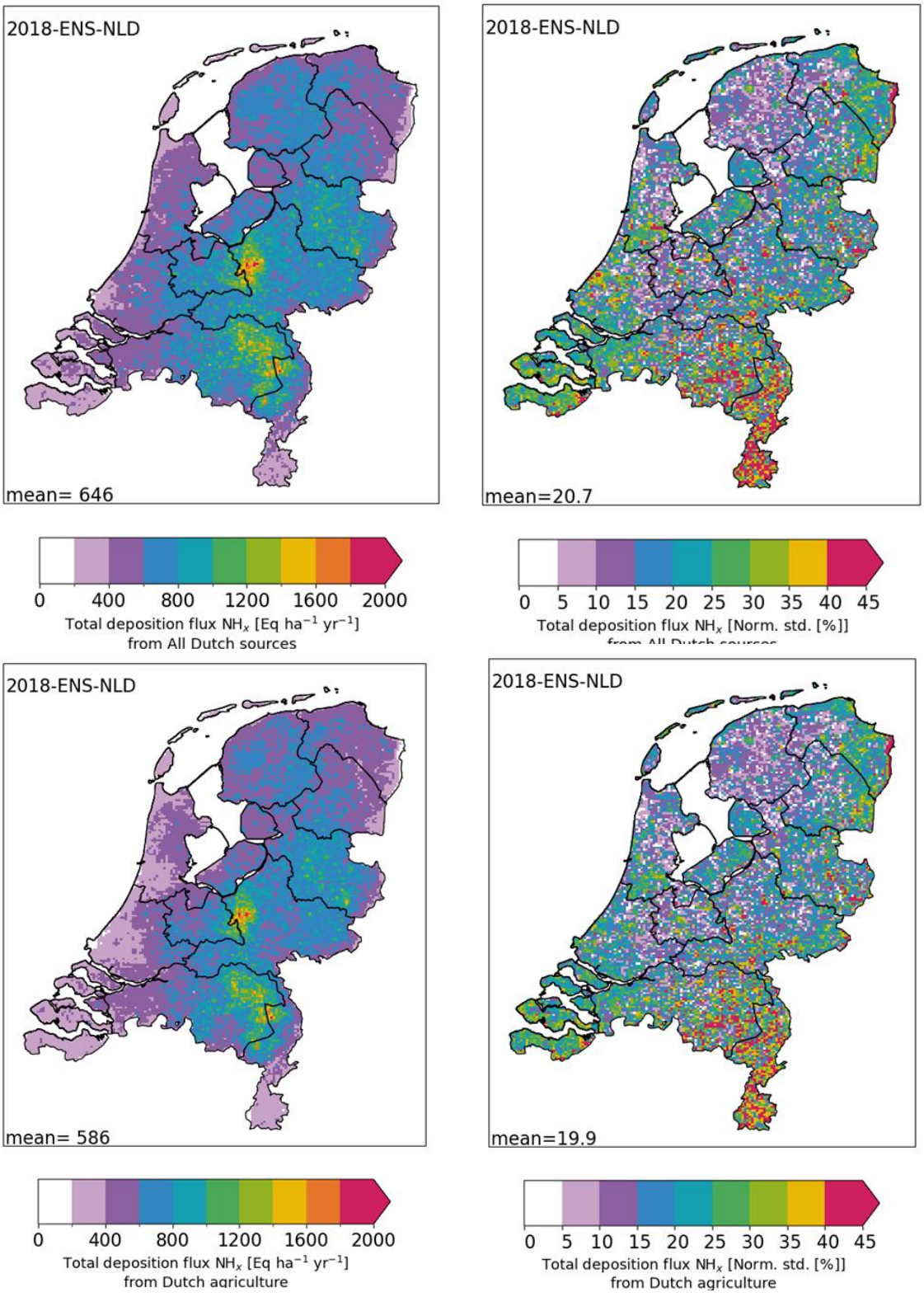

Figure 50: Total deposition flux of NHx for the ensemble of three Dutch models (OPS, LOTOS, and EMEP4NL). Left panels show the flux from all Dutch sources (top) and Dutch agriculture (bottom). The right panels show the normalized standard deviation [%] for both fluxes of the ensemble.

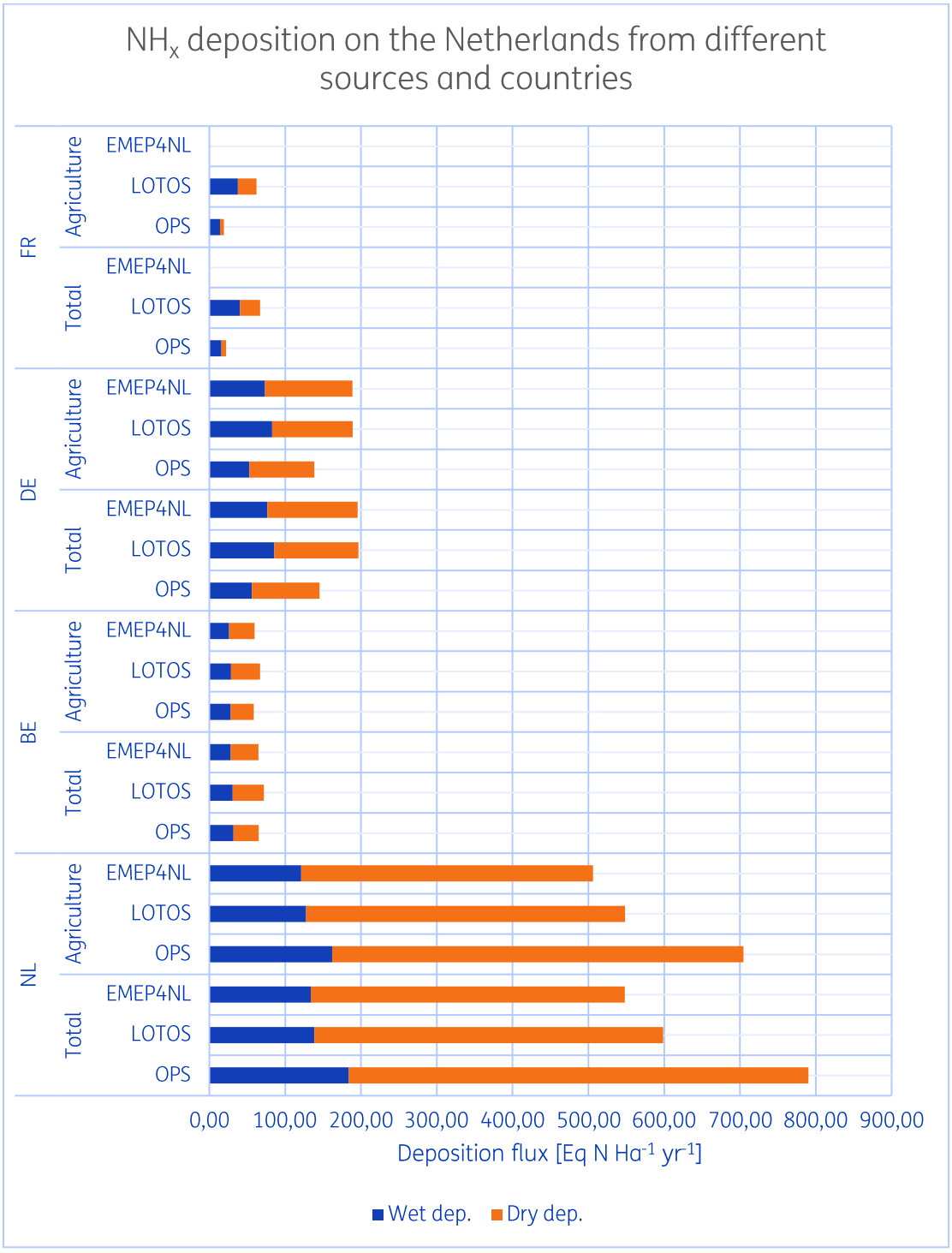

Figure 51: Source apportionment results for OPS, LOTOS, EMEP4NL for deposition of NH_x from most important source (Agriculture) and countries (Netherlands, Belgium, Germany, and France) for 2018.

Oxidized nitrogen (NO_y)

The total modelled deposition of NO_y in OPS (455) is larger compared to LOTOS (347) and EMEP4NL (404). The source apportionment results in this section shows that these differences are for a large part driven by different contributions from domestic sources. In Figure 52, deposition fluxes on the Netherlands are shown for NO_y. At the top row, contributions from all Dutch sources are displayed, the second and third row show the most important sectors for NO_y, transport and industry respectively. The results of the Dutch ensemble and the spread are shown in Figure 53. The normalized standard deviation for the ensemble with all Dutch sources is around 28 %, with even a larger spread of 36 % for contribution from Dutch transport and a similar value of 27 % for Dutch industry. Further, the spread between the models for Dutch transport is the largest in Zeeland, the coastal area and the road network. The spread for industry peaks at urban locations and the southeast of the country. For OPS, the Dutch contribution to NO_y deposition is 46 % (207 Dutch/454 total), while LOTOS and EMEP both have a domestic contribution of 33 %. This indicates that the travel distance of NO_y is smaller in OPS compared to the grid models. Furthermore, the Dutch contribution has a much larger share of wet deposited NO_y in OPS than in the other models, causing the spread between the models to be largest for this deposition pathway (see Table 10). This aspect indicates that a considerable part of the different transport distance may be related to the particulate matter formation and subsequent wet deposition in OPS. For all models the contribution of the transport sector, from the Netherlands and neighbouring countries, is more important than the industry sector from those countries (Figure 54). As percentage to deposition of NO_y contributions are 49 % vs 16 % for OPS, 37 % vs 15 % for LOTOS, and 35 % vs 10 % for EMEP4NL.

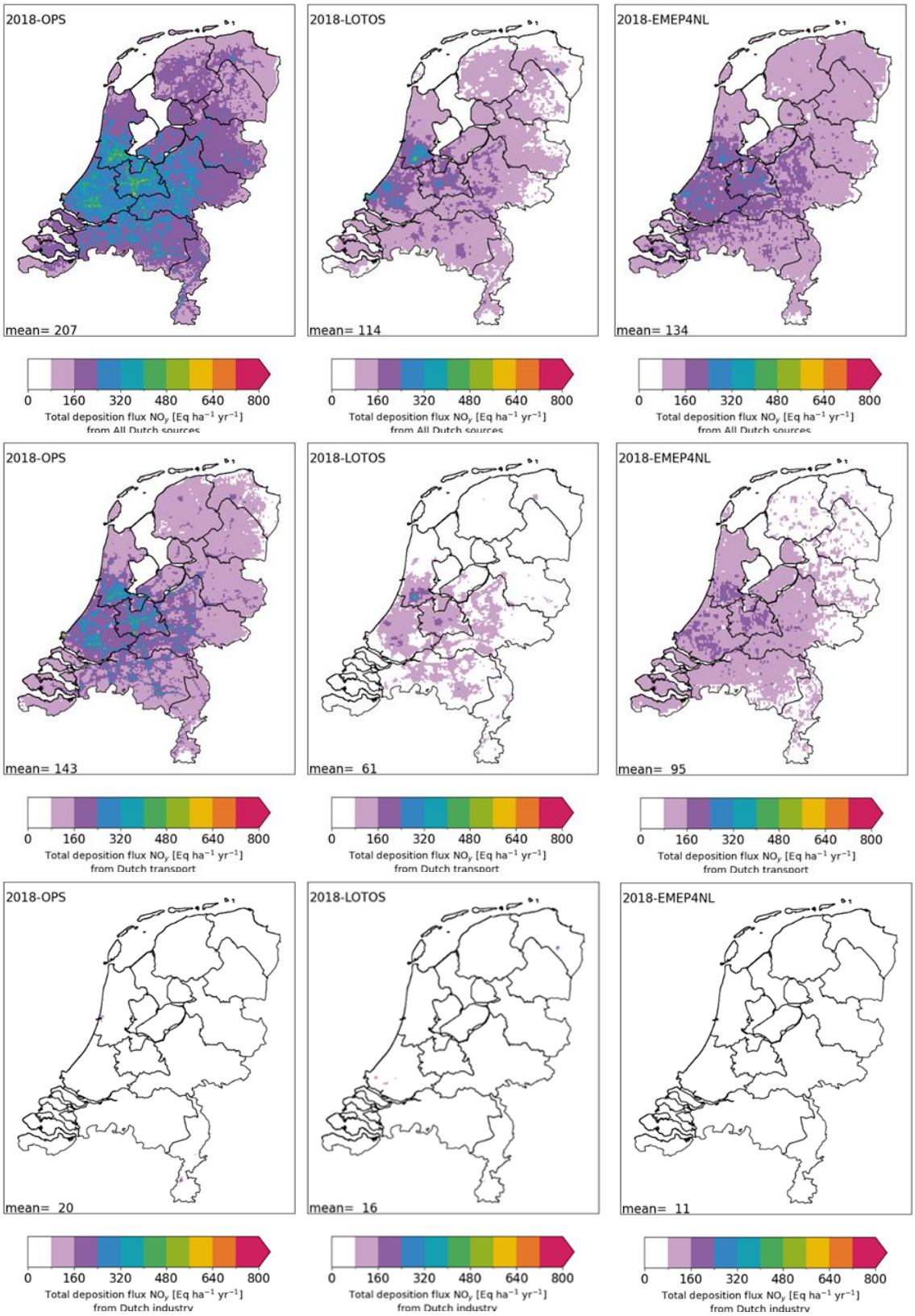

Figure 52:Total deposition of NO_y in 2018 from all Dutch sources (top), from Dutch transport (middle) and from Dutch Industry (bottom) for OPS (left), LOTOS (middle) and EMEP4NL (right).

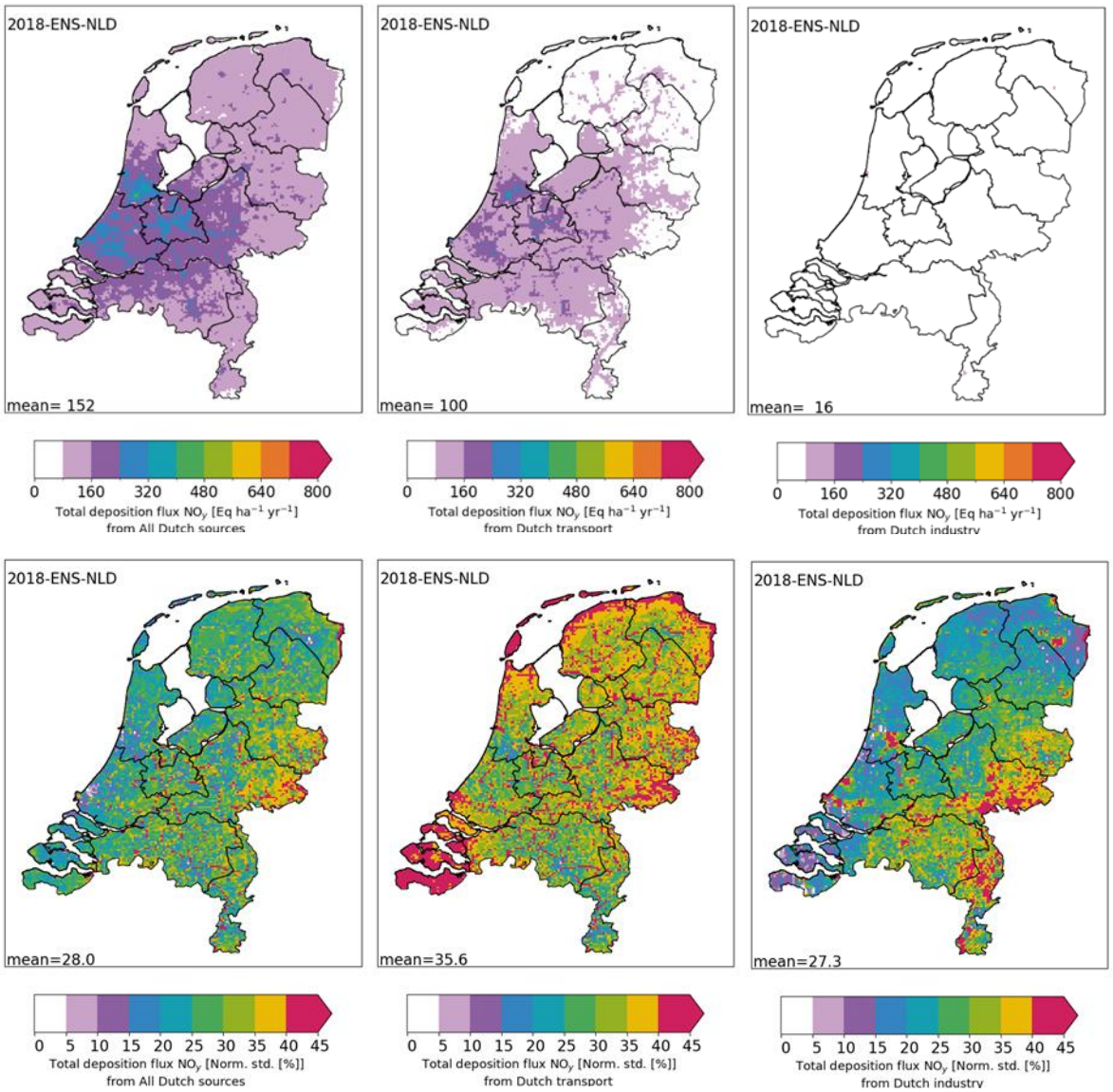

Figure 53: Total deposition flux of NO_y for the ensemble of three Dutch models (OPS, LOTOS, and EMEP4NL). top panels show the flux from all Dutch sources (left), Dutch transport (middle) and Dutch industry (right). The bottom panels show the normalized standard deviation [%] for the respective distributions.

Table 10: Normalized standard deviations [%] of the ensemble from three Dutch models for different sources and deposition types.

Tracer	Source	Total deposition	Dry deposition	Wet deposition
Total N	NL-Total	20.5	21.8	21.9
NH_x	NL-Total	20.7	24.2	17.6
	NL-Agriculture	19.9	23.5	17.2
NO_y	NL-Total	28.0	22.0	57.8
	NL-Transport	35.6	28.8	67.9
	NL-Industry	27.3	21.9	52.5

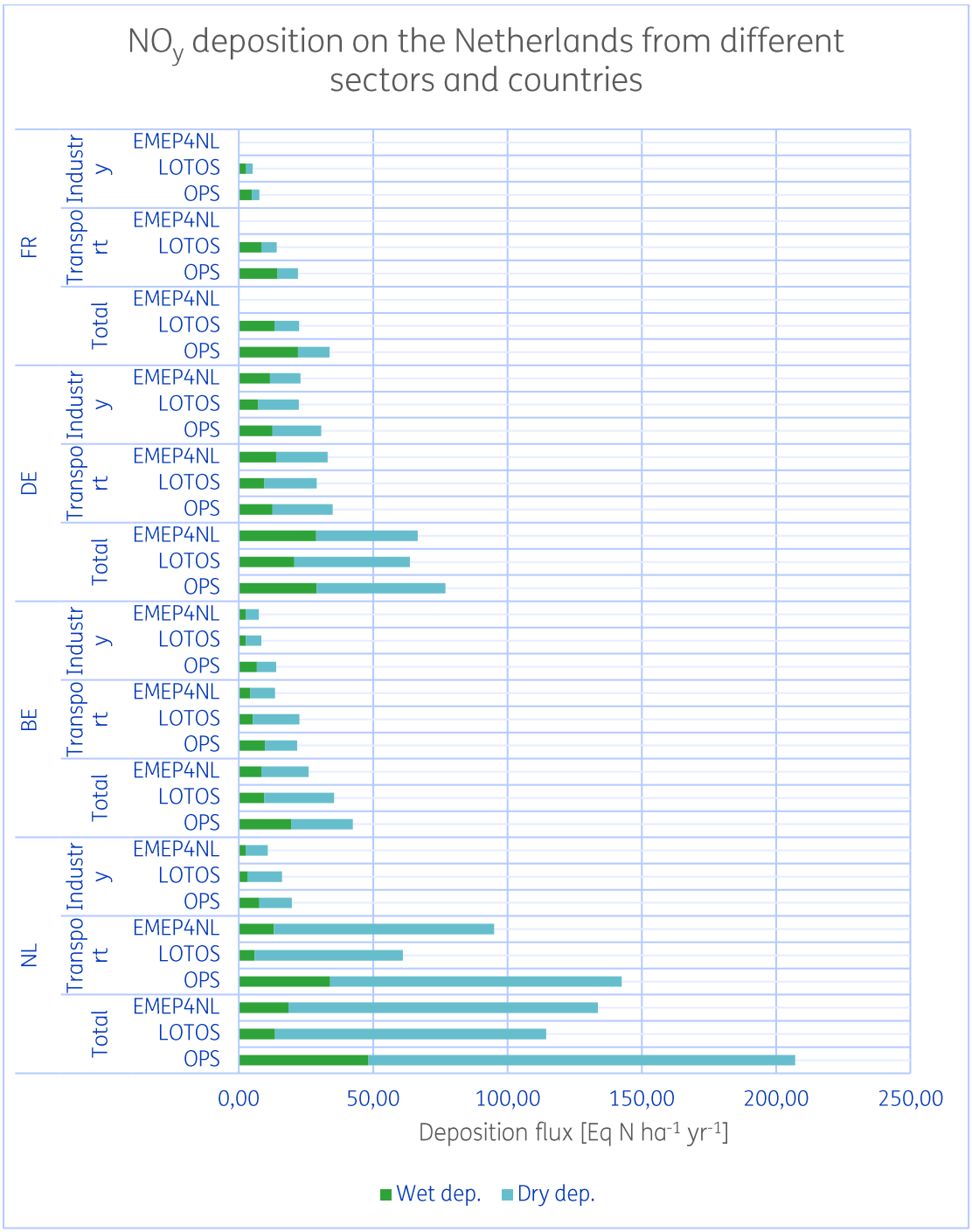

Figure 54: Source apportionment results for OPS, LOTOS, EMEP4NL for deposition of NO_y from most important sources (Transport, Industry) and countries (Netherlands, Belgium, Germany, and France) for 2018.

5 Synthesis and recommendations

This study documents the first model intercomparison study aimed at quantifying nitrogen deposition in the Netherlands at a national scale. For this purpose, 5 modelling systems were applied to model the concentration and deposition distributions of nitrogen components over the Netherlands for 2019. In addition, the models in use in the Netherlands performed simulations for additional years and provided additional information on source apportionment. The benchmark protocol prescribed uniform emission distributions. Therefore, the differences between the model results are only due to modelling aspects. Hence, in comparison to earlier assessments on similarities and differences between modelling results (based on non-uniform emission information), the current study allows to draw stronger conclusions. Furthermore, the level of detail in the available model output is much larger than that what was available before. Below, we synthesize the main results and shortly discuss their implications. Furthermore, we provide recommendations for next steps.

Modelled total deposition and spread between models

The average total nitrogen deposition in the Netherlands as calculated by the five models amounts to 1476 mol or equivalent nitrogen per hectare per year (eq ha^{-1} yr^{-1}). The individual model estimates are 1296 (EMEP4NL), 1334 (LOTOS), 1508 (SILAM), 1569 (OPS) and 1669 (MATCH) eq ha^{-1} yr^{-1}. The standard deviation (1 σ) around the ensemble mean is 141 eq ha^{-1} yr^{-1} or 10 %.

The modelled total nitrogen deposition shows a large variability across the country. Highest deposition fluxes are calculated for the regions with intensive animal husbandry and for forested areas. In the maxima the modelled ensemble mean deposition exceeds 2000 eq ha^{-1} yr^{-1}. In the western coastal provinces of Zeeland, South and North Holland and southern Limburg large areas show central estimates slightly below 1250 eq ha^{-1} yr^{-1}. The country-average standard deviation (1 σ) for the modelled deposition at a kilometer scale is about 15 % of the mean. Only for forested areas, most notably the Veluwe, the spread in the model results is considerably larger. These results suggest that in large parts of the Netherlands the modelled deposition of nitrogen is smaller than the observation-anchored uncertainty reported by Hoogerbrugge et al. (2024). Hoogerbrugge et al. (2024) estimated the uncertainty of the total deposition at a random location in the Netherlands to be around 30-35 % (1 σ). It should be noted that the spread or uncertainty provided in the present study does not include the uncertainty introduced due to uncertainty in emissions, but are solely due to differences in modelling practice, using the same emissions and not fully accounting for the uncertainty in model parameters. In the study of Hoogerbrugge et al. (2024), the uncertainty was estimated based (as much as possible) on a comparison of model results with measurements.

Table 11: Overview of the modelled dry and wet deposition for NH_x, NO_y and total N deposition for the country as a whole (eq N ha^{-1} yr^{-1}). For the ensembles the standard deviation of the mean is also provided.

	Dry-NH_x	Wet-NH_x	Dry-NO_y	Wet-NO_y	Total	% NH_x	% NO_y
OPS	733	374	260	201	1569	71	29
LOTOS	655	330	209	139	1334	74	26
EMEP4NL	573	308	268	147	1296	68	32
Ensemble mean NLD	654	337	246	162	1400	71	29
Std. ensemble mean NLD	131	38	32	30	173		
MATCH	968	356	184	162	1669	79	21
SILAM	952	220	246	90	1508	78	22
Ensemble mean INT	777	317	234	148	1476	74	26
Std. ensemble mean INT	246	59	44	38	250		

Reduced nitrogen (particularly the dry deposition of ammonia) explains a large part of the total deposition and the variability between the models. The dry ammonia deposition contributes on average almost half of the total nitrogen deposition in the Netherlands. The wet reduced nitrogen deposition contributes about 20 – 25 %. The modelled contribution of oxidized nitrogen to total nitrogen deposition varies between 21 and 32 %. The models vary a lot regarding the relative importance of dry and wet deposition for oxidized nitrogen. Thus, the spread or uncertainty between the models increases when the different contributing fluxes to the total are considered. The lower uncertainty in the totals is due to compensating effects. For example, when a model less efficiently removes nitrogen dioxide by dry deposition, dry or wet deposition of nitric acid will subsequently be enhanced. Similar compensation mechanisms apply to the spatial dimension. The uncertainty for the mean over the whole of the Netherlands, is much smaller than for individual squares of one by one kilometre.

Reduced nitrogen deposition

The largest variability between the models was determined for the dry deposition of ammonia. On average across the Netherlands, the standard deviation was about 30 % of the mean. This number means that on average there is a 95 percent probability that a model outcome falls within the range of the mean plus or minus 60 %. For comparison, the average normalized standard deviation was 23 % for ammonia and 19 % for the reduced nitrogen wet deposition. The largest variability in the modelled reduced nitrogen dry deposition with a standard deviation of about 50 % is found for the Veluwe area. The latter is due to the contrasting results of MATCH and SILAM as compared to the other three models in the ensemble. This is illustrative for the fact that these two models were often the envelope within which the other models performed. The effective dry deposition velocity, computed from the average concentration and deposition from the models, varies by a factor of two. This illustrates that the atmospheric lifetime and transport distances vary between models. An interesting case was provided by the different treatment of arable land and grassland in EMEP4NL as compared to OPS and LOTOS. This difference appears to affect the national-scale ammonia concentration and deposition patterns, highlighting the impact of differing approaches to describe ammonia exchange for agricultural land.

Oxidized nitrogen

Nitrogen dioxide is directly emitted or formed immediately after emission of nitrogen monoxide (NO). The dry and wet deposition of nitrogen dioxide is a minor loss term (~20 %) for this component, which is largely due to the low water solubility of this compound. Most nitrogen dioxide is oxidized to nitric acid (HNO_3) and may subsequently form particulate matter. The large similarity in the annual mean concentration distribution for nitrogen dioxide indicates that the mean dispersion is very similar among the models. Differences observed between the models near industrial areas and inland shipping lanes could be caused by differences in the assumptions on the effective emission height. The nationwide good agreement between modelled and observed annual mean concentrations provides evidence that the totals and spatial distribution of nitrogen oxides emissions are generally well understood. The variability between the model results increases for the reaction products of nitrogen oxides and their dry and wet deposition fluxes. This is understandable, as the number of processes involved, and the dependencies on the model skill for other reactants such as ammonia, become larger. For some key species, such as nitric acid, or key processes, such as particle deposition fluxes, no information was available for evaluation of the models. Moreover, in the regions where the models show some of the largest variability in oxidized reactive nitrogen wet deposition, likely related to differences in particulate nitrate, no observations of the quantity were available in the air quality monitoring networks. In these regions additional observations would be useful for model validation.

Skill of the ensemble

Evaluation against measurements indicates that the ensemble mean generally performs as well as, or better than, the best individual model for the quantities evaluated. The best performing model system varies per quantity. Hence, it is the consistency of the skill for all evaluated parameters that makes the ensemble model perform better than the ensemble members. This also shows that models that individually perform not as well for a certain component, still contribute to the performance of the whole ensemble. The ensemble mean model shows the largest added value for parameters that are most uncertain. In other words, for components with little uncertainty such as the nitrogen dioxide the ensemble brings less added value than for parameters where the models are further apart, such as oxidized nitrogen deposition. These features could also be observed for the small ensemble of Dutch models. At the national scale the OPS model performs comparable to the other models for ammonia and nitrogen dioxide concentrations, where the more complex models performed better for secondary components. This is in line with earlier studies in which the OPS model has been compared with LOTOS and EMEP4NL (Van Der Swaluw et al., 2017, 2021).

Domestic contribution to NH_x and NO_y deposition

The domestic contribution may be the first indicator to assess the effectiveness of national mitigation measures. The contribution of Dutch sources to the total nitrogen deposition, the so-called domestic contribution, modelled by OPS is on average 66 % in the Netherlands. In an absolute sense, this is about 1000 eq ha^{-1} yr^{-1}. The source apportionment simulations using LOTOS and EMEP4NL yield domestic contributions of 53 %. In an absolute sense the N deposition attributed to domestic sources are 300 eq ha^{-1} yr^{-1} lower. Within the domestic contribution the shares of the source sectors are similar according to all models. The systematic differences in the contribution of domestic and international contributions highlight the different ‘source receptor relationships’ in the models. The transport distance in OPS is shorter than in EMEP4NL and LOTOS, for both nitrogen oxides and ammonia. The reason for the shorter transport distance in OPS might be partly attributed to the larger concentrations of precursor gas near source areas. Such higher concentrations are expected

to yield higher deposition values on the average. Hence more nitrogen is deposited in source areas in the OPS model than in the Eulerian models.

The source attribution results indicate that the fraction of the Dutch emissions exported is larger when calculated by LOTOS-EUROS and EMEP4NL than calculated by OPS, indicating a potentially 30 % lower effectiveness of national mitigation measures as compared to OPS. Correspondingly, the LOTOS and EMEP4NL model calculations would indicate that the Netherlands can benefit more strongly from international mitigation efforts. Because the differences between the models may lead to different policy conclusions, we recommend to conduct dedicated model simulations to compare the effectiveness of potential mitigation strategies.

An assessment of the differences between OPS and the ensemble members

The mean values for the different fluxes (dry and wet deposition of reduced nitrogen and oxidized reactive nitrogen), as modelled by the OPS model, are all within the range of the other models in this study. The only exception is the wet deposition of oxidized nitrogen, in which the OPS model clearly yields the highest value of the five models (see Table 2). The above might be linked to the different spatial distributions for the modelled particulate nitrate (pNO_3^-) concentrations in the OPS model as compared to the other models: the annual average particulate nitrate distribution from OPS shows an impact of the ammonia emission distribution, whereas the other models show much less gradients across the country.

The OPS model uses chemical conversion rates derived from calculations by the EMEP4NL model (Hoogerbrugge et al., 2020). Rates for conversion from, for example, nitrogen oxides to particulate pNO_3^- are derived which are consistent with the annual mass conversion computed by EMEP4NL. As such, annual mean conversion rates are produced for use in OPS on kilometre scale resolution over the Netherlands. In reality, conversion rates vary, depending on meteorological conditions and chemical regime, from day to day and from season to season. An improvement of the application of the chemical conversion rates from EMEP4NL in OPS could be established by differentiating them according to the meteorological classes in the OPS model, instead of using a constant value over the whole year. The same reasoning applies to the formation of particulate ammonium from ammonia.

Recommendations for model development for the individual ensemble members

The analysis of the results and discussions yielded model specific recommendations:

- For OPS we recommend to address the PM formation conversion rates and subsequent wet removal efficiency (as explained above);
- For LOTOS we observed a lower dry and wet removal efficiency for (coarse) particles and we recommend to look into these aspects;
- For EMEP4NL we recommend to test the use of ECMWF meteorology and to incorporate an exchange module for arable land in line to that of OPS. Both aspects aim to improve consistency required for deriving the conversion rates to be used in OPS;
- For MATCH we recommend to look into the deposition efficiency above forests and the particulate ammonium formation;
- For SILAM we recommend to move away from the current approach for deposition and introduce a land use dependent scheme closer to those used in the other systems.

Recommendations for improvement of the ensemble as a whole

The differences between modelled and observed ammonia concentrations as well as the variability between the models is much larger for ammonia than it is for nitrogen dioxide. We have identified that four models show a pattern in which annual mean ammonia concentrations in the western coastal provinces are underestimated and those in the eastern provinces overestimated. SILAM shows a systematic underestimation nationwide. The underestimation in the coastal provinces has been subject to discussions about the source contributions of ammonia from the sea and the underestimation is popularly called "Duinengat" (in English, "Dune Gap") in the Netherlands, suggesting that the underestimation is limited to the Dune areas. The current study shows that the underestimation is also seen further inland, gradually turning into an overestimation by the models in the (south-) eastern part of the country. Currently, an explanation for this underestimation in the west and overestimation in the east is lacking. However, we can conclude that this is not an OPS specific issue but a general feature.

The underestimation of ammonia concentrations in the coastal provinces has been extensively investigated by RIVM. Three possible causes were considered in this study: the measurements, missing sources and the model calculations (Bleeker et al., 2023; R. J. Wichink Kruit et al., 2025). This research has shown that it is unlikely to be caused by the measurements, nor is it likely to that important sources are overlooked. Follow-up work has looked more closely at a number of possible modelling explanations revising the ammonia emissions from sea to very small numbers and updating the meteorological information for the Province of Zeeland. As a consequence, the systematic underestimation of OPS has declined somewhat (by about 20 %) but remains present (R. J. Wichink Kruit et al., 2025). Considering that the pattern of over and underestimations across the country is not model specific, we postulate that the origin of the biases in the different regions may have the same cause(s).

Based on the current study (and previous experiences) we postulate that the underlying causes need to be sought in a number of directions. The common aspect in these directions of research is that they move away from national scale assumptions that neglect regional variability towards detailing the spatiotemporal variability in the ammonia budget. Three directions of research are highlighted:

A. Detailing the regional variability in ammonia emissions for manure and fertilizer application: Instead of using a constant emission fraction for the whole country regional variability due to varying application practices, soil types, and soil characteristics should be introduced.
B. Detailing the temporal variability in ammonia emissions: The current practice assumes a single seasonal cycle in ammonia emissions across the country, whereas different crops and housing systems would induce variability within the country. Moreover, ammonia evaporation and this emissions are favoured under fair weather conditions that are more often associated with south, southeasterly and easterly wind conditions. First steps towards the detailing of the variability in ammonia emissions, largely based on German information, have shown a significant increase in model performance for ammonia (Ge et al., 2020; Ge, Schaap, Dammers, et al., 2023; Ge, Schaap, & de Vries, 2023). We recommend to consolidate these efforts for the Dutch practice, and expand the methodology to incorporate managed grassland.
C. Detailing the role of agricultural land as a source and sink of ammonia: Arable land and pastures cover a large part of the Netherlands and are important for the nitrogen budget. Hence, the parameterization of exchange of ammonia for these areas impacts the travel distance of ammonia and the local to national reduced nitrogen budget. For example, EMEP4NL assumes no dry deposition to arable land during the growing season. It is

unclear why a similar assumption is not made for managed grasslands, although they are manured more often throughout the growing season. In reality, agricultural crops alternate from being a source and a sink for ammonia dependent on many factors (Meyers et al., 2006). The crude assumption in EMEP4NL has a considerable impact on the modelled distributions and shows that detailing the exchange of ammonia for agricultural lands (crops and pastures on different soils) will impact the transport distances of ammonia and is required to improve the national scale ammonia modelling. In this study, the coastal areas were shown to be sensitive to differences in transport distances. Hence, we recommend to expand the current efforts to measure ammonia dry deposition to natural ecosystems towards agricultural ecosystems and further develop modelling of ammonia exchange accordingly.

These directions are not independent from each other but can be addressed simultaneously. It is important to address them all as experience learns it is never a single development that improves such complicated models. Furthermore, the integration of emission and exchange process descriptions in a single framework with an explicit soil module introduced in the chemistry transport models is a long-anticipated and fundamental step in this direction and requires all abovementioned activities.
The preparation and execution on the benchmark study opened the possibility to track the impact of future developments in the national scale models. Moreover, it is possible to extend the effort by attracting more international modelling teams that bring international knowledge and experience to the Netherlands.

Closing remarks

For the first time, we have performed a national scale benchmark study of nitrogen deposition over the Netherlands. The intercomparison showed that the national scale models developed (OPS, LOTOS) and applied (EMEP4NL) in the Netherlands are consistent with the current state of modelling practice in Europe. The ensemble proves to be an elegant way to quantify the uncertainty in modelled nitrogen deposition and pollutant concentrations. Based on the analysis presented here, we were able to give recommendations for model development of both the individual ensemble members as well as for the ensemble as a whole. We recommend to complement the benchmark with a recent year (2025) and to repeat the full intercomparison exercise 2 years from now as part of a structural quality assurance for policy modelling. Repeating the benchmark would also benefit from the current activities in expanding the LML network, and from activities in regional monitoring networks in agricultural areas. Moreover, the repetition allows for the incorporation of the advised model improvements and to further address the performance of the ensemble (mean) in comparison to a larger set of dry and wet deposition measurements.

References

Appel, K. W., Bash, J. O., Fahey, K. M., Foley, K. M., Gilliam, R. C., Hogrefe, C., Hutzell, W. T., Kang, D., Mathur, R., Murphy, B. M., Napelenok, S. L., Nolte, C. G., Pleim, J. E., Pouliot, G. A., Pye, H. O. T., Ran, L., Roselle, S. J., Sarwar, G., Schwede, D. B., ... Wong, D. C. (2021). The Community Multiscale Air Quality (CMAQ) model versions 5.3 and 5.3.1: System updates and evaluation. *Geoscientific Model Development, 14*, 2867–2897.

Banzhaf, S., Schaap, M., Kerschbaumer, A., Reimer, E., Stern, R., Van Der Swaluw, E., & Builtjes, P. (2012). Implementation and evaluation of pH-dependent cloud chemistry and wetdeposition in the chemical transport model REM-Calgrid. *Atmospheric Environment, 49*, 378–390. https://doi.org/10.1016/j.atmosenv.2011.10.069

Banzhaf, S., Schaap, M., Kranenburg, R., Manders, A. M. M., Segers, A. J., Visschedijk, A. J. H., Denier Van Der Gon, H. A. C., Kuenen, J. J. P., Van Meijgaard, E., Van Ulft, L. H., Cofala, J., & Builtjes, P. J. H. (2015). Dynamic model evaluation for secondary inorganic aerosol and its precursors over Europe between 1990 and 2009. *Geoscientific Model Development, 8*(4), 1047–1070. https://doi.org/10.5194/gmd-8-1047-2015

Barrie, L. A. (1992). Scavenging ratios: Black magic or a useful scientific tool? In S. E. Schwartz & W. G. N. Slinn (Eds.), *Precipitation scavenging and atmosphere-surface exchange* (Vol. 1, pp. 403–419). Hemisphere Publ. Corp.

Berge, E. (1993). Coupling of wet scavenging of sulphur to clouds in a numerical weather prediction model. *Tellus B, 45*(1), 1–22. https://doi.org/10.1034/j.1600-0889.1993.00001.x

Berge, E., & Jakobsen, H. A. (1998). A regional scale multilayer model for the calculation of long-term transport and deposition of air pollution in Europe. *Tellus B, 50*(3), 205–223. https://doi.org/10.1034/j.1600-0889.1998.t01-2-00001.x

Bergström, R., & Olenius, T. (2025). Atmospheric Ammonia in Sweden: Regional Modeling and Assessment of National Emission Reduction Benefits. *Submitted to Tellus B*.

Binkowski, F. S., & Shankar, U. (1995). The Regional Particulate Matter Model: 1. Model description and preliminary results. *Journal of Geophysical Research: Atmospheres, 100*(D12), 26191–26209. https://doi.org/10.1029/95JD02093

Bleeker, A., Poelhuis, M., van Pul, A., Siteur, K., & Stolk, A. (2023). *Stand van zaken ammoniak van zee. Tussenrapportage april 2023*. Rijksinstituut voor Volksgezondheid en Milieu RIVM. https://doi.org/10.21945/RIVM-2023-0308

Bott, A. (1989). A Positive Definite Advection Scheme Obtained by Nonlinear Renormalization of the Advective Fluxes. *Monthly Weather Review, 117*(5), 1006–1016. https://doi.org/10.1175/1520-0493(1989)117%253C1006:APDASO%253E2.0.CO;2

Bove, M. C., Brotto, P., Cassola, F., Cuccia, E., Massabò, D., Mazzino, A., Piazzalunga, A., & Prati, P. (2014). An integrated PM2.5 source apportionment study: Positive Matrix Factorisation vs. the chemical transport model CAMx. *Atmospheric Environment, 94*, 274–286. https://doi.org/10.1016/j.atmosenv.2014.05.039

Brandt, J., Christensen, J. H., Frohn, L. M., & Berkowicz, R. (2001). Operational air pollution forecasts from regional scale to urban street scale. Part 1: System description. *Physics and Chemistry of the Earth, Part B: Hydrology, Oceans and Atmosphere, 26*(10), 781–786. https://doi.org/10.1016/S1464-1909(01)00086-7

Briggs, G. A. (1971). Plume Rise: A Recent Critical Review. *Nuclear Safety*, *12*, 15–24.

Briggs, G. A. (1975). Plume rise predictions. In: Lectures on air pollution and environmental impact analyses, D. Haugen (editor). Workshop proceedings, Boston, Massachusetts. *American Meteorological Society, Boston, Massachusetts, USA.*, 59–111.

Briggs, G. A. (1982). Plume Rise Predictions. In D. A. Haugen, *Lectures on Air Pollution and Environmental Impact Analyses* (pp. 59–111). American Meteorological Society. https://doi.org/10.1007/978-1-935704-23-2_3

Burridge, D. M., & Gadd, (joint author.), A. J. (1977). *The Meteorological Office operational 10-level numerical weather prediction model (December 1975).* London : H.M.S.O.

Byun, D. W., & Ching, J. K. S. (1999). *SCIENCE ALGORITHMS OF THE EPA MODELS-3 COMMUNITY MULTISCALE AIR QUALITY (CMAQ) MODELING SYSTEM.* https://cfpub.epa.gov/si/si_public_record_report.cfm?dirEntryId=63400&Lab=NERL

Carter, W. P. L. (1996). Condensed atmospheric photooxidation mechanisms for isoprene. *Atmospheric Environment*, *30*(24), 4275–4290. https://doi.org/10.1016/1352-2310(96)00088-X

Colette, A., Andersson, C., Manders, A., Mar, K., Mircea, M., Pay, M.-T., Raffort, V., Tsyro, S., Cuvelier, C., Adani, M., Bessagnet, B., Bergström, R., Briganti, G., Butler, T., Cappelletti, A., Couvidat, F., D'Isidoro, M., Doumbia, T., Fagerli, H., … Wind, P. (2017). EURODELTA-Trends, a multi-model experiment of air quality hindcast in Europe over 1990–2010. *Geoscientific Model Development*, *10*(9), 3255–3276. https://doi.org/10.5194/gmd-10-3255-2017

Colette, A., Collin, G., Besson, F., Blot, E., Guidard, V., Meleux, F., Royer, A., Petiot, V., Miller, C., Fermond, O., Jeant, A., Adani, M., Arteta, J., Benedictow, A., Bergström, R., Bowdalo, D., Brandt, J., Briganti, G., Carvalho, A. C., … Rouïl, L. (2024). Copernicus Atmosphere Monitoring Service – Regional Air Quality Production System v1.0. *EGUsphere*, *2024*, 1–92. https://doi.org/10.5194/egusphere-2024-3744

De Souza Fernandes Duarte, E., Franke, P., Lange, A. C., Friese, E., Juliano da Silva Lopes, F., João da Silva, J., Souza dos Reis, J., Landulfo, E., Santos e Silva, C. M., Elbern, H., & Hoelzemann, J. J. (2021). Evaluation of atmospheric aerosols in the metropolitan area of São Paulo simulated by the regional EURAD-IM model on high-resolution. *Atmospheric Pollution Research*, *12*(2), 451–469. https://doi.org/10.1016/j.apr.2020.12.006

De Vries, W., Leip, A., Reinds, G. J., Kros, J., Lesschen, J. P., & Bouwman, A. F. (2011). Comparison of land nitrogen budgets for European agriculture by various modeling approaches. *Environmental Pollution*, *159*(11), 3254–3268. https://doi.org/10.1016/j.envpol.2011.03.038

De Vries, W., & Sauter, F. (2020, October). *OPS User manual OPS 5.0.0.0 / OPS-Pro 5.1.1.*

de Vries, W., & Sauter, F. (2022). *OPS User manual OPS 5.1.0.2 / OPS-Pro 5.2.0.* RIVM.

Dentener, F., Drevet, J., Lamarque, J. F., Bey, I., Eickhout, B., Fiore, A. M., Hauglustaine, D., Horowitz, L. W., Krol, M., Kulshrestha, U. C., Lawrence, M., Galy-Lacaux, C., Rast, S., Shindell, D., Stevenson, D., Van Noije, T., Atherton, C., Bell, N., Bergman, D., … Wild, O. (2006). Nitrogen and sulfur deposition on regional and global scales: A multimodel evaluation. *Global Biogeochemical Cycles*, *20*(4), 2005GB002672. https://doi.org/10.1029/2005GB002672

Donahue, N. M., Robinson, A. L., & Pandis, S. N. (2009). Atmospheric organic particulate matter: From smoke to secondary organic aerosol. *Atmospheric Environment*, *43*(1), 94–106. https://doi.org/10.1016/j.atmosenv.2008.09.055

Dore, A. J., Carslaw, D. C., Braban, C., Cain, M., Chemel, C., Conolly, C., Derwent, R. G., Griffiths, S. J., Hall, J., Hayman, G., Lawrence, S., Metcalfe, S. E., Redington, A., Simpson, D., Sutton, M. A., Sutton, P., Tang, Y. S., Vieno, M., Werner, M., & Whyatt, J. D. (2015a). Evaluation of the performance of different atmospheric chemical transport models and inter-comparison of nitrogen and sulphur deposition estimates for the UK. *Atmospheric Environment*, *119*, 131–143. https://doi.org/10.1016/j.atmosenv.2015.08.008

Dore, A. J., Carslaw, D. C., Braban, C., Cain, M., Chemel, C., Conolly, C., Derwent, R. G., Griffiths, S. J., Hall, J., Hayman, G., Lawrence, S., Metcalfe, S. E., Redington, A., Simpson, D., Sutton, M. A., Sutton, P., Tang, Y. S., Vieno, M., Werner, M., & Whyatt, J. D. (2015b). Evaluation of the performance of different atmospheric chemical transport models and inter-comparison of nitrogen and sulphur deposition estimates for the UK. *Atmospheric Environment*, *119*, 131–143. https://doi.org/10.1016/j.atmosenv.2015.08.008

EEA. (2017). *European Union emission inventory report 1990–2015 under the UNECE Convention on Long-range Transboundary Air Pollution (LRTAP)* (EEA Report No. No 9/2017; p. 126). https://www.eea.europa.eu/publications/annual-eu-emissions-inventory-report/at_download/file

Elberse, J., Mennen, M., Hoogerbrugge, R., Mooibroek, D., Zoch, J., Dusseldorp, A., & Janssen, N. (2021). *Tussentijdse resultaten Gezondheidsonderzoek in de IJmond*. Rijksinstituut voor Volksgezondheid en Milieu. https://doi.org/10.21945/RIVM-2021-0061

Eliassen, A., Saltbones, J., Stordal, F., Hov, Ø., Isaksen, I. S. A., & Stordal, F. (1982). A Lagrangian Long-Range Transport Model with Atmospheric Boundary Layer Chemistry. *Journal of Applied Meteorology*, *21*(11), 1645–1661. https://doi.org/10.1175/1520-0450(1982)021%253C1645:ALLRTM%253E2.0.CO;2

Emberson, L. D., Ashmore, M. R., Cambridge, H. M., Simpson, D., & Tuovinen, J. P. (2000). Modelling stomatal ozone flux across Europe. *Environmental Pollution*, *109*(3), Article 3. https://doi.org/10.1016/S0269-7491(00)00043-9

Emberson, L. D., Cooperative Programme for Monitoring and Evaluation of the Long Range Transmission of Air Pollutants in Europe, Norske meteorologiske institutt, Simpson, D., Tuovinen, J. P., & Meteorological Synthesizing Centre--West (Oslo, N. (2000). *Towards a Model of Ozone Deposition and Stomatal Uptake Over Europe*. Norwegian Meteorological Institute. https://books.google.nl/books?id=hj_ntgAACAAJ

Emberson, L. D., Simpson, D., Tuovinen, J., Ashmore, M. R., & Cambridge, H. M. (2000). Towards a model of ozone deposition and stomatal uptake over Europe. In *Environment* (Issue July).

Emberson, L. D., Wieser, G., & Ashmore, M. R. (2000). Modelling of stomatal conductance and ozone flux of Norway spruce: Comparison with field data. *Environmental Pollution*, *109*(3), 393–402. https://doi.org/10.1016/S0269-7491(00)00042-7

ENVIRON. (2010). *CAMx User Guide, Comprehensive air quality model with extensions Version 5.20* (p. 279) [Technical report]. ENVIRON.

Erisman, J. W., Sutton, M. A., Galloway, J., Klimont, Z., & Winiwarter, W. (2008). How a century of ammonia synthesis changed the world. *Nature Geoscience*, *1*, 636–639. https://doi.org/10.1038/ngeo325

Erisman, J. W., Van Pul, A., & Wyers, P. (1994). Parametrization of surface resistance for the quantification of atmospheric deposition of acidifying pollutants and ozone. *Atmospheric Environment*, *28*(16), Article 16. https://doi.org/10.1016/1352-2310(94)90433-2

Fagerli, H., Benedictow, A., & Blake, L. (2024). *EMEP Status Report 1/2024*.

Foley, K. M., Roselle, S. J., Appel, K. W., Bhave, P. V., Pleim, J. E., Otte, T. L., Mathur, R., Sarwar, G., Young, J. O., Gilliam, R. C., Nolte, C. G., Kelly, J. T., Gilliland, A. B., & Bash, J. O. (2010). Incremental testing of the Community Multiscale Air Quality (CMAQ) modeling system version 4.7. *Geosci. Model Dev.*

Fowler, D., Pilegaard, K., Sutton, M. A., Ambus, P., Raivonen, M., Duyzer, J., Simpson, D., Fagerli, H., Fuzzi, S., Schjoerring, J. K., Granier, C., Neftel, A., Isaksen, I. S. A., Laj, P., Maione, M., Monks, P. S., Burkhardt, J., Daemmgen, U., Neirynck, J., … Erisman, J. W. (2009). Atmospheric composition change: Ecosystems–Atmosphere interactions. *Atmospheric Environment*, *43*(33), 5193–5267. https://doi.org/10.1016/j.atmosenv.2009.07.068

Fox, D.G. (1984). Uncertainty in Air Quality Modeling. *Bull. Am. Meteor. Soc.*, *65*(1), 27–47.

Frohn, L. M., Geels, C., Ye, Z., Andersen, C., Christensen, J. H., Massenberg, J. R., Simpson, D., Andersson, C., Bergström, R., Bredahl Jacobsen, J., Laage-Thomsen, T., Magnussen, K., & Sigurdsson, B. D. (2025). *Nitrogen deposition in the Nordic countries: Results from two research projects focused on Nordic nature and air pollution*. Nordic Council of Ministers. https://doi.org/10.6027/NA2025-901

Galloway, J. N., Aber, J. D., Erisman, J. W., Seitzinger, S. P., Howarth, R. W., Cowling, E. B., & Cosby, B. J. (2003). The Nitrogen Cascade. *BioScience*, *53*(4), 341. https://doi.org/10.1641/0006-3568(2003)053%255B0341:TNC%255D2.0.CO;2

Galperin, M. V. (2000). *The Approaches to Correct Computation of Airborne Pollution Advection. Problems of Ecological Monitoring and Ecosystem Modelling, 17, pp. 54–68.*

Ge, X., Schaap, M., Dammers, E., Shephard, M., & De Vries, W. (2023). Impact of interannual weather variation on ammonia emissions and concentrations in Germany. *Agricultural and Forest Meteorology*, *334*, 109432. https://doi.org/10.1016/j.agrformet.2023.109432

Ge, X., Schaap, M., & de Vries, W. (2023). Improving spatial and temporal variation of ammonia emissions for the Netherlands using livestock housing information and a Sentinel-2-derived crop map. *Atmospheric Environment: X*, *17*. https://doi.org/10.1016/j.aeaoa.2023.100207

Ge, X., Schaap, M., Kranenburg, R., Segers, A., Reinds, G. J., Kros, H., & De Vries, W. (2020). Modeling atmospheric ammonia using agricultural emissions with improved spatial variability and temporal dynamics. *Atmospheric Chemistry and Physics*, *20*(24), 16055–16087. https://doi.org/10.5194/acp-20-16055-2020

Genikhovich, E. L. (2003). Indicators of performance of dispersion models and their reference values. *International Journal of Environment and Pollution*, *20*(1–6), 321–329. Scopus. https://doi.org/10.1504/ijep.2003.004295

Giorgi, F., & Chameides, W. L. (1986). Rainout lifetimes of highly soluble aerosols and gases as inferred from simulations with a general circulation model. *Journal of Geophysical Research*, *91*(D13), 14367. https://doi.org/10.1029/JD091iD13p14367

Gong, S. L. (2003). Canadian Aerosol Module: A size-segregated simulation of atmospheric aerosol processes for climate and air quality models 1. Module development. *Journal of Geophysical Research*, *108*(D1), 4007. https://doi.org/10.1029/2001JD002002

Granier, C., Darras, S., Denier van der Gon, H., Doubalova, J., Elguindi, N., Galle, B., Gauss, M., Guevara, M., Jalkanen, J.-P., Kuenen, J., Liousse, C., Quack, B., Simpson, D., &

Sindelarova, K. (2019). *The Copernicus Atmosphere Monitoring Service global and regional emissions (April 2019 version)*. https://doi.org/10.24380/D0BN-KX16

Hänninen, R. M., Kouznetsov, R., & Sofiev, M. (2023a). *Positive semi-definite variants of CBM4 and CBM05 chemistry schemes for atmospheric composition models*. https://doi.org/10.5194/gmd-2023-3

Hänninen, R. M., Kouznetsov, R., & Sofiev, M. (2023b). Positive semi-definite variants of CBM4 and CBM05 chemistry schemes for atmospheric composition models. *Geoscientific Model Development Discussions*, *2023*, 1–16. https://doi.org/10.5194/gmd-2023-3

Hass, H., Builtjes, P. J. H., Simpson, D., & Sternii, R. (1997). Comparison of model results obtained with several european regional air quality models. *Atmospheric Environment*, *31*(19), 3259–3279. https://doi.org/10.1016/S1352-2310(97)00066-6

Heimann, M., & Keeling, C. D. (1989). A three-dimensional model of atmospheric CO2 transport based on observed winds: 2. Model description and simulated tracer experiments. In *Aspects of Climate Variability in the Pacific and the Western Americas* (pp. 237–275). https://doi.org/10.1029/GM055p0237

Henzing, J. S., Olivié, D. J. L., & Van Velthoven, P. F. J. (2006). A parameterization of size resolved below cloud scavenging of aerosols by rain. *Atmospheric Chemistry and Physics*, *6*(11), 3363–3375. https://doi.org/10.5194/acp-6-3363-2006

Holtslag, A. A. M. (1991). Eddy diffusivity and countergradient transport in the convective atmospheric boundary layer. *Journal of the Atmospheric Sciences*, *48*(14), 1690–1698. Scopus. https://doi.org/10.1175/1520-0469(1991)048%253C1690:EDACTI%253E2.0.CO;2

Holtslag, A. A. M., Van Meijgaard, E., & De Rooy, W. C. (1995). A comparison of boundary layer diffusion schemes in unstable conditions over land. *Boundary-Layer Meteorology*, *76*(1), 69–95. https://doi.org/10.1007/BF00710891

Hoogerbrugge, R., Braam, M., Siteur, K., Jacobs, C., & Hazelhorst, S. (2024). *Uncertainty in the determined nitrogen deposition in the Netherlands. Status report 2023*. National Institute for Public Health and the Environment. https://doi.org/10.21945/RIVM-2022-0085

Hoogerbrugge, R., Geilenkirchen, G., den Hollander, H., Schuch, W., de Vries, W., & Wichink Kruit, R. J. (2020). *Grootschalige concentratie- en depositiekaarten Nederland. Rapportage 2020*. Rijksinstituut voor Volksgezondheid en Milieu. https://doi.org/10.21945/RIVM-2020-0091

Hoogerbrugge, R., Geilenkirchen, G. P., Hazelhorst, S., Den Hollander, H. A., Huitema, M., Marra, W., Siteur, K., De Vries, W. J., & Wichink Kruit, R. J. (2022). *Grootschalige concentratie- en depositiekaarten Nederland. Rapportage 2022*. Rijksinstituut voor Volksgezondheid en Milieu RIVM. https://doi.org/10.21945/RIVM-2022-0059

Hov, Ø., Hjøllo, B. A., & Eliassen, A. (1994). Transport distance of ammonia and ammonium in Northern Europe: 1. Model description. *Journal of Geophysical Research: Atmospheres*, *99*(D9), 18735–18748. https://doi.org/10.1029/94JD00909

Im, U., Bianconi, R., Solazzo, E., Kioutsioukis, I., Badia, A., Balzarini, A., Baró, R., Bellasio, R., Brunner, D., Chemel, C., Curci, G., Denier Van Der Gon, H., Flemming, J., Forkel, R., Giordano, L., Jiménez-Guerrero, P., Hirtl, M., Hodzic, A., Honzak, L., … Galmarini, S. (2015). Evaluation of operational online-coupled regional air quality models over Europe and North America in the context of AQMEII phase 2. Part II: Particulate matter. *Atmospheric Environment*, *115*, 421–441. https://doi.org/10.1016/j.atmosenv.2014.08.072

Im, U., Markakis, K., Unal, A., Kindap, T., Poupkou, A., Incecik, S., Yenigun, O., Melas, D., Theodosi, C., & Mihalopoulos, N. (2010). Study of a winter PM episode in Istanbul using the high resolution WRF/CMAQ modeling system. *Atmospheric Environment*, *44*(26), 3085–3094. https://doi.org/10.1016/j.atmosenv.2010.05.036

Janssen, A. J., & Ten Brink, H. M. (1985). *De samenstelling van neerslag onder een rookgaspluim: Modellering, berekening en validatie*. ECN rapport ECN-170.

Jongenelen, T., van Zanten, M., Dammers, E., Wichink Kruit, R., Hensen, A., Geers, L., & Erisman, J. W. (2025). Validation and uncertainty quantification of three state-of-the-art ammonia surface exchange schemes using NH_3 flux measurements in a dune ecosystem. *Atmospheric Chemistry and Physics*, *25*(9), 4943–4963. https://doi.org/10.5194/acp-25-4943-2025

Kaiser, J. W., Heil, A., Andreae, M. O., Benedetti, A., Chubarova, N., Jones, L., Morcrette, J.-J., Razinger, M., Schultz, M. G., Suttie, M., & van der Werf, G. R. (2012). Biomass burning emissions estimated with a global fire assimilation system based on observed fire radiative power. *Biogeosciences*, *9*(1), Article 1. https://doi.org/10.5194/bg-9-527-2012

Kiesewetter, G., Borken-Kleefeld, J., Schöpp, W., Heyes, C., Thunis, P., Bessagnet, B., Terrenoire, E., Fagerli, H., Nyiri, A., & Amann, M. (2015). Modelling street level PM_{10} concentrations across Europe: Source apportionment and possible futures. *Atmospheric Chemistry and Physics*, *15*(3), 1539–1553. https://doi.org/10.5194/acp-15-1539-2015

Köhler, I., Sausen, R., & Klenner, G. (1995). *NOx production from lightning, The impact of NOx emissions from aircraft upon the atmo sphere at flight altitudes 8–15 km (AERONOX)* [Final report to the Commission of the European Communities]. Deutch Luft und Raumfart.

Kouznetsov, R., & Sofiev, M. (2012a). A methodology for evaluation of vertical dispersion and dry deposition of atmospheric aerosols. *Journal of Geophysical Research: Atmospheres*, *117*(D1), 2011JD016366. https://doi.org/10.1029/2011JD016366

Kouznetsov, R., & Sofiev, M. (2012b). A methodology for evaluation of vertical dispersion and dry deposition of atmospheric aerosols. *Journal of Geophysical Research Atmospheres*, *117*(1). Scopus. https://doi.org/10.1029/2011JD016366

Kouznetsov, R., & Sofiev, M. (2012c). A methodology for evaluation of vertical dispersion and dry deposition of atmospheric aerosols: DRY DEPOSITION OF AEROSOLS. *Journal of Geophysical Research: Atmospheres*, *117*(D1), n/a-n/a. https://doi.org/10.1029/2011JD016366

Kranenburg, R., Segers, A. J., Hendriks, C., & Schaap, M. (2013). Source apportionment using LOTOS-EUROS: Module description and evaluation. *Geoscientific Model Development*, *6*(3), Article 3. https://doi.org/10.5194/gmd-6-721-2013

Krupa, S. V. (2003). Effects of atmospheric ammonia (NH3) on terrestrial vegetation: A review. *Environmental Pollution*, *124*(2), 179–221. https://doi.org/10.1016/S0269-7491(02)00434-7

Laakso, L. (2003). Ultrafine particle scavenging coefficients calculated from 6 years field measurements. *Atmospheric Environment*, *37*(25), 3605–3613. https://doi.org/10.1016/S1352-2310(03)00326-1

Langner, J., Robertson, L., Persson, C., & Ullerstig, A. (1998). Validation of the operational emergency response model at the Swedish Meteorological and Hydrological Institute using data from etex and the chernobyl accident. *Atmospheric Environment*, *32*(24), 4325–4333. https://doi.org/10.1016/S1352-2310(98)00175-7

Leip, A., Billen, G., Garnier, J., Grizzetti, B., Lassaletta, L., Reis, S., Simpson, D., Sutton, M. A., Vries, W. de, Weiss, F., & Westhoek, H. (2015). Impacts of European livestock production: Nitrogen, sulphur, phosphorus and greenhouse gas emissions, land-use, water eutrophication and biodiversity. *Environmental Research Letters*, *10*(11), 115004. https://doi.org/10.1088/1748-9326/10/11/115004

Loosmore, G. A., & Cederwall, R. T. (2004). Precipitation scavenging of atmospheric aerosols for emergency response applications: Testing an updated model with new real-time data. *Atmospheric Environment*, *38*(7), 993–1003. https://doi.org/10.1016/j.atmosenv.2003.10.055

Manders, A. M. M., Builtjes, P. J. H., Curier, L., Denier van der Gon, H. A. C., Hendriks, C., Jonkers, S., Kranenburg, R., Kuenen, J. J. P., Segers, A., Timmermans, R. M. A., Visschedijk, A. J. H., Wichink Kruit, R. J., van Pul, A., Sauter, F., van der Swaluw, E., Swart, D. P. J., Douros, J., Eskes, H., van Meijgaard, E., … Schaap, M. (2017). Curriculum vitae of the LOTOS–EUROS (v2.0) chemistry transport model. *Geoscientific Model Development*, *10*(11), 4145–4173. https://doi.org/10.5194/gmd-10-4145-2017

Manders-Groot, A. M. M., Segers, A. J., & Jonkers, S. (2023). *LOTOS-EUROS v2.2.003 Reference Guide* (p. 82) [Reference Guide]. TNO.

Marécal, V., Peuch, V.-H., Andersson, C., Andersson, S., Arteta, J., Beekmann, M., Benedictow, A., Bergström, R., Bessagnet, B., Cansado, A., Chéroux, F., Colette, A., Coman, A., Curier, R. L., Denier Van Der Gon, H. A. C., Drouin, A., Elbern, H., Emili, E., Engelen, R. J., … Ung, A. (2015). A regional air quality forecasting system over Europe: The MACC-II daily ensemble production. *Geoscientific Model Development*, *8*(9), 2777–2813. https://doi.org/10.5194/gmd-8-2777-2015

Marra, W., Hazelhorst, S., de Jongh, L., Wichink Kruit, R., & Schram, J. (2024). *Monitor stikstofdepositie in Natura 2000-gebieden 2024*. Rijksinstituut voor Volksgezondheid en Milieu RIVM. https://doi.org/10.21945/RIVM-2024-0076

MATCH - transport and chemistry model—SMHI. (n.d.). Retrieved October 10, 2025, from https://www.smhi.se/en/research/research-units/meteorology/method-and-models/match---transport-and-chemistry-model

Meyers, T., Luke, W., & Meisinger, J. (2006). Fluxes of ammonia and sulfate over maize using relaxed eddy accumulation. *Agricultural and Forest Meteorology*, *136*(3–4), 203–213. https://doi.org/10.1016/j.agrformet.2004.10.005

Michou, M., Laville, P., Serça, D., Fotiadi, A., Bouchou, P., & Peuch, V.-H. (2005). Measured and modeled dry deposition velocities over the ESCOMPTE area. *Atmospheric Research*, *74*(1–4), 89–116. https://doi.org/10.1016/j.atmosres.2004.04.011

Mozurkewich, M. (1993). The dissociation constant of ammonium nitrate and its dependence on temperature, relative humidity and particle size. *Atmospheric Environment. Part A. General Topics*, *27*(2), 261–270. https://doi.org/10.1016/0960-1686(93)90356-4

Mues, A., Manders, A., Schaap, M., Kerschbaumer, A., Stern, R., & Builtjes, P. (2012). Impact of the extreme meteorological conditions during the summer 2003 in Europe on particulate matter concentrations. *Atmospheric Environment*, *55*, 377–391. https://doi.org/10.1016/j.atmosenv.2012.03.002

Nemitz, E., Milford, C., & Sutton, M. A. (2001). A two-layer canopy compensation point model for describing bi-directional biosphere-atmosphere exchange of ammonia. *Quarterly Journal of the Royal Meteorological Society*, *127*(573), 815–833. https://doi.org/10.1002/qj.49712757306

Nho-Kim, E. (2004). Parameterization of size-dependent particle dry deposition velocities for global modeling. *Atmospheric Environment*, *38*(13), 1933–1942. https://doi.org/10.1016/j.atmosenv.2004.01.002

Ots, R., Loot, A., & Kaasik, M. (2014). Scale-Dependent and Seasonal Performance of SILAM Model in Estonia. In D. G. Steyn, P. J. H. Builtjes, & R. M. A. Timmermans (Eds.), *Air Pollution Modeling and its Application XXII* (pp. 593–597). Springer Netherlands. https://doi.org/10.1007/978-94-007-5577-2_100

Petroff, A., Mailliat, A., Amielh, M., & Anselmet, F. (2008a). Aerosol dry deposition on vegetative canopies. Part I: Review of present knowledge. *Atmospheric Environment*, *42*(16), 3625–3653. https://doi.org/10.1016/j.atmosenv.2007.09.043

Petroff, A., Mailliat, A., Amielh, M., & Anselmet, F. (2008b). Aerosol dry deposition on vegetative canopies. Part II: A new modelling approach and applications. *Atmospheric Environment*, *42*(16), 3654–3683. https://doi.org/10.1016/j.atmosenv.2007.12.060

Petroff, A., & Zhang, L. (2010). Development and validation of a size-resolved particle dry deposition scheme for application in aerosol transport models. *Geoscientific Model Development*, *3*(2), 753–769. https://doi.org/10.5194/gmd-3-753-2010

Pleim, J., Venkatram, A., & Yamartino, R. (1984). *ADOM/TADAP Model Development Program: The Dry Deposition Module* (p. 4). Ministry of the Environment.

Poupkou, A., Giannaros, T., Markakis, K., Kioutsioukis, I., Curci, G., Melas, D., & Zerefos, C. (2010). A model for European Biogenic Volatile Organic Compound emissions: Software development and first validation. *Environmental Modelling and Software*, *25*(12), 1845–1856. Scopus. https://doi.org/10.1016/j.envsoft.2010.05.004

Robertson, L., Langner, J., & Engardt, M. (1999a). An Eulerian Limited-Area Atmospheric Transport Model. *Journal of Applied Meteorology and Climatology*, *38*(2), 190–210. https://doi.org/10.1175/1520-0450(1999)038%253C0190:AELAAT%253E2.0.CO;2

Robertson, L., Langner, J., & Engardt, M. (1999b). An Eulerian Limited-Area Atmospheric Transport Model. *Journal of Applied Meteorology*, *38*(2), 190–210. https://doi.org/10.1175/1520-0450(1999)038%253C0190:AELAAT%253E2.0.CO;2

Robinson, A. L., Donahue, N. M., Shrivastava, M. K., Weitkamp, E. A., Sage, A. M., Grieshop, A. P., Lane, T. E., Pierce, J. R., & Pandis, S. N. (2007). Rethinking Organic Aerosols: Semivolatile Emissions and Photochemical Aging. *Science*, *315*(5816), 1259–1262. https://doi.org/10.1126/science.1133061

Roselle, S., & Binkowski, F. (1999). Cloud Dynamics and Chemistry. In *Science Algorithms of the EPA Models-3 Community Multiscale Air Quality (CMAQ) Modeling System* (pp. 11-1-11–18). United States Environmental Protection Agency.

Ruijgrok, W., Nicholson, K. W., & Davidson, C. I. (1993). *Dry deposition of particles*. Models and methods for the quantification of atmospheric input to ecosystems. Nordic Council of Ministers, Copenhagen.

Sauter, C., Fowler, H. J., Westra, S., Ali, H., Peleg, N., & White, C. J. (2023). Compound extreme hourly rainfall preconditioned by heatwaves most likely in the mid-latitudes. *Weather and Climate Extremes*, *40*, 100563. https://doi.org/10.1016/j.wace.2023.100563

Sauter, F., Sterk, M., Van Der Swaluw, E., Wichink Kruit, R. J., De Vries, W., & Van Pul, A. (2022). *The OPS model—Description of OPS 5.0.2.1 (Technical report)*. RIVM.

Schaap, M., Banzhaf, S., Scheuschner, T., Geupel, M., Hendriks, C., Kranenburg, R., Nagel, H.-D., Segers, A. J., Von Schlutow, A., Wichink Kruit, R. J., & Builtjes, P. J. H. (2017).

Atmospheric nitrogen deposition to terrestrial ecosystems across Germany. Biogeochemistry: Air - Land Exchange. https://doi.org/10.5194/bg-2017-491

Schaap, M., Hendriks, C., Kranenburg, R., Kuenen, J. J. P., Segers, A. J., Schlutow, A., Nagel, H. D., Ritter, A., & Banzhaf, S. (2018a). *PINETI-3: Modellierung atmosphärischer Stoffeinträge von 2000 bis 2015 Zur Bewertung der ökosystem-spezifischen Gefährdung von Biodiversität durch Luftschadstoffe in Deutschland.* (No. No. ISSN 1862-4359). UBA.

Schaap, M., Hendriks, C., Kranenburg, R., Kuenen, J. J. P., Segers, A. J., Schlutow, A., Nagel, H. D., Ritter, A., & Banzhaf, S. (2018b). *PINETI-3: Modellierung atmosphärischer Stoffeinträge von 2000 bis 2015 Zur Bewertung der ökosystem-spezifischen Gefährdung von Biodiversität durch Luftschadstoffe n Deutschland.* (No. ISSN 1862-4359). UBA.

Schaap, M., Timmermans, R. M. A., Roemer, M., Boersen, G. A. C., Builtjes, P. J. H., Sauter, F. J., Velders, G. J. M., & Beck, J. P. (2008). The LOTOS-EUROS model: Description, validation and latest developments. *International Journal of Environment and Pollution*, *32*(2), Article 2. https://doi.org/10.1504/IJEP.2008.017106

Scott, B. C. (1978). Parameterization of Sulfate Removal by Precipitation. *Journal of Applied Meteorology*, *17*(9), 1375–1389. https://doi.org/10.1175/1520-0450(1978)017%253C1375:POSRBP%253E2.0.CO;2

Seinfeld, J. H., & Pandis, S. N. (1998). *Atmospheric Chemistry and Physics, From Air Pollution to Climate Change*. Wiley & Sons, inc.

Seinfeld, J. H., & Pandis, S. N. (2006). *Atmospheric Chemistry and Physics: From Air Pollution to Climate Change* (2nd ed.). John Wiley & Sons, Inc.

Simpson, D., Andersson, C., Christensen, J. H., Engardt, M., Geels, C., Nyiri, A., Posch, M., Soares, J., Sofiev, M., Wind, P., & Langner, J. (2014). Impacts of climate and emission changes on nitrogen deposition in Europe: A multi-model study. *Atmospheric Chemistry and Physics*, *14*(13), 6995–7017. https://doi.org/10.5194/acp-14-6995-2014

Simpson, D., Benedictow, A., Berge, H., Bergström, R., Emberson, L. D., Fagerli, H., Flechard, C. R., Hayman, G. D., Gauss, M., Jonson, J. E., Jenkin, M. E., Nyíri, A., Richter, C., Semeena, V. S., Tsyro, S., Tuovinen, J.-P., Valdebenito, Á., & Wind, P. (2012a). The EMEP MSC-W chemical transport model – technical description. *Atmospheric Chemistry and Physics*, *12*(16), 7825–7865. https://doi.org/10.5194/acp-12-7825-2012

Simpson, D., Benedictow, A., Berge, H., Bergström, R., Emberson, L. D., Fagerli, H., Flechard, C. R., Hayman, G. D., Gauss, M., Jonson, J. E., Jenkin, M. E., Nyíri, A., Richter, C., Semeena, V. S., Tsyro, S., Tuovinen, J.-P., Valdebenito, Á., & Wind, P. (2012b). The EMEP MSC-W chemical transport model – technical description. *Atmospheric Chemistry and Physics*, *12*(16), Article 16. https://doi.org/10.5194/acp-12-7825-2012

Simpson, D., & Darras, S. (2021). *Global soil NO emissions for Atmospheric Chemical Transport Modelling: CAMS-GLOB-SOIL v2.2*. Atmosphere – Atmospheric Chemistry and Physics. https://doi.org/10.5194/essd-2021-221

Simpson, D., Fagerli, H., Hellsten, S., Knulst, J. C., & Westling, O. (2006). Comparison of modelled and monitored deposition fluxes of sulphur and nitrogen to ICP-forest sites in Europe. *Biogeosciences*, *3*(3), 337–355. https://doi.org/10.5194/bg-3-337-2006

Simpson, D., Fagerli, H., Jonson, J. E., Tsyro, S., Wind, P., & Tuovinen, J.-P. (2003). Transboundary acidification, eutrophication and ground level ozone in Europe, Part I.

Unified EMEP model description, EMEP Status Report 1/2003, Norwegian Meteorological Institute, Oslo, 74 p. *EMEP Report 1/2003*, *August*, Article August.

Singles, R., Sutton, M. A., & Weston, K. J. (1998). A multi-layer model to describe the atmospheric transport and deposition of ammonia in Great Britain. *Atmospheric Environment*, *32*(3), 393–399. https://doi.org/10.1016/S1352-2310(97)83467-X

Sintermann, J., Neftel, A., Ammann, C., Häni, C., Hensen, A., Loubet, B., & Flechard, C. R. (2012). Are ammonia emissions from field-applied slurry substantially over-estimated in European emission inventories? *Biogeosciences*, *9*(5), 1611–1632. https://doi.org/10.5194/bg-9-1611-2012

Skamarock, W. C., Klemp, J., Dudhia, J., Gill, D. O., Barker, D., Wang, W., & Powers, J. G. (2008). *A Description of the Advanced Research WRF Version 3*. *27*, 3–27.

Skjøth, C. A., Geels, C., Berge, H., Gyldenkærne, S., Fagerli, H., Ellermann, T., Frohn, L. M., Christensen, J., Hansen, K. M., Hansen, K., & Hertel, O. (2011). Spatial and temporal variations in ammonia emissions – a freely accessible model code for Europe. *Atmospheric Chemistry and Physics*, *11*(11), 5221–5236. https://doi.org/10.5194/acp-11-5221-2011

Slinn, S. A., & Slinn, W. G. N. (1980). Predictions for particle deposition on natural waters. *Atmospheric Environment (1967)*, *14*(9), 1013–1016.

Slinn, W. G. N. (1982). Predictions for particle deposition to vegetative canopies. *Atmospheric Environment (1967)*, *16*(7), 1785–1794. https://doi.org/10.1016/0004-6981(82)90271-2

Slinn, W. G. N. (1984). Precipitation scavenging. In D. Randerson (Ed.), *Atmospheric Science and Power Production* (pp. 466–532). OSTI.

Smith, R., Fowler, D., & Sutton, M. A. (2003). *The external surface re sistance in the EMEP Eulerian model, Technical note to EMEP MSC-W*.

Smith, R. I., Fowler, D., Sutton, M. A., Flechard, C., & Coyle, M. (2000). Regional estimation of pollutant gas dry deposition in the UK: Model description, sensitivity analyses and outputs. *Atmospheric Environment*, *34*(22), 3757–3777. https://doi.org/10.1016/S1352-2310(99)00517-8

Sofiev, M. (2000a). A model for the evaluation of long-term airborne pollution transport at regional and continental scales. *Atmospheric Environment*, *34*(15), 2481–2493. https://doi.org/10.1016/S1352-2310(99)00415-X

Sofiev, M. (2000b). A model for the evaluation of long-term airborne pollution transport at regional and continental scales. *Atmospheric Environment*, *34*(15), 2481–2493. https://doi.org/10.1016/S1352-2310(99)00415-X

Sofiev, M. (2002). Extended resistance analogy for construction of the vertical diffusion scheme for dispersion models. *Journal of Geophysical Research: Atmospheres*, *107*(12), ACH10-1. Scopus. https://doi.org/10.1029/2001jd001233

Sofiev, M., Genikhovich, E., Keronen, P., & Vesala, T. (2010). Diagnosing the Surface Layer Parameters for Dispersion Models within the Meteorological-to-Dispersion Modeling Interface. *Journal of Applied Meteorology and Climatology*, *49*(2), 221–233. https://doi.org/10.1175/2009JAMC2210.1

Sofiev, M., Soares, J., Prank, M., de Leeuw, G., & Kukkonen, J. (2011). A regional-to-global model of emission and transport of sea salt particles in the atmosphere. *Journal of Geophysical Research: Atmospheres*, *116*(D21). https://doi.org/10.1029/2010JD014713

Sofiev, M., Vira, J., Kouznetsov, R., Prank, M., Soares, J., & Genikhovich, E. (2015). Construction of the SILAM Eulerian atmospheric dispersion model based on the advection algorithm of Michael Galperin. *Geoscientific Model Development*, *8*(11), 3497–3522. Scopus. https://doi.org/10.5194/gmd-8-3497-2015

Sportisse, B., & Bois, L. du. (2002). Numerical and theoretical investigation of a simplified model for the parameterization of below-cloud scavenging by falling raindrops. *Atmospheric Environment*, *36*(36–37), 5719–5727. https://doi.org/10.1016/S1352-2310(02)00576-9

Stern, R., Builtjes, P., Schaap, M., Timmermans, R., Vautard, R., Hodzic, A., Memmesheimer, M., Feldmann, H., Renner, E., Wolke, R., & Kerschbaumer, A. (2008). A model inter-comparison study focussing on episodes with elevated PM10 concentrations. *Atmospheric Environment*, *42*(19), 4567–4588. https://doi.org/10.1016/j.atmosenv.2008.01.068

Strand, A., & Hov, Ø. (1994). A two-dimensional global study of tropospheric ozone production. *Journal of Geophysical Research: Atmospheres*, *99*(D11), 22877–22895. https://doi.org/10.1029/94JD01945

Sutton, M. A., Nemitz, E., Milford, C., Fowler, D., Moreno, J., San José, R., Wyers, G. P., Otjes, R. P., Harrison, R., Husted, S., & Schjoerring, J. K. (2000). Micrometeorological measurements of net ammonia fluxes over oilseed rape during two vegetation periods. *Agricultural and Forest Meteorology*, *105*(4), 351–369. https://doi.org/10.1016/S0168-1923(00)00203-3

Ten Brink, H. M., Janssen, A. J., & Slanina, J. (1988). Plume wash-out near a coal-fired power plant: Measurements and model calculations. *Atmospheric Environment (1967)*, *22*(1), 177–187.

Thunis, P., Cuvelier, C., Roberts, P., White, L., Post, L., Tarrason, L., Tsyro, S., Stern, R., Kerschbaumer, A., Rouil, L., Bessagnet, B., Bergström, R., Schaap, M., Boersen, G., & Builtjes, P. (2008). *EURODELTA – II: Evaluation of a sectoral approach to integrated assessment modelling including the Mediterranean Sea*. European Commission. Joint Research Centre. Institute for Environment and Sustainability. https://data.europa.eu/doi/10.2788/87066

Thunis, P., Degraeuwe, B., Pisoni, E., Ferrari, F., & Clappier, A. (2016). On the design and assessment of regional air quality plans: The SHERPA approach. *Journal of Environmental Management*, *183*, 952–958. https://doi.org/10.1016/j.jenvman.2016.09.049

Thürkow, M., Banzhaf, S., Butler, T., Pültz, J., & Schaap, M. (2023). Source attribution of nitrogen oxides across Germany: Comparing the labelling approach and brute force technique with LOTOS-EUROS. *Atmospheric Environment*, *292*, 119412. https://doi.org/10.1016/j.atmosenv.2022.119412

Tiedtke, M. (1989). A Comprehensive Mass Flux Scheme for Cumulus Parameterization in Large-Scale Models. *Monthly Weather Review*, *117*(8), 1779–1800. https://doi.org/10.1175/1520-0493(1989)117%253C1779:ACMFSF%253E2.0.CO;2

Timmermans, R., van Pinxteren, D., Kranenburg, R., Hendriks, C., Fomba, K. W., Herrmann, H., & Schaap, M. (2022). Evaluation of modelled LOTOS-EUROS with observational based PM10 source attribution. *Atmospheric Environment: X*, *14*, 100173. https://doi.org/10.1016/j.aeaoa.2022.100173

TNO. (2024). *Het gedrag van stikstofverbindingen in de atmosfeer*. R10757.

Tomlinson, S. J., Carnell, E. J., Dore, A. J., & Dragosits, U. (2021). Nitrogen deposition in the UK at 1 km resolution from 1990 to 2017. *Earth System Science Data*, *13*(10), 4677–4692. https://doi.org/10.5194/essd-13-4677-2021

Troen, I. B., & Mahrt, L. (1986). A simple model of the atmospheric boundary layer; sensitivity to surface evaporation. *Boundary-Layer Meteorology*, *37*(1–2), 129–148. https://doi.org/10.1007/BF00122760

Turner, D. B., Chico, T., & Catalano, J. A. (1986). TUPOS - A multiple source gaussian dispersion algorithm using on site turbulence data. *U.S. Environmental Protection Agency, EPA Publication No. EPA-600/8-86/010*(Research Triangle Park, North Carolina).

Uusitalo, L., Lehikoinen, A., Helle, I., & Myrberg, K. (2015). An overview of methods to evaluate uncertainty of deterministic models in decision support. *Environmental Modelling & Software*, *63*, 24–31. https://doi.org/10.1016/j.envsoft.2014.09.017

van der Swaluw, E., de Vries, W., Sauter, F., Aben, J., Velders, G., & van Pul, A. (2017). High-resolution modelling of air pollution and deposition over the Netherlands with plume, grid and hybrid modelling. *Atmospheric Environment*, *155*, 140–153. https://doi.org/10.1016/j.atmosenv.2017.02.009

Van Der Swaluw, E., De Vries, W., Sauter, F., Aben, J., Velders, G., & Van Pul, A. (2017). High-resolution modelling of air pollution and deposition over the Netherlands with plume, grid and hybrid modelling. *Atmospheric Environment*, *155*, 140–153. https://doi.org/10.1016/j.atmosenv.2017.02.009

Van Der Swaluw, E., De Vries, W., Sauter, F., Wichink Kruit, R. J., Vieno, M., Fagerli, H., & Van Pul, A. (2021). Trend analysis of reduced nitrogen components over the Netherlands with the EMEP4NL and OPS model. *Atmospheric Environment*, *248*, 118183. https://doi.org/10.1016/j.atmosenv.2021.118183

van der Swaluw, E., de Vries, W., Sauter, F., Wichink Kruit, R., Vieno, M., Fagerli, H., & van Pul, A. (2021). Trend analysis of reduced nitrogen components over the Netherlands with the EMEP4NL and OPS model. *Atmospheric Environment*, *248*, 118183. https://doi.org/10.1016/j.atmosenv.2021.118183

Van Dingenen, R., Dentener, F., Crippa, M., Leitao, J., Marmer, E., Rao, S., Solazzo, E., & Valentini, L. (2018). TM5-FASST: a global atmospheric source–receptor model for rapid impact analysis of emission changes on air quality and short-lived climate pollutants. *Atmospheric Chemistry and Physics*, *18*(21), 16173–16211. https://doi.org/10.5194/acp-18-16173-2018

Van Loon, M., Roemer, M. G. M., & Builtjes, P. J. H. (2004). *Model intercomparison in the framework of the review of the unified EMEP model (TNO-Report No. R2004/282).* TNO, Apeldoorn, The Netherlands.

Van Loon, M., Vautard, R., Schaap, M., Bergström, R., Bessagnet, B., Brandt, J., Builtjes, P. J. H., Christensen, J. H., Cuvelier, C., Graff, A., Jonson, J. E., Krol, M., Langner, J., Roberts, P., Rouil, L., Stern, R., Tarrasón, L., Thunis, P., Vignati, E., … Wind, P. (2007). Evaluation of long-term ozone simulations from seven regional air quality models and their ensemble. *Atmospheric Environment*, *41*(10), 2083–2097. https://doi.org/10.1016/j.atmosenv.2006.10.073

van Ulden, A. P., & Holtslag, A. A. M. (1985). Estimation of Atmospheric Boundary Layer Parameters for Diffusion Applications. *Journal of Climate and Applied Meteorology*, *24*(11), 1196–1207. JSTOR.

Van Zanten, M. C. (2010). *Description of the DEPAC module Dry deposition modelling with DEPAC_GCN2010*. www.rivm.nl

Vautard, R., Schaap, M., Bergström, R., Bessagnet, B., Brandt, J., Builtjes, P. J. H., Christensen, J. H., Cuvelier, C., Foltescu, V., Graff, A., Kerschbaumer, A., Krol, M., Roberts, P., Rouïl, L., Stern, R., Tarrason, L., Thunis, P., Vignati, E., & Wind, P. (2009). Skill and uncertainty of a regional air quality model ensemble. *Atmospheric Environment*, *43*(31), 4822–4832. https://doi.org/10.1016/j.atmosenv.2008.09.083

Versie-informatie rekenmodel ISL3a | Informatiepunt Leefomgeving. (n.d.). Informatiepunt Leefomgeving. Retrieved November 11, 2025, from https://iplo.nl/thema/lucht/vaststellen-luchtkwaliteit/rekenmodel-luchtkwaliteit-isl3a/versie-informatie-rekenmodel-isl3a/

Vieno, M., Dore, A. J., Wind, P., Marco, C. D., Nemitz, E., Phillips, G., Tarrasón, L., & Sutton, M. A. (2009). Application of the EMEP Unified Model to the UK with a Horizontal Resolution of 5× 5 km2. In *Atmospheric Ammonia: Detecting emission changes and environmental impacts* (pp. 367–372). Springer.

Vivanco, M. G., Bessagnet, B., Cuvelier, C., Theobald, M. R., Tsyro, S., Pirovano, G., Aulinger, A., Bieser, J., Calori, G., Ciarelli, G., Manders, A., Mircea, M., Aksoyoglu, S., Briganti, G., Cappelletti, A., Colette, A., Couvidat, F., D'Isidoro, M., Kranenburg, R., … Ung, A. (2017). Joint analysis of deposition fluxes and atmospheric concentrations of inorganic nitrogen and sulphur compounds predicted by six chemistry transport models in the frame of the EURODELTAIII project. *Atmospheric Environment*, *151*, 152–175. https://doi.org/10.1016/j.atmosenv.2016.11.042

Vivanco, M. G., Theobald, M. R., García-Gómez, H., Garrido, J. L., Prank, M., Aas, W., Adani, M., Alyuz, U., Andersson, C., Bellasio, R., Bessagnet, B., Bianconi, R., Bieser, J., Brandt, J., Briganti, G., Cappelletti, A., Curci, G., Christensen, J. H., Colette, A., … Galmarini, S. (2018). Modeled deposition of nitrogen and sulfur in Europe estimated by 14 air quality model systems: Evaluation, effects of changes in emissions and implications for habitat protection. *Atmospheric Chemistry and Physics*, *18*(14), 10199–10218. https://doi.org/10.5194/acp-18-10199-2018

Wall, S. M., John, W., & Ondo, J. L. (1988). Measurement of aerosol size distributions for nitrate and major ionic species. *Atmospheric Environment (1967)*, *22*(8), Article 8. https://doi.org/10.1016/0004-6981(88)90392-7

Wesely, M. L. (1989). PARAMETERIZATION OF SURFACE RESISTANCES TO GASEOUS DRY DEPOSITION IN REGIONAL-SCALE NUMERICAL MODELS. *Atmospheric Environment*, *23*(6), 1293–1304.

Whitten, G. Z., Hogo, H., & Killus, J. P. (1980). The carbon-bond mechanism: A condensed kinetic mechanism for photochemical smog. *Environmental Science and Technology*, *14*(6), 690–700. https://doi.org/10.1016/S1352-2310(00)00326-5

Wichink Kruit, R. J., Aben, J., De Vries, W., Sauter, F., Van Der Swaluw, E., Van Zanten, M. C., & Van Pul, W. A. J. (2017). Modelling trends in ammonia in the Netherlands over the period 1990–2014. *Atmospheric Environment*, *154*, 20–30. https://doi.org/10.1016/j.atmosenv.2017.01.031

Wichink Kruit, R. J., Bleeker, A., C Jacobs, Meijer, P., & Poelhuis, M. (2025). *Eindrapport Ammoniak van Zee. Samenvatting van het onderzoek naar de onderschatting van de ammoniakconcentraties langs de kust*. Rijksinstituut voor Volksgezondheid en Milieu RIVM. https://doi.org/10.21945/RIVM-2024-0095

Wichink Kruit, R. J. (Roy), van Pul, W. A. J., Otjes, R. P., Hofschreuder, P., Jacobs, A. F. G., & Holtslag, A. A. M. (2007). Ammonia fluxes and derived canopy compensation points over non-fertilized agricultural grassland in The Netherlands using the new gradient ammonia-high accuracy-monitor (GRAHAM). *Atmospheric Environment*, *41*(6), Article 6. https://doi.org/10.1016/j.atmosenv.2006.09.039

Wichink Kruit, R. J., Schaap, M., Sauter, F. J., Van Zanten, M. C., & Van Pul, W. A. J. (2012). Modeling the distribution of ammonia across Europe including bi-directional surface-atmosphere exchange. *Biogeosciences*, *9*(12), 5261–5277. Scopus. https://doi.org/10.5194/bg-9-5261-2012

Wichink Kruit, R. J., Van Pul, W. A. J., Sauter, F. J., Van Den Broek, M., Nemitz, E., Sutton, M. A., Krol, M., & Holtslag, A. A. M. (2010). Modeling the surface–atmosphere exchange of ammonia. *Atmospheric Environment*, *44*(7), 945–957. https://doi.org/10.1016/j.atmosenv.2009.11.049

Willis, P. T., & Tattelman, P. (1989). Drop-size Distributions Associated with Intense Rainfall. *Journal of Applied Meteorology*, *28*, 3–15.

Zender, C. S., Bian, H., & Newman, D. (2003). Mineral Dust Entrainment and Deposition (DEAD) model: Description and 1990s dust climatology. *Journal of Geophysical Research: Atmospheres*, *108*(D14). https://doi.org/10.1029/2002JD002775

Zhang, L. (2001). A size-segregated particle dry deposition scheme for an atmospheric aerosol module. *Atmospheric Environment*, *35*(3), 549–560. https://doi.org/10.1016/S1352-2310(00)00326-5

Zhang, L., Brook, J. R., & Vet, R. (2003). A revised parameterization for gaseous dry deposition in air-quality models. *Atmospheric Chemistry and Physics*, *3*(6), Article 6. https://doi.org/10.5194/acp-3-2067-2003

Zhang, L., Gong, S., Padro, J., & Barrie, L. (2001). A size-segregated particle dry deposition scheme for an atmospheric aerosol module. *Atmospheric Environment*, *35*(3), Article 3. https://doi.org/10.1016/S1352-2310(00)00326-5

Zilitinkevich, S., & Mironov, D. V. (1996). A multi-limit formulation for the equilibrium depth of a stably stratified boundary layer. *Boundary-Layer Meteorology*, *81*(3), 325–351. https://doi.org/10.1007/BF02430334

Signature

TNO › Energy & Materials Transition › Utrecht, 4 December 2025

ValidSigned by Sam van Goethem
on 2025-12-05 17:42:47

Sam van Goethem
Research Manager
Air Quality and Emissions Research

ValidSigned by Martijn Schaap
on 2025-12-09 13:26:46

Martijn Schaap
Principal Scientist Air Quality
Air Quality and Emissions Research

Appendix A

Model descriptions

In this appendix, we provide the more technical model descriptions of the participating models OPS, LOTOS-EUROS, EMEP4NL, MATCH and SILAM. Finally, a list of all (also the ones that did not participate) international model candidates is given.

A.1 OPS-LT

A.1.1 Introduction

The long-term version of the Operational Priority Substances (OPS-LT) model has been developed at RIVM to assess the present state and trends of the concentration and deposition within the Netherlands of pollutants like NH_3, NO_x, SO_2 and particulate matter. Official background maps of these quantities, based on computations with OPS-LT, are provided annually (e.g., Hoogerbrugge et al., 2022) and an outlook of the developments is given as well. The information is provided in support of policy making and licensing practice. The OPS-LT-model is an important component of AERIUS, the calculation tool for the living environment, ultimately targeting assessment of nitrogen deposition (www.aerius.nl). OPS-LT has also been applied to analyze the air quality in specific situations, e.g., where there may be an impact on public health in a particular region (e.g. Elberse et al., 2021)) as well as for research applications (see Van Der Swaluw et al. (2021) for more references in this regard).

OPS-LT is a source-receptor model. The equations governing the transport, dispersion and deposition processes are solved analytically. This allows the use of non-gridded sources and receptors as well as gridded configurations. In the latter case, the grid-size can be varied according to the needs. Using combinations of gridded receptors and non-gridded sources, including point sources, is also possible. Since OPS-LT is a source-receptor model it has implemented source apportionment in its calculations by construct. Thus, sectoral contributions from local, regional and foreign sources can be easily combined and distinguished (De Vries & Sauter, 2020). The area for which concentrations and depositions can be calculated is determined by the size of the area for which meteorological parameters are known. Since the standard climatological data set used for this model is based on observations from the Royal Netherlands Meteorological Institute (KNMI), the maximum size of the receptor area becomes, in effect, the Netherlands and adjoining regions (F. Sauter et al., 2022).

A.1.2 Lagrangian model system

The so-called long-term version of the model used in this study, OPS-LT, simulates the process sequence of emission into the atmosphere, transport and dispersion, chemical conversion and deposition of pollutants. It is based on the well-established principles of Gaussian dispersion in the atmosphere (Seinfeld & Pandis, 2006). Gaussian plumes from point or area sources are combined with a Lagrangian trajectory model for long-range transport to describe relations between individual sources or source areas, and individual

receptors even at long distances. As such, it can also be classified as a long-term climatological trajectory model that treats impacts of sources on a receptor independently (F. Sauter et al., 2022).

The model is considered statistical in the sense that concentration and deposition values are calculated for a number of typical situations, called classes. Long-term values are obtained by summation of the outcomes per class, weighted with their relative frequencies of occurrence. Classes are defined by meteorological conditions in combination with travel distance of air parcels between source and receptor. Regarding travel distance, four representative trajectory distance classes are distinguished, representing the contribution from local sources (within 50 km from the receptor, or ~1-2 hours of transport time) and from sources at intermediate (100km), long (300 km) and very long (1000km or ~2-4 days of transport time) distances. The meteorological classes are based on wind direction (12 wind sectors of 30°) and a combination of atmospheric static stability and distance-dependent criteria of the maximum mixing height over the trajectory (see Figure 55, from Sauter et al., 2022).

The construction of the trajectories in OPS-LT is based on the meteorological conditions in the Netherlands, provided by KNMI. Using the observed average wind speed and direction in the Netherlands, the path followed by an air parcel arriving at a receptor point is traced back during 96 hours (4 days). These are the trajectory paths describing the transport between the sources and the receptors. For each trajectory, the meteorological conditions and related parameters are determined. Trajectories are grouped according to the aforementioned classes, using the meteorological preprocessor METPRO, and the relative number of occurrences (frequency) of each class is determined. For each class, the corresponding average primary meteorological conditions (windspeed, temperature, humidity, solar radiation) and derived, secondary, parameters (e.g., maximum mixing layer height, aerodynamic resistance at 4 m, rainfall probability and duration) are computed (F. Sauter et al., 2022).

OPS-LT assesses if a specific source is present in a trajectory, and contributes to the concentration at a given receptor point. It then links this contribution to a specific trajectory class. For any arbitrary source-receptor combination, the trajectory characteristics are inter- and extrapolated between distances and wind directions. Ultimately, contributions from each class are summed, weighted with their relative frequencies of occurrence.

Class	Atmospheric stability	Monin-Obukhov length L (m)	Trajectory: 0 km	Trajectory: 100 km	Trajectory: 300 km	Trajectory: 1000 km
			Maximum mixing height over trajectory (m)			
U1	Unstable	$L < 0$ (1)	< 500	< 800	< 900	< 1000
U2			≥ 500	≥ 800	≥ 900	≥ 1000
N1	Neutral	$L > 100$ (1)	< 400	< 400	< 500	< 800
N2			≥ 400	≥ 400	≥ 500	≥ 800
S1	Stable	$0 < L < 100$	< 80	< 150	< 400	< 800
S2			≥ 80	≥ 150	≥ 400	≥ 800

Figure 55: Criteria for the atmospheric stability, mixing height and transport distance classes. U, N, S denote Unstable, Neutral and Stable classes; the indices 1 and 2 denote relatively low and high mixing height

respectively. [1)] Values of Monin-Obukhov length (L) < -100 are put into the classes U1 or U2 instead of in one of the neutral classes to avoid averaging of very large positive and very large negative values of L. [From Sauter et al., 2022]. The classes mentioned in the table are determined in each of the 12 wind direction classes.

A.1.3 Emissions

OPS-LT is quite flexible regarding specification of emissions. Users can specify the location of each source individually, along with various characteristics of each source. The main source area for OPS-LT is a circle with a radius of 1000 km, with the Netherlands located in the centre. The contribution of sources in this area to concentration and deposition in the Netherlands may be calculated for countries and economic sectors individually. The contribution of sources outside this area, but within Europe, can be estimated as well, but with less accuracy (de Vries & Sauter, 2022).

Point sources are distinguished from area sources. Emissions of either type can be input to the model in any number and in any combination. For both types of sources, a diurnal emission variation can be specified per individual source, on a two-hourly basis. Default variations are available, describing, e.g., effects of traffic intensity, average industrial activity or a source with an emission that is constant in time. User-defined variations are allowed as well. In the case of emissions due to space heating in buildings a seasonal effect is modelled (F. Sauter et al., 2022). Emission of NH_3 from manure application and from animal housing systems are a special case. For these emissions, correction factors (relative to the average emission strength) related to meteorological conditions are applied to account for weather-related temporal variations. All emission variations are linked to the OPS meteorological classes and as such weighed with frequency of occurrence of these classes.

OPS-LT distinguishes gaseous and particulate emissions (de Vries & Sauter, 2022). In the case of gaseous emissions, the rise of plumes due to momentum (Turner et al., 1986) and heat (Briggs, 1971, 1975, 1982) is accounted for, based on user-specified source characteristics of heat content or of stack diameter, exit flow and - temperature. Furthermore, building effects on emissions using correction factors determined offline on the basis of calculations with ISL3a (*Versie-Informatie Rekenmodel ISL3a | Informatiepunt Leefomgeving*, n.d.) can be included. To deal with particulate emissions a particle-size distribution has to be specified. In this case, the emission is considered to be distributed over six particle-size classes (<0.95 µm; 0.95-2.5 µm; 2.5-4 µm; 4-10 µm; 10-20 µm; >20 µm). Pre-defined distributions are available, but the user-specified distributions can be prescribed as well (de Vries & Sauter, 2022).

A.1.4 Transport

Based on the meteorological conditions in the Netherlands, the paths followed by air parcels arriving at a receptor point are traced back during 96 hours. These are the trajectories described in Section A.1.2. The trajectories are grouped into the meteorological classes, that have been discussed before, and which are used to assess the removal processes during the transport. The removal processes include dry- and wet deposition and chemical conversion.

In OPS-LT, the approach to account for the effect of deposition on the concentration in air can be described as ‘source depletion with surface correction’. In this approach the loss of airborne material due to deposition is accounted for by appropriately reducing the source strength as a function of down-wind distance.

Locally, at the receptor points, the concentration is computed using the contributions from each source to a specific receptor, by summation of the contributions per class, weighted with their relative frequencies of occurrence. Local deposition is using the local conditions regarding wind speed (statistics) and precipitation (statistics), along with aerodynamic roughness and (other) land-surface properties relevant to dry deposition.

Dispersion parameters are intimately linked with the transport. They are described as a function of distance from the source and the development of the plume: within an area source, not yet fully mixed and uniformly mixed in the mixing layer. In OPS-LT, the lateral dispersion parameter is taken equal to the wind sector angle, also taking into account the horizontal dimension of area sources. Regarding the vertical dispersion parameter related to point source emissions a distinction is made between local dispersion near the source and dispersion at longer distances. The local dispersion parameter is described as a function of source height, mixing height and a stability-dependent vertical dispersion length. Further away from the source, the vertical dispersion length becomes equal to the mixing layer height, which is the maximum mixing layer height over the part of the trajectory path considered. In the case of area sources, the local dispersion length is taken to be a function of the variability of source heights within the area and approximating the area source as an infinite number of point sources (F. Sauter et al., 2022).

A.1.5 Chemical conversion

Since OPS-LT applies analytical solutions for plumes, implementation of a full chemistry scheme involving many species and reactions, is not feasible. Only pseudo first-order chemical reactions are permitted in the present model. Thus, chemistry in the OPS-LT model is strongly parameterized, and therefore expected to be less robust regarding chemical conversion than a Eulerian chemistry transport model (van der Swaluw et al., 2017). This is the reason why OPS-LT currently has the option to use chemical conversion rates derived from the EMEP model (Simpson et al., 2012a) in the configuration for the Netherlands (EMEP4NL; Van Der Swaluw et al., 2021; also see Section A.3). Since the use of this option has become the default in the production of the concentration and deposition maps in the Netherlands it was used in the benchmark runs as well.

The chemistry scheme in EMEP computes the removal of the precursors SO_2, NO_x, and NH_3 and their transformation into secondary inorganic sulphate, nitrate and ammonium aerosols (Simpson et al., 2012a). In order to derive corresponding conversion rates for use in OPS-LT, a special routine was added in EMEP. In this routine, for each grid cell and for each time step, the mass of the precursors at the start of the time step and the mass chemically converted into a secondary species during that time step are obtained. Masses are integrated over the mixing layer depth and ultimately stored as yearly averaged mass values. The maps of precursor and converted mass produced in this way are read in OPS-LT. The masses obtained from the maps are averaged over a trajectory between source and receptor and then used to compute net conversions rates, in %/hour (F. Sauter et al., 2022). The computed rates can be used directly in the pseudo first-order chemical reaction equations applied in OPS-LT. See Simpson et al. (2012a) for more details on the treatment of chemical conversion in EMEP.

A.1.6 Wet deposition

For wet deposition, OPS-LT follows the common approach of discerning in-cloud and below-cloud scavenging. The below cloud scavenging rate is assumed to be relevant at short distances from the source only, where interactions between a plume and clouds may be

ignored. In-cloud scavenging is assumed to be the most relevant wet deposition process at distances further away from the source.
Below-cloud scavenging is related to precipitation intensity, determined from meteorological observations, and to drop size distribution. Furthermore, the molecular diffusivity of the species under consideration is taken into account (Janssen & Ten Brink, 1985). During the calculations, it is assumed that in-cloud scavenging is more effective than below-cloud scavenging. Below-cloud scavenging of NO_x is ignored because of its low solubility in water (Sauter et al., 2022). In the case of particles, below-cloud scavenging is also assumed to depend on precipitation intensity and the droplet size. This includes the effect of the precipitation characteristics on the particle-droplet collision efficiency, which depends on both the droplet and particle size.

Within-cloud scavenging is described by means of the commonly applied scavenging rate. This quantity is given by the scavenging ratio, defined as the concentration ratio between the initial concentration in air and in precipitation, the scavenging depth, and the precipitation intensity derived from meteorological observations. The scavenging ratio may be determined empirically, or theoretically from Henry's law equilibrium. In the case of particles, empirical values are taken, also assuming dependence of in-cloud scavenging on particle-size may be neglected. The scavenging depth is taken to be equal to the two times the dispersion length for plumes that are located completely above the mixed layer, and equal to mixed layer depth for other plumes. A summary of the implementation is given in Table 12.

Table 12: Coverage of different processes in the wet deposition scheme of OPS (F. Sauter et al., 2022).

Process description		Implementation
In-cloud scavenging (Barrie, 1992)	Species dependence	Henry's law equilibrium, empirical for SO_2, NH_3, NO_x Fixed scavenging ratio for particles
	Precipitation dependence	Precipitation rate
	Scavenging depth	Dependency of mixing height or vertical dispersion length
	Aerosol size dependence	-
Below-cloud scavenging (Ten Brink et al., 1988)	Species dependence	Correlation with species diffusivity
	Precipitation dependence	Drop size distribution
	Scavenging depth	-
	Aerosol size dependence	Particle size to drop size ratio

A.1.7 Dry deposition

For estimations of gaseous dry deposition, OPS-LT uses the DEPAC dry deposition routines (Van Zanten, 2010). The DEPAC module is driven by the average meteorological conditions that characterize a specific meteorological class. It is called for all source-receptor combinations that contribute to a concentration, and hence deposition, at a specific receptor point. Estimates of dry deposition are made by computing the deposition velocity v_d for all land use types occurring in a receptor grid cell or over a trajectory. The deposition velocity is the land use fraction weighted average from all contributing land use types ("tiling" approach), an overview of all dependencies is given in Table 13.

Dry deposition of aerosols in general is related to the dimension of the particles, using data from Slinn (1982). Per particle size class a settling velocity is computed, based on Stokes law. If the settling velocity leads to a significant contribution to dry deposition, the settling velocity is used in an alternative resistance scheme in which an extra deposition path is

introduced parallel to the aerodynamic path (described by $r_a + r_b$) which enhances the deposition velocity of the particles.
In case of acidifying aerosols, which are generally relatively small in size, the approach is to introduce a surface resistance for particles, r_{part}, that depends on the surface roughness. For roughness lengths below 0.5m, the model proposed by Wesely (1985) is used, which computes r_{part} as a function of the friction velocity and atmospheric stability. In the case of rougher surfaces, like forests, a collection efficiency is computed based on relative humidity, wind speed and friction velocity (Ruijgrok et al., 1993). See Table 14 for an implementation summary.

Table 13: *Coverage of different processes in the dry deposition scheme (DEPAC).*

Process description		Implementation
Number of land use classes		9
Photosynthetically active radiation (PAR)		sunlit & shaded fraction of leaves
Growing season dependency		LAI parameters for each LUC
Surface area dependence		SAI linearly related to LAI roughness
Stomatal Resistance R_{sto} (Emberson, Ashmore, et al., 2000; Emberson, Simpson, et al., 2000)	Phenology influence	LAI variation prescribed
	Light influence	Based on PAR
	Temperature influence	Optimum curve, assumed constant within canopy
	Vapor pressure deficit (VPD) influence	Linear dependence on VPD
	Soil water influence	-
	Particulars	HNO_3 always small Rc
	Speciation	Stomatal resistance is scaled from ozone on basis of diffusivity ratio
	Compensation point NH_3	Determined from T-dependent NH_3/NH_4^+ equilibrium (Nemitz et al., 2001; R. J. (Roy) Wichink Kruit et al., 2007)
Non-stomatal resistances	External resistance R_{ext}	Dependent on SAI and RH, low-temperature correction for freezing conditions
	In-canopy resistance R_{inc}	Dependent on canopy height, friction velocity & SAI
	Ground surface resistance R_{gs}	Tabulated values (LUC & species dependent) with low-temperature and snow coverage correction
	Particulars	SO2 high deposition rate for wet surfaces
	Co-deposition NH_3/SO_2	Factor dependent on NH_3/SO_2 balance in external surface compensation point
	Speciation	Other species interpolated between O_3 and SO_2 using solubility and reactivity indices
	Compensation point NH_3	Both for external surface and soil, determined from T-dependent NH_3/NH_4^+ equilibrium (Nemitz et al., 2001; R. J. (Roy) Wichink Kruit et al., 2007)

Table 14: Coverage of different processes in the aerosol dry deposition scheme of OPS (F. Sauter et al., 2022).

Process description		Implementation
Aerosols	Size dependence	Non-acidifying: 6 size classes Acidifying: -
	Land use dependence	Non-acidifying: - Acidifying: Schemes of Wesely or Ruijgrok, depending on roughness length
	Species dependence	Non-acidifying: - Acidifying: Tabulated parameters for collection efficiency
	Height dependence	-

A.1.8 Source apportionment

Source apportionment output is standard within OPS, because calculations are done per specific source sector. These calculations are straightforward given the linearized nature of the OPS model.

A.2 LOTOS-EUROS

A.2.1 Eulerian model system

LOTOS-EUROS (short: LOTOS) is an open source air quality model developed by TNO in cooperation with national and international partners for scientific applications and for policy support (Schaap et al., 2008). The model is aimed at the simulation of air pollution in the lower troposphere. The model is of intermediate complexity in the sense that the relevant processes are parameterized in such a way that the computational demands are modest enabling hour-by-hour calculations over extended periods of several years within acceptable computational time. The model is a so-called eulerian grid model, which means that the calculations for advection, vertical mixing, chemical transformations and removal by wet and dry deposition are performed on a three dimensional grid. Applications in Europe typically cover the continent as a whole, with higher resolution domains on the region of interest. Meteorological data are standard taken from ECMWF. The LOTOS-EUROS model has a long history studying the atmospheric nitrogen budget, and is also applied for ozone, particulate matter, methane and other organic compounds. It is operationally applied to provide air quality analyses and forecasts within the CAMS service. The system contributes to the benchmarking of the UNECE EMEP model and is used for policy support for national authorities of the Netherlands, Germany and Croatia. LOTOS is an integral part of the nitrogen deposition mapping approach for Germany. The resulting deposition maps are used for international reporting obligations and are provided as a background deposition for use in permit applications in Germany.

LOTOS-EUROS is an Eulerian code with the continuity equation as its main prognostic equation. It describes the change in time of the concentration of a species as a result of advective and turbulent transport, entrainment, emissions, chemical reactions, and wet and dry deposition. Currently, resolutions up to 1 x 1 km^2 can be used in LOTOS-EUROS calculations. The vertical layer system is a hybrid one with 12 sigma levels up to a pressure of 300 hPa. The description below is based on the LOTOS-EUROS Reference Guide of version 2.2.003 (Manders-Groot et al., 2023).

A.2.2 Emissions

The emission module of LOTOS-EUROS describes releases of trace gases and aerosols from various sources. The following emission groups of sources are present by default in the current model:

- Anthropogenic sources: by default, CAMS emissions are used, but EMEP, EDGAR, MEIC, US EPA and HTAP compilations are also possible. Very often, the CAMS emission are combined with national inventories from e.g the Netherlands or Germany. Even special components like heavy metals can be studied. CAMS emissions include NO_x, SO_x, NH_3, NMVOC, CH_4, CO, EC, OC, SO_4, Na and PPM. LOTOS-EUROS calculates plume rise for anthropogenic point emissions
- Biogenic sources: these include isoprene and monoterpenes from trees, grass, and crops. They depend on temperature, photosynthetically active radiation and leaf area index,

and are calculated on-line. For some land use classes, NO_x emissions from soil are calculated on-line.

- **Sea-spray sources**: sea salt from whitecaps on seas is modelled as a function of windspeed.
- **Dust sources**: natural windblown dust, re-suspended dust from traffic, and dust from agricultural land management are included in the model. These emissions are calculated as a function of meteorology, traffic intensity (in time and space) and land management intensity (in time and space).
- **Forest fires**: Both the GFAS fire emissions and the SILAM fire emissions are supported. A height dependence is incorporated in the emission calculations.
- **Special components**: these include heavy metals and base cations (from PM speciation) at the moment

For particles that are part of emission inventories, only the fine and coarse fractions are defined, as the emission inventories do not provide more detail. For dust and sea salt the emissions are calculated on-line and five size classes are used.

A.2.3 Transport

Transport terms in LOTOS-EUROS include advection, entrainment, vertical and horizontal diffusion. Advection is driven by meteorological winds that are terrain following (i.e. orography dependent). The vertical component of the wind velocity is determined from the divergence of the horizontal wind speed to satisfy continuity. Entrainment is caused by the growth of the mixing layer during the day. Each hour the vertical structure of the model is adjusted to the new mixing layer depth.

Horizontal diffusion was reintroduced in v2.2.003, since the concentrations from stacks would be too much aligned with the north-south and east-west directions for high resolution calculations. The introduction of a horizontal eddy diffusivity based on the velocity deformation tensor remedies this problem. Vertical diffusion is described using the standard K_z-theory.

A.2.4 Chemistry

CBM-IV chemistry is used for the gas phase reaction mechanisms (Whitten et al., 1980). Originally, 81 reactions are covered, including photo-chemical formation of sulfuric and nitric acid and the formation of secondary inorganic aerosols. LOTOS-EUROS uses a modified version of the CBM-IV scheme with 33 species and 104 reactions (inc. 14 photolytic reactions).

Most of the organic species in the mechanism are represented by carbon-carbon bond types, except for ethene, isoprene and formaldehyde which are represented explicitly. The carbon-bond types include carbon atoms that contain only single bonds, double-bons, 7-carbon ring structures represented by toluene, and 8-carbon ring structures represented by xylene, the carbonyl group with adjacent carbon atom, and higher molecular weight aldehydes represented by acetaldehyde, and non-reactive carbon atoms. Many organic compounds are apportioned to the carbon-bond species based simply on the basis of molecular structure. In addition to the inorganic gas phase reactions, an oxidation pathway in clouds is included for sulphate formation and a pathway for the nocturnal formation of nitric acid from dinitrogen pentoxide.

Aerosol chemistry is split into two approaches: secondary inorganic (SIA) and secondary organic aerosol (SOA) formation. SIA formation is modelled as the equilibrium between gaseous nitric acid, sulphuric acid, ammonia, particulate ammonium nitrate and sulphate, and water. ISORROPIA2 is the default scheme that is applied in LOTOS-EUROS, but EQSAM may also be used as a simpler and faster algorithm. For SOA formation, the broadly applied Volatile Basis Set (VBS) approach is used. This approach defines classes of volatile organic compounds (VOC) of which a fraction of material is partitioned in the gas phase and the rest in the aerosol phase. The balance between these classes and phases is formed by production from anthropogenic/biogenic sources, changing volatility due to chemical reactions, and deposition processes.

A.2.5 Wet deposition

Most wet deposition models in current CTMs, LOTOS-EUROS included, follow a similar approach. Specifically, LOTOS-EUROS follows the approach of CAMx with both in-cloud and below-cloud scavenging (Banzhaf et al., 2012; ENVIRON, 2010). In this approach, in-cloud scavenging is integrated over the height of the cloud by accumulating the scavenged species in the cloud droplets at each level on their way to the ground. In particular, the implementation in LOTOS-EUROS includes the influence of temperature and cloud pH on the scavenging coefficients (Banzhaf et al., 2012).

A.2.6 Dry deposition

The dry deposition scheme for gases is implemented according to the DEPAC model (Van Zanten, 2010). The biggest implementation difference between the LOTOS-EUROS implementation of DEPAC and the original, is the incorporation of 9 extra land use classes representing Mediterranean conditions. These classes are used for the dry deposition modelling in Southern Europe. A schematic overview is shown in Figure 56. Dry deposition of particles follows the parametrization of Zhang (Zhang et al., 2001), the different dependencies are given in Table 15.

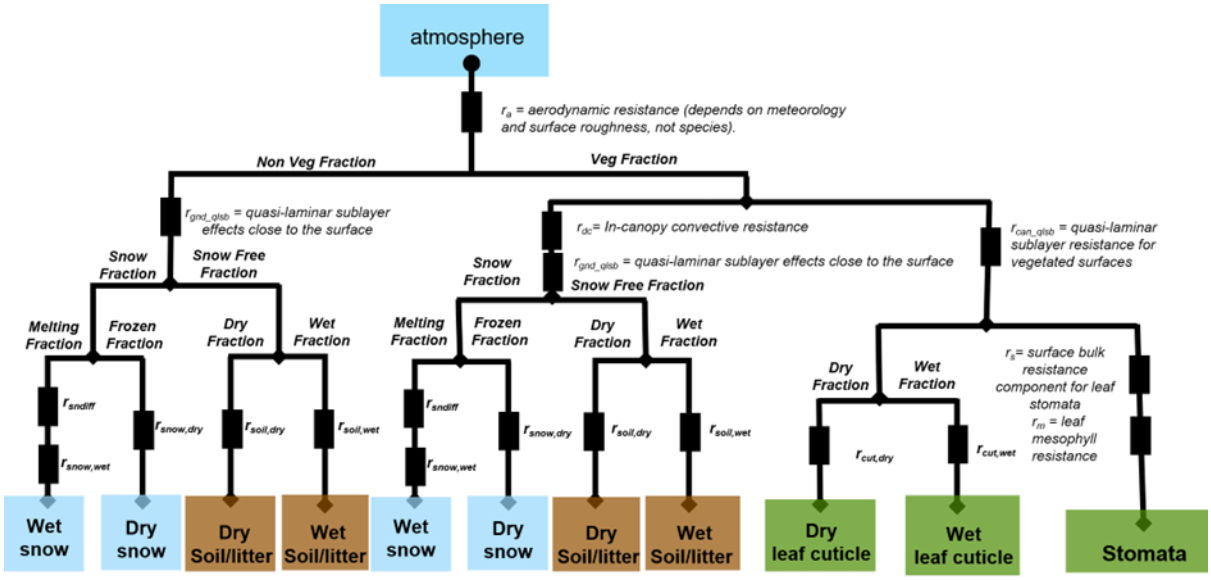

Figure 56: Schematic representation of the dry deposition model (DEPAC) in LOTOS-EUROS.

Table 15: Dependencies for aerosol deposition in the LOTOS-EUROS model.

Dependency	Implementation
Size dependence	Bimodal log-normal distribution, but 5 class approach for sea salt and dust
Land use dependence	Collection efficiency terms are LUC dependent
Species dependence	-
Height dependence	Aerodynamic resistance is height dependent

A.2.7 Source apportionment

Within the FP7 project EnerGEO, TNO has developed a system to track the impact of emission categories within a LOTOS-EUROS simulation based on a labelling technique (Kranenburg et al., 2013). In addition to species concentrations and deposition fluxes, the contributions and depositions of predefined source categories are calculated and tracked for each process description in the model. The labelling routine is designed for chemically active tracers with a C, N (reduced and oxidized), or S atom, since these are conserved and traceable. The source attribution module for LOTOS-EUROS provides source attribution valid for current atmospheric conditions, since all chemical transformations occur at the same concentrations of oxidants. For details and validation of this source attribution module, we refer to Kranenburg et al. (2013). The source attribution technique has previously been used with a focus on Germany to study the origin of nitrogen deposition (Schaap et al., 2018b).

A.3 EMEP4NL

A.3.1 Introduction

The European Monitoring and Evaluation Programme (EMEP) / Meteorological Synthesizing Centre-West (MSC-W) model is a Eulerian atmospheric chemical transport model (ACTM) described in Simpson et al. (2012) and developed at the Norwegian Meteorological Institute. The EMEP model supports the development of air quality policies in the European Union (see https://emep.int) and is available under an open-source GPLv3 license. It includes a detailed atmospheric chemistry scheme and is used to monitor the yearly developments in particulate matter, photo-oxidants, acidifying and eutrophying components across Europe (see e.g. the EMEP Status Report 2022).

A.3.2 Version for the Netherlands

Specifically for the Netherlands, the EMEP4NL configuration was developed (Van Der Swaluw et al., 2021). The current version of EMEP4NL is based on the EMEP/MSC-W model version 4.45. EMEP4NL uses one-way nested horizontal grids, in order to scale up from a coarser resolution on a European level, to a higher resolution over the domain over the Netherlands. This set-up is similar as the one used for the United Kingdom, i.e. the EMEP4UK model (Vieno et al., 2009). The basic domain (level 1) has a coarse resolution (0.5° x 0.5°) over the whole European domain. Subsequently, for each level, the resolution is increased by a factor of 3, while the spatial extent of the domain is reduced. In this way, moving from the coarsest level 1 (which covers all of Europe) to the finest level 4 (which covers all of the Netherlands), one obtains a horizontal resolution of roughly 1–2 km over the domain of the Netherlands.

In its vertical direction, EMEP4NL uses 21 layers with pressure coordinates: the bottom layer is at 1000 hPa (with a height of ~50 m) and reaches up to 100 hPa (~15 km).

The EMEP4NL model is driven by meteorological data input obtained from the Weather Research Forecast (WRF) model version 3.8 (Skamarock et al., 2008). The grid configuration as used in the WRF model is identical to the grid configuration in the EMEP4NL model described above. The WRF model uses Newtonian nudging (Vieno et al., 2009), which is applied every six simulated hours, using the reanalysis of the global numerical weather prediction model (Global Forecast System (GFS)) from the US National Centers for Environmental Prediction (NCEP) and National Center for Atmospheric Research (NCAR) at a resolution of 1°.

A.3.3 Emissions

Emission datasets from various sources can be used in the EMEP model. These emissions can be assigned to a sector. A sector defines three properties: the split into sub-species, the emission height release distribution and the emission timefactors. The number of sectors is flexible and can be defined by the user, in the EMEP4NL setup the 13 GNFR CAMS sectors are used with their pre-defined settings, except for ammonia, where for the Netherlands, monthly timefactors are used that better reflect the local agricultural practice. In general, the following emissions are considered:

1. **Anthropogenic emissions (country level):** these include NH_3, NO_x, SO_x, primary PM_{coarse}, primary $PM_{2.5}$, NMVOC and CO. Dust emissions due to road traffic are included using the provided datasets by EMEP/MSC-W.
2. **Aircraft emissions:** emissions during landing and take-off are included in the sectoral emissions per country, for cruising heights, the CAMS-GLOB-AIR dataset is used (Granier et al., 2019).
3. **Biogenic emissions:** various biogenic emission sources can be used:
   a. *Sea salt:* sea salt calculations include primarily particles with diameters up to 10 µm (Simpson et al., 2012a).
   b. *Lightning:* Emissions of NO_x from lightning are included in the model as monthly averages on T21 (5.65° x 5.65°) resolution (Köhler et al., 1995).
   c. *NO_x from soil*: natural NO_x emissions from soils due to nitrification (Simpson & Darras, 2021). NO_x emissions from fertilizer are excluded, these are included in the sectoral emissions per country.
   d. *Isoprene and monoterpene*: these are calculated in the model as a function of temperature and solar radiation, using the landuse datasets (Simpson & Darras, 2021).
   e. *Dust*: The sources of natural mineral dust in the model include windblown dust from deserts, semi-arid areas, agricultural and bare lands within the model domain, as well as dust produced beyond the model grid (e.g. on African deserts) and transported to the calculation domain (Simpson et al., 2012).
   f. *Dimethylsulfide (DMS) from sea:* these are computed by taking into account sea surface temperature and wind speed. Surface water concentrations of DMS (needed for the flux calculation) are taken from SOLAS (Surface Ocean Lower Atmosphere Study, SOLAS).
   g. *Forest and vegetation fires:* daily emissions from forest and vegetation fires can be used from the “Fire INventory from NCAR version 1.0” (FINNv1, Wiedinmyer et al. 2011). These are not enabled in the current EMEP4NL setup.

h. *Emissions of volcanoes:* can be introduced into the model as point sources, at a height determined by the height of each volcano (Simpson et al., 2012a). These are not enabled in the current EMEP4NL setup.

Additionally, boundary conditions of ozone are developed from climatological ozone-sonde datasets, modified monthly against clean-air surface observations for 2015 (the so-called "Mace-Head" adjustment, see Simpson et al. (2012).

A.3.4 Transport

The numerical solution of the advection terms of the continuity equation is based on the scheme of Bott (Bott, 1989). The fourth order scheme is utilized in the horizontal directions. In the vertical direction a second order version applicable to variable grid distances is employed (Simpson et al., 2012a). The turbulent eddy diffusivity coefficients (Kz) are first calculated for the whole 3D model domain on the basis of local Richardson numbers. The planetary boundary layer (PBL) height is then calculated using methods described in Simpson et al. (2012). For stable conditions, new Kz values are calculated by the method described in Troen & Mahrt (1986). For unstable situations, new Kz values are calculated for layers below the mixing height using the O'Brien interpolation (Simpson et al., 2012a).

An optional convective mass flux scheme has been implemented in the EMEP model, based on Tiedtke (1989). If used with European-scale simulations, worse model results compared to observations were obtained.

A.3.5 Chemistry

The chemical scheme traces its origins to the EMEP chemical mechanisms that began with Eliassen et al. (1982). This scheme has been updated and tested against other schemes in a number of studies The latest scheme was largely developed in 2008–2019 and is denoted EmChem19. It contains approximately 70 chemical species, 140 chemical reactions and 30 photo-dissociation reactions (Simpson et al., 2012a). The EMEP model uses the MARS equilibrium module of Binkowski & Shankar (1995) to calculate the partitioning between gas and fine-mode secondary inorganic aerosol phase in the system of SO_4 - HNO_3 - NO_3 - NH_3 - NH_4. A volatility basis set (VBS) approach is used (Donahue et al., 2009; Robinson et al., 2007) for secondary organic aerosols (SOA). The EMEP model distinguishes five classes of fine and coarse particles, which for dry deposition purposes are assigned various physical parameters. A more detailed description of the chemistry scheme is provided in Simpson et al. (2012).

A.3.6 Wet deposition

Parameterization of the wet deposition processes in the EMEP model includes both in-cloud and sub-cloud scavenging of gases and particles. The parameterization of the wet deposition is described in (Berge & Jakobsen, 1998) and Simpson et al. (2012). In-cloud scavenging is modelled by in-cloud scavenging ratios (dependent on the substance), the precipitation rate and the characteristic scavenging depth (set to 1 km). The effect that dissolved material may be released if clouds or rain water evaporate is not taken into account. Sub-cloud scavenging of gases is modelled in the same way as in-cloud scavenging, but a different set of sub-cloud scavenging ratios per substance are used. For particles, the sub-cloud scavenging is calculated, based on (Scott, 1978) and depends on the raindrop fall speed, the empirical coefficient (a Marshall-Palmer size distribution is assumed for rain drops) and the collection efficiency of aerosols by the raindrops. The collection

efficiency is size dependent, with a minimum for fine particles (see Henzing et al., 2006; Laakso, 2003). More details and values of the various constants are given in Simpson et al. (2012).

A.3.7 Dry deposition

In the EMEP model, dry deposition velocities are calculated using a resistance approach. A detailed explanation is given in Simpson et al. (2012). In summary, the three calculated resistances that are used in the model are the aerodynamic resistance R_a between the modelled height *z* and the top of the vegetation canopy (the displacement height plus the roughness length), the quasi-laminar layer resistance R_b and the surface (or canopy) resistance R_c. Over grid cells which are 100 % sea, the NWP model's meteorological parameters (and roughness length) are used to calculate the resistances. Where grid cells contain other land-classes, a so-called mosaic approach is used, where the grid-average deposition rate is calculated from the deposition velocity of each land use type, weighted by the frequency of occurrence of that land use type in the current grid cell. The EMEP model uses 16 land use types, a schematic overview is shown in Figure 57.

The calculation of the aerodynamic resistance R_a is based on various meteorological parameters such as the Obukhov length L and the friction velocity u*, and on local parameters such as the displacement height and the surface roughness. The quasi-laminar resistance R_b depends on the friction velocity, the roughness length and parameters describing the diffusivity of the pollutant. The surface (or canopy) resistance R_c is based on surface characteristics and the chemical characteristics of the depositing pollutant. It is split into stomatal and non-stomatal conductance pathways. Stomatal conductance is calculated with a multiplicative model, a development of the model described in Emberson et al. (2000). Non-stomatal conductance is split into deposition via external surfaces and deposition directly to the soil, for which a correction is applied for freezing temperatures and snow cover. Details of the calculation of the resistances are given in Simpson et al. (2012).

Specifically for ammonia, during the growing season for crop land-covers, the surface resistance is set to a very high value, which ensures zero deposition. This procedure is designed to account for the fact that many croplands are actually emitters of NH_3, rather than sinks (e.g. Fowler et al., 2009, and references therein; Sutton et al., 2000). In the calculation of the (non-stomatal) surface resistance for ammonia, the effect of SO_2 co-deposition is taken into account following an adapted method proposed by (R. Smith et al., 2003) Smith et al. (2003). Additional parameters taken into account in the calculation of the surface resistance are the relative humidity and the temperature.

For aerosol deposition the system is described by (Petroff et al., 2008a, 2008b), implementations of different dependencies are given in Table 16.

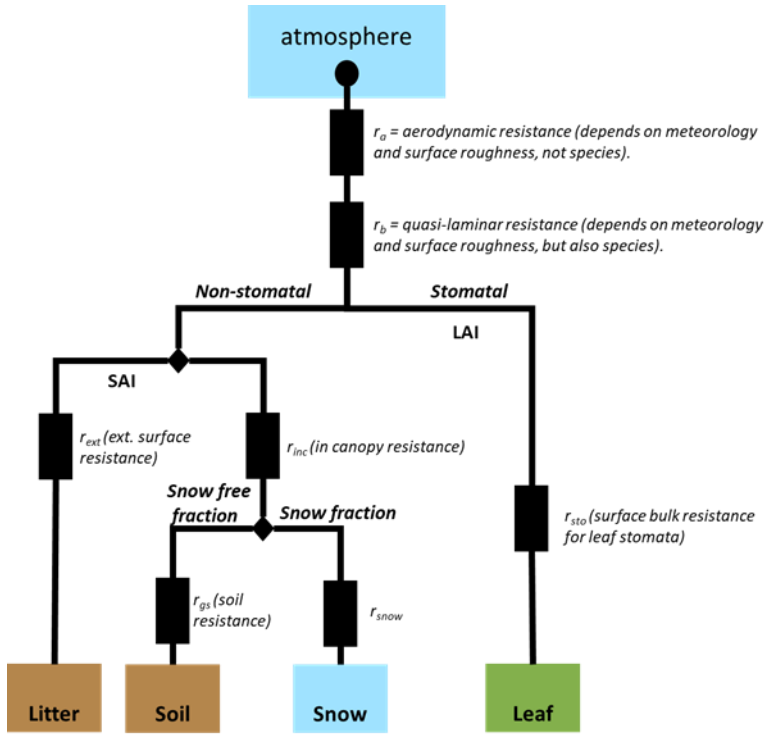

Figure 57: Schematic representation of the dry deposition scheme for gases in EMEP MSC-W (based on (Simpson et al., 2012a)).

Table 16: Dependencies for aerosol deposition in the EMEP-model.

Dependency	Implementation
Size dependence	Bimodal log-normal distribution
Land use dependence	SAI dependent deposition velocity only for forests
Species dependence	Enhancement factor for fine nitrate & ammonium
Height dependence	Aerodynamic resistance is height dependent

A.3.8 Source apportionment

EMEP4NL uses a so-called brute-force method to calculate source contributions. A brute-force method (BF or emission reduction impact) is a sensitivity analysis technique which estimates the change in pollutant concentration or deposition (impact) that results from a change in one or more emission sources. The impact in terms of concentration or deposition is attributed to the source of the emission change. Sensitivity analysis techniques have been widely used to estimate the impact of different sources on pollution levels (e.g. Kiesewetter et al., 2015; Thunis et al., 2016; Van Dingenen et al., 2018).

A.4 SILAM

A.4.1 Eulerian model system

The System for Integrated modeLling of Atmospheric coMposition SILAM v.6.1 (http://silam.fmi.fi) is a Eulerian chemical transport model with the transport module based

on advection scheme of Galperin (2000) refined by Sofiev et al. (2015) and adaptive vertical diffusion algorithm of Sofiev (2002). Apart from the transport and physico-chemical cores described below, SILAM includes a set of supplementary tools including a meteorological pre-processor, input-output converters, reprojection and interpolation routines, etc. In the operational forecasts, these enabled direct forcing of the model by the ECMWF IFS meteorological fields.

A.4.2 Transport

The SILAM Eulerian transport core (Sofiev et al., 2015) is based on the coupled developments: refined advection scheme of Galperin (2000) and vertical diffusion algorithm of Sofiev (2002) and Kouznetsov & Sofiev (2012b). The methods are compatible, in a sense that both use the same set of variables to determine the sub-grid distribution of tracer mass. The approach, in particular, allows computing correct vertical exchange using high-resolution input data but low-resolution chemistry and diffusion grids. The later feature is used in the vertical setup with 9 thick layers.

Diffusion is parameterised following the first-order K-theory based closure. Horizontal diffusion is embedded into the advection routine, which itself has zero numerical viscosity, thus allowing full control over the diffusion fluxes. The vertical diffusivity parameterisation follows the approach suggested by Genikhovich (2003), as described in Sofiev et al. (2010). The procedure diagnoses all the similarity theory parameters using the profiles of the basic meteorological quantities: wind, temperature and humidity.

A.4.3 Chemistry

The main gas-phase chemical mechanism is a modified version of CBM-5 (Hänninen et al., 2023b), supplemented with the oxidation scheme for semi-volatile organics. The heterogeneous sulfur scheme is an updated version of the DMAT model scheme (Sofiev, 2000a). It incorporates the formation pathways of secondary inorganic aerosols.

Emission of 2 sets of compounds is embedded into the simulations: biogenic VOC, sea salt, and desert dust. The bio-VOC computations follow the Poupkou et al. (2010) model and provide isoprene and mono-terpene emissions. The sea salt emission parameterisation is the original development generally based on Sofiev et al. (2011), with refinements and spume formation mechanism.

A.4.4 Deposition

Dry deposition parameterisation follows the resistive analogy of Wesely (1989). Deposition velocity for aerosols are evaluated using the original (Kouznetsov & Sofiev, 2012b) algorithm. Wet deposition parameterisation is based on the scavenging coefficient after Sofiev (2000a) for gas species and a new deposition scheme for aerosols following the generalised formulations of Kouznetsov & Sofiev (2012b).

A.5 MATCH

A.5.1 Model system

The Multi-scale Atmospheric Transport and Chemistry model (MATCH; Robertson et al., 1999b; Bergström & Olenius, 2025; *MATCH - Transport and Chemistry Model — SMHI*, n.d.) is

an off-line chemical transport model (CTM) with a flexible design, accommodating different weather data forcing on different resolutions and projections, and a range of alternative schemes for deposition and chemistry.

For this study meteorological data were taken from the ECMWF IFS weather forecast system. A nested modelling approach was employed, starting with a European-scale simulation at a horizontal resolution of 0.2° × 0.2°, utilizing 50 vertical levels from IFS, which were reduced to 25 levels in MATCH, corresponding to a vertical extent of about 6–8 km. This was followed by a higher-resolution simulation covering the BeNeLux area, parts of western Germany and northern France, with a 2.5 km × 2.5 km grid resolution, with 36→18 vertical levels (reaching ~4km height). The lowest model level is about 40 m thick. Chemical boundary conditions for the European-scale domain were obtained from the IFS global forecasts, similar to the operational CAMS system (Colette et al., 2024). The results from this large-scale simulation were then used as boundary data for the nested, high-resolution BeNeLux-scale simulations.

A.5.2 Emissions

MATCH offers various options for handling emissions, covering different sectors, vertical distribution, and temporal variations from multiple sources. For European-scale simulations, anthropogenic emissions are often taken from the CAMS or EMEP emission inventories, sometimes combined with finer resolution national emission datasets.

In this study, European-scale MATCH simulations utilized CAMS-REG-V5.1c emissions (for 2018), while the high-resolution simulations used the emissions from the NKS emission inventory (Appendix B.1). The temporal variation of the emissions in both model setups followed the CAMS-REG-TEMPO-v3.1 profiles for 2019.

Natural emissions can also be treated in a variety of ways in MATCH. In the present study biogenic emissions of isoprene and monoterpenes were calculated in the model (based on the methodology of Simpson et al. (2012a); sea salt aerosol emissions were modelled using a parameterization from Sofiev et al. (2011), and aeolian dust emissions were modelled based on the DEAD model (Zender et al., 2003). Vegetation fire emissions were taken from the GFAS fire emission database (Kaiser et al., 2012). A simplified treatment of sulfur emissions from seas and volcanoes were also included. The version of MATCH used in this study does not include soil-NO_x emissions.

Further details on the emission setup, including the sector-dependent speciation of VOCs, are provided in Bergström & Olenius (2025). In the high-resolution simulations for the Netherlands, emissions from the Agricultural, Road Transport and Solvents sectors were constrained to the lowest model level (~40 m thick), whereas in the coarser European-scale simulations, these emissions were distributed over the lowest 92 m.

A.5.3 Transport

Mass conservative transport schemes are used for advection and turbulent transport. The advection is formulated as a Bott-like scheme (Robertson et al., 1999b). A second order transport scheme is used in the horizontal as well as the vertical. The vertical diffusion is described by an implicit mass conservative first order scheme, where the exchange coefficients for neutral and stable conditions are parameterized following (Holtslag, 1991). In the convective case the turbulent Courant number is directly determined from the turnover time in the ABL.

Part of the dynamical core is the initialization and adjustment of the horizontal wind components. This is a very important step to ensure mass conservative transport. The initialization is based on a procedure proposed by (Heimann & Keeling, 1989), where the horizontal winds are adjusted by means of the difference between the input surface pressure tendency, and the calculated pressure tendency assumed to be an error in the divergent part of the wind field.

Boundary layer parameterization is based on surface heat and water vapor fluxes as described by van Ulden & Holtslag (1985) for land surfaces, and Burridge & Gadd (1977) for sea surfaces. The boundary layer height is calculated from formulations proposed by Zilitinkevich & Mironov (1996) for the neutral and stable case, and from Holtslag et al. (1995) for the convective case. These parameterisations drive the formulations for dry deposition and vertical diffusion.

A.5.4 Chemistry

The photochemistry scheme used in this study is based on the EMEP MSC-W EmChem09 scheme (Simpson et al., 2012b), with a modified scheme for isoprene oxidation (Carter, 1996; Langner et al., 1998) and updated reaction rates from EmChem19 (Bergström et al., 2022; Bergström & Olenius, 2025). Gas-to-particle conversions include the formation of secondary inorganic aerosol (SIA; consisting of ammonium sulfate and nitrate) and secondary organic aerosol (SOA). Particles are treated as bulk aerosol in two size classes, corresponding to fine and coarse PM with diameters smaller and larger than 2.5 µm, respectively. Ammonium nitrate (NH_4NO_3) equilibrium is calculated according to temperature- and RH-dependent equilibrium coefficient (Mozurkewich, 1993), and coarse nitrate formation is described by transfer of gaseous nitric acid (HNO_3) to aerosol-phase NO_3 (pNO_3^-) (Strand & Hov, 1994). Further details regarding the chemistry scheme can be found in Bergström & Olenius (2025).

A.5.5 Deposition

Dry deposition of gases and aerosols is modelled using a resistance-based approach (based on the scheme in (Simpson et al., 2012b). This accounts for stomatal and non-stomatal deposition pathways for vegetated surfaces. In this study the treatment of NH_3 dry deposition has been updated to a bidirectional flux parameterization based on Frohn et al. (2025) and Wichink Kruit et al. (2012)

MATCH uses 3D-precipitation (estimated in the model, based on the surface precipitation and 3D cloud water information from the IFS forecast) and separates wet scavenging into in-cloud and sub-cloud scavenging. In-cloud scavenging of gases depends on the solubility. The sub-cloud scavenging is assumed to be proportional to the precipitation intensity for highly soluble gases and it is neglected for low-solubility gases. For particulate components in-cloud scavenging is treated using simple scavenging ratios while the sub-cloud scavenging is treated using a scheme based on (Berge, 1993) with size dependent collection efficiencies (as in (Simpson et al., 2012b)).

A.6 International model candidates

To enable an informed selection of the international model systems, an overview of candidate systems was created. The models were evaluated on a number of simple criteria. These criteria basically check if modelling systems have been used in the past to address

nitrogen deposition at the national scale. 17 model systems have been assessed using these criteria (see Table 17). They were evaluated on the following criteria:

- The model contains a dynamic dry deposition module discriminating the major land use classes for nitrogen compounds (reference to relevant literature).
- The model contains a wet deposition process description (reference to relevant literature).
- There is a proven case of a national scale assessment at 2 x 2 km^2 resolution or better (reference to relevant literature).
- The model is regularly applied for national or European nitrogen deposition assessment for policy support (if yes, country or region is mentioned).
- The model has participated in model intercomparison studies for deposition (if yes, the name of the project is mentioned).

The 17 air quality models are categorized into three groups based on these criteria. The models in Group A are most suitable for the ensemble, since they provide all features necessary, are validated on a national scale, are used for policy support for N deposition in Europe and participated in intercomparison studies on N deposition. Group B consists of models that are not used for policy support or did not participate in intercomparison studies, but do meet the other criteria. Group C is the group of models that do not meet some or all of the criteria.

Table 17: Grouping of 17 international air quality models on the basis of (N) deposition criteria.

Model	Dynamic dry deposition module	Wet deposition module	Proven case @ national scale	N deposition assessment policy support	Deposition inter-comparison studies	Group
CAMx	(S. A. Slinn & Slinn, 1980; Wesely, 1989; Zhang et al., 2001, 2003)	(Seinfeld & Pandis, 1998)	(Bove et al., 2014) (local: Genoa, IT)	No	AQMEII	B
CHIMERE	(Emberson, Ashmore, et al., 2000; Wesely, 1989)	(Loosmore & Cederwall, 2004; Willis & Tattelman, 1989)	-	No	AQMEII, AQMEII3, EURODELTA	C
CMAQ	M3DRY (Pleim et al., 1984) or STAGE (Appel et al., 2021)	(Roselle & Binkowski, 1999)	(Im et al., 2010) (local: Istanbul, TR)	No	AQMEII3, AQMEII4	B
COSMO-MUSCAT	(Seinfeld & Pandis, 2006)	(Simpson et al., 2012a)	-	No	AQMEII4	C
DEHM	EMEP (Emberson, Simpson, et al., 2000; Simpson et al., 2003)	Based on Henry coefficients (Simpson et al., 2003)	(Brandt et al., 2001) (DEOM, operational version of DEHM)	Yes (DK)	AQMEII3	A
EMEP/MSC-W	DO3SE (Emberson, Ashmore, et al., 2000), EMEP-12 (Petroff et al., 2008a, 2008b)	(Berge & Jakobsen, 1998)	(van der Swaluw et al., 2021) (EMEP4NL)	Yes (NO, Europe)	AQMEII, EURODELTA	A

Model	Dynamic dry deposition module	Wet deposition module	Proven case @ national scale	N deposition assessment policy support	Deposition inter-comparison studies	Group
EURAD	(Petroff & Zhang, 2010; Zhang et al., 2003)	(Roselle & Binkowski, 1999)	(De Souza Fernandes Duarte et al., 2021)	No	AQMEII	B
FRAME	NH_3 (Singles et al., 1998), SO_2 & NO_2 follows big leaf CBED (R. I. Smith et al., 2000)	Similar to EMEP Lagrangian model	(Tomlinson et al., 2021)	Yes (UK)	(Dore et al., 2015b)	A
GEM-MACH	Robichaud (Wesely, 1989) (adapted), (Zhang et al., 2001)	(Gong, 2003)	-	No	AQMEII4	C
MATCH	Based on EMEP (Simpson et al., 2012a)	Similar to (Simpson et al., 2012a)	-	Yes (SE)	EURODELTA	A
MINNI	(Wesely, 1989)	EMEP, 2003		No	EURODELTA	C
MOCAGE	(Michou et al., 2005; Nho-Kim, 2004)	(Giorgi & Chameides, 1986)	-	No	-	C
MONARCH	(Nho-Kim, 2004; Wesely, 1989)	(Byun & Ching, 1999; Foley et al., 2010)	-	No	-	C
POLYPHEMUS	(Zhang et al., 2001, 2003)	(W. G. N. Slinn, 1984; Sportisse & Bois, 2002)	-	No	-	C
RemCalgrid	(Erisman et al., 1994)	Parametrization w. simple washout	-	No	-	C
SILAM	(Kouznetsov & Sofiev, 2012c; Wesely, 1989)	(Kouznetsov & Sofiev, 2012c; Sofiev, 2000b)	(Ots et al., 2014)	No	AQMEII3	B
WRF-CHEM	(Erisman et al., 1994)	GOCART	-	No	AQMEII4	C

Some general conclusions can be drawn from the literature search of the above mentioned models:

- Out of the 17 models, there are 16 Eulerian models, and 1 is Lagrangian (FRAME).
- Wet deposition is modelled following the same principle in all models
- Dry deposition follows one of three variants: constant deposition velocities per species (and sometimes land use class) or a resistance approach, either with (DEPAC) or without compensation points (EMEP).
- Differences in dry deposition implementation are often subtle and are usually found in number and type of land use classes, the incorporation of diurnal or seasonal patterns, the distinction between wet and dry surfaces and the influence of ice and snow.

- For particulate ammonium nitrate formation the modelling approaches also show a lot of resemblance: ISORROPIA is used in 9 cases, MARS in 4 cases and the rest according to an unnamed and often simplified equilibrium model.
- Gas phase chemistry modules show a more variation between the air quality models. Many air quality models include a single chemistry scheme, but some include a list of chemistry schemes from which the user can choose. Most used chemistry schemes are the carbon bond schemes CBM-IV and CB05, the regional atmospheric chemistry mechanism RACM (version 2), and a collection of related EMEP-type chemistry schemes (such as EmChem in EMEP-MSC-W or a variant on Simpson et al. (2012) in MATCH).

The application of very similar approaches for the dry and wet deposition has consequences. The differences between modelled deposition can be driven by the modelled approach (Eulerian), by the choice in dry deposition scheme, by the subtle differences in the implementation or by all the other factors than the deposition modules they used. The latter is obvious for models that use the same dry deposition scheme. Hence, it is important have models with different approaches for the dry deposition in the current study.

To attract interest an open invitation was sent to modelling groups in Europe (through CAMS and personal network). Three teams reacted positively: SILAM, MATCH and MINNI. The first two were able to deliver the results in time for this report. We approached the team connected to the only other Langrangian model (FRAME), but learned that the development and maintenance of this model was stopped two years ago.

Appendix B

NKS vs OPS emission inventory

In this section, the difference between the general harmonized emission set for this project is compared with the emission set used by OPS. Both emission sets contain the same information but due to scaling issues and different projections, small differences are present between both sets. First the properties of the NKS-emission inventory is listed, second the OPS emission inventory is described together with the adjustments to harmonize it with the NKS set. Finally the differences are displayed between both sets.

B.1 NKS emission inventory

The NKS emission inventory is created from different inputs to have a high resolution for the Netherlands and surrounding on a highly detailed level on emission sectors.

- Europe
  - CAMS – v5.1 REF2 (submission 2020, year 2018)
  - 0.1x0.05 lon/lat resolution
  - GNFR sector classification
- NCP and OSPARII
  - ER-emissions based on MARIN data (spatial distribution 2016, year 2018)
  - 1x1 km resolution on NCP, spatial distribution + emission totals 2021
  - 5x5 km resolution on OSPARII except NCP, emission totals updated according to relative change in NCP emission totals
  - GNFR sector classification
- Netherlands
  - ER-emissions (submission 2022, year 2018)
  - 1x1km resolution
  - ER-sector-classification converted to GNFR sector classification
- Germany
  - Greta (submission 2022, year 2018)
  - 1/60 x 1/120 lon/lat resolution
  - GNFR sector classification
- *Belgium*
  - VMM-emissions (VLOPS) for 2018, from submission 2020.
  - Only for NO_x and NH_3
  - 1x1km resolution for Flanders, 5x5 km resolution for Wallonia
  - GNFR-classification

B.2 OPS emission inventory

Unfortunately, it was not feasible to fully use the same identical set (NKS emission inventory) by all models. By design, the OPS model is able to use point sources in the standard settings using a Gaussian plume. In the OPS model, point sources are an integral part of the parametrization, allowing more precise modelling of localized sources such as industrial or agricultural exhausts. Utilizing this important model feature requires an emission set which includes explicit definitions of point sources, their emission heights and codes for diurnal variations, heat content etc. The NKS emission set provided for this study do not include this specific information. Therefore, a special set of emissions was generated for OPS ("OPS emission inventory"). To design this set, an existing set of emissions for OPS was taken as base and adjusted as much as possible to match the emission totals and the spatial distribution of the NKS set, especially for the Netherlands and neighboring countries.

The OPS emission inventory consists of the following emissions, of which most of them were harmonized with the NKS-set.

- Europe
  - CAMS – reg v4.2, spatial distribution of 2017. Totals rescaled to submission of 2020, resulting in the same totals as the NKS set.
  - 5x5 km and subsequently 25x25 km up to 75x75 km further away from the Netherlands. This is a coarser resolution with respect to NKS set, but only at large distance from the Netherlands
  - GNFR sector classification, identical to NKS-set.
- NCP and OSPARII
  - Exactly the same data as in the NKS set.
- Netherlands
  - ER-emissions(Submission of 2021, year 2018). Totals updated to submission 2022, resulting in the same totals as the NKS-set, with slightly different spatial distribution.
  - 1x1 km resolution and point sources (Specifically needed for OPS).
  - ER sectors converted to GCN sector classification, thus more detail compared to GNFR classification.
- Germany
  - Greta (UBA), spatial distribution of 2019. Totals updated to submission 2022 for year 2018, resulting is same totals as NKS set with a slightly different spatial distribution.
  - Aggregated to 5x5 km and subsequently 25x25 km further away from the Netherlands, resulting in coarser resolution at large distance from the Netherlands
  - GNFR sector classification, identical to NKS-set
- Belgium
  - VMM-emissions (VLOPS) for 2018, from submission 2020, identical to NKS-set.
  - Including point sources (needed for OPS).
  - 1x1 km resolution for Flanders, 5x5 km resolution for Wallonia, identical to NKS-set.
  - GNFR-classification, identical to NKS-set.

B.3 Differences between NKS and OPS inventory

The spatial differences in emissions between the NKS and OPS emissions inventories were determined. for the smallest domain (highest resolution) because this is the most important part of the emission set, with the largest expected impact on concentrations in the Netherlands. The emissions of and the differences between the two emission sets are shown in Figure 58 for NO_x and in Figure 59 for NH_3. Additionally, Table 18 lists the differences in total emissions per country. As can be seen in the tables, the largest differences grouped by

country are 2.3 kton (3 %) for NH_3 in France and 5 kton (1 %) for NO_x in Germany (see Table 18). While the emission totals were homogenized on a GNFR sector and country level, the spatial distribution used in the OPS emission set differs from the one in the NKS emission set for Germany. Because only part of Germany and France is included in the smallest domain, differences in emissions can arise in spite of the scaling of the emission totals.

Also for the Netherlands, the spatial distribution is slightly different between the two sets. This is a result of the projection used in both sets. The OPS emissions are created on a regular grid with grid cells of exactly 1x1km^2, while the NKS set uses a regular grid on longitudes and latitudes of approximately 1x1km^2. Showing the differences on the same projection basically leads to alternating red and blue points in the difference plots of Figure 58 and Figure 59, while the top panels show a large cohesion between both sets.

In conclusion, in spite of the effort to homogenize the emissions, differences remain, especially in spatial distribution. Because the differences are considered to be small, these were not studied in further detail. Further note that by using grid models like LOTOS or EMEP4NL, emissions are directly spread over a complete grid cell, thus in the model this impact is even smaller.

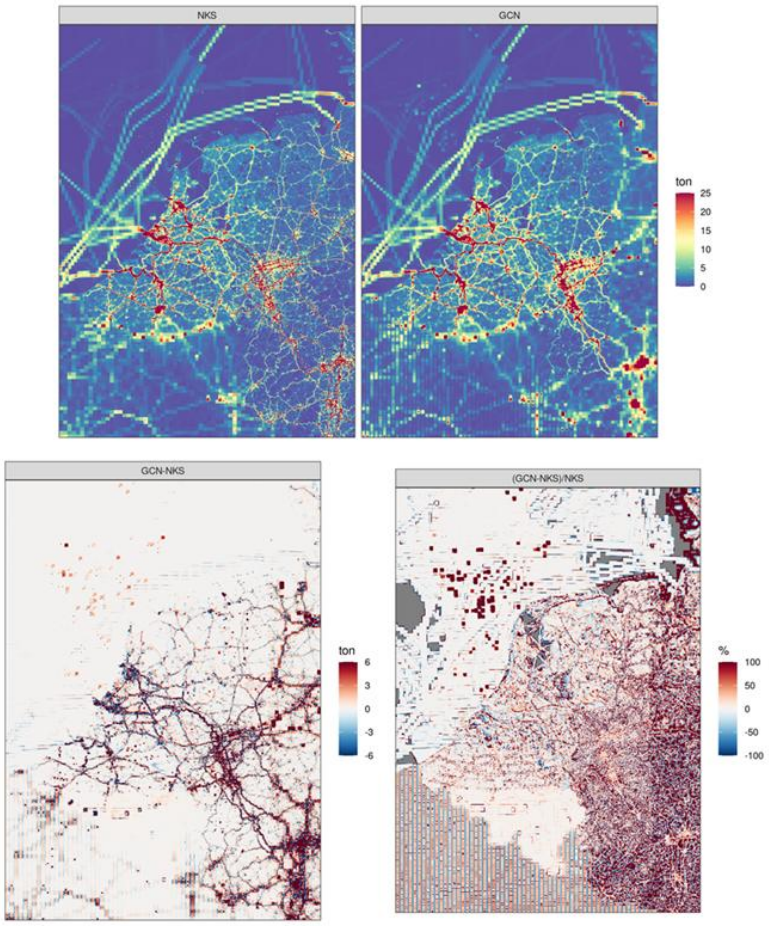

Figure 58: NO_x emissions for NKS inventory (upper left) and OPS inventory (upper right). Absolute (left) and relative (right) differences are shown in the lower panels.

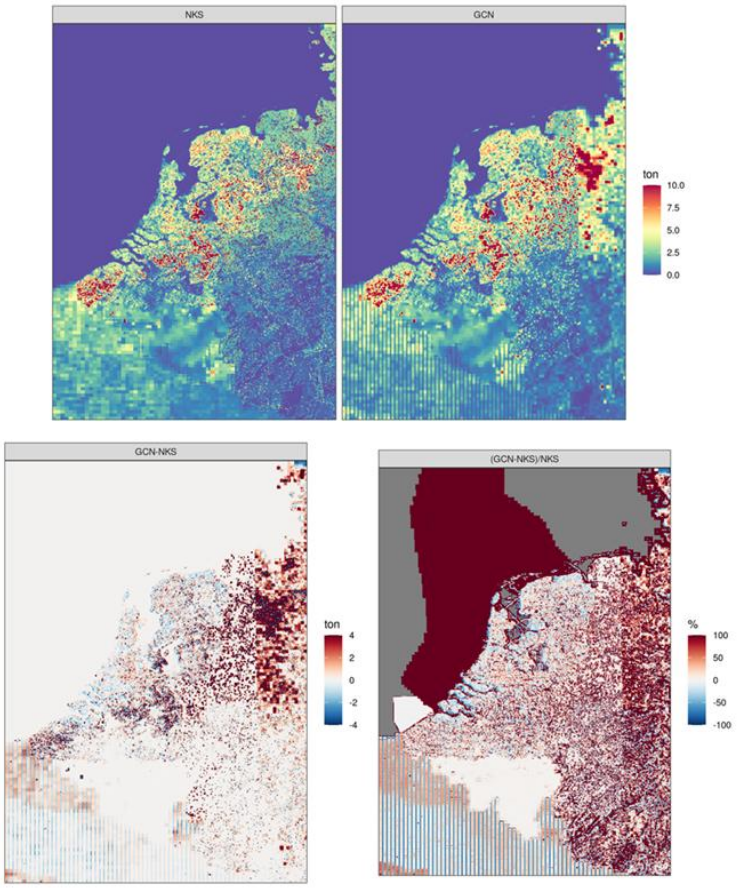

Figure 59: NH_3 emissions for NKS inventory (upper left) and OPS inventory (upper right). Absolute (left) and relative (right) differences are shown in the lower panels.

Table 18: Emission totals per country for NKS and OPS emission inventory on the smallest domain covering the Netherlands and neighbouring countries.

Comp.	Country	NKS	OPS	GCN-OPS [ton]	(OPS-NKS)/NKS [%]
NH_3	BE	69269.7	69269.7	0.1	0.0
NH_3	DE	221866.9	221786.4	-55.4	0.0
NH_3	DK	812.9	832.6	19.7	2.4
NH_3	FR	70228.2	67409.6	-2338.8	-3.3
NH_3	LU	5771.3	5771.3	0.1	0.0
NH_3	NL	129632.7	129756.9	124.1	0.1
NO_x	BE	162564.8	162566.0	1.2	0.0
NO_x	DE	484023.1	488673.2	5011.3	1.0
NO_x	DK	191.5	194.5	3.1	1.6
NO_x	FR	102870.0	103622.8	1601.5	1.6
NO_x	LU	11760.8	11760.4	-0.2	0.0
NO_x	NL	400215.7	400704.0	488.3	0.1

Appendix C
Requested output

The requested output from all participating models is described in this section, two tiers of outputs were prescribed. Tier 1 consists of all variables necessary for constructing the ensemble, while tier 2 contains all other variables of interest, which are used to gain more insight in the model processes. Outputs are divided into four categories: concentrations (Table 19), depositions (Table 20), emissions (Table 21), and meteorological parameters (Table 22).

Table 19: Requested output of concentrations.

Type	Variables	Tier 1	Tier 2
Gaseous concentrations [µg/m^3]	NH_3	X	X
	NO	X	X
	NO_2	X	X
	O_3		X
	SO_2		X
	HNO_3		X
	N_2O_5		X
	PAN		X
	Organic nitrogen		X
Aerosol concentrations [µg/m^3]	PM2.5	X	X
	PM10	X	X
	pNO_3^- (fine,coarse)	X	X
	pNH_4^+ (fine,coarse)	X	X
	pSO_4^{2-} (fine, coarse)		X
	Organic nitrate		X

Table 20: Requested output of depositions.

Type	Variables	Tier 1	Tier 2
Depositions (wet + dry) Units: kg (N/S)/ha	NH_x as N	X	X
	NO_y as N	X	X
	SO_x as S		X
Dry-deposition-fluxes [mol m^{-2} s^{-1}] + Landuse dependent dry-deposition velocities [m s^{-1}] for: Grassland Arable land Coniferous forest Deciduous forest Water Urban Semi-natural Resolution: 1 month	O_3		X
	NO	X	X
	NO_2	X	X
	HNO_3		X
	NH_3	X	X
	SO_2		X
	pSO_4^{2-} (fine, coarse)		X
	pNO_3^- (fine, coarse)		X
	pNH_4^+ (fine, coarse)	X	X

Table 21: Requested output of emissions.

Variables	Tier 1	Tier 2
Boundary layer height [m]	X	X
Temperature [K]	X	X
Wind u and v [m s^{-1}]	X	X
Pressure-3d [Pa]	X	X
Relative humidity [%]	X	X
Rain [mm hr^{-1}]	X	X
Soil water content [kg kg^{-1}]	X	X
Atmospheric resistance (per landuse, identical to deposition output) [s m^{-1}]		X
U* (per landuse) [m s^{-1}]		X

Table 22: Requested output of meteorological parameters.

Variables	Tier 1	Tier 2
Boundary layer height [m]	X	X
Temperature [K]	X	X
Wind u and v [m s^{-1}]	X	X
Pressure-3d [Pa]	X	X
Relative humidity [%]	X	X
Rain [mm hr^{-1}]	X	X
Soil water content [kg kg^{-1}]	X	X
Atmospheric resistance (per landuse, identical to deposition output) [s m^{-1}]		X
U* (per landuse) [m s^{-1}]		X

Appendix D

Comparison with observations (statistics)

In this appendix, indicators are given for the comparison of all models and both ensembles with respect to the available observations (wet deposition (Table 23 and Table 24), gaseous concentrations (Table 25, Table 26, and Table 28), and aerosol concentrations (Table 27 and Table 29). For all year and models, the parameters for the regression line are given (Offset and Slope), together with the statistical indicators: spatial correlation, normalized root mean squared error (NRMSE), normalized mean bias (NMB), and the ratio. The column spread represents the normalized standard deviation of the different models which forms the given ensemble.

Table 23: Statistics for wet deposition of reduced nitrogen (NH_x).

Model	Year	Offset	Slope	Correlation	NRMSE	NMB	Ratio	Spread
OPS	2016	-4.09	1.71	0.83	0.30	-0.03	0.94	-
LOTOS	2016	-0.96	1.05	0.87	0.24	-0.13	0.86	-
EMEP4NL	2016	-0.20	0.88	0.85	0.28	-0.16	0.85	-
ENS-NLD	2016	-1.65	1.19	0.87	0.22	-0.10	0.88	9 %
OPS	2017	-2.86	1.37	0.56	0.32	-0.11	0.88	-
LOTOS	2017	-0.29	0.88	0.77	0.28	-0.17	0.83	-
EMEP4NL	2017	1.37	0.64	0.62	0.27	-0.13	0.89	-
ENS-NLD	2017	-0.30	0.91	0.71	0.25	-0.14	0.87	8 %
OPS	2018	-0.57	0.89	0.55	0.33	-0.22	0.80	-
LOTOS	2018	3.68	0.27	0.36	0.29	-0.06	1.00	-
EMEP4NL	2018	2.67	0.29	0.29	0.38	-0.22	0.83	-
ENS-NLD	2018	2.17	0.44	0.55	0.30	-0.17	0.88	14 %
OPS	2019	-2.88	1.55	0.49	0.39	0.00	0.99	-
LOTOS	2019	0.46	0.80	0.66	0.29	-0.11	0.90	-
EMEP4NL	2019	1.25	0.55	0.18	0.50	-0.21	0.81	-
ENS-NLD	2019	0.09	0.69	0.56	0.58	-0.30	0.71	11 %
SILAM	2019	0.95	0.40	0.77	0.79	-0.41	0.60	-
MATCH	2019	-0.53	1.07	0.53	0.27	-0.03	0.97	-
ENS-INT	2019	0.10	0.80	0.56	0.40	-0.18	0.83	19 %

Table 24: Statistics for wet deposition of oxidized nitrogen (NO_y).

Model	Year	Offset	Slope	Correlation	NRMSE	NMB	Ratio	Spread
OPS	2016	0.75	0.97	0.30	0.76	0.27	1.28	-
LOTOS	2016	0.35	0.44	0.57	1.13	-0.42	0.58	-
EMEP4NL	2016	-1.01	1.29	0.49	0.40	-0.11	0.88	-
ENS-NLD	2016	0.51	0.71	0.69	0.29	-0.09	0.91	24 %
OPS	2017	1.09	0.90	0.18	1.00	0.34	1.35	-
LOTOS	2017	0.28	0.53	0.20	1.04	-0.36	0.65	-

Model	Year	Offset	Slope	Correlation	NRMSE	NMB	Ratio	Spread
EMEP4NL	2017	-1.44	1.60	0.51	0.37	0.02	1.02	-
ENS-NLD	2017	0.62	0.75	0.61	0.20	0.00	1.01	20 %
OPS	2018	1.51	0.46	0.15	0.43	0.18	1.22	-
LOTOS	2018	0.85	0.31	0.00	0.59	-0.28	0.75	-
EMEP4NL	2018	3.34	-0.68	0.02	0.42	-0.07	0.96	-
ENS-NLD	2018	1.50	0.22	0.01	0.33	-0.06	0.98	15 %
OPS	2019	1.46	0.64	0.01	0.93	0.34	1.37	-
LOTOS	2019	0.75	0.38	0.62	0.69	-0.26	0.75	-
EMEP4NL	2019	-1.03	1.45	0.28	0.45	-0.05	0.96	-
ENS-NLD	2019	0.64	0.47	0.40	0.60	-0.22	0.79	19 %
SILAM	2019	0.47	0.37	0.54	1.03	-0.40	0.60	-
MATCH	2019	0.66	0.74	0.30	0.33	0.06	1.07	-
ENS-INT	2019	0.75	0.55	0.40	0.34	-0.09	0.92	26 %

Table 25: Statistics for ammonia concentrations in air (observations of the MAN-network).

Model	Year	Offset	Slope	Correlation	NRMSE	NMB	Ratio	Spread
OPS	2016	-2.79	1.78	0.69	0.17	0.24	1.16	-
LOTOS	2016	-0.81	1.48	0.61	0.17	0.32	1.31	-
EMEP4NL	2016	0.27	1.20	0.59	0.13	0.25	1.28	-
ENS-NLD	2016	-0.88	1.44	0.67	0.15	0.27	1.25	13 %
OPS	2017	-3.16	1.80	0.73	0.18	0.19	1.10	-
LOTOS	2017	-1.15	1.54	0.64	0.18	0.32	1.29	-
EMEP4NL	2017	0.03	1.24	0.62	0.14	0.24	1.26	-
ENS-NLD	2017	-1.20	1.48	0.71	0.16	0.25	1.22	13 %
OPS	2018	-3.99	1.63	0.74	0.15	0.05	0.97	-
LOTOS	2018	-1.52	1.30	0.67	0.12	0.08	1.06	-
EMEP4NL	2018	-0.15	1.02	0.63	0.10	0.00	1.01	-
ENS-NLD	2018	-1.65	1.28	0.72	0.11	0.04	1.02	13 %
OPS	2019	-4.95	1.86	0.68	0.19	0.06	0.98	-
LOTOS	2019	-2.16	1.47	0.62	0.15	0.12	1.09	-
EMEP4NL	2019	-0.76	1.22	0.60	0.13	0.10	1.10	-
ENS-NLD	2019	-2.35	1.48	0.67	0.14	0.09	1.06	14 %
SILAM	2019	-0.21	0.65	0.67	0.19	-0.39	0.62	-
MATCH	2019	-2.65	1.35	0.58	0.14	-0.08	0.88	-
ENS-INT	2019	-1.89	1.27	0.67	0.12	-0.04	0.93	23 %

Table 26: Statistics for ammonia concentrations in air (observations of the LML-network).

Model	Year	Offset	Slope	Correlation	NRMSE	NMB	Ratio	Spread
OPS	2016	-1.83	1.23	0.79	0.19	0.05	0.99	-
LOTOS	2016	0.35	0.76	0.92	0.16	-0.21	0.84	-
EMEP4NL	2016	1.14	0.67	0.76	0.21	-0.21	0.88	-
ENS-NLD	2016	0.08	0.87	0.86	0.15	-0.12	0.90	13 %
OPS	2017	-1.96	1.22	0.70	0.21	0.03	0.99	-
LOTOS	2017	0.30	0.75	0.89	0.16	-0.22	0.85	-
EMEP4NL	2017	1.12	0.69	0.70	0.21	-0.20	0.91	-
ENS-NLD	2017	0.02	0.87	0.79	0.16	-0.13	0.92	13 %
OPS	2018	-1.31	0.99	0.74	0.19	-0.10	0.86	-
LOTOS	2018	0.35	0.59	0.97	0.26	-0.38	0.64	-
EMEP4NL	2018	0.91	0.50	0.91	0.31	-0.43	0.61	-
ENS-NLD	2018	0.13	0.69	0.87	0.23	-0.30	0.70	13 %
OPS	2019	-4.62	1.50	0.87	0.23	0.05	0.94	-

Model	Year	Offset	Slope	Correlation	NRMSE	NMB	Ratio	Spread
LOTOS	2019	-1.03	0.85	0.97	0.18	-0.25	0.74	-
EMEP4NL	2019	0.11	0.79	0.87	0.19	-0.20	0.81	-
ENS-NLD	2019	-1.56	1.02	0.95	0.12	-0.13	0.83	14 %
SILAM	2019	-0.34	0.52	0.96	0.39	-0.52	0.49	-
MATCH	2019	-0.32	0.63	0.80	0.32	-0.40	0.62	-
ENS-INT	2019	-1.02	0.86	0.95	0.18	-0.24	0.74	23 %

Table 27: Statistics for ammonium aerosol concentrations in air (observations of the LML-network).

Model	Year	Offset	Slope	Correlation	NRMSE	NMB	Ratio	Spread
OPS	2016	-0.84	1.90	0.11	0.87	0.23	1.25	-
LOTOS	2016	0.57	0.81	0.44	0.70	0.26	1.28	-
EMEP4NL	2016	0.35	1.03	0.38	0.82	0.31	1.32	-
ENS-NLD	2016	0.12	1.17	0.26	0.76	0.27	1.28	8 %
OPS	2017	-0.85	1.84	0.51	0.56	0.17	1.17	-
LOTOS	2017	0.35	0.93	0.81	0.44	0.21	1.22	-
EMEP4NL	2017	0.43	1.00	0.85	0.68	0.34	1.35	-
ENS-NLD	2017	0.04	1.21	0.73	0.52	0.24	1.25	10 %
OPS	2018	-1.18	1.86	0.87	0.36	0.00	0.99	-
LOTOS	2018	0.92	0.50	0.57	0.49	0.16	1.18	-
EMEP4NL	2018	1.03	0.44	0.64	0.53	0.18	1.20	-
ENS-NLD	2018	0.33	0.88	0.88	0.32	0.12	1.12	11 %
OPS	2019	-0.67	1.94	0.69	0.82	0.31	1.30	-
LOTOS	2019	0.78	0.60	0.50	0.81	0.34	1.36	-
EMEP4NL	2019	0.68	0.74	0.46	0.93	0.39	1.41	-
ENS-NLD	2019	0.35	1.01	0.70	0.82	0.35	1.36	9 %
SILAM	2019	0.47	0.36	0.48	0.53	-0.20	0.81	-
MATCH	2019	0.32	1.67	0.57	2.25	0.97	1.99	-
ENS-INT	2019	0.38	1.00	0.66	0.85	0.36	1.37	30 %

Table 28: Statistics for nitrogen dioxide concentrations in air (observations of the LML-network, GGD-Amsterdam, and DCMR).

Model	Year	Offset	Slope	Correlation	NRMSE	NMB	Ratio	Spread
OPS	2016	-1.78	1.11	0.86	0.10	0.02	1.02	-
LOTOS	2016	-0.97	1.10	0.89	0.09	0.05	1.05	-
EMEP4NL	2016	-1.29	1.04	0.90	0.08	-0.02	0.97	-
ENS-NLD	2016	-0.91	1.06	0.92	0.07	0.02	1.02	5 %
OPS	2017	-1.12	1.05	0.86	0.10	-0.01	1.00	-
LOTOS	2017	-0.64	1.10	0.89	0.11	0.06	1.07	-
EMEP4NL	2017	-0.63	1.04	0.86	0.10	0.01	1.01	-
ENS-NLD	2017	-0.36	1.04	0.91	0.08	0.02	1.03	5 %
OPS	2018	-1.78	1.10	0.80	0.12	0.00	1.00	-
LOTOS	2018	-2.61	1.23	0.83	0.15	0.09	1.09	-
EMEP4NL	2018	-1.48	1.08	0.83	0.11	0.00	1.00	-
ENS-NLD	2018	-1.54	1.11	0.85	0.11	0.03	1.03	4 %
OPS	2019	-2.24	1.17	0.80	0.13	0.05	1.05	-
LOTOS	2019	-2.76	1.31	0.84	0.19	0.16	1.15	-
EMEP4NL	2019	-1.44	1.14	0.82	0.13	0.06	1.06	-
ENS-NLD	2019	-1.73	1.18	0.85	0.13	0.09	1.09	5 %
SILAM	2019	1.56	1.02	0.84	0.14	0.11	1.12	-
MATCH	2019	-0.32	1.14	0.79	0.16	0.12	1.13	-
ENS-INT	2019	-0.76	1.14	0.86	0.13	0.10	1.10	5 %

Table 29: Statistics for nitrate aerosol concentrations in air (observations of the LML-network).

Model	Year	Offset	Slope	Correla-tion	NRMSE	NMB	Ratio	Spread
OPS	2016	-0.93	1.57	0.01	1.15	0.34	1.37	-
LOTOS	2016	2.17	0.64	0.12	0.67	0.20	1.23	-
EMEP4NL	2016	2.30	0.66	0.17	0.77	0.25	1.27	-
ENS-NLD	2016	1.58	0.86	0.06	0.84	0.26	1.29	7 %
OPS	2017	-2.24	1.80	0.13	0.85	0.24	1.26	-
LOTOS	2017	0.84	0.91	0.32	0.43	0.12	1.13	-
EMEP4NL	2017	1.76	0.81	0.46	0.68	0.24	1.26	-
ENS-NLD	2017	0.51	1.08	0.28	0.62	0.20	1.21	7 %
OPS	2018	-1.74	1.51	0.17	0.67	0.13	1.14	-
LOTOS	2018	3.21	0.37	0.02	0.43	0.07	1.08	-
EMEP4NL	2018	3.15	0.40	0.19	0.41	0.08	1.09	-
ENS-NLD	2018	2.01	0.66	0.18	0.45	0.09	1.10	6 %
OPS	2019	-3.09	1.94	0.17	0.78	0.17	1.17	-
LOTOS	2019	2.15	0.56	0.01	0.47	0.10	1.11	-
EMEP4NL	2019	1.95	0.64	0.07	0.51	0.13	1.14	-
ENS-NLD	2019	0.84	0.92	0.13	0.53	0.13	1.14	7 %
SILAM	2019	4.06	-0.16	0.00	0.56	-0.15	0.86	-
MATCH	2019	-0.64	1.25	0.03	0.55	0.09	1.10	-
ENS-INT	2019	1.02	0.82	0.10	0.43	0.08	1.09	12 %

Appendix E
Deposition fluxes

In this appendix, all the modelled deposition fluxes are displayed for all models (2016-2019).

Table 30: Modelled deposition fluxes of nitrogen by OPS. Fluxes represent the average value of the Netherlands.

Year	Tracer	Fluxdry	Fluxwet	FluxTotal
2016	**N**	1064	610	1675
	NH_x	787	381	1168
	NH_3	762	291	1053
	NH_4^+	25	90	115
	NO_y	277	230	507
	HNO_3+NO_3^-	98	201	299
	NO_x	179	28	207
2017	**N**	1016	621	1637
	NH_x	748	380	1128
	NH_3	725	287	1013
	NH_4^+	23	93	115
	NO_y	268	241	509
	HNO_3+NO_3^-	94	213	307
	NO_x	174	28	203
2018	**N**	1024	489	1513
	NH_x	746	312	1057
	NH_3	721	241	962
	NH_4^+	25	70	95
	NO_y	278	177	455
	HNO_3+NO_3^-	97	160	257
	NO_x	181	18	198
2019	**N**	993	575	1569
	NH_x	733	374	1107
	NH_3	709	291	1000
	NH_4^+	24	83	107
	NO_y	260	201	462
	HNO_3+NO_3^-	87	178	265
	NO_x	173	23	196

Table 31: Modelled deposition fluxes of nitrogen by LOTOS. Fluxes represent the average value of the Netherlands.

Year	Tracer	Fluxdry	Fluxwet	FluxTotal
2016	**N**	860	489	1349
	NH_x	645	356	1001
	NH_3	622	280	902
	NH_4^+	23	76	99
	NO_y	215	133	348
	HNO_3+NO_3^-	69	109	178
	NO_x	139	0	139
	N_2O_5	7	23	30
2017	**N**	856	513	1368
	NH_x	644	363	1007
	NH_3	622	282	904
	NH_4^+	21	82	103
	NO_y	212	149	361
	HNO_3+NO_3^-	68	119	187
	NO_x	137	0	137
	N_2O_5	7	29	36
2018	**N**	860	489	1349
	NH_x	643	359	1002
	NH_3	620	280	900
	NH_4^+	23	79	102
	NO_y	217	130	347
	HNO_3+NO_3^-	79	105	185
	NO_x	129	0	129
	N_2O_5	9	24	33
2019	**N**	865	469	1334
	NH_x	655	330	985
	NH_3	635	258	893
	NH_4^+	20	72	92
	NO_y	209	139	349
	HNO_3+NO_3^-	74	111	185
	NO_x	127	0	127
	N_2O_5	8	28	36

Table 32: Modelled deposition fluxes of nitrogen by EMEP4NL. Fluxes represent the average value of the Netherlands.

Year	Tracer	Fluxdry	Fluxwet	FluxTotal
2016	**N**	857	497	1354
	NH_x	588	338	926
	NH_3	535	237	772
	NH_4^+	52	101	153
	NO_y	270	159	429
	HNO_3+NO_3^-	108	145	253
	NO_x	146		146
2017	**N**	836	557	1392
	NH_x	570	370	940
	NH_3	516	251	767
	NH_4^+	53	119	172
	NO_y	266	187	453
	HNO_3+NO_3^-	111	169	280
	NO_x	139		139
2018	**N**	857	433	1291
	NH_x	585	297	882
	NH_3	535	209	745
	NH_4^+	49	88	137
	NO_y	272	137	409
	HNO_3+NO_3^-	117	124	240
	NO_x	138		138
2019	**N**	841	454	1296
	NH_x	573	308	881
	NH_3	526	218	744
	NH_4^+	47	90	137
	NO_y	268	147	415
	HNO_3+NO_3^-	107	132	239
	NO_x	145		145

Table 33: Modelled deposition fluxes of nitrogen for the Dutch Ensemble (ENS-NLD). Fluxes represent the average value of the Netherlands.

Year	Tracer	Fluxdry	Fluxwet	FluxTotal
2016	**N**	928	532	1460
	NH_x	674	358	1032
	NH_3	640	269	909
	NH_4^+	33	89	122
	NO_y	254	174	428
	HNO_3+NO_3^-	92	152	243
	NO_x	155		
2017	**N**	903	563	1467
	NH_x	654	371	1025
	NH_3	622	273	895
	NH_4^+	32	98	130
	NO_y	249	192	441
	HNO_3+NO_3^-	91	167	258
	NO_x	150		
2018	**N**	914	470	1385
	NH_x	658	322	981
	NH_3	626	243	869
	NH_4^+	32	79	111
	NO_y	256	148	404
	HNO_3+NO_3^-	98	130	227
	NO_x	149		
2019	**N**	900	500	1400
	NH_x	654	337	991
	NH_3	624	256	879
	NH_4^+	30	82	112
	NO_y	246	162	409
	HNO_3+NO_3^-	89	140	230
	NO_x	149		

Table 34: Modelled deposition fluxes of nitrogen for SILAM. Fluxes represent the average value of the Netherlands.

Year	Tracer	Fluxdry	Fluxwet	FluxTotal
2019	N	1198	310	1508
	NH_x	952	220	1172
	NH_3	951		
	NO_y	246	90	336
	HNO_3	66		
	NO_x	174		

Table 35: Modelled deposition fluxes of nitrogen for MATCH. Fluxes represent the average value of the Netherlands.

Year	Tracer	Fluxdry	Fluxwet	FluxTotal
2019	N	1152	517	1669
	NH_x	968	356	1324
	NH_3	905		
	NO_y	184	162	346

Table 36: Modelled deposition fluxes of nitrogen for the international ensemble of five models (ENS-INT). Fluxes represent the average value of the Netherlands.

Year	Tracer	Fluxdry	Fluxwet	FluxTotal
2019	N	1011	465	1476
	NH_x	777	317	1094
	NH_3	706		
	NO_y	234	148	382
	NO_x	155		

Appendix F

Prompts for Large Language Models

If you would like to get a 2-pages summary of this report using Large Language Models (such as Copilot, Chat-GPT, etc.), we recommend using the following prompts we designed specifically for this purpose. You can find below 3 prompts you can directly copy and use to get a targeted summary of the report "TNO 2025 R11248 National scale modelling of nitrogen deposition in the Netherlands", either policy-focused (in English and in Dutch) or science-focused (in English).

1. Prompt for Policy Makers (in English):

Please provide a concise, policy-focused summary of the key findings and recommendations from the report "TNO 2025 R11248 National scale modelling of nitrogen deposition in the Netherlands." Specifically, address:

1. What are the main results for total nitrogen deposition in the Netherlands, and how do the different models compare?
2. What is the estimated contribution of Dutch sources versus international sources to nitrogen deposition?
3. Which sectors are the main contributors to nitrogen emissions and deposition?
4. What are the main uncertainties in the modelling results, and how do they affect policy decisions?
5. What recommendations does the report make for improving nitrogen policy, emission inventories, and monitoring?
6. What are the implications for the effectiveness of Dutch-only versus international mitigation measures?

Summarize the answers in clear, actionable language suitable for policy decision-making. Highlight any critical uncertainties or caveats that should be considered when using these results for policy.

---

2. Prompt for Policy Makers (in Dutch):

Geef een beknopte, beleidsgerichte samenvatting van de belangrijkste bevindingen en aanbevelingen uit het rapport “TNO 2025 R11248 National scale modelling of nitrogen deposition in the Netherlands”. Beantwoord daarbij specifiek de volgende vragen:

1. Wat zijn de belangrijkste resultaten voor de totale stikstofdepositie in Nederland, en hoe vergelijken de verschillende modellen?
2. Wat is de geschatte bijdrage van Nederlandse bronnen versus internationale bronnen aan de stikstofdepositie?
3. Welke sectoren dragen het meest bij aan de stikstofemissies en -depositie?
4. Wat zijn de belangrijkste onzekerheden in de modelresultaten, en wat betekent dit voor beleidsbeslissingen?
5. Welke aanbevelingen doet het rapport voor verbetering van het stikstofbeleid, de emissie-inventarisaties en de monitoring?
6. Wat zijn de implicaties voor de effectiviteit van uitsluitend Nederlands beleid versus internationale maatregelen?

Vat de antwoorden samen in duidelijke, actiegerichte taal die geschikt is voor beleidsbeslissingen. Benoem expliciet eventuele kritische onzekerheden of kanttekeningen die van belang zijn bij het gebruik van deze resultaten voor beleid.

---

3. Prompt for International Scientists:

Please provide a scientifically detailed summary of the report “TNO 2025 R11248 National scale modelling of nitrogen deposition in the Netherlands,” focusing on the following aspects:

Scientific novelty:
1. What is new or unique about this national-scale benchmark and ensemble study?
2. How does it compare to previous national or European nitrogen modelling efforts?

Methodology:
1. Which models were included in the intercomparison, and how were emissions, meteorology, and land use harmonized?
2. How were model outputs validated?

Key results:
1. What are the main findings regarding total nitrogen deposition, spatial distribution, and quantified uncertainties?
2. How do the models differ in their treatment of ammonia and nitrogen oxides?

Source attribution and transboundary issues:
1. What is the estimated contribution of domestic versus international sources to nitrogen deposition?
2. How do model differences affect the assessment of national versus international mitigation effectiveness?

Model performance and evaluation:
1. How well do the models and the ensemble reproduce observed concentrations and deposition fluxes?
2. What are the main sources of model uncertainty and bias?

3. Are there recommendations for model improvement or future intercomparison studies?

Policy and research implications:

1. What are the implications for national and European nitrogen policy?
2. What recommendations are made for emission inventories, monitoring, and future research?
3. Are there identified research gaps or priorities for the international modelling community?

Data and collaboration:

1. Is the benchmark protocol, emission inventory, or model output available for external researchers?
2. Are there opportunities for international collaboration or participation in future benchmarking exercises?

Please summarize the answers in clear, scientifically precise language, and highlight any critical uncertainties, methodological innovations, or opportunities for further research and collaboration.

Energy & Materials Transition

Princetonlaan 6
3584 CB Utrecht
www.tno.nl

TNO innovation for life